



**NASA CONTRACT  
NASW 1920**

**SPACE GEODESY  
ALTIMETRY**

**VERIFICATION  
EXPERIMENT  
DESIGN STUDY (VEDS)  
FINAL REPORT**

**April 1970**

FACILITY FORM 602

**N71-14791**  
(ACCESSION NUMBER)

**436**  
(PAGES)

**CR-115897**  
(NASA CR OR TMX OR AD NUMBER)

**G3**  
(THRU)  
**13**  
(CODE)  
(CATEGORY)



Reproduced by  
**NATIONAL TECHNICAL  
INFORMATION SERVICE**  
Springfield, Va. 22151

SPACE GEODESY ALTIMETRY  
VERIFICATION EXPERIMENT DESIGN STUDY  
(VEDS)

FINAL REPORT

SR70-4108


APRIL 1970


PREPARED UNDER


NASA CONTRACT NASW — 1920

FOR

NASA  
CODE RED-IDB-RSS  
Wallops Station  
Wallops Island, Virginia 23337  
H. R. Stanley, Technical Monitor

  
\_\_\_\_\_  
E. WEISS  
TECHNICAL DIRECTOR

APPROVED BY   
\_\_\_\_\_  
M. KOLKER  
PROGRAM MANAGER

  
\_\_\_\_\_  
C. MUNDO  
PROGRAM SCIENTIST

PREPARED BY

RAYTHEON COMPANY  
EQUIPMENT DIVISION  
Wayland Laboratories  
Advanced Technology Programs  
Sudbury, Massachusetts 01776

## FOREWORD

This report contains the results of the Verification Experiment Design Study awarded Raytheon Company under Contract No. NASW-1920 by the Geodetic Satellite Program Office, Office of Space Science and Applications, National Aeronautics and Space Administration.

The study was conducted by the Equipment Division of Raytheon Company, under the direction of Mr. Myer Kolker as Program Manager with Mr. Ephraim Weiss as Technical Director and Dr. Charles J. Mundo, Jr. as Program Scientist.

Successful implementation of this effort was due largely to Mr. Jerome D. Rosenberg, Manager, Geodetic Satellite Programs, NASA OSSA, who initiated the effort, and provided the necessary initial direction and guidance, and to Mr. H.R. Stanley, Technical Monitor, NASA Wallops Station, who continued the direction and guidance through the conclusion of the study.

The primary objective of this study was to design an experiment to verify the performance of a 5-meter satellite altimeter operating over the sea surface in 1972, and to derive data to aid in the design of higher performance altimeters.

## ABSTRACT

A study was conducted by Raytheon Company, Equipment Division, for NASA OSSA & NASA Wallops Station to design an experiment to verify the performance of a 5-meter spaceborne altimeter operating over the sea surface in 1972 and to derive data to aid in the design of higher performance altimeters.

Four methods of verification are presented and analyzed, indicating that precision can currently be verified to within 3 meters, and with appropriate modifications, accuracy can be verified to 5 meters. Error studies identify current limitations on verification. Design data requirements and altimeter implications are identified for echo waveform, backscatter coefficient, and correlation time. Recommendations are proposed to ensure success of the Verification Experiment.



## ACKNOWLEDGEMENTS

Earlier efforts in satellite altimetry have been acknowledged in our earlier Space Geodesy Altimetry and Pulse Compression Radar Studies for NASA.

This study was largely the result of the combined efforts of Mr. S. W. Henriksen, Mr. M. Kolker, Dr. C. Mundo, Jr., and Mr. E. Weiss.

Substantial contributors to the study included: Mr. S. W. Henriksen (Section 4), Dr. C. Mundo, Jr. (Sections 5 and 6) Mr. S. Riceman (Section 7), Messrs. J. Bartlett, W. Fordon and J. H. Tatsch (Appendices O, Q and R), and Mr. E. F. Hudson.

Other contributors included Mr. D. K. Barton, Dr. T. Berger (Consultant) of Cornell University, Messrs. C. Brown and M. Crombie (of Raytheon's Autometric Operation), Mr. E. Genest, Mr. H. Kahler.

Dr. B. Kinsman, of the Johns Hopkins University and Chesapeake Bay Institute, consulted on ocean truth and was responsible for Appendix O.

Dr. W. Von Arx of Woods Hole Oceanographic Institute and M. I. T., consulted on geodetic ocean measurements, and prepared Appendix S.

This report was prepared by Mr. E. Weiss, edited by Mr. L. F. Coppenrath, and reviewed by Dr. C. Mundo, Jr., Mr. E. F. Hudson and Mr. M. Kolker.

SPACE GEODESY ALTIMETRY VERIFICATION  
EXPERIMENT DESIGN STUDY (VEDS)

EXECUTIVE SUMMARY

Study Objective

The objective of this study is to design an experiment which will:

- a. Verify the ability of a satellite-borne altimeter to provide useful geodetic data and determine how well it can perform this function.
- b. Derive empirical data to aid in the design of higher performance altimeters for use in the mid-70's.

These experiment objectives apply to the first satellite altimeter flight, anticipated to be GEOS-C in 1972. SEA SAT - A is assumed to be the second. Empirical data from the GEOS-C altimeter will be used to aid in the design of the SEA SAT - A altimeter for higher performance. For purpose of this study, the GEOS-C altimeter is assumed to measure altitude with an accuracy of  $\pm 5$  meters and a precision of  $\pm 5$  meters.

The experiment objectives are listed above in order of decreasing priority. The first experimental objective (to "verify") is interpreted to mean that this study determines methods of verifying the altimeter accuracy and precision to  $\pm 5$  meters, errors in the methods, and the geographic regions in which they can be conducted. The second experimental objective (to "derive empirical data") is interpreted to mean that this study determines what capability is needed on the GEOS-C altimeter for obtaining design data, and the implications of including such capability upon the altimeter model system parameters and related telemetry requirements. The major effort in this study concentrated on the first objective: to "verify".

A third priority experiment objective for GEOS-C, not considered in this study, is to:

- c. Obtain geodetic and other scientific data consistent with the satellite configuration and mission constraints without compromising the above objectives.

## Conclusions

This study indicates the following:

- (1) Within the scope of this study, a verification experiment has been outlined, including methods and procedures necessary to verify the performance of an altimeter to an accuracy of 5 meters, and to a precision of better than 2 meters.
- (2) There currently exists tracking capability which can be used to measure altitude to better than 5 meters for limited regions and ocean surface conditions; this represents only part of the requirements for verification. Based on current capabilities, accuracy can be verified to 15 to 25 meters, precision to 3 meters.
- (3) With relatively minor modifications in procedure and techniques, and updating hardware to conform to that of the more accurate tracking stations, accuracy could be verified to 5 meters, precision to 1 to 2 meters.
- (4) With the best use of currently available technology, verification could be performed to an accuracy of 1 to 2 meters, precision to better than 1 meter.
- (5) Verification of accuracy to better than one meter is beyond the scope of this study; the major limitations on further error reduction are tracking errors and geoid location errors.
- (6) The principal sources of error in verification are identified as follows:
  - a. Tracking accuracy.
  - b. Tracking station location.
  - c. Time synchronization between tracking stations.
  - d. Geoid location relative to the Ellipsoid.
  - e. Location of IMSL (Instantaneous Mean Sea Level) relative to the Geoid or to the Ellipsoid.

- (7) The primary geographic area for performing the Verification Experiment is the Caribbean Sea; secondary is the Hawaiian region.
- (8) Four categories of verification should be incorporated in the Verification Experiment, with cross-checking by using more than one where feasible.
- (9) The ocean surface wave spectrum cannot be fully described with currently available and operational instrumentation. A spectral description of the ocean surface is necessary for verification.
- (10) If the altimeter is designed to collect design data, then the assumed power limitation of 25 watts will be exceeded both in the altimeter and in the design data modes of operation. STADAN telemetry capability is adequate.
- (11) The coordination and processing of data to perform verification requires the development of new data processing software.

#### Recommendations

- (1) An Implementation Plan should be initiated immediately to develop the specifics of the Verification Experiment.
- (2) Some modifications should be made to existing operational facilities to upgrade performance to a level acceptable for verification.
- (3) An early determination should be made as to extent of Design Data capability to be included and whether it can be accommodated on board GEOS-C. This will have a direct impact on the GEOS-C radar altimeter design.
- (4) Planning should include use of the best available instrumentation for ocean surface wave spectrum. This includes evaluation of the combination of laser profilometer, Stilwell photography, and techniques for measurement of capillary ocean waves.

- (5) An aircraft should be flown over the satellite ground track to obtain Design Data and Ocean Truth simultaneously with Design Data from the GEOS-C satellite.
- (6) A software and data processing study should be implemented immediately to provide the necessary support to the Verification Experiment.
- (7) An early study should investigate the design and use in conjunction with the altimeter of surface-based transponders to perform self-verification.
- (8) An early study should investigate the use of receiver/clocks for supporting verification.
- (9) An Aircraft Experiment Program and the GEOS-B program should include a phase to test simulation of the verification categories.

## CONTENTS

	FORWARD	<u>Page</u> ii
	ABSTRACT	iii
	ACKNOWLEDGEMENTS	iv
	EXECUTIVE SUMMARY	I
	<u>Section</u>	
1	INTRODUCTION AND SUMMARY	1-1
1.1	Study Objective	1-1
1.2	Assumptions	1-2
1.3	Study Rationale and Approach	1-3
1.4	Verification	1-5
1.4.1	Performance Levels of Verification	1-5
1.4.2	Results of Error Analyses	1-6
1.4.3	Geography	1-7
1.4.4	Advantages and Disadvantages of Each Category	1-9
1.4.5	Integration of Experimental Methods	1-11
1.5	Design Data Summary	1-12
1.6	Conclusions	1-13
1.7	Recommendations	1-15
2	BACKGROUND	2-1
2.1	Ground Rules for the Verification Experiment Design Study	2-1
2.2	VEDS Radar Altimeter Model	2-2
2.3	Role of VEDS in the GEOS-C Program	2-4
3	APPROACHES TO VERIFICATION	3-1
3.1	Definition of the Problem of Verification	3-1
3.2	Classification of Verification Methods	3-3
3.3	Calibration and Verification	3-3
4	ABSOLUTE VERIFICATION	4-1
4.1	Summary and Conclusions	4-1
4.2	Description of Absolute Verification	4-7
4.2.1	Absolute Verification Concept	4-7
4.2.2	Location of Instantaneous Mean Sea Level (IMSL)	4-9

## Contents (Continued)

<u>Section</u>	<u>Page</u>
4.2.3 Location of Altimeter	4-15
4.3 Regions for Absolute Verification	4-17
4.3.1 The Caribbean Sea	4-19
4.3.1.1 Characteristics (Caribbean)	4-19
4.3.1.2 Tracking Station Location (Caribbean)	4-29
4.3.1.3 Conduct of Experiment (Caribbean)	4-40
4.3.1.4 Error Analysis (Caribbean)	4-57
4.3.2 Hawaiian Islands Region	4-88
4.3.2.1 Characteristics (Hawaii)	4-89
4.3.2.2 Tracking Station Location (Hawaii)	4-95
4.3.2.3 Additional Data Required (Hawaii)	4-98
4.3.2.4 Conduct of Experiment (Hawaii)	4-98
4.3.2.5 Error Analysis (Hawaii)	4-100
4.3.3 Marshall Islands	4-103
4.3.4 Lake Maracaibo	4-103
4.3.4.1 Tracking Station Location (Maracaibo)	4-104
4.3.4.2 Additional Data Required (Maracaibo)	4-104
4.3.5 Lago De Nicaragua	4-104
4.3.5.1 Region Characteristics (Lago De Nicaragua)	4-105
4.3.5.2 Tracking Station Location (Lago De Nicaragua)	4-108
4.3.5.3 Additional Data Required (Lago De Nicaragua)	4-108
4.3.6 Lake Titicaca	4-108
4.3.7 Other Regions	4-109
4.4 Critique of Absolute Verification	4-109
5 RELATIVE VERIFICATION	5-1
5.1 Summary	5-1
5.2 Description of Relative Verification	5-3
5.2.1 Relative Verification Concept	5-3
5.3 Geometry	5-5
5.4 Error Analysis	5-7
5.4.1 Errors due to X:	5-7
5.4.2 Establishing Instantaneous Mean Sea Level	5-10

## Contents (Continued)

<u>Section</u>	<u>Page</u>
5.4.3 The Measurement System for Range (R)	5-11
5.4.3.1 Current Ranging Capability	5-11
5.4.4 Possible Alternative Ranging Instrumentation Surface Transponders	5-14
6 VERIFICATION OF ALTIMETER PRECISION	6-1
6.1 Self-consistent Verification	6-1
6.1.1 Error Summary	6-1
6.1.2 Geography	6-1
6.1.3 Ground Support System	6-2
6.1.4 Data Requirements	6-4
6.1.4.1 Tracking Data	6-4
6.1.4.2 Surface Data	6-4
6.1.4.3 Sea State Monitoring	6-5
6.1.5 Advantages and Disadvantages	6-5
6.1.6 Self Consistently Verification Concept	6-5
6.1.7 Error Analysis	6-8
6.1.8 Variants of the Self Consistent Method	6-11
6.2 Differential Verification	6-14
6.2.1 Summary	6-14
6.2.2 Support Data	6-19
6.2.3 Geography	6-19
6.2.4 Theory	6-20
6.2.5 Error Analysis	6-22
6.2.6 Regions of Experimentation	6-27
6.2.6.1 Differential Measurements Over the Caribbean	6-27
6.2.6.2 Differential Measurements in the Lake Nicaragua Region	6-28
6.2.6.3 Differential Measurements in the Gulf of Panama - Panama North Coast Region	6-28
6.2.6.4 Differential Measurements in the Puerto Rico Trench Region	6-29/6-30
6.2.6.5 Differential Measurements East of the Caribbean	6-29/6-30



## Contents (Continued)

<u>Section</u>	<u>Page</u>
7 DESIGN DATA (INCLUDING DISCUSSION OF VEDS RADAR ALTIMETER MODELS)	7-1
7.1 Radar Altimeter Model - For Verification Only	7-2
7.1.1 General Description	7-2
7.1.2 Expected Radar Altimeter Characteristics	7-4
7.1.2.1 The Echo Shape	7-7
7.1.2.2 Range Ambiguities	7-7
7.1.2.3 Signal Integration	7-8
7.1.2.4 Atmospheric Effects	7-9
7.1.3 Detailed Description of the VEDS Radar Altimeter Model	7-9
7.1.3.1 Altimeter Parameters	7-11
7.1.3.2 Radar Range Equation	7-11
7.1.4 Altimeter Data Output	7-12
7.1.4.1 Altitude Measurements	7-12
7.1.4.2 Timing	7-12
7.1.4.3 Performance Monitoring	7-12
7.1.4.4 Altimeter Data Rate	7-13
7.1.4.5 Processing of the Altimeter Data at Ground Stations	7-13
7.2 Collection of Design Data for SEA SAT-A	7-14
7.2.1 Purpose	7-14
7.2.2 Data Collection	7-14
7.2.2.1 Echo Waveform Data	7-14
7.2.2.2 Backscatter Coefficient Measurement	7-17
7.2.3 Correlation Time	7-17
7.2.4 Monitoring Conditions	7-18
7.3 Radar Altimeter Model - Incorporating Design Data Capability	7-19
7.3.1 Model Characteristics	7-20
7.3.2 GEOS-C Radar Altimeter Measurements	7-21
7.3.3 Altitude Measurements	7-21
7.3.4 Design Data Measurements	7-22
7.3.5 Size, Weight and Power Requirements	7-23

## Contents (Continued)

<u>Section</u>	<u>Page</u>
7.4 Implications of Pulse Compression in the Altimeter	7-24
7.5 Telemetry Capability	7-25/7-26
8 EXPERIMENT INTEGRATION CONSIDERATIONS	8-1
8.1 Introduction	8-1
8.2 Design Data and Verification	8-1
8.3 Storage and Telemetry	8-2
8.4 Time and Timing	8-5
8.5 Power, Weight and Volume	8-7
8.6 Ocean Truth and Atmospherics	8-9
8.7 Instantaneous Mean Sea Level (IMSL)	8-9
8.8 Software and Data Handling	8-10
8.8.1 Software Recommendation	8-12
8.9 Experiment Integration	8-13
APPENDIX A LIST OF TRACKING STATIONS	
APPENDIX B MATHEMATICAL BASIS FOR GEOMETRIC ERROR ANALYSIS	
APPENDIX C CHARACTERISTICS OF FREQUENCY AND TIME STANDARDS	
APPENDIX D MATHEMATICAL BASIS FOR ANALYSIS OF ERROR IN SATELLITE LOCATIONS (DYNAMICAL SITUATIONS)	
APPENDIX E EFFECT OF ORBITAL CONSTRAINTS ON LOCATION ERRORS	
APPENDIX F INFLUENCE OF LAND TOPOGRAPHY ON RETURN PULSE	
APPENDIX G VERIFICATION METHOD USING PATH INTERSECTIONS	
APPENDIX H NOTE ON RELATIONS BETWEEN STANDARD DEVIATIONS INVOLVED IN THE VERIFICATION EXPERIMENT	
APPENDIX I NOTES ON BIASES, SHORT-PERIOD VARIATIONS, AND OTHER COMMON CONCEPTS	
APPENDIX J REMOVAL OF EFFECTS OF CERTAIN TYPES OF SYSTEMATIC ERRORS FROM OBSERVATIONS	
APPENDIX K PURPOSE AND ORGANIZATION OF ERROR ANALYSIS	
APPENDIX L CONFIDENCE LIMITS FOR THE STANDARD DEVIATION OF THE ALTIMETER HEIGHT	
APPENDIX M CONSTRAINTS ON VEDS	
APPENDIX N TERMINOLOGY AND DEFINITIONS	
APPENDIX O OCEAN SURFACE CONDITIONS (OCEAN TRUTH)	
APPENDIX P SURFACE VERIFICATION OF ALTITUDE UTILIZING ALTIMETER SIGNAL	

## Contents (Continued)

### Section

APPENDIX Q TROPOSPHERIC AND IONOSPHERIC EFFECTS

APPENDIX R CONTRIBUTIONS TO MEAN SEA LEVEL IN THE OPEN  
OCEAN

APPENDIX S THE FIGURE OF THE SEA: AN ESTIMATE OF ERROR

GENERAL REFERENCES

## LIST OF ILLUSTRATIONS

<u>Figure</u>		<u>Page</u>
1-1	Verification Categories	1-4
2-1	Radar Altimeter Model Simplified Block Diagram	2-3
3-1	VEDS Geometry	3-2
3-2	Verification Categories	3-5
4-1A	Percent of area of total Caribbean in which total error is less than 6 meters.	4-6
4-1	Absolute Verification Geometry	4-8
4-2	Absolute Verification Block Diagram	4-10
4-3	VEDS Geometry	4-11
4-4	Verification Experiment Region (Caribbean)	4-20
4-5	Traces of the Altimeter Orbit	4-21
4-6	Density of Oceanographic Observations (S. T. P.) in the Verification Experiment Region (Number of Observations per 5° x 5° Square).	4-23
4-7	Regions of Substantial Gravity Data in the Caribbean	4-24
4-8	Astrogeodetic Geoid in the Verification Experiment Region (Caribbean)	4-25
4-9	Satellite Geoid in the Verification Experiment Region (a) Anderle, 1965 (heights in meters)	4-26
4-9	Satellite Geoid in the Verification Experiment Region (b) Bursa 1969. (heights in meters)	4-27
4-10	Average Cloudiness in American Mediterranean	4-28
4-11	Wave Heights (in meters) in Caribbean Sea Region. <sup>10</sup>	4-31
4-12	Coverage of Tracking Stations in the Caribbean (a) Optical Tracking Stations	4-32
4-12	Coverage of Tracking Stations in the Caribbean (b) Electronic Tracking Stations	4-33
4-12	Coverage of Tracking Stations in the Caribbean (c) 4 or more radar stations for tracking	4-34
4-13	Stations which are located so that they can observe the altimeter (at 60° zenith distances or less) when the altimeter is within 90° (in longitude) of the Caribbean	4-36
4-14	Stations Which Can Observe the Satellite Only Outside the 90° Limit	4-37

## List of Illustrations (Continued)

<u>Figure</u>		<u>Page</u>
4-15	Subregions where a Higher Density of Measurements should be Made	4-41
4-16	Typical Measurement and Trace Intervals	4-43
4-17	Location of Electronic Tracking Stations	4-52
4-18	Geometric Arrangement of Ranging Station Locations	4-60
4-19	Verification Experiment Area (Hawaii)	4-90
4-20	Inter-Island Geodetic Control (Hawaii)	4-91
4-21	Satellite Geoid in Hawaiian Islands Area	4-92
4-22	Data on S. T. P. in the Verification Experiment Area (Hawaii)	4-93
4-23	Satellite - Tracking Radars and Cameras in the Hawaiian Islands - Johnston Island Region	4-96
4-24	Region Containing Lago De Nicaragua	4-106
4-25	Astro Geodetic Geoid Around Lago De Nicaragua	4-107
5-1	Relative Verification Geometry	5-4
5-2	Relative Verification Block Diagram	5-6
5-3	Ground Track Error	5-8
6-1	Sub-Satellite Tracking Density	6-3
6-2	Self-consistent Category Test	6-7
6-3	The Path-Intersection Grid	6-12
6-4	Measurement of Altimeter Repeatability by Multiple Passes on Same Ground Trace	6-13
6-5	Differential Verification	6-15
6-6	Differential Verification Block Diagram	6-16
6-7	Geometric Relations Between Heights in Differential Verification	6-21
7-1	Radar Altimeter Operation	7-3
7-2	Radar Altimeter Model Simplified Block Diagram	7-5
7-3	The Echo Waveform	7-8
7-4	Time Relationships Between Transmitted and Received Pulses and the Time Interval Measured by the Altimeter	7-9
7-5	Detailed Block Diagram of the VEDS Radar Altimeter Model	7-10
7-6	Echo Waveform Measurement	7-23

# List of Illustrations (Continued)

<u>Figure</u>		<u>Page</u>
B-2		B-2
G-1	The Path-Intersection Grid	G-2
L-1	Graphs of sample size required to insure with a given probability $\gamma$ that a confidence interval for the mean with confidence coefficient .99 will be shorter than L	L-3
L-2	Power curves for testing $H_0: \sigma^2 = \sigma_0^2$ against $\sigma^2 > \sigma_0^2$ at 0.005 significance level. $H_1:$	L-4
M-1	Optical Tracking Stations	M-7
M-2	Electronic Tracking Stations	M-8
N-1	VEDS Geometry	N-7/N-8
O-1	Portions of Wave Profiles Obtained From Stereo-photographs	O-25
O-2	Facet Length as Determined by Flatness Tolerance	O-26
O-3	Average Facet Length Versus Slope for Waves 1-1.5 Feet High (radar wavelength = 3 cm)	O-27
O-4	Slope Probability for Waves 1-1.5 Feet High	O-29
Q-1	Typical Day and Night Profiles: Electron Density vs. Altitude	Q-6
R-1A	Distributions of Water Surface Displacement (July)	R-3
R-1B	Distributions of Water Surface Displacement (November)	R-4

## LIST OF TABLES

<u>Table</u>		<u>Page</u>
1-1	VEDS Error Summary	1-7
1-2	Geographic Regions for Verification	1-8
1-3	Estimated Impact on GEOS-C Radar Altimeter of Design Data	1-13
2-1	VEDS Radar Altimeter Characteristics	2-4
3-1	Verification Methods	3-4
4-1	Summary of R.M.S. Errors in Verification Experiments (Absolute Category)	4-2
4-1A	Percent of Caribbean with Error Less than 6 Meters*	4-5
4-2	Principal Areas of Possible Interest to VEDS	4-18
4-3	Percent Observing Time Favorable for Observing Satellite During 1962, 1963	4-30
4-4	Locations of Tracking Stations for Caribbean Tests	4-38
4-5	Tracking Station Locations for the Caribbean	4-65
4-6	Station Configurations (See Table 4-5 for Locations)	4-66
4-7	Results of Error Analyses for the Caribbean	4-67
4-8	Standard Deviations of Horizontal Coordinates of Certain Tracking Station Sites Relative to Grand Turk Station*	4-70
4-9	Wave Height Data for East Equatorial Pacific	4-94
4-10	Cloud-Cover Data for Maui (in % of observing time lost)	4-94
4-11	Tracking Stations in Hawaiian Islands -- Johnston Island Region	4-97
4-12	Geometric Error in Satellite Height for Ground Tracking in Hawaii Area	4-102
5-1	Relative Verification Error Summary	5-1
5-2	Propagation Errors	5-13
6-1	Self-Consistent Verification Error Summary	6-2
6-2	Tracking Errors in Self-Consistent Verification	6-9
6-3	Errors that Result from Location Difference and Time Difference Between Points i and j	6-10
6-4	Differential Verification Error Summary	6-17

# List of Tables (Continued)

<u>Table</u>		<u>Page</u>
7-1	VEDS Radar Altimeter Characteristics	7-6
7-2	VEDS Radar Altimeter Transmission Characteristics	7-7
7-3	Estimated Physical Parameters of Optional Altimeter Designs	7-24
A-1	C-Band Radars	A-1
A-2	C-Band Radars	A-2
A-3	USB	A-3
A-4	GRARR	A-4
A-5	MOTS	A-5
A-6	USAF	A-6
A-7	Special Optical Cameras (MOTS 40 and P TH 100 <sup>1</sup> )	A-7
A-8	TRANET	A-8
A-9	SAO Tracking Net (Baker-Nunn and Special Cameras)	A-9
A-10	Satellite Positions for the Caribbean	A-10
A-11	Fictitious Satellite Positions Over Puerto Rico	A-11
A-12	Tracking Station Locations for the Caribbean	A-12
A-13	List of Stations for the Hawaii Area	A-13/A-14
C-1	Frequency Standard Specification	C-2
O-1	Sea State Classification	O-6
O-2	Wave Classification by Steepness	O-7
O-3	Deep-Wave Relationships for Fully Developed Sea	O-8
O-4	Minimum Fetch and Duration vs., Wind Speed for a Fully Developed Sea	O-9
O-5	Relative Frequency of Waves of Different Heights in Different Regions	O-10
Q-1	One-Way Troposphere-Induced Range Errors (m)	Q-2
Q-2	One-Way Ionosphere-Induced Range Errors (m)	Q-3
Q-3	One-Way Atmospherically-Induced Range Errors (m)	Q-3
Q-4	Values of Constants a, b, and c Based on ICAO	Q-9
R-1	Equilibrium Tides Due to Moon and Sun	R-7
R-2	Errors in Instantaneous Mean Sea Level (IMSL) Relative to Mean Sea Level (MSL) for Deep Oceans	R-10



## SECTION 1. INTRODUCTION AND SUMMARY

## SECTION 1. INTRODUCTION AND SUMMARY

### 1.1 Study Objective

The objective of this study is to design an experiment which will:

- a. Verify the ability of a satellite-borne altimeter to provide useful geodetic data and determine how well it can perform this function.
- b. Derive empirical data to aid in the design of higher performance altimeters for use in the mid-70's.

These experiment objectives apply to the first satellite altimeter flight, anticipated to be GEOS-C in 1972. SEA SAT - A is assumed to be the second. Empirical data from the GEOS-C altimeter will be used to aid in the design of the SEA SAT - A altimeter for higher performance. For purpose of this study, the GEOS-C altimeter is assumed to measure altitude with an accuracy of  $\pm 5$  meters and a precision of  $\pm 5$  meters.

The experiment objectives are listed above in order of decreasing priority. The first experimental objective (to "verify") is interpreted to mean that this study determines methods of verifying the altimeter accuracy and precision to  $\pm 5$  meters, errors in the methods, and the geographic regions in which they can be conducted. The second experimental objective (to "derive empirical data") is interpreted to mean that this study determines what capability is needed on the GEOS-C altimeter for obtaining design data, and the implications of including such capability upon the altimeter model system parameters and related telemetry requirements. The major effort in this study concentrated on the first objective: to "verify".

A third priority experiment objective for GEOS-C, not considered in this study, is to:

- c. Obtain geodetic and other scientific data consistent with the satellite configuration and mission constraints without compromising the above objectives.

## 1.2 Assumptions

The Verification Experiment Design Study was initiated in support of GEOS-C, and initial assumptions were based on existing concepts of this satellite.

The GEOS-C flight is anticipated in approximately 1972. The fundamental mission of satellite altimetry for geodesy is to measure mean sea level - not to measure ocean state conditions. The GEOS-C satellite is assumed to be limited in coverage by a 20° inclination. Apogee at 850 nautical miles (1575 km) establishes maximum power requirements; together with perigee at 600 nautical miles (1100 km), this specifies the range of altitudes. The satellite is expected to have a useful life of two years.

The radar altimeter uses 25 watts average power and transmits 5 kilowatts peak power. The altimeter is expected to measure altitude with an accuracy of 5 meters, precision of 5 meters and a resolution of 1 meter. The radar will operate at X-band (8 to 10 GHz), and will have a useful life of 200 to 500 hours.

The available tracking and communications networks are assumed to be similar to those used for GEOS-B. In addition, at least one Apollo Tracking Ship is assumed to be available for a limited time.

It is assumed that aboard the satellite there is access to a clock stable to one part in  $10^{11}$ . It is assumed that there will be no interference between the radar altimeter and other experiments and instrumentation, including house-keeping functions. Short-term data storage is assumed available, and long-term storage not available.

In addition to the explicit assumptions, there are numerous implicit constraints involving time, equipment, money, geography, additional equipment and the orbit. Assumptions and constraints are further enumerated in Appendix M.

### 1.3 Study Rationale and Approach

The approach to verification is that the instrument measurement should agree with an independent standard measurement of the same quantity in a consistent manner, under a variety of operating conditions. The variety of operating conditions must be sufficient to ensure operation within the specifications under the many conditions likely to be encountered, and not just under an ideal environment. This requires many geographical, meteorological and ocean surface (sea state) combinations, with sufficient redundancy to provide suitable statistical confidence in the results.

Of the many ways of performing verification measurements, four categories evolved. While each individually can be considered a form of verification, all four are proposed to contribute to verifying the performance of the altimeter. The four categories are illustrated in Figure 1-1:

- a. In the ABSOLUTE category, accuracy is verified by measuring the location of the satellite with a tracking system, and determining the location of the instantaneous mean sea level (IMSL) at the sub-satellite point by way of geoid-ellipsoid determinations along the reference ellipsoid.
- b. In the RELATIVE category, accuracy is verified by means of a direct measurement of the satellite height near the zenith, with a local determination of IMSL. These measurements are both relative to the ranging instrument.
- c. In the SELF-CONSISTENT category, precision is verified by comparing the difference in altimeter measurements on two successive passes at a crossing with the measured difference in orbit heights and in ocean surface heights.
- d. In the DIFFERENTIAL category, precision is verified by comparing the difference in altimeter measurements over short intervals of time with changes in satellite altitude determined by tracking and topographical differences (in IMSL).

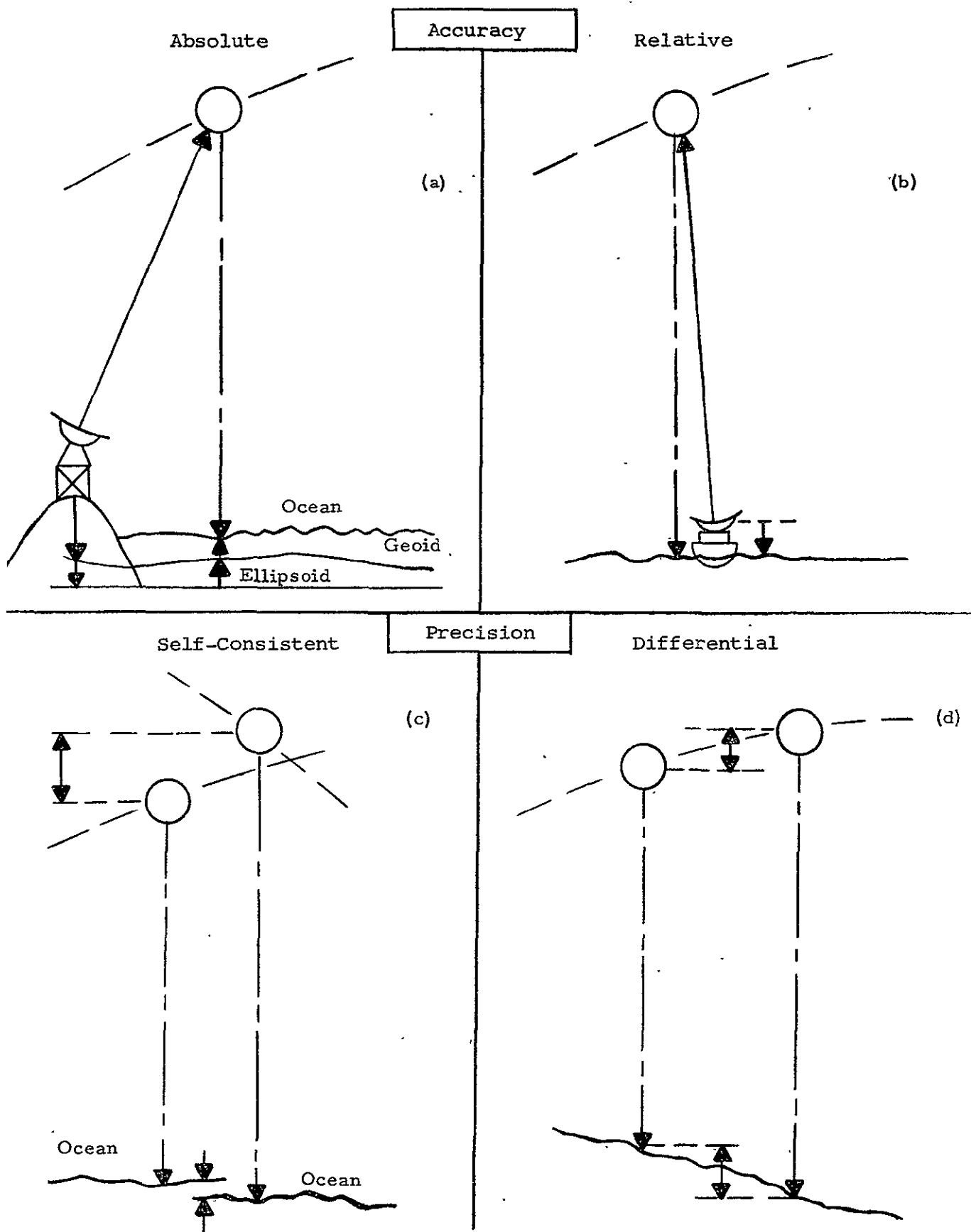


Figure 1-1. Verification Categories

#### 1.4 Verification

The study results indicate that precision of the satellite altimeter can be verified to within 1 meter, and that accuracy can be verified to 5 meters.

##### 1.4.1 Performance Levels of Verification

Three levels of performance were analyzed:

- o Operational
- o Capable
- o Feasible

The Operational Level of performance is that expected with the use of C and S Band tracking equipment as it now performs in the field and the personnel and procedures that are used on Apollo tracking missions.

The Capable level of performance is that expected of the system if all components are upgraded to the best level currently operational in only limited regions, and tested modifications were made to the network. The changes considered would include:

- o Upgrading the performance level of all C-Band tracking radars to better than 5 meters tracking accuracy, in accordance with that of better systems currently in use. (Includes incorporating digital range tracking where not currently in use.)
- o Upgrading timing synchronization for tracking stations to 100 microseconds.
- o For the absolute category of verification,
  - (a) Assuming all tracking stations that have been operational are operational at the time of verification.
  - (b) Basing computations on new spheroid fitted to the geoid at Grand Turk.
- o Assuming that currently existing geodetic and oceanographic data have been collected and put in useable form.
- o Assuming implementation of existing computer programs and equations, with minor modifications where necessary.

The Feasible level of performance is that expected of the system if the system were operating at the best level that could be obtained within the limits of technology and of available time and money. Modifications would require equipment and software redesign. This would include:

- o Upgrading all tracking stations to the same or better level of operation as the best currently available.
- o Adding tracking instruments where necessary to provide good geometry and improve coverage.
- o Assuming use of computer programs and equations designed to make best use of data.
- o For absolute and differential verification, obtaining and incorporating additional survey data in selected areas to upgrade geodetic information (e.g., off the coast of Yucatan).

#### 1.4.2 Results of Error Analyses

The results of the error analyses for each verification category at each level of performance are summarized in Table 1-1.

Tracking errors are the dominant source of error for all except the absolute category, for which station location and geoid-ellipsoid errors are at times the dominant error sources. This applies with minor exception to the three levels of performance.

The results indicate that precision can be verified at the operational level of performance to 3 meters, at the capable level to 1-2 meters, and at the feasible level to better than 1 meter.

The results also indicate that accuracy could be verified at the feasible level to 1-2 meters with the absolute method, to 2-3 meters with the relative method. Although some individual tracking measurements may currently be made to better than 5 meters, the analyses indicate that verification of accuracy cannot be currently performed (at the operational level) to better than 15 meters. At the capable level, the absolute method can be used to verify accuracy to 2-20 meters, the relative method to 5-7 meters.

Table 1-1. VEDS Error Summary

Verification Category: Accuracy			Precisión		
Level of Performance:	Absolute	Relative	Differential	Self-Consistent	
	Operational	15 - 55 m	15 - 25 m	3 m	3 m
	Capable	2 - 20 m	5 - 7 m	1 - 2 m	1 - 2 m
	Feasible	1 - 2 m	2 - 3 m	<1 m	<1 m

#### 1.4.3 Geography

The geographic regions for performance of the verification experiment were investigated. The satellite orbit limits all altimeter and surface measurements to the 20° latitude belt about the equator. Additional constraints are imposed by tracking station location and the availability of geodetic and environmental data.

Table 1-2 is a qualitative summary of the suitability of different geographic regions for the performance of the verification experiment at each level of performance. The relative category of verification can be performed at all three levels of performance throughout the 20° zone. The Caribbean and Hawaiian regions are the only ones where all four categories of verification can be performed at three levels of performance.

The differential and self consistent categories lend themselves to measuring precision in areas where less tracking support and less surface data are available. The self consistent method can also be implemented near Mozambique and in the Indian Ocean west of Australia. In addition, variants of this method may be possible at any longitude in the vicinity of 20° latitude.



Table 1-2. Geographic Regions for Verification

Geographic Region:	Verification Category:	Accuracy		Precision	
		Absolute	Relative*	Differential	Self-Consistent
Universally within 20°		X	OCF	O	O
Universally within 1° of 20°		X	OCF	OC	OC
Regions of Large Geoidal Slope		X	OCF	OCF	OCF
Caribbean		OCF	OCF	OCF	OCF
Hawaii		OCF	OCF	OCF	OCF
North and West of Australia		O	OCF	OC	OC
Mozambique		O	OCF	-	OC
* 2 data runs per day per ship O Operational level of performance C Capable level of performance F Feasible level of performance X Cannot be performed satisfactorily - Not adequately investigated					

The differential method is also applicable beyond the scope of extensive tracking support, particularly in regions of large topographical variations. Suitable regions are the Marianas Trench, the Java Trench, the Puerto Rico Trench and the Venezuela Trench.

The conclusion of the geographic investigation is that the primary region for verification should be the Caribbean.

#### 1.4.4 Advantages and Disadvantages of Each Category

##### Verification - Advantages:

- . Related directly to phenomena of geodetic and oceanographic importance.
- . Provides more information per unit cost than other categories
- . Often employable without extensive special instrumentation in subsatellite region (such as ship or local surface measurements).

##### Absolute Verification - Disadvantages:

- . Employs extensive computation, thereby increasing possibility of undetected and/or cumulative errors.
- . Errors vary considerably with locale, restricting present geographic areas and times for experiments.
- . Effort required to reduce errors increases as function of size more rapidly than for other categories.

##### Relative Verification - Advantages:

- . Incorporates a direct measurement of satellite height above instantaneous mean sea level.
- . Does not require as precise orbital estimation as the Absolute Category, with the associated errors and coordination requirements.
- . Does not require height of geoid above spheroid, or of sea surface above geoid.
- . Measurement may be performed from a ship in any portion of a large geographical region.

##### Relative Verification - Disadvantages:

- . Small number of measurements due to limited opportunities.
- . Dependence on limited measurements on a pass, without opportunity for statistical improvement by tracking over larger portion of track.
- . Imposes cost and schedule problems of deployment of an Apollo ship (except for measurements near shore based tracking stations).

#### Self-Consistent Verification - Advantages:

- . Computationally simple.
- . Requires minimal additional expenditure of effort; i. e., no additional hardware demand.
- . Relatively insensitive to errors in tracking system, such as equipment biases, propagation errors and tracking station location errors.
- . Requires no knowledge of the geoid.
- . Requires only changes in IMSL, principally tides.
- . Can be used as check on continuity of operational performance of the altimeter during its lifetime.
- . Variations of this method can be performed in areas having little or no direct tracking support.

#### Self-Consistent Verification - Disadvantage:

- . For large crossing angles, is sensitive to (geometric) propagation of errors.

#### Differential Verification - Advantages:

- . Can be performed almost anywhere; in areas with no geoidal changes, can monitor drift in altimeter system.
- . Errors in the tracking system such as equipment biases and propagation errors, are practically cancelled out.
- . Relatively insensitive to tracking station location errors.
- . Requires only changes in IMSL, and therefore only changes in oceanographic correction and geoid slope.
- . Relatively insensitive to absolute location error.
- . Exercises a method for scientific application of the altimeter to measurement of the slope of the geoid.

#### Differential Verification - Disadvantages:

- . None apparent.

#### 1.4.5 Integration of Experimental Methods

The results of this study lead to the conclusion that the four verification methods considered complement each other, and all contribute to the verification program. In addition to the technical justification, economic justification of the use of all four verification methods is based on the consideration that the percentage increase in cost over that for a single verification category is relatively small.

In order to implement a primary objective of the verification experiment - verification of altimeter accuracy - the Absolute or Relative method must be implemented, under a variety of conditions. The Relative method is limited as to the number of data sequences by virtue of the geometric configuration requirement for a ranging station almost directly under the satellite.\* The Absolute method is limited geographically to those regions where adequate geodetic and environmental data are available. These limitations inhibit measurements under a variety of operational and environmental conditions, which are essential to high confidence in the verification of the altimeter.

Simultaneous implementation of Absolute and Relative verification not only serves to increase confidence in the reliability of the measurements by virtue of the use of independent methods for performing the same measurement, but also provides increased confidence in the geodetic and environmental data and data processing used in the Absolute verification. The improved geodetic and environmental data can be used to extend the region of applicability of the Absolute verification method, thereby increasing the confidence in the verification results. In this sense, the Relative method, which has a conceptually more direct approach, may be thought of as a calibration of the Absolute method.

---

\* See Figure 5-3. From this figure, it is apparent that the satellite must pass within  $2\frac{1}{2}^{\circ}$  of zenith of the tracking station when the tracking station position is known relative to the subsatellite point to an accuracy of 50 meters.

In principle, either Self-consistent or Differential verification can be used to determine the precision of the altimeter. Precision verification can be determined to a smaller numerical value than is achievable by verification of accuracy, and provides essential information on the performance of the altimeter while increasing confidence in the performance results. This can be implemented with the same equipment used for accuracy verification, and largely from the same body of data. In a manner similar to that described in the preceding paragraph, precision verification can be used to extend the geographical region of applicability of verification.

#### 1.5 Design Data Summary

The following represent at a minimum the types of data that should be derived from the GEOS-C experiment:

- . Echo Waveform
- . Backscatter Coefficient
- . Correlation Time

These data should be gathered as a function of various transmitter pulse lengths (20 to 200 nanoseconds) and various ocean (sea state) conditions.

The estimated impact on the GEOS-C radar altimeter of adding capability of design data is shown in Table 1-3. NASA's STADAN facilities can provide the capacity for the maximum telemetry rate of 1020 bits per second.

Table 1-3. Estimated Impact On GEOS-C Radar Altimeter of Design Data

	Basic Altimeter	Altimeter To Collect Design Data	
		Altimeter Mode	Design Data Mode
Volume, (in <sup>3</sup> )	620	1200	1200
Electronics Weight, (lbs)	20	40 <sup>(1)</sup>	40 <sup>(1)</sup>
Antenna Weight, (lbs)	5	5	5
Power, (watts)	25	42	57 <sup>(1)</sup>
Maximum Output Data <sup>(2)</sup> Rate, (Bits/Sec)	220	220	1020
<p>(1) Recent efforts indicate that A to D converter state-of-the-art design can reduce Design Data requirements to about 36 lbs and 45 watts.</p> <p>(2) At 10 altitude measurements per second.</p>			

## 1.6 Conclusions

This study indicates the following:

- (1) Within the scope of this study, a verification experiment has been outlined, including methods and procedures necessary to verify the performance of an altimeter to an accuracy of 5 meters, and to a precision of better than 2 meters.
- (2) There currently exists tracking capability which can be used to measure altitude to better than 5 meters for limited regions and ocean surface conditions; this represents only part of the requirements for verification. Based on current capabilities, accuracy can be verified to 15 to 25 meters, precision to 3 meters.
- (3) With relatively minor modifications in procedure and techniques, and updating hardware to conform to that of the more accurate tracking stations, accuracy could be verified to 5 meters, precision to 1 to 2 meters.

- (4) With the best use of currently available technology, verification could be performed to an accuracy of 1 to 2 meters, precision to better than 1 meter.
- (5) Verification of accuracy to better than one meter is beyond the scope of this study; the major limitations on further error reduction are tracking errors and geoid location errors.
- (6) The principal sources of error in verification are identified as follows:
  - a. Tracking accuracy.
  - b. Tracking station location.
  - c. Time synchronization between tracking stations.
  - d. Geoid location relative to the Ellipsoid.
  - e. Location of IMSL (Instantaneous Mean Sea Level) relative to the Geoid or to the Ellipsoid.
- (7) The primary geographic area for performing the Verification Experiment is the Caribbean Sea; secondary is the Hawaiian region.
- (8) Four categories of verification (absolute, relative, differential and self-consistent) should be incorporated in the Verification Experiment, with cross-checking by using more than one where feasible.
- (9) The ocean surface wave spectrum cannot be fully described with currently available and operational instrumentation. A spectral description of the ocean surface is necessary for verification.
- (10) If the altimeter is designed to collect design data, then the assumed power limitation of 25 watts will be exceeded both in the altimeter and in the design data modes of operation. STADAN telemetry capability is adequate.
- (11) The coordination and processing of data to perform verification requires the development of new data processing software.

## Recommendations

- (1) An Implementation Plan should be initiated immediately to develop the specifics of the Verification Experiment.
- (2) Some modifications should be made to existing operational facilities to upgrade performance to a level acceptable for verification (enumerated in Section 1.4.1).
- (3) An early determination should be made as to extent of Design Data capability to be included and whether it can be accommodated on board GEOS-C. This will have a direct impact on the GEOS-C radar altimeter design.
- (4) Planning should include use of the best available instrumentation for ocean surface wave spectrum. This includes evaluation of the combination of laser profilometer, Stilwell photography, and techniques for measurement of capillary ocean waves.
- (5) An aircraft should be flown over the satellite ground track to obtain Design Data and Ocean Truth simultaneously with Design Data from the GEOS-C satellite.
- (6) A software and data processing study should be implemented immediately to provide the necessary support to the Verification Experiment.
- (7) An early study should investigate the design and use in conjunction with the altimeter of surface-based transponders to perform self-verification.
- (8) An early study should investigate the use of receiver/clocks for supporting verification.
- (9) An Aircraft Experiment Program and the GEOS-B program should include a phase to test simulation of the verification categories (e.g., Differential over the Puerto Rico trench).



## SECTION 2. BACKGROUND

When plans for a NASA GEOS-C Radar Altimeter Experiment were announced in 1969<sup>1</sup>, it was apparent that some way of verifying the performance of the altimeter on the satellite would be required. The altimeter would be providing measurements of the satellite's height above the ocean. But there should also be another measurement of the satellite's height made by an independent system so that the satellite altimeter's performance could be evaluated. This led to the study of a Verification Experiment.

### 2.1 Ground Rules for the Verification Experiment Design Study

The radar altimeter whose performance is to be verified will be flown aboard the GEOS-C satellite. For purposes of this study, some assumptions pertaining to both the satellite and the altimeter were expressed as constraints. They are reviewed in detail in Appendix M. Briefly, however, they are as follows.

It is assumed that the satellite will be in a 600 mile by 850 mile orbit for two years, with the inclination of the orbit at 20°. The satellite is assumed to have a communications and tracking network similar to that available to GEOS-B, and much of the on-board instrumentation will be similar to that aboard GEOS-B. It is assumed that a clock will be available, and that the satellite will be attitude-stabilized with respect to the vertical to within  $\pm 2^\circ$ .

For purposes of this study, the radar altimeter is assumed to measure with an accuracy of 5 meters, with a resolution of readout of 1 meter. It is expected to have a useful life of 200 to 500 hours. An average power of 25 watts is assumed to be available to the radar altimeter, and the peak radiated power is assumed to be 5 kilowatts.

These are some of the more explicit constraints. In addition, there are some implicit constraints, such as time, equipment, money, geographical regions, additional equipment, and details of the orbit. All have implications on the design and conduct of the verification experiment, and therefore require careful consideration.

It is likely that some of the constraints will change between the time of this study and the launching of GEOS-C. If so, the implications of the change in constraints must be reviewed for the effect on verification.

## 2.2 VEDS Radar Altimeter Model

The Satellite Radar Altimeter to be flown on GEOS-C has not been built, nor even designed. Yet the purpose of the study is to verify the performance of the GEOS-C Satellite Radar Altimeter. Accordingly, an early portion of the study was devoted to formulating a model for the instrument to be used for purposes of this study.

The VEDS Radar Altimeter Model was based on many earlier study efforts of a satellite altimeter, including efforts at NASA, C&S, Geonautics, Raytheon, G.E., APL, RTI, University of Kansas, NYU and others. The model was intended to be general enough to preclude orientation toward a specific altimeter design, yet specific enough to provide a meaningful instrument concept for purposes of this study.

The radar altimeter for GEOS-C will have two functions. First, it is to measure altitude. Second, it is to provide data to aid in the development of altimeters of higher accuracy.

The initial characteristics of the VEDS radar altimeter model were as shown in Table 2-1. A simplified block diagram is shown in Figure 2-1.

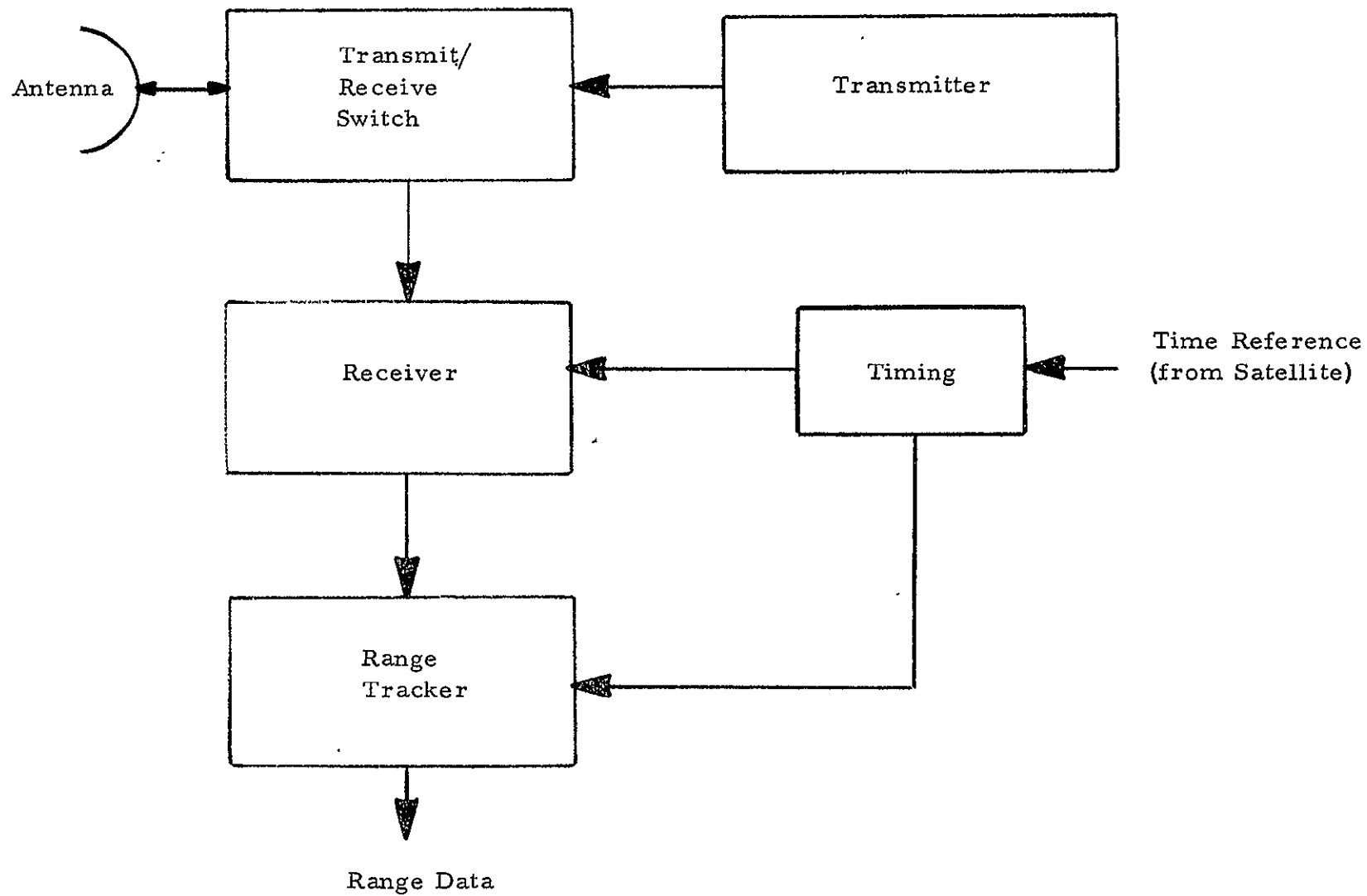


Figure 2-1. Radar Altimeter Model Simplified Block Diagram

Table 2-1. VEDS Radar Altimeter Characteristics

Weight of Electronics	20 lbs
Size of Electronics	620 cubic inches
Weight of Antenna	5 lbs.
Size of Antenna	2 feet in diameter
Transmitter Tube Life	200 - 500 hours
Prime Power	25 watts
Maximum Peak Power	5 kw
Readout Resolution	1 meter
Altitude Accuracy	5 meters
Altitude Ambiguity	1000 meters

However, as the study progressed, it became apparent that the initial characteristics would have to change if the function of providing design data were to be included along with the altitude measuring function. The final radar altimeter model resulting from this study is described in detail in Section 7.

### 2.3 Role of VEDS in the GEOS-C Program

The present study is an element in the planning for the GEOS-C Program. Proper utilization of the satellite requires not only that the satellite, its sensors and the launch vehicle be on schedule, but also that all the support be on schedule. The support includes provisions for verification and for the collection of design data.

Verification is needed to check the altitude measurement capability of the GEOS-C altimeter independently of the altimeter itself. These independent determinations will provide the basis for evaluating the performance of the altimeter.

The design data function of the GEOS-C altimeter will be to provide data to aid in the development of altimeters of higher accuracy, such as the altimeter for SEA SAT-A. In addition to answering some of the design questions directly, the design data from GEOS-C will be used to establish a correlation at satellite altitude with the data from the Aircraft Experiment Program (NASW-1932).

The major contribution of this study to the GEOS-C Program is to define the verification problem and to delineate a number of ways in which the Verification Experiment can be performed. This study does not make the choice of which specific methods should be implemented, nor does it provide a final detailed experimental plan; these are beyond the scope of the present study.

It is clear from this study that a decision is needed on which methods should be planned in detail and implemented. It is necessary to make such a commitment well in advance of the GEOS-C launch date to allow sufficient lead time for the extensive planning required. Among the considerations imparting a sense of urgency are the need for considerable interagency cooperation, the requirement for the development and acquisition of hardware and software to satisfy requirements of the verification experiment, and the possible requirement of some auxiliary field measurements and deployment of field measurement instruments.

## SECTION 3. APPROACHES TO VERIFICATION

### 3.1 Definition of the Problem of Verification

When dealing with a simple problem of verification in which we have complete control of the experiment's variables, we can devise a correspondingly simple, short, and straightforward experiment. This would be the case if we were, for example, engaged in verifying in a laboratory the length of a measuring tape, or the readings of a pyrometer, or the geometric fidelity of an optical image. Verification of the performance of a satellite altimeter is defined to mean confirmation of the ability to measure to within specified limits. This is not a simple problem; there is no readily accessible standard with which the altimeter's height can be compared. Furthermore, the environment in which the measurements will be made is entirely uncontrollable, and the times and places at which measurements may be made are limited.

What does the altimeter measure? The radar altimeter transmits pulses of electromagnetic radiation and receives the echoes from the ocean surface. It measures the time interval between the transmission and reception of the signal (pulse) and converts the time interval into a distance measurement. This is a measure of the altitude from the satellite to the ocean surface. But the relation between the measurement and the quantity being measured is not a priori clear. The radar manufacturer is assumed to claim that the altimeter measures the distance to some easily definable location on the ocean surface, identifiable to the radar and identifiable to the user of the radar altimeter. The surface assumed for this purpose is the instantaneous mean sea level (IMSL), defined in Appendix N, which is a momentary average height of the ocean over a specified area. (See Figure 3-1).

The problem of verification is then to verify how well the radar altitude measurement,  $H_r$ , compares with  $H_1$ .

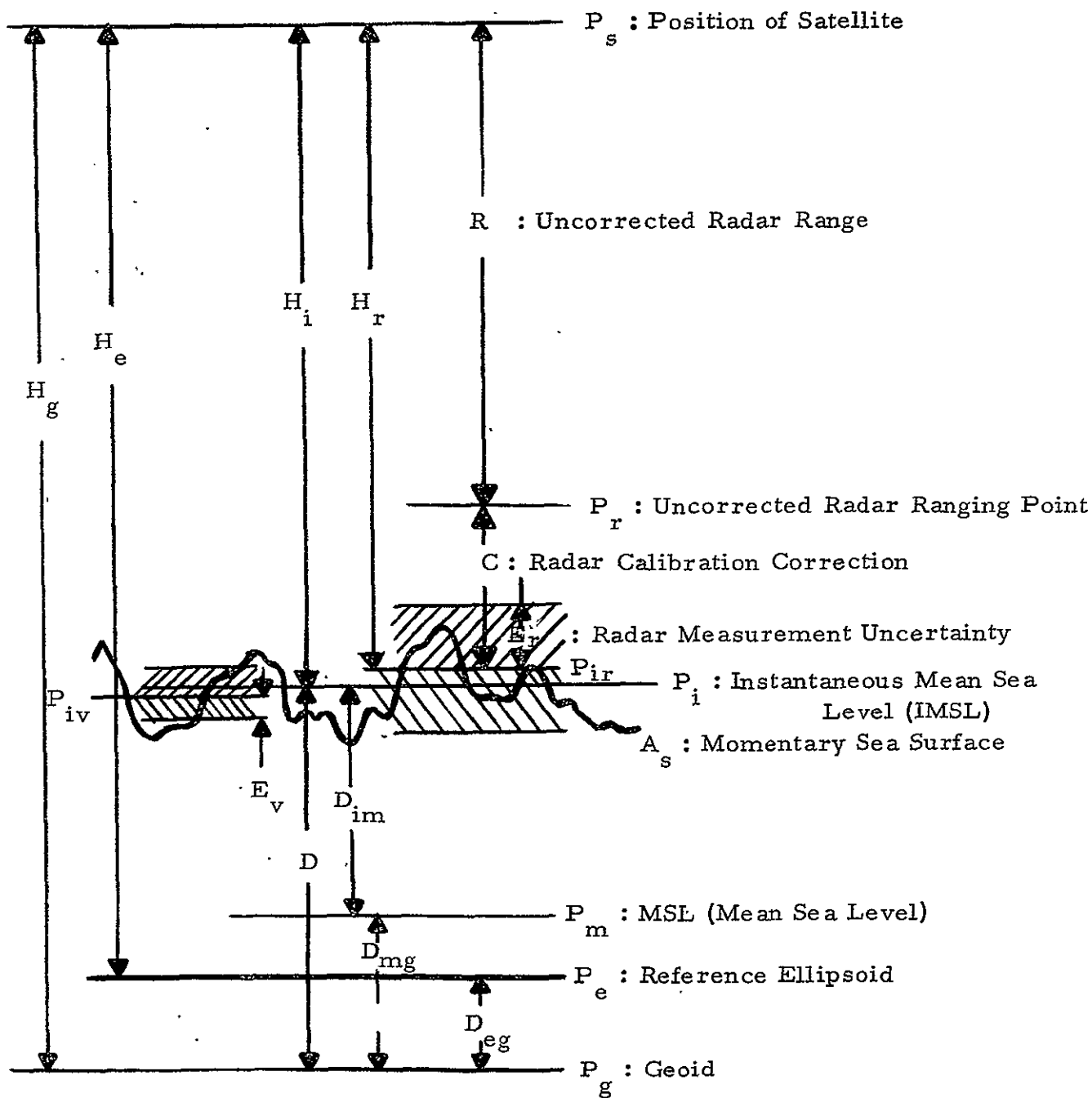


Figure 3-1. VEDS Geometry

### 3.2 Classification of Verification Methods

The verification methods considered may be conveniently classified into two types (see Table 3-1): (a) accuracy verification, which concerns the measurement of the total distance between the satellite altimeter and the subsatellite ocean surface (Instantaneous Mean Sea Level); (b) precision verification, which concerns comparison between altimeter measurements over either the same or nearby locations.

Considering the first (accuracy) type of verification (see Figure 3-2) distinction is made between (a) absolute verification, in which both satellite altimeter position and subsatellite ocean surface are measured with respect to a pre-established spheroid, and (b) relative verification, in which a range measurement is made (independently of the altimetry) between the satellite altimeter and the subsatellite ocean surface. The relative measurements are made substantially directly, without reference to a spheroid.

In precision verification, two categories are considered (Figure 3-2): (a) differential verification in which changes in known ocean surface topography may be correlated with changes in altimeter measurements; and (b) self-consistent verification, in which substantially the same measurement is repeated over the same location at different times (in different orbits).

### 3.3 Calibration and Verification

We consider two approaches to calibration and verification. First, we consider an approach in which calibration and verification are kept separate and distinct. The radar altimeter manufacturer makes a calibration prior to the delivery to the user. Instructions are included which instruct the user how to convert the raw data coming out of the instrument into corrected measurements which the manufacturer claims will meet specifications,



Table 3-1. Verification Methods

<u>Type of Verification</u>	<u>Category</u>	<u>Measurement Comparison</u>
Accuracy	Absolute	Measure satellite position and Instantaneous Sea Level with respect to established coordinates
	Relative	Measure satellite position relative to Instantaneous Sea Level by independent means
Precision	Differential	Measure changes in satellite position and in Instantaneous Sea Level to determine change in altitude
	Self-Consistent	Repeat altimeter measurement at same location at different times, knowing satellite position

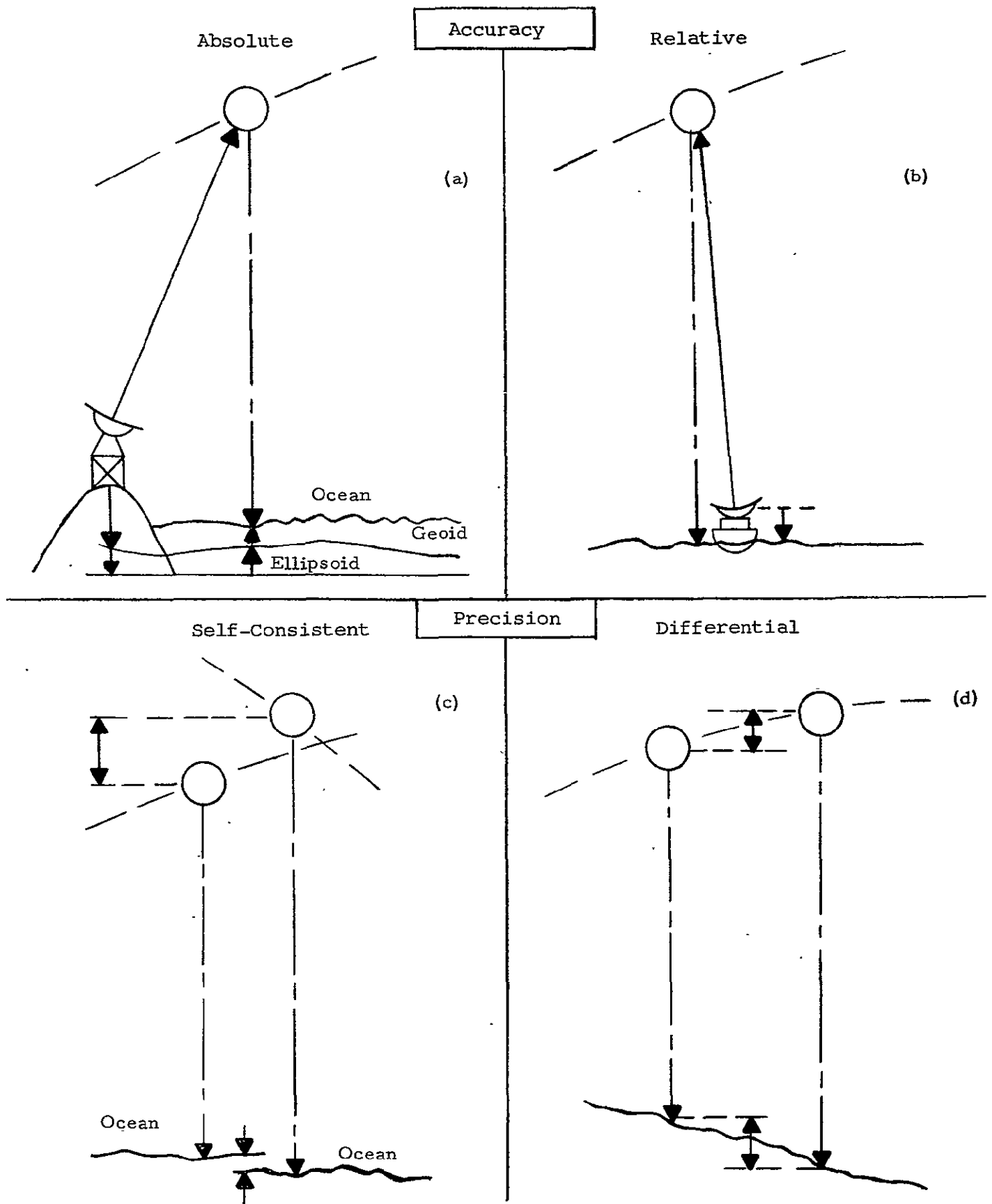


Figure 3-2. Verification Categories

in this case,  $\pm 5$  meters. In principle, the verifier is not concerned with how measurements are made but only with an independent check on the measurements. In practice the verifier is also intimately concerned with the operation of the instrument, the principal reason being that it indicates the set of experimental operating conditions under which it is necessary to perform the verification.

In the case of the radar altimeter instrument under consideration, the manufacturer's calibration is most likely to be performed in flight. Calibration is not distinguishable from verification in methodology. However, use of the same measurements for both calibration and verification would lead to truisms and verify nothing. One must, therefore, assume that some time will be spent on calibration and other time on verification. It is perfectly reasonable to inter-twine the two in time providing the same data are not used for both.

An alternate approach to calibration and verification does not keep them as separated as that of the preceding paragraph, but considers the calibration and verification to be different mathematical aspects of the same procedure. In particular, a precision verification is a measure of the narrowness of the distribution curve of the results; that is, of the spread or rms error in the results. On the other hand, some constant (or bias) terms are considered part of the calibration and some part of the accuracy verification. In this approach, clear separation is not warranted between applicability of data for calibration or for verification.

Whichever of these two concepts of calibration and verification are used, the result must be an honest evaluation of the performance of the instrument.

## SECTION 4. ABSOLUTE VERIFICATION

### 4.1 Summary and Conclusions

Absolute verification derives an altitude for comparison with the altimeter-measured altitude by computing independently of each other the altimeter location at the instant of measurement and the shape of the instantaneous mean sea surface at that instant. Both location and shape are determined in the same absolute system of reference, i. e., a system that is independent of the altimeter location and the shape of the sea surface.

A careful evaluation of the characteristics of possible regions throughout the world where experiments in the absolute and other categories might be made, led to the selection of the Caribbean Sea and contiguous water areas as a choice for region where most work should be done and of a small portion of the Pacific Ocean just south of Hawaii (island) as a region where experiments should be made but on a smaller scale of effort. The process of selection of the sites involved making gross estimates of the errors that would result if the experiments were carried out there, but after selection more detailed error analyses were made.

The sizes of the errors of the altitudes computed for comparison with measured altitudes lie in the range 1 meter to 55 meters. They depend on the locality of the experiment, the time of the experiment, the method of data reduction, and other factors. This wide range can be broken down into a set of narrower ranges by using the concept of "performance levels" as shown in Table 4-1. The range of errors (r.m.s.) at the operational level is then from 15 to 55 meters, at the capable level from 2 to 20 meters and, at the feasible level, from 1 to 2 meters.\*

---

\* The error analysis in the following text was made before introduction of "performance levels" and some of the error size values given in this paragraph and in Table 4-1 are not supported by the same careful analysis as are the others, but must be considered plausible estimates.

Table 4-1. Summary of R.M.S. Errors<sup>(a)</sup>  
In Verification Experiments (Absolute Category)

Performance Level (b)	Ground Tracking	R.M.S. ERROR (Meters)		Altitude Above Ellipsoid
		Atmospheric Correction*	Station Instrument Location Horiz/Vert.	
OPERATIONAL (c)	15 - 25	1	1-10/1-50	15-55
CAPABLE (d)	1 - 5**	1	1-3 /1-3	2-6
FEASIBLE (e)	0.5 - 2	0.5	1-2 /1-2	1-2
* See Appendix Q ** (Ref.): Anonymous: AFETR Plan for Use of Calibration Satellite for Calibration and Evaluation of Range Instrumentation. Pan American World Airways, Guided Missile Range Division, Patrick AFB, Fla., 15 Dec. 1965.				

Performance Level	Altitude Above Ellipsoid	R.M.S. ERROR (Meters)		Altitude Above IMS Surface
		Geoid Above Ellipsoid	IMSL (Above Geoid)	
OPERATIONAL	15 - 55	1 - 50	2	15 - 55
CAPABLE	2 - 6	1 - 20	1	2 - 20
FEASIBLE	1 - 2	1 - 2	0.5	1 - 2

NOTES:

- (a) See footnote, Section 4.1. Use of the term "r.m.s. error" implies they are the result of a more detailed and reliable analysis than was actually provided for most of them, but it is hoped that the values given do not differ too much from those that a more detailed analysis would have provided.
- (b) The difference between the definitions for the performance levels given below (c, d, e) and those used in Section 1 should not be sufficient to affect the numerical results.

- (c) The operational performance level is the quality (measured as r.m.s. error) of performance to be expected from a given system if it continues operating exactly in the manner in which it was believed to be operating in Aug. 1969 (This date is chosen because the r.m.s. errors given here and in other sections of the report are based on data gathered earlier than that date). This definition differs from that given in Section 1 previously, but the difference is, I hope, verbal; it should not make any difference to the numbers; it is given to allow a more definite scheme by which errors are assigned. The "system" referred to includes all the (world-wide) electronic and optical tracking systems operating up to and on the given date and tracking satellites of the GEOS-A and GEOS-B type. It includes all personnel and equipment involved in the tracking, communications, and data reduction, as well as the operations and programs actually being used for data reduction. It does not include the GEOS-C satellite and altimeter, of course, and a satellite of the GEOS-B type in the orbit specified for GEOS-C must be assumed. A number of other assumptions are implicit in the evaluation but are for brevity not stated.
- (d) The "capable" performance level of a system is here defined to be that level at which one could reasonably expect the system to be operating on a date 1 week after launch of the GEOS-C satellite containing an altimeter. This implies the functioning (at the August, 1969 level) of all tracking stations operating in August 1969 with the same level of personnel and equipment and the functioning of such other stations and personnel as were operating in the past, were not operating in August, 1969, and be put into operation by NASA or other responsible organizations. It also implies the use of such equations and computer programs as may be required for reduction of the data, provided such equations were in existence in August 1969 or could result by minor modification of the existing equations and programs. It implies, furthermore, that all tracking instruments are located at sites that have been surveyed to the same level of accuracy as similar instruments were located in August 1969, and that relevant geodetic and oceanographic data existing on in August, 1969 have been collected and put in usable form. Existence of GEOS-C is of course implicit in the definition. It is also implied that in the reduction of the data, measurements of range, etc., will be introduced with their proper weights.
- (e) The "feasible" performance level is that level of performance of a system which could be attained by a system operating two years after the successful launch of a GEOS-C satellite containing an altimeter if, at the date of launch, the system was the best possible within the limitations of technology, money available, time available, etc. For the system under consideration this implies (1) all tracking instruments operating at the same or better level as the best of those operating in August, 1969; (2) modification of tracking instruments to ensure (1) if necessary; (3) emplacement of tracking instruments on such sites as necessary to provide good geometry and full coverage; (4) use of equations and programs designed to make best use of data.

The percent of the total Caribbean in which the total error in altitude verification is less than 6 meters is listed in Table 4-1A, and shown geographically in Figure 4-1A, for each performance level.

The principal advantages of experiments of the absolute type are:

- (1) as a by-product, they are directly related to phenomena of geodetic and oceanographic importance;
- (2) they require no knowledge of or assumptions about the functioning of the altimeter;
- (3) they provide more information per unit cost than other types;
- (4) they have minimal involvement of other types of equipment as reference standards.

The principal disadvantages of experiments of the absolute type are:

- (1) the number of factors that must be considered and the amount of computation required are considerably larger than for other types, with the consequent increased chance of undetected errors being introduced;
- (2) some of the component factors have associated errors that vary considerably with the geographic locale of the experiment (geoid-spheroid separation, for example) or other experiment parameters, thus restricting at present the areas and times where experiments can be made;
- (3) the effort involved in reducing the errors inherent in experiments of the absolute type increases more rapidly as a function of error size than does the effort needed to reduce errors in other types of experiments.

Table 4-1A. Percent of Caribbean with Error Less than 6 Meters\*

Performance Level**	Percent of Caribbean with Error Less than 6 Meters*	Notes
OPERATIONAL	<10	Assumes that stations at Grand Turk, Antigua, and Bermuda have total r.m.s. error of less than $\pm 5$ meters. Land probably occupies about 40% of this area, so usable area is <6%.
CAPABLE	<60	Assuming that all stations concerned have systematic errors <5 m. and random errors <1 meter. Assuming that C&GS and Lamont gravity data are made available.
FEASIBLE	>97	Small area just off Yucatan omitted.
<p>* Percent of area of total Caribbean in which the total error (altitude above IMA surface) is less than 6 meters.</p> <p>** See description of performance levels in footnotes to Table 4-1.</p>		



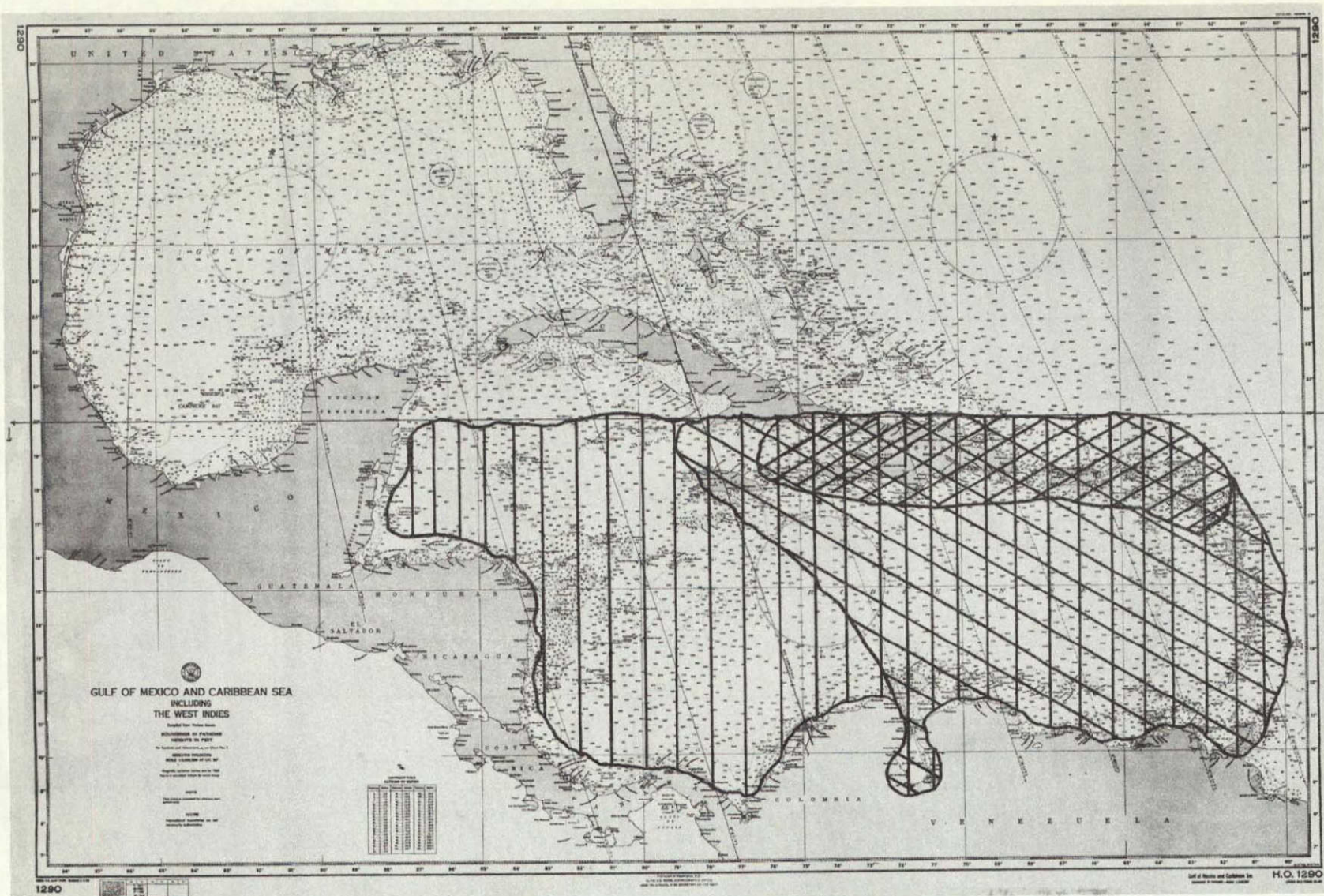


Figure 4-1A. Percent of area of total Caribbean in which total error is less than 6 meters. (See relevant footnotes to Table 4-1)  
(a) Operational: <10% [Cross-hatch pattern]; (b) Capable: <60% [Diagonal line pattern]; (c) Feasible: >97% [Vertical line pattern]

## 4.2 Description of Absolute Verification

### 4.2.1 Absolute Verification Concept

Verification is the process of showing that some theory is or does what it is supposed to be or do. The thing may be a number, a process, an instrument, or a person. We can do the verification by comparing the given number, etc., directly with the supposedly correct value (called the standard), or indirectly by going through a chain of sub-standards, or negatively by showing that the hypothesis, that it disagrees with the standard by more than allowed, is false. In the present case, we hope to verify the performance of an altimeter by comparing it with a standard. Since no standard altitudes between 1100 km and 1400 km exist at present, the comparison must be indirect (compare, however, the discussion in Section 5, on relative types of experiments). It will be made by computing comparison altitudes from data whose errors are known and small enough in size to give computed total error size within the allowed limits ( $\pm 5$  meters). For convenience, the data used will be referred to as a coordinate system which is absolute - that is, independent of any assumptions regarding the location of the altimeter, its motion, the size and shape of the earth and its oceans, etc. The verification experiment is then said to be in the "absolute" category. Figure 4-1 suggests the physical situation involved, and Figures 4-2 and 4-3 give a more detailed schematic picture of the numerical relationships involved.

Primary data are:

- (1) locations of the tracking instruments, in the absolute reference system;
- (2) coordinates of the satellite in the tracking instrument coordinate system (as range, velocity radially from the station, right ascension and/or declination, etc.), including time;
- (3) coordinates of the reference ellipsoid in the absolute reference system;
- (4) height of the geoid above the ellipsoid;
- (5) height of mean sea-surface above the geoid (mean sea level);
- (6) height of the instantaneous mean sea surface above the mean sea surface (instantaneous mean sea level or IMSL is this height plus the preceding).

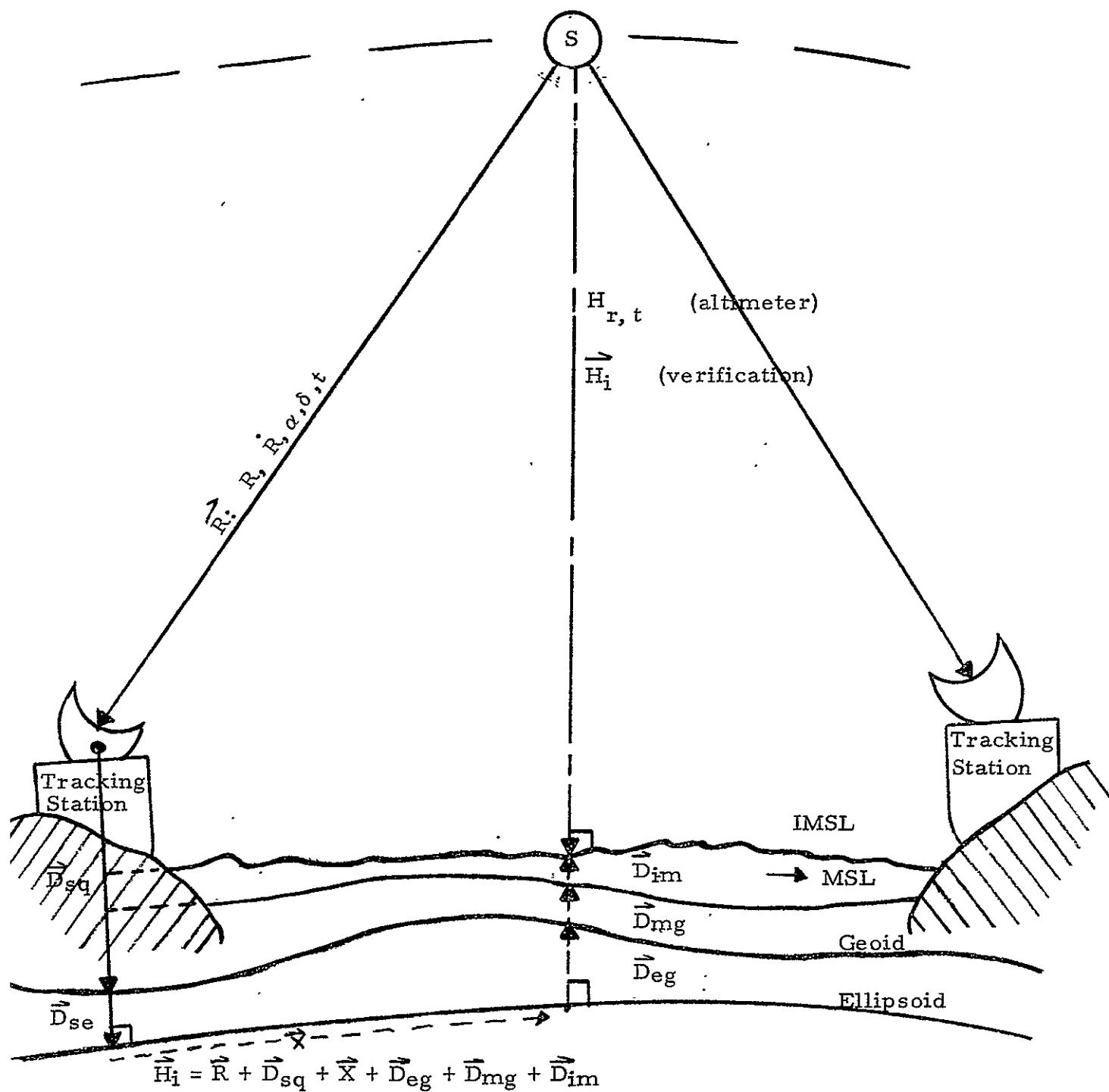


Figure 4-1. Absolute Verification Geometry

Satellite tracking station locations are combined with tracking station measurements, using auxiliary data on ionosphere electron density, troposphere temperature, density, and humidity, tracking instrument corrections, transponder (and similar corrections) etc. and using suitable orbital constraints, to compute altimeter location (in the absolute system) as a function of time. At the same time, or at least independently of the satellite computation procedure, geoid-above-ellipsoid data are collected or computed from other data and converted to the absolute reference system selected. Mean sea level is computed and added to the geoid-above-spheroid separation. It is convenient, although not necessary, to compute from the satellite locations at times of measurements the approximate horizontal coordinates of the footpoint of the altimeter on the mean sea surface (or on the spheroid, at this stage). A circular area approximately 3.5 km in radius about this point returns to the altimeter that part of the pulsed radiation that is used for altitude measurement. Within this area, therefore, the effects of tide, air pressure, wind waves, etc., are added together to give the height of the instantaneous mean sea surface above mean sea level, and all these various heights from the ellipsoid on out are added together (possibly with corrections for different directions, although such corrections are utterly too small to be significant at present) to give, within the limited area under the satellite, the height of the instantaneous mean sea surface above the ellipsoid. It is now a simple matter to compute, from the altimeter coordinates and the instantaneous mean sea surface heights, the actual horizontal coordinates of the satellite foot point on that surface and to make suitable corrections (which will be negligible most of the time). A block diagram of the computational procedure is shown in Figure 4-2.

To carry out an absolute procedure, we have to be able to locate in an absolute system (1) the altimeter and (2) its foot point on the IMSL surface. Because the second requirement is the more restrictive, we consider it first.

#### 4.2.2 Location of Instantaneous Mean Sea Level (IMSL)\*

We are concerned with IMSL and the associated surface not because it is important to the geodesist or oceanographer but because it is a visualizable surface that the radar engineer thinks he can connect to the altimeter readings

---

\* See also Appendix S.

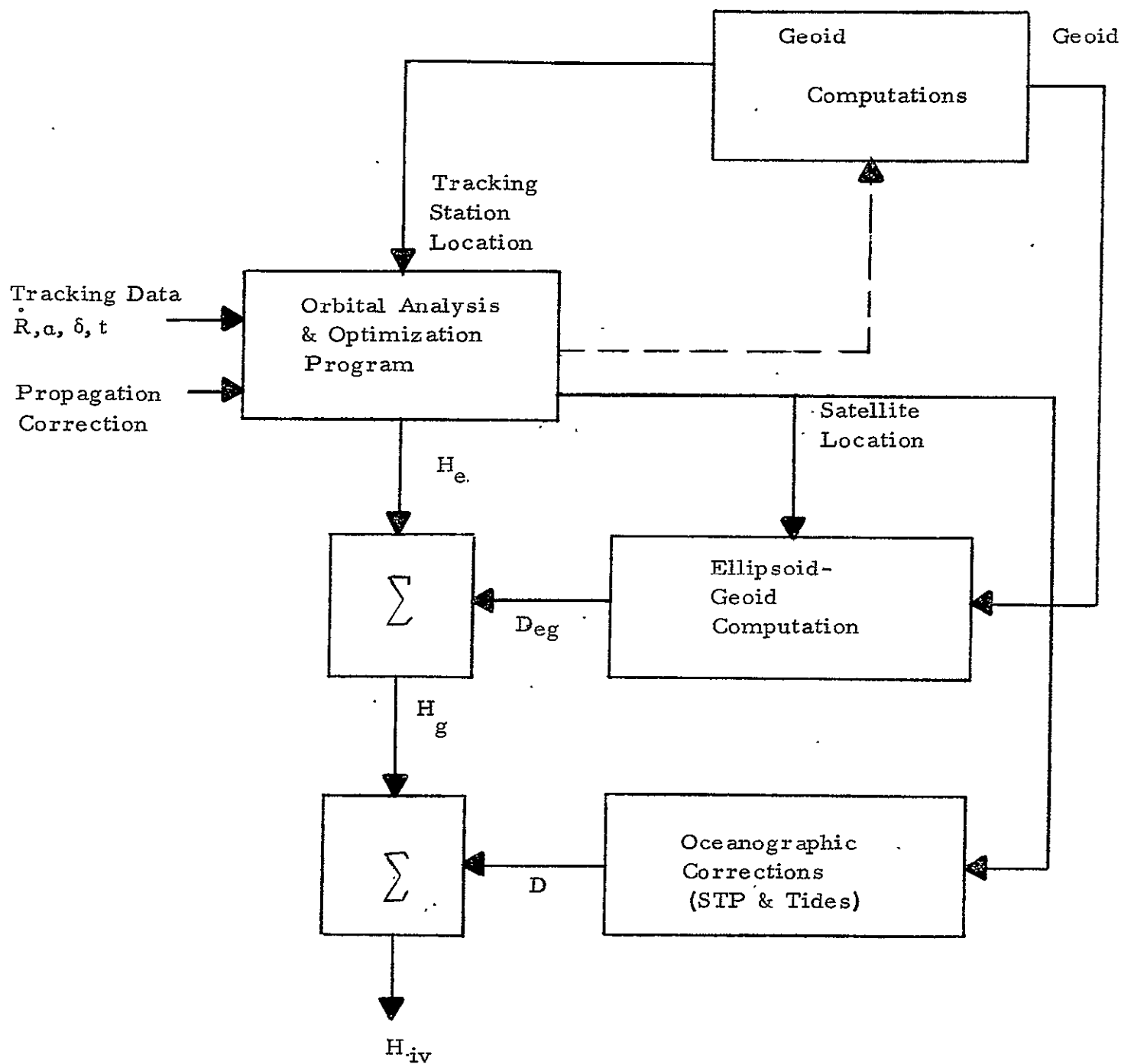


Figure 4-2. Absolute Verification Block Diagram

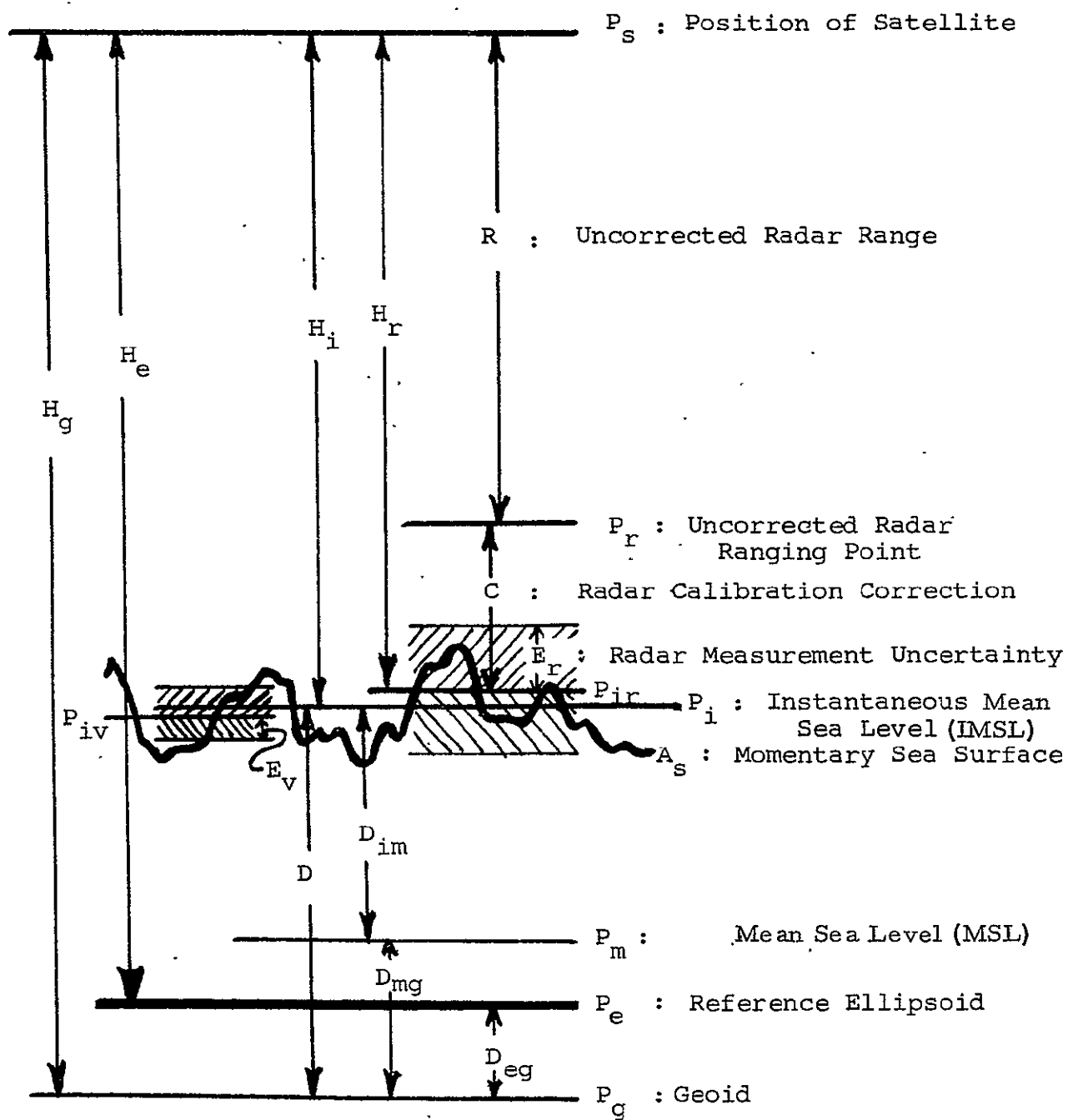


Figure 4-3. VEDS Geometry



(not measurements). Since the radar engineer could have dragged in a hypothetical surface even less remotely connected to the physical world, we should not complain too much about the difficulties in locating the IMSL by some means other than radar.

Accepting IMSL surface as the surface to which radar measurements refer, we look for ways of locating it. The definition requires that the instantaneous sea surface be known at the instant for which a distance measurement is given, since otherwise we cannot average over the surface. If we assume that the maximum rate of change of sea level with respect to IMSL surface is 10 m/sec. (gravity waves), then a change of 1 meter can take place in 0.1 sec. We would therefore have to catch the ocean surface within an interval of 0.1 sec. of the measurement time to avoid getting an error of more than 1 meter in sea level. Such a requirement cannot be met. Even if it were possible to photograph the ocean surface adequately from airplanes at the time of measurement, the airplanes would prevent the altimeter from getting a true value for IMSL. With fewer airplanes, we would interfere less with the altimeter but we would get less adequate pictures of the sea surface.

To get over this difficulty, we assume that IMSL is not really sensitive to changes in instantaneous sea level. Again, this invokes that powerful scientific ju-ju, ergodicity. The integral

$$\overline{H}(t) = \frac{1}{S} \int_S H_{SL}(\vec{r}, t) dS$$

is set approximately equal to

$$\overline{H}(r) = \frac{1}{T} \int_t H_{SL}(\vec{r}, t) dt.$$

This is an assumption, necessary but reasonable, and making it we can send out airplanes into the area S at convenient times before (and/or after also, preferably) distance measurement. In fact, if we push this assumption to its logical conclusion, we can send in only one airplane, which can fly as low as it pleases to pick up minute ocean wave detail, or we can dispense with the airplane entirely by waiting for a quiet day and then measuring IMSL. The

latter conclusion of course sets the radar engineer into gyrations, since he has been insisting all along that he doesn't know how waves are going to affect his results. How did he get himself impaled on both horns of the dilemma at once? Logically, we sat him there when we allowed time averages to substitute for area averages. But the time-averaging is perfectly reasonable from a physical point of view, so that we must assign his trouble to his own insistence on the IMSL as being what the altimeter measures. We must therefore be completely honest and admit that, at the present moment, we do not know if IMSL is the proper surface for the radar engineer to choose or not. If it is, then we, the verifiers, need only carry out a few experiments to verify the ergodicity of the surface to within a few decimeters (which is perfectly adequate error for GEOS-C altimeter verification). If it is not, this implies that either the radar engineer has been unable to calibrate the altimeter to measure IMSL or that our assumption that the IMSL is close to the time averages SL is wrong.

In summary, then, we state the procedure for finding by an absolute procedure, altimeter height above IMSL as follows.

1. Location of the altimeter in the absolute system is gotten from a combination of tracking data with satellite orbit theory. The methods for doing this as used in the experiment are a minor modification of well-known and tested methods.
2. Location of the altimeter foot point on the IMSL surface proceeds in stages.
  - a. First, the International Spheroid is defined in the same coordinate system as that used for locating the altimeter. The spheroid equation

$$\sum a_{ij} x^i x^j = 0 \quad i, j = 0, 1, 2$$

relates the spheroid directly to the  $x^i$ -system in which the altimeter moves; geodetic or spheroidocentric coordinates are more convenient and will be used instead since the transformation from one kind to the other is easy to make.



- b. From available survey, astrogeodetic, gravity, and satellite data (including non-altimetric data from the altimeter satellite itself) the geoid is mapped with respect to the spheroid in the area of our experiment.
- c. From available data on ocean currents, salinity, temperature, pressure and meteorological conditions, the mean sea level surface is mapped with respect to the geoid.
- d. From available data on tides and seiches, the "quiet" sea surface is mapped with respect to the mean sea level surface at the instants of time at which the height measurements are given.
- e. The last stage would be the mapping of the instantaneous sea surface on the quiet sea surface and the mapping therefore of the IMSL with respect to the quiet sea surface. There are no data which give this other than data gathered at the spot at the instant corresponding to the height measurement. We therefore either have to map, at considerable expense, the instantaneous sea surface during the experiment and derive IMSL from it or to measure some other quantities that will differ (we hope) insignificantly from IMSL. Methods for carrying out the former alternative are discussed in Appendix O; some of those for carrying out the second were discussed in a preceding paragraph. In either case, we have at least defined the problem and found methods of solving it, so that for the time being we take the possibility of the last stage as established.

3. Finally, we compute by straightforward mathematical means the distance from the point

$$P_S (x_m^1, x_m^2, x_m^3)$$

at which the altimeter is located to the surface (IMSL surface) which existed at that instant  $I_m$  at which the altimeter was at point  $P_S$  and made the height measurement  $h_m$ . The surface  $S$  is at a constant height above the spheroid and can with negligible error be assumed to be a section of a spheroid homothetic to our reference spheroid; the formula for the distance from an external point to a spheroid is well known, is given in elementary analytic geometry texts, and has been programmed for computation.

#### 4.2.3 Location of Altimeter

Primary data that go into the determination of altimeter location are (1) the locations, in various reference systems, of the instruments that provide ranges to and/or directions to and/or velocity components of the altimeter, and (2) the measurements of these coordinates (range, etc.). Auxiliary data are (i) instrument calibration constants, (2) troposphere and ionosphere characteristics that affect the measurements, and (3) reliable values for the Earth's gravity field as far as it affects the altimeter motion.

It is possible to derive the altimeter location in a series of steps, as was done in deriving the location of the instantaneous mean sea surface. The first step would be conversion of the given tracking instrument coordinates from their various reference systems to the absolute reference system. Some of the instruments use several sets of coordinates, corresponding to their location simultaneously in different coordinate systems. This is the situation, for example, of the tracking instruments at Cape Canaveral, which have coordinates derived by the usual triangulation and leveling procedures, as well as coordinates derived by several different satellite tracking methods. Existence of these several sets of coordinates implies that the final single set of coordinates for each such instrument in the absolute reference system will have a smaller r.m.s. error ellipsoid than any one of the parent sets has. Note that

to some extent this step is actually contained within the first and second steps of the IMSL-derivation process (Section 4.2.2) and could be made along with the IMSL-derivation.

The second step is combination of the measurements made by the various tracking instruments with the tracking instruments' coordinates and with each other. Each measurement made by a tracking instrument is a coordinate of the target in a coordinate system peculiar to the tracking instrument. Conversion of the measurement coordinates to absolute reference system coordinates produces observation equations containing the reference system coordinates as variables. Combination of the observation equations from the different instruments for the same times yields values for the variables; i.e., locations for the altimeter. The third step is to introduce condition equations that will allow use of observation equations for different tracking instruments at different times. These condition equations are the equations of motion of the altimeter. The equations of motion restrict the allowable variation in altimeter location from instant to instant and connect observations made at different times.

While the step-by-step approach just described is adequate and desirable for initial stages of the verification experiment, it has the drawback that it does not make full use of the information available. The constraints placed by the orbital conditions on the measurements and, through the measurements, on the station locations are so strong, even over "short" segments of the orbit, that they can and should be used to improve the tracking instrument locations and reduced measurements. This improvement is best achieved by adjusting all unknowns together (but not necessarily all data simultaneously). A sequential analysis procedure, while not as efficient theoretically as a complete, simultaneous reduction procedure, combines most of the desirable features of the step-by-step and simultaneous procedure, as is therefore recommended for use after less powerful but more rapid analyses have shown that the data being accumulated are of satisfactory quality.

#### 4.3 Regions for Absolute Verification

Verification experiments in an absolute system must be carried out in regions where computation can be accurately made of (a) altimeter location, (b) the spheroid, (c) the geoid, (d) mean sea level and (e) IMSL. It must also be feasible to make those measurements from which IMSL is computed: measurements that map the instantaneous sea surface or measurements that, by time-averaging, lead to an IMSL approximation. In practical terms, consideration is given to regions where there are many tracking stations of high accuracy, where the geoid is well known, and where many observations have been made of ocean characteristics. A survey of data on these matters shows that there is no region in the  $+20^{\circ}$  to  $-20^{\circ}$  zone which meets all the requirements completely. It also shows that there are a few regions which meet the requirements to some extent; these are:

1. Caribbean Sea\*
2. Hawaiian Islands - Johnston Island region
3. Marshall Islands
4. Persian Gulf
5. Lake Maracaibo
6. Lake Nicaragua
7. Lake Victoria
8. Lake Titicaca
9. Lake Chad
10. Indian Ocean

The dimensions and area of the regions are given in Table 4-2.

These regions have the following characteristics in common: (1) they are of adequate size to allow use of an altimeter with a 7-km diameter illumination area; (2) their surfaces are, or can easily be, located in a geodetic frame of reference; (3) with the exceptions of Lake Chad and the Marshall Islands areas, all regions are within a short distance of NASA-supported tracking stations.

---

\* For the convenience of the reader, a Bathymetric chart of the Caribbean Sea is included inside the rear cover.

Table 4-2. Principal Areas of Possible Interest to VEDS

REGION	AREA* (Sq. km)	DIMENSIONS (km) *	
		Length	Width
LAKE VICTORIA	69,900	400	240
CHAD	20,800	230	50
MARACAIBO	16,500	135	120
TITICACA	9,000	175	45
NICARAGUA	7,900	170	65
SEA CARIBBEAN	1,960,000	2,800	580
RED	417,000	1,785	260
OCEAN INDIAN	73,500,000	---	---
GULF PERSIAN	230,000	875	200

\* Mostly based on "The Times Atlas of the World", Comprehensive Edition, Houghton Mifflin Co., Boston, 1967.

They differ in ways that are quite important. Some of these are:

1. the cost of using them as experimental areas
2. the number of measurements that can be made during the altimeter lifetime
3. the accuracy with which IMSL can be measured;
4. the variety of surface conditions to be encountered

It is impractical to attempt to use all the regions intensively. One region is therefore selected as the site of primary experimentation; others are used on an "as opportunity offers" basis.

#### 4.3.1 The Caribbean Sea

The Caribbean Sea and the Gulf of Mexico are shown in Figure 4-4. The Gulf of Mexico lies for the most part above the +20° parallel and is of no concern; it is worth mentioning only because stations able to track the altimeter lie along its perimeter. The Caribbean Sea itself, together with a 200 km wide strip of the Atlantic Ocean running along the Puerto Rico-Leeward Islands coasts is selected as the primary region for making verification experiments in an absolute system. The characteristics of the region that make it desirable as a primary experimentation site are discussed in the following sections.

##### 4.3.1.1 Characteristics (Caribbean)

The Caribbean Sea, (Figure 4-4) has an area of about  $2.75 \times 10^5$  sq. km. It is about 2600 km long, from the tip of Yucatan Peninsula to the Granadine Islands, and about 1200 km wide between Cape Tiburon (Haiti) and the north-western coast of Panama. These dimensions, taken with the fact that the Caribbean includes the footpoints of the upper part of the GEOS-C orbit, lead to the conclusion that most tracks of the altimeter over the region will be along the long dimension of the Caribbean. Figure 4-5 shows the traces (locus of foot points) of a series of passes of the altimeter over the Caribbean; the traces are numbered to show the pass sequence; a similar series of passes begins about 12 hours later in time. From the dimensions of the sea and from the orbit characteristics it follows that the altimeter measuring at the rate of one measurement per second could make up to 390 measurements during the descending phase of each passage and up to 360 measurements during the ascending phase. Since the altimeter will, during a 2-year period, make approximately 800 passes in a south-to-north direction and 300 passes in a north-to-south direction over the region, the approximately  $1.8 \times 10^6$  observations that can be made (at one per second) in a 500-hour altimeter lifetime are about four times what would be made if the altimeter were always turned on while over the Caribbean.

1290

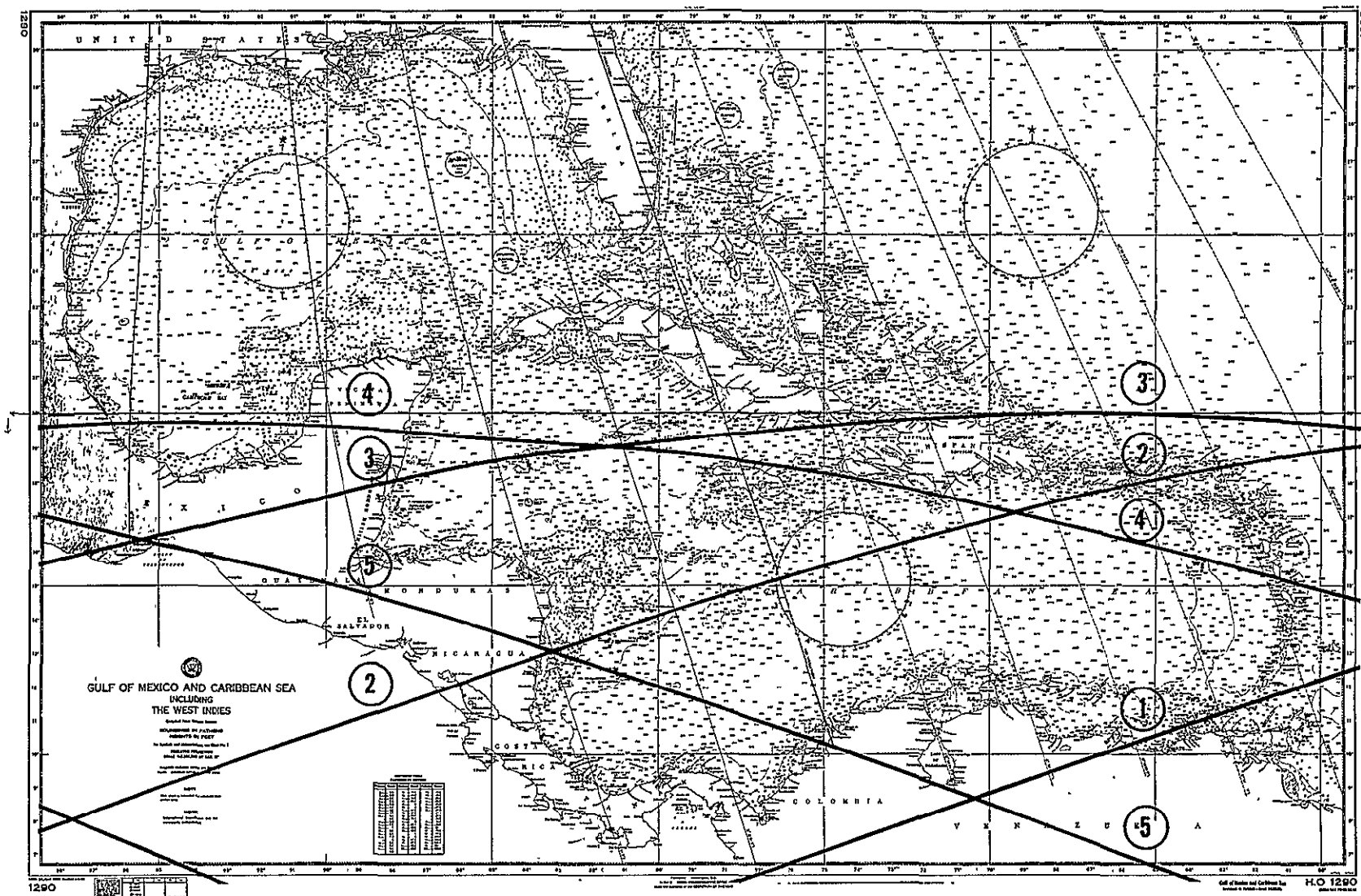


Figure 4-5. Traces of the Altimeter Orbit



Figure 4-6 shows the number of observations of salinity, temperature, and pressure (STP) made in  $5^{\circ} \times 5^{\circ}$  "squares" in the Caribbean-Gulf of Mexico region and available from the National Oceanographic Data Center<sup>4</sup>.

These data were taken at different times and under various conditions; a study of the temporal variation of the quantities represented will be necessary and, if the temporal variation is large, more data may have to be gathered to provide enough information to allow a reasonable guess at the correct time function. Figure 4-7 shows the estimated distribution of gravity data available for the area<sup>5,66,67</sup>. While the number of gravity observations in the Caribbean is considerable, many of the data are under military control or were obtained by exploratory groups for oil companies and are not readily accessible. The extent to which such restricted data will be needed cannot be determined until the totality of unrestricted information has been explored.

The astrogeodetic geoid (i.e., the geoid determined by geometric procedures from astronomic longitude and latitude measurements) has been computed for most of the perimeter of the Caribbean; the latest<sup>2</sup> computation results are shown in Figure 4-8. Note the gap in the geoid along the north coast of South America. While the gap will not make it impossible or even difficult to use the astrogeodetic geoid, a stronger solution would of course be possible if the gap could be filled in. Finally, to complete the picture on data relevant to the geoid, diagrams of the "geoid" inferred from satellite dynamics are shown in Figure 4-9. The geoid representation in Figure 4-9(a) dates from 1965<sup>6</sup>. The representation in Figure 4-9(b) is from 1969<sup>7</sup>. These two representations differ considerably (tens of meters) in detail, and only the general patterns are similar. In the small area of the Caribbean, the relative differences in geoids are also small, as comparison of the diagrams shows. In the present developmental stages of satellite geodesy, no dependence should be placed on absolute values of the satellite geoids.

Figures 4-10a and 4-10b show the amount of cloud cover to be expected in the Caribbean region in March, when cloud cover is least, and September when cloud cover is greatest. These figures are based on charts given in Berry,

21	11	18	77	16	8	55	37	42	91	605	1337	1					1873	1201	1281	351	89	101			
126		120		124		123		122		121		120		119		118		115		113		114			
16	14	9	30	16	11	17	212	123	94	349	3008	3721	42				13	95	1426	401	1007	584	36	28	
58	18	13	22	44	48	47	145	97	44	106	404	2862	1732	22		70	229	265	509	956	160	124	68	44	41
040		039		038		037		036		035		034		033		032	031	030	029	028	027	026	025	024	
9	13	18	60	606	166	60	9	12	14	9	35	228	810	230		60	119	201	727	1063	161	186	124	35	47
1	11	15	27	273	139	56	7	7	3	8	21	17	21	38	45	101	28	14	71	132	116	258	426	39	50
054		053		052		051		050		049		048		047		046	045	044	043	042	041	040	039	038	037
5	20	10	13	66	123	65	11	8		9	15	10	7	30	30	82	52	31	40	59	57	86	409	161	43
15	24	10	10	28	13	17	20	17	4	6	13	17	5	10	16	42	27	72	121	186		46	59	39	
018		017		016		015		014		013		012		011		010	009	008	007	006	005	004	003	002	001
13	24	18	16	34	19	20	58	24	5	4	13	23	5	7	12	45	34	31	76	27				15	
18	22	17	6	27	18	14	35	43	10	7	6	23	18	6	7	50	39	66	374	1					
317		316		315		314		313		312		311		310		309	308	307	306	305	304	303	302	301	
10	13	9	2	9	11	5	16	18	7		5	3	7	3	3	30	30	27	622	332					
5	14	3	5	7	11	11	16	14	3	4	2	1	14	2	1	20	20	12	48	829	1				
353		352		351		350		349		348		347		346		345	344	343	342	341	340	339	338	337	
2	3	3	5	2	7	70	13	7	7	2			2			23	24	1	7	147	268				
3	8	1	1	1	2	6	1	2				1	2			14	3	4	13	17	67				
339		338		337		336		335		334		333		332		331	330	329	328	327	326	325	324	323	
5		4		2		2	3		2			1	2	7	1	3	7		7	4	34				

Figure 4-6. Density of Oceanographic Observations (S. T. P.) in the Verification Experiment Region (Number of Observations per 5° x 5° Square).<sup>4</sup>



Figure 4-7. Regions of Substantial Gravity Data in the Caribbean

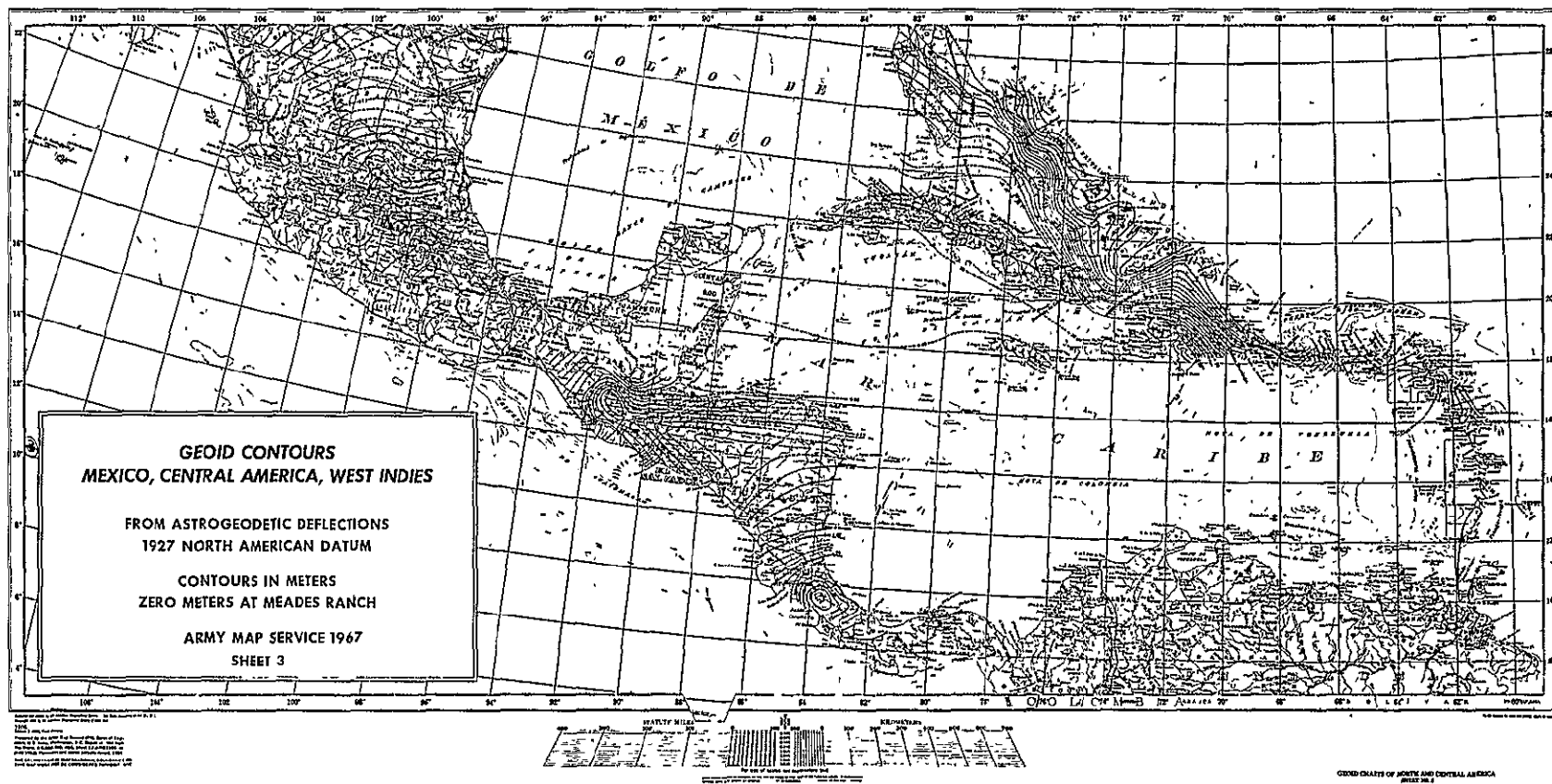
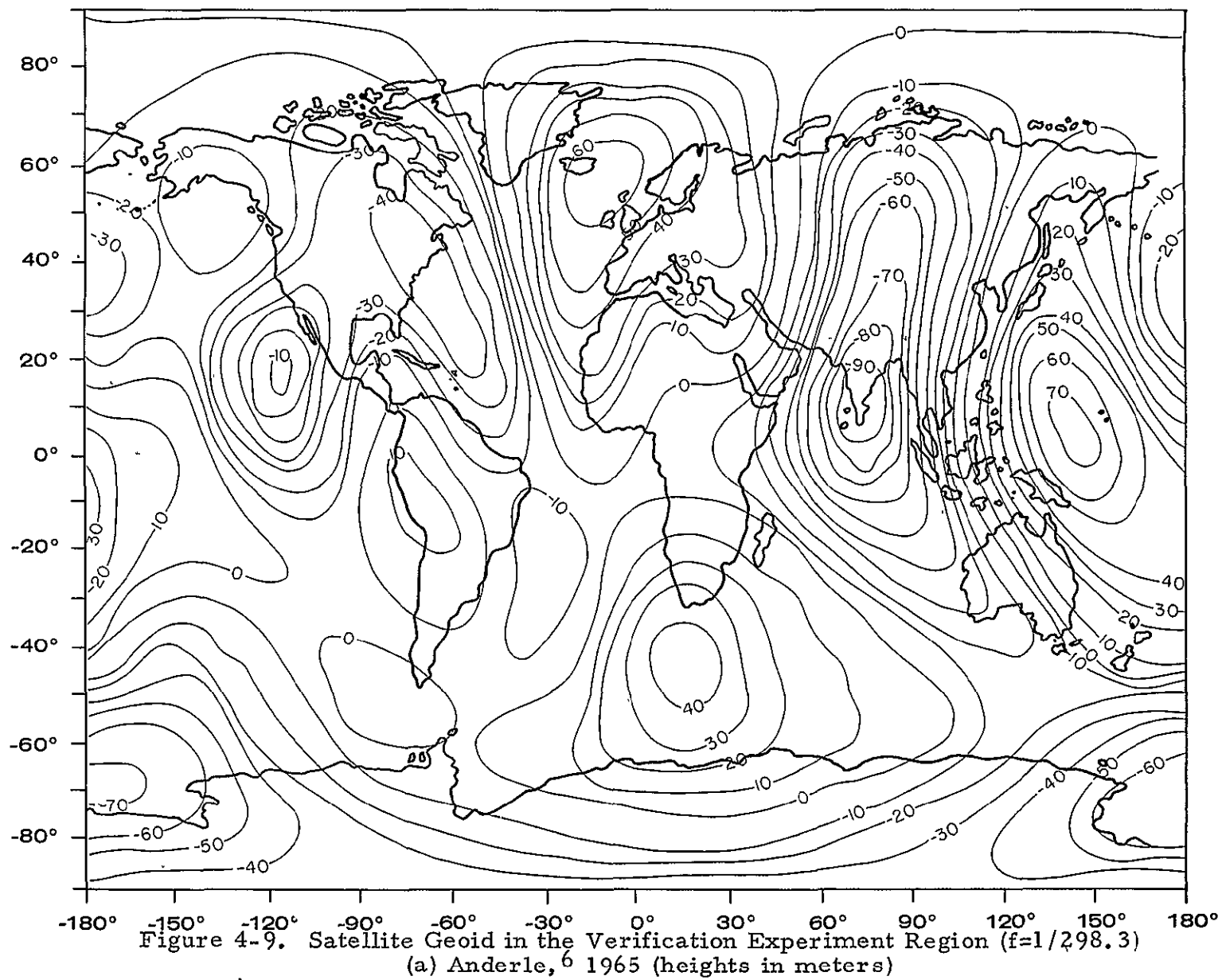


Figure 4-8. Astrogeodetic Geoid in the Verification Experiment Region (Caribbean)





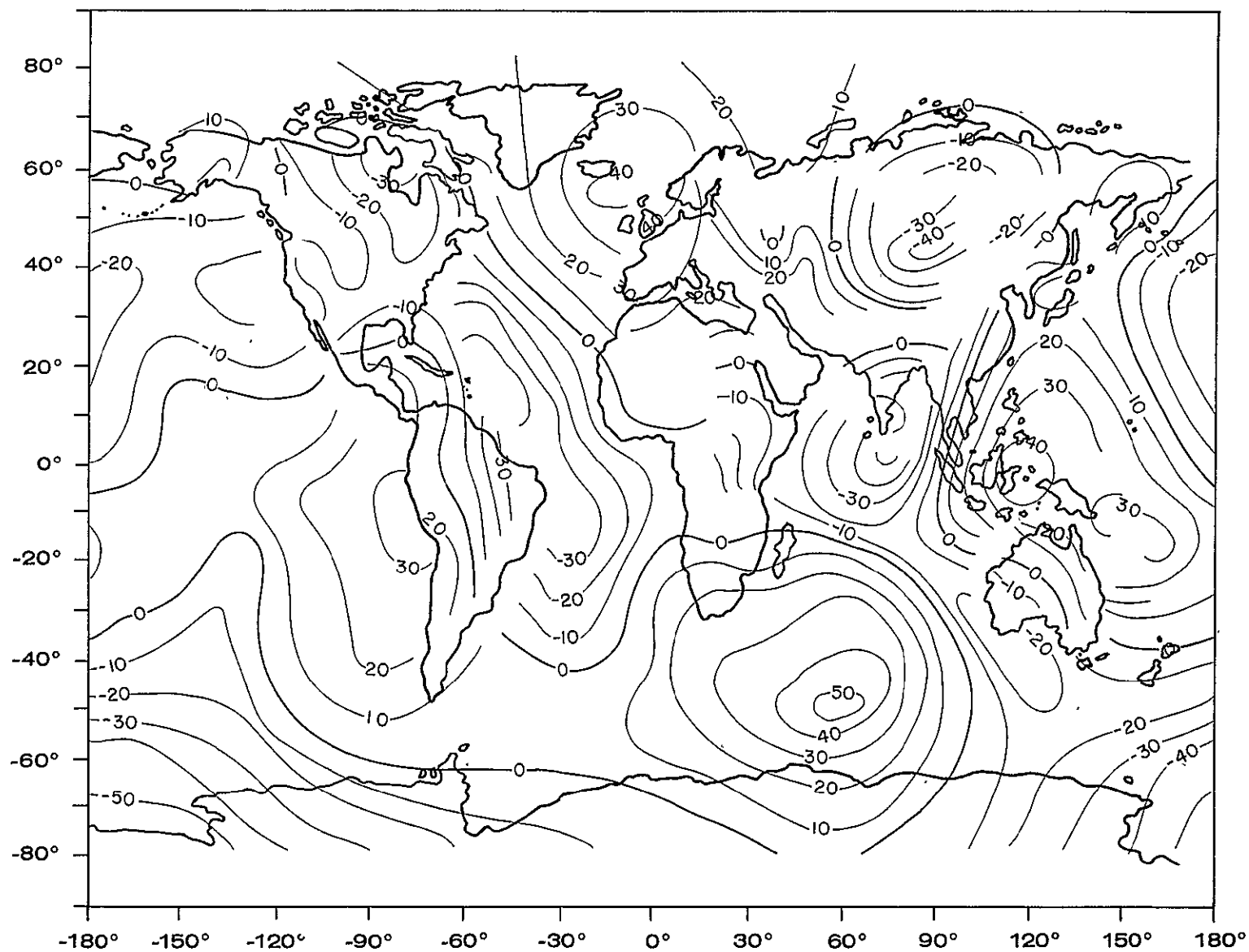
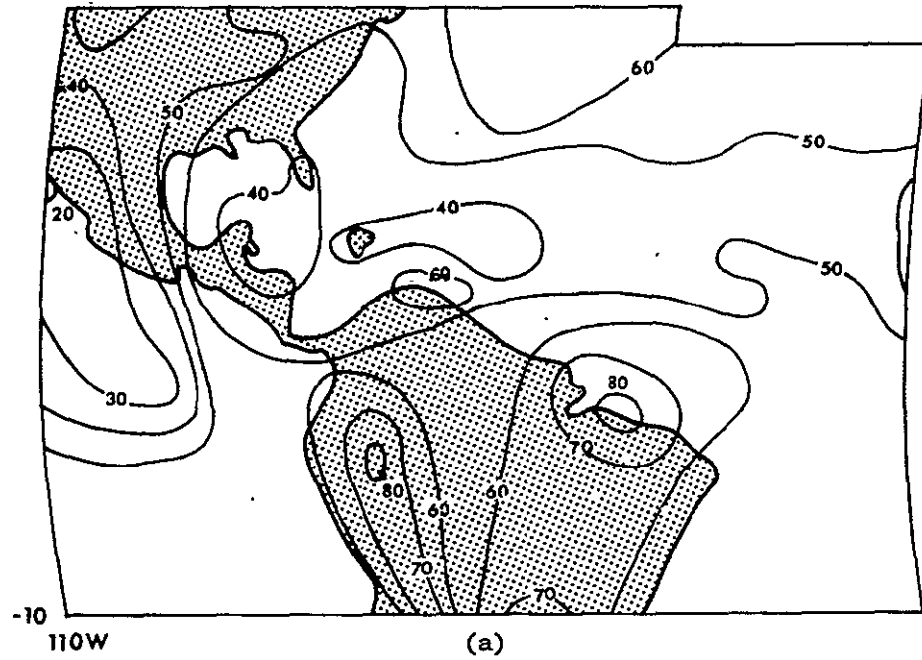
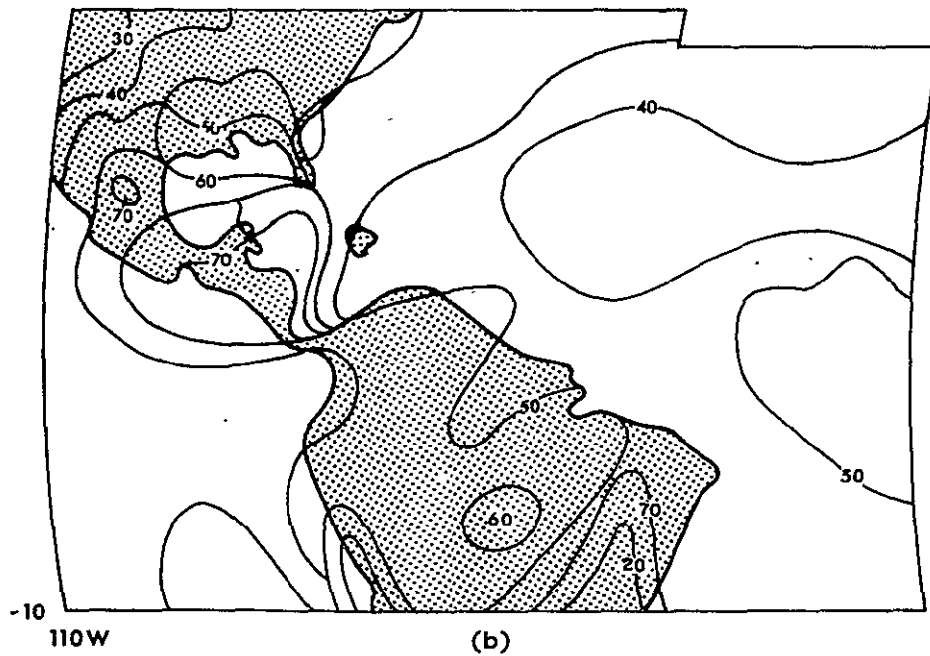


Figure 4-9. Satellite Geoid in the Verification Experiment Region ( $f=1/298.3$ )  
 (b) Bursa<sup>7</sup> 1969. (heights in meters)



AVERAGE PERCENTAGE OF CLOUDINESS IN MARCH



AVERAGE PERCENTAGE OF CLOUDINESS IN SEPTEMBER

Figure 4-10. Average Cloudiness in American Mediterranean<sup>3</sup>

Bolay, and Beers.<sup>3</sup> The data used in assembling the charts were assembled prior to 1943 and were obtained for the most part from land-based stations. Cloud cover estimates based on a larger volume of data is described in Ref. 8. Table 4-3, taken from Ref. 9, shows the percentage of time favorable for observations at Baker-Nunn camera stations in Florida and Curacao. Cloud cover data are summarized by the estimate that the probability of successful optical observation (by virtue of skies sufficiently clear) is less than 60% in the 2 - 3 most favorable months, and less than 40% the remainder of the year.

Wave height data shown in Figure 4-11 were taken from Hogben and Lumb<sup>10</sup>. Height numbers 1 to 19 are twice the wave height (and four times the wave amplitude) in meters. The numbers within the rectangular outline are the number of reported occurrences of the heights corresponding to the listed height numbers. The region (area 16 of Hogben and Lumb) to which the data apply does not include the western portion of the Yucatan Basin nor the banks just off Nicaragua.

#### 4.3.1.2 Tracking Station Location (Caribbean)

The verification experiment will require, for the absolute category, altimeter locations at the instants of height measurement. These locations will come from a combination of observational data taken at or close to the time of height measurement with computations based on the theory of satellite motion. Many tracking stations other than those able to observe the altimeter while it is directly over the Caribbean will be able to contribute useful data; the usefulness of tracking data will therefore depend not only on the kind of tracking station involved but on its location with respect to the Caribbean region and to the satellite orbit. The locations of tracking stations that are expected to contribute useful data are shown in three figures. Figure 4-12 shows the coverages of the tracking stations in the Caribbean region. Optical tracking stations locations are indicated in Figure 4-12a; electronic tracking station locations are indicated in Figure 4-12b (which also indicates C-band and S-band coverage). The distinction



Table 4-3. Percent Observing Time Favorable for Observing  
Satellite During 1962, 1963

MONTH	STATION			
	Curacao		Florida	
	1962	1963	1962	1963
January	48	30	45	43
February	57	41	60	42
March	44	45	38	53
April	47	32	45	72
May	26	30	64	50
June	34	60	39	58
July	54	36	59	56
August	62	45	45	71
September	40	37	48	51
October	61	50	55	68
November	55	35	45	51
December	50	38	57	57

Ref. 9

		WAVE PERIOD CODE											TOTALS
		X	2	3	4	5	6	7	8	9	0	1	
4-31 WAVE HEIGHT CODE	00	1212	1661	55	22	12	1	1	4	1	42	48	3059
	01	62	5129	541	131	51	18	3	1	3	3	273	6215
	02	65	10311	4145	687	182	67	9	7	10	26	79	15588
	03	59	5350	7324	1790	336	109	32	12	2	3	19	15036
	04	17	1154	3629	2005	434	94	28	4			3	7368
	05	7	317	1460	1246	328	107	33	10	4		2	3514
	06	3	105	484	583	233	68	17	7				1500
	07	1	43	224	247	159	69	9	4				756
	08	1	12	65	112	62	37	12	4	2			307
	09	1	4	40	79	61	14	12	4		1		216
	10	3	2	10	6	10	11	1				2	45
	11	1	1	6	7	9	1	1	2				28
	12	2	4	18	12	2	4	2	2				46
	13		5	7	6	8	8	1					35
	14	1	1	3	2	1	1						9
	15			3	3	1	1		2				10
	16				3								3
	17						1						1
	18											1	1
	19		1			2	2						5
TOTALS		1435	24100	18014	6941	1891	613	161	63	22	75	427	53742

Figure 4-11. Wave Heights (in meters) in Caribbean Sea Region. 10

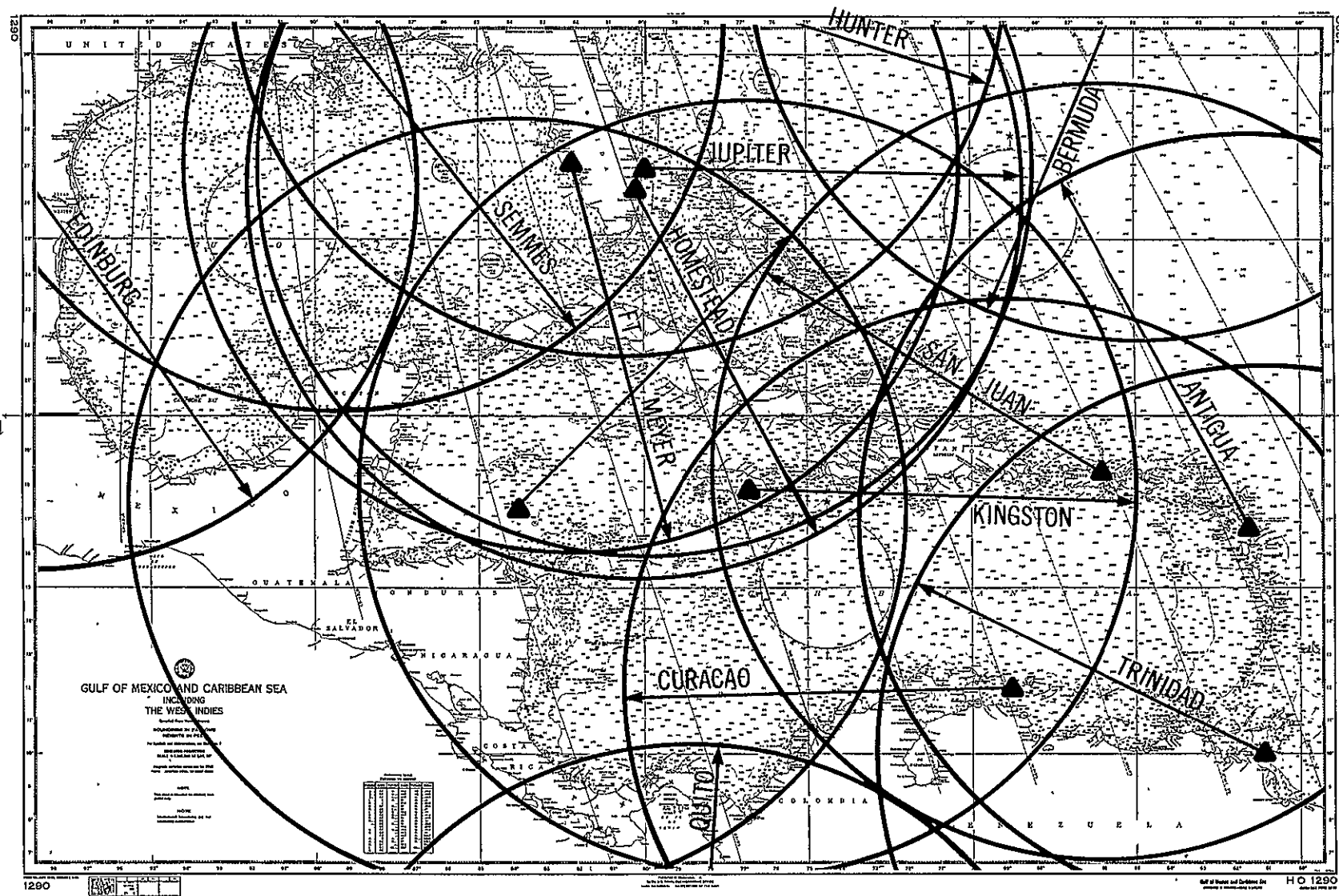


Figure 4-12. Coverage of Tracking Stations in the Caribbean  
(a) Optical Tracking Stations

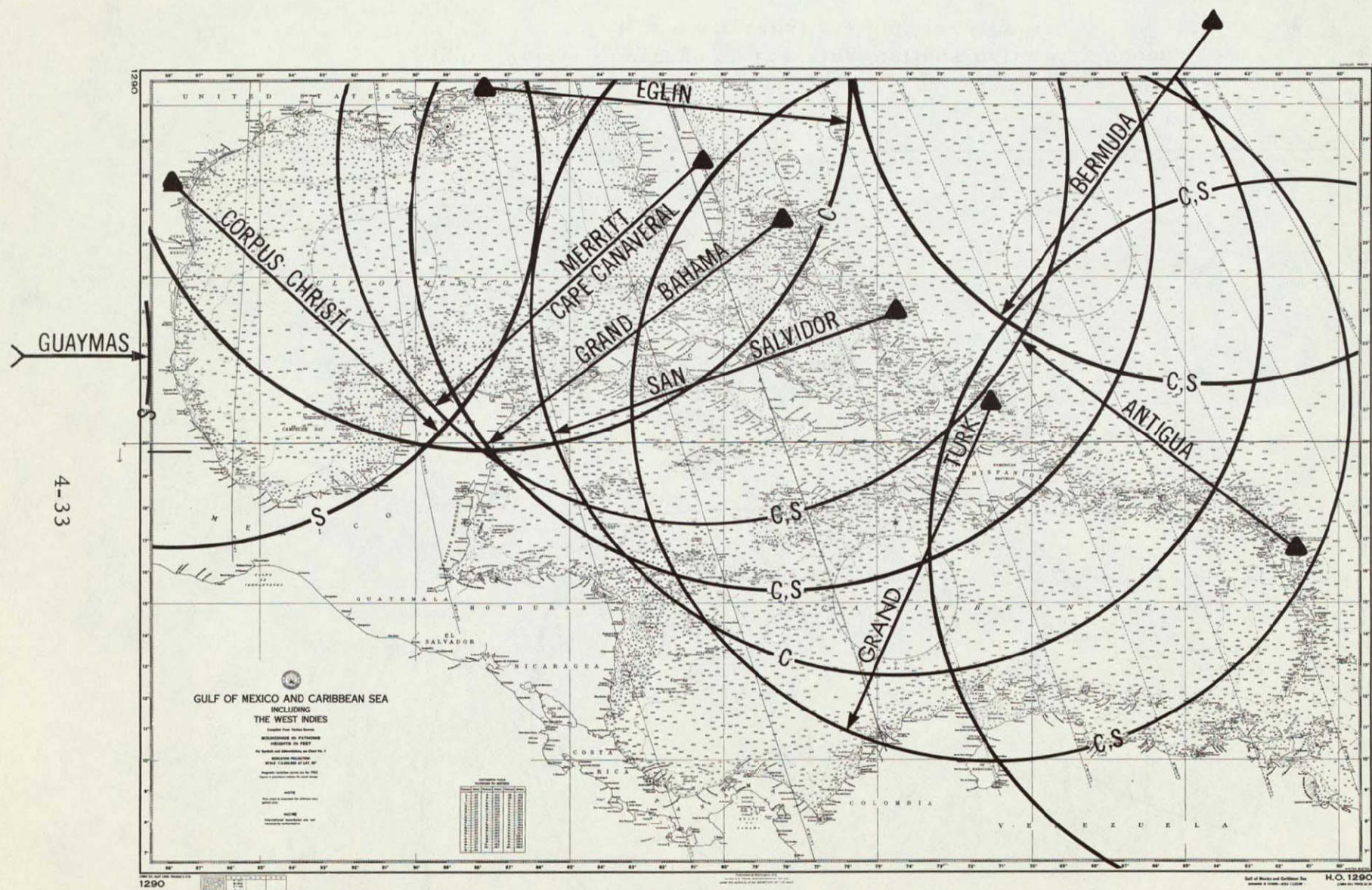


Figure 4-12. Coverage of Tracking Stations in the Caribbean  
(b) Electronic Tracking Stations



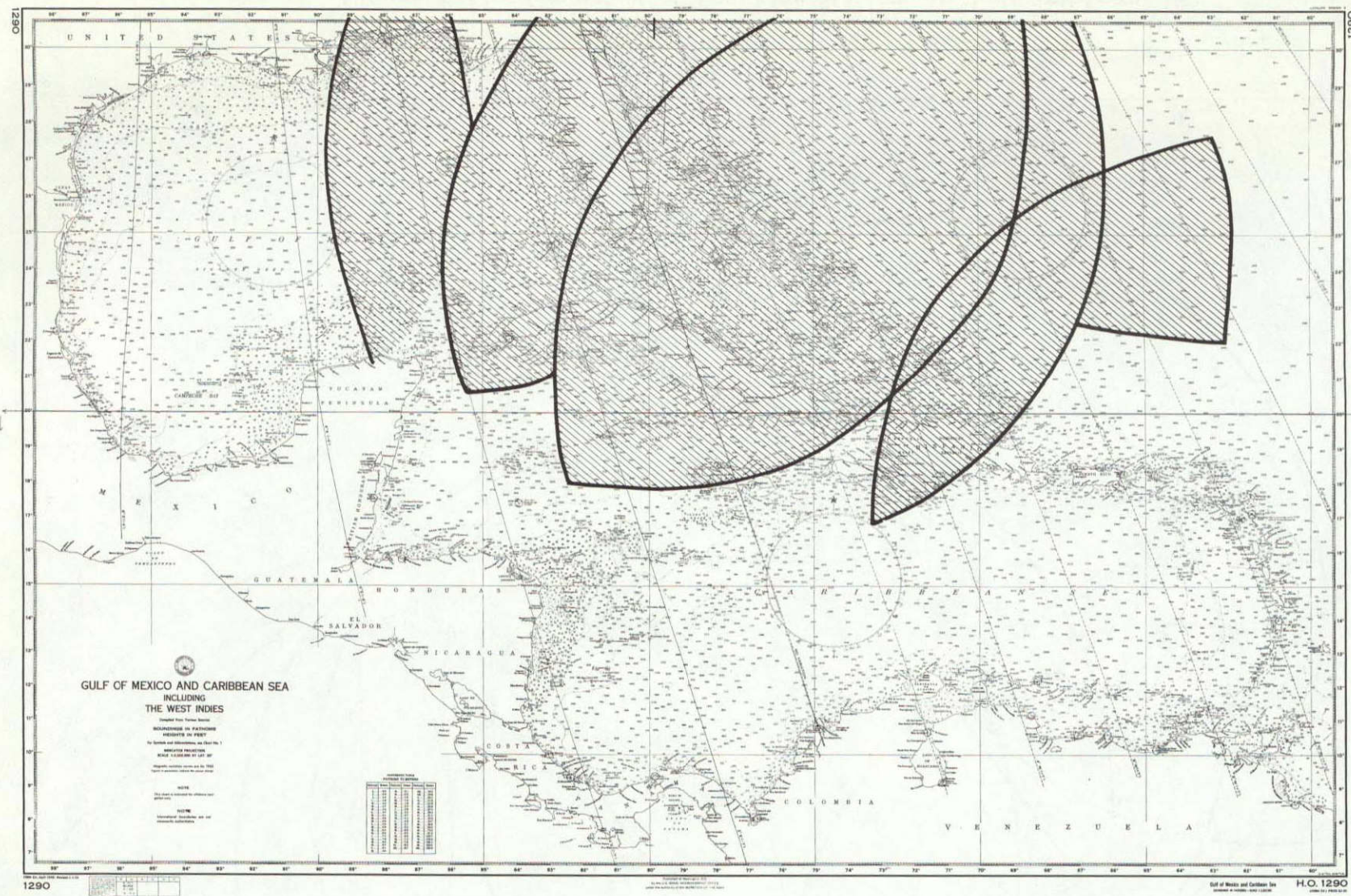


Figure 4-12. Coverage of Tracking Stations in the Caribbean  
(c) 4 or more radar stations for tracking

is necessary because, for observations in the Caribbean region, optical observations will have only a 60% to 30% chance of being successful when operating alone, and of course a much smaller chance when operating with other optical tracking stations. A satellite altitude of 1100 km was used, and a limiting zenith distance of  $60^\circ$  was set for both electronic and optical tracking stations. Although useful observations can be made at greater zenith distances (except perhaps by laser tracking devices), the  $60^\circ$  limit is safe and, because accuracy in determining the normal component is more important than accuracy in determining the tangent and binormal components, is adequate for preliminary planning purposes. In Figure 4-12c, those regions within which 4 or more radar stations can simultaneously track the altimeter are indicated. Those stations which are located so that they can observe the altimeter (at  $60^\circ$  zenith distances or less) when the altimeter is within  $90^\circ$  (in longitude) of the Caribbean region are shown in Figure 4-13, and those stations which can observe the satellite only outside the  $90^\circ$  limits are shown in Figure 4-14. The TRANET instrument locations are shown in Figures 4-13 and 4-14, even those locations from which observation of the altimeter within the Caribbean would not be possible, because the TRANET instruments will not be used to provide locations directly but will be used for strengthening the location as derived from the orbit. Except in the case of the TRANET stations, a circle showing the limits within which the altimeter nadir point must lie in order to be observable from that station (at less than  $60^\circ$  zenith distance and above 1100 km) are drawn about each station in Figures 4-12(a), (b) and (c).

Table 4-4, following, lists the relevant tracking stations, grouping them into regional categories according to their relevance to the problem. Section 4.3.1.3 below, under "Conduct of Experiment (Caribbean)"; discusses both existing and hypothetical tracking station locations in their relation to the possible experiments.

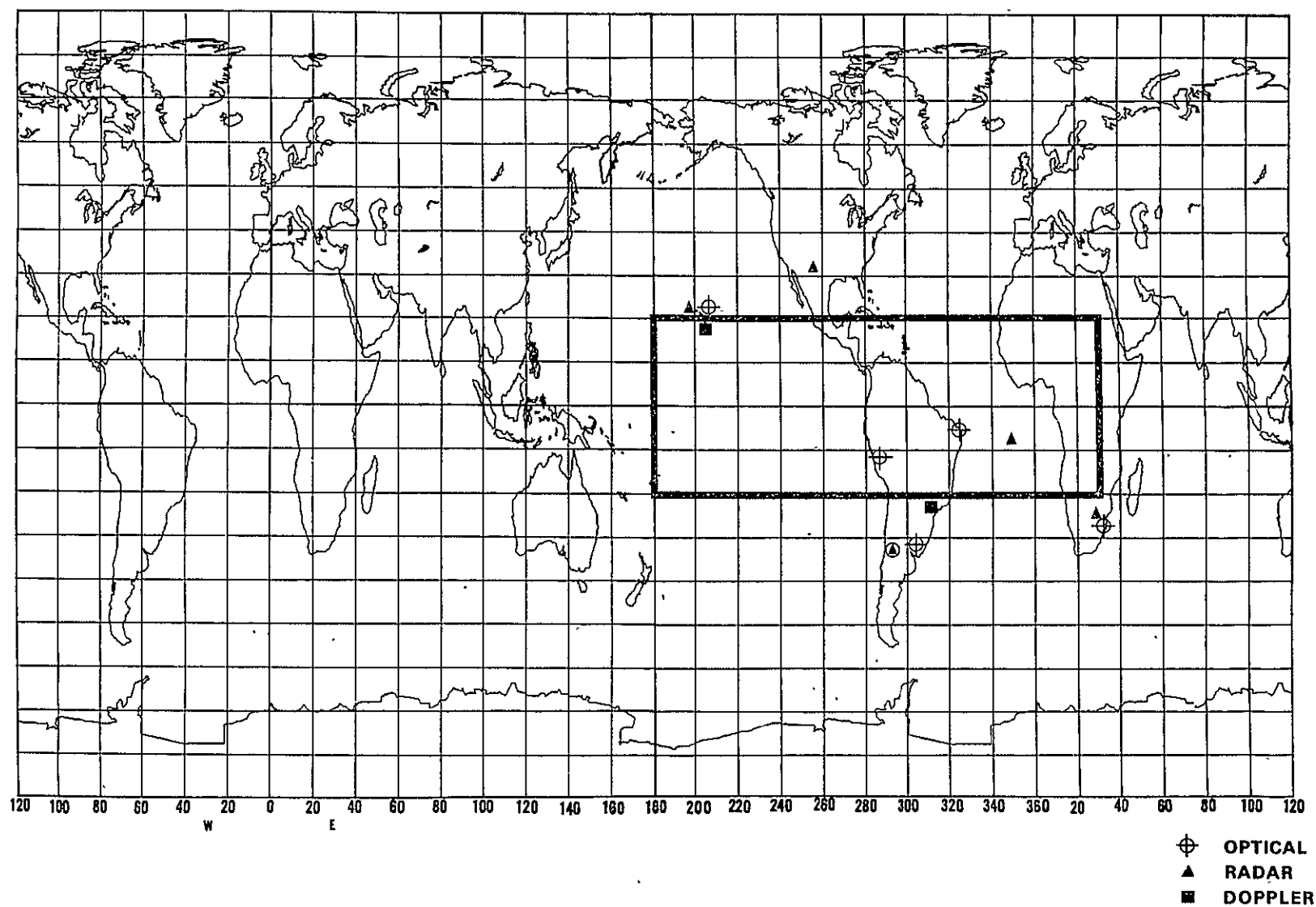


Figure 4-13. Stations which are located so that they can observe the altimeter (at  $60^\circ$  zenith distances or less) when the altimeter is within  $90^\circ$  (in longitude) of the Caribbean

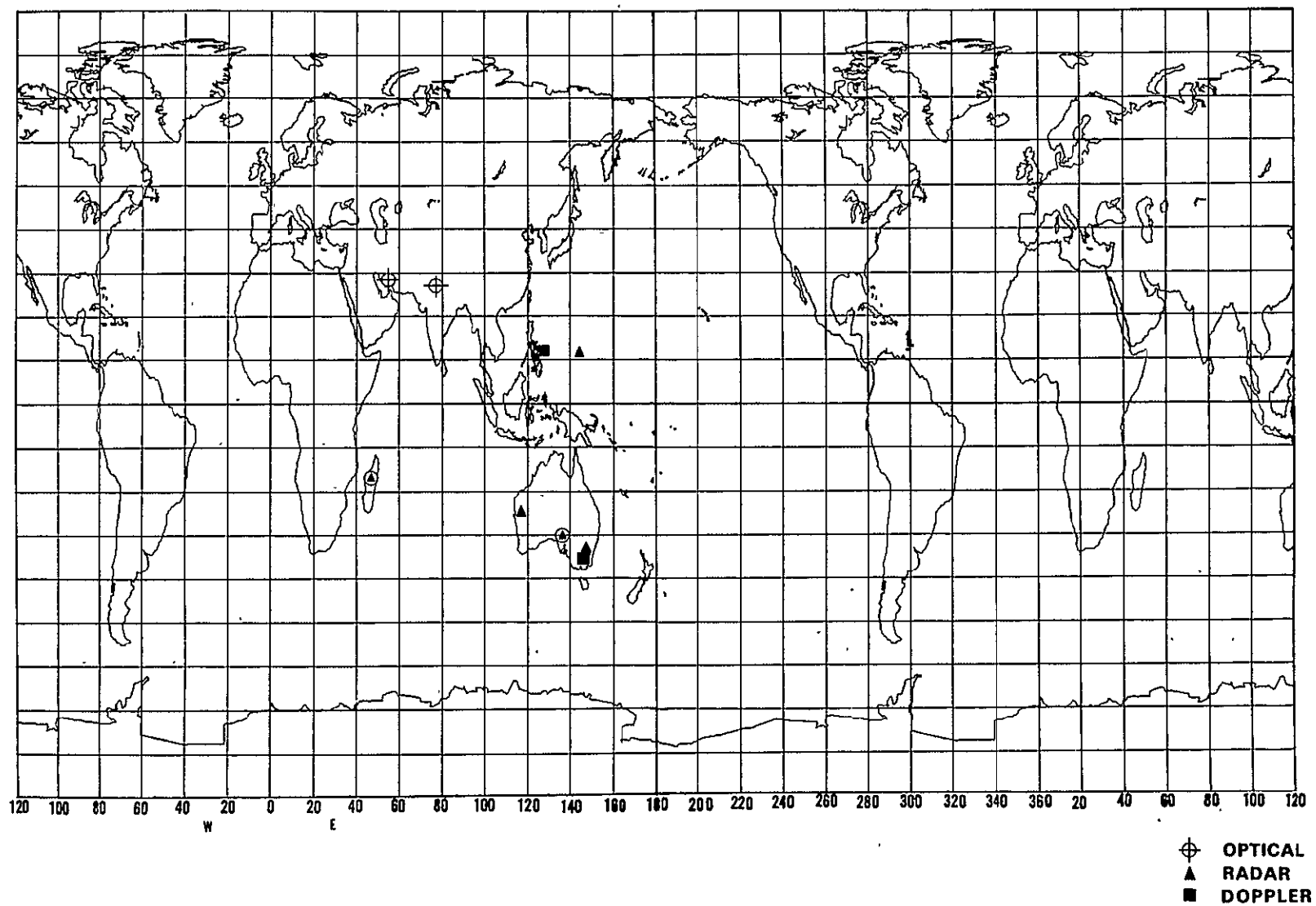


Figure 4-14. Stations Which Can Observe the Satellite Only Outside the 90° Limit



Table 4-4. Locations of Tracking Stations for Caribbean Tests

CATEGORY A						
Name	Location		h	Source	TYPE	
	$\lambda$	$\phi$				
Cape Canaveral (Kennedy)	279° 24' 01"78	28° 13' 33"98	15	2	FPQ-6	
and Vicinity	279° 18' 22"93	28° 30' 28"22	3	2	USB	
Homestead, Fla.	279° 36' 42"69	25° 30' 24"69	18	1	PC-1000	
San Salvador	285° 29' 43"96	24° 07' 05"52	13	2	FPS-16(a)	
Eglin AFB	273° 12' 06"44	30° 25' 17"06	28	2	FPS-16	
Corpus Christi	262° 37' 17"92	27° 39' 11"78	6		USB	
Grand Turk	288° 52' 03"04	21° 27' 43"68	36	2	TPQ-18	
Antigua	298° 12' 23"84	17° 08' 35"00	42	2	FPQ-6	
	298° 12' 37"41	17° 08' 51"68	7	1	PC-1000	
					USB	
	291° 09' 42"55	12° 05' 21"55	23	1	Baker-Nunn	
	283° 11' 26"52	18° 04' 31"98	485	1	MOTS-40	
San Juan	294° 00' 22"17	18° 15' 26"22	58	1	MOTS-40	
Trinidad	298° 23' 23"67	10° 44' 32"78	269	1	PC-1000	
Swan Isl.	276° 03' 29.87	17° 24' 16"57	83	1	PC-1000	

(a) No longer exists. (H.R. Stanley, private communication)

CATEGORY B						
Name	Location		h	Source	Type	
	$\lambda$	$\phi$				
Bermuda	295° 20' 46"53	32° 20' 47"53	21	3	FPQ-6	USB
Quito	281° 25' 14"81	-0° 37' 28"00	3649	1	MOTS	
Grand Bahama	281° 39' 06"88	26° 36' 54"95	14	2	FPS-16	USB
Cape Canaveral (Kennedy)	279° 25' 23"77	28° 28' 52"79	14	2	FPS-16	
Las Cruces	253° 14' 48"25	32° 16' 43"75	1201	1	Doppler	
Stoneville	269° 09' 10"70	33° 25' 31"57	44	1	Doppler	

Table 4-4 (Cont.)

## CATEGORY C

Name	Location			h (meters)	Source	Type
	$\lambda$	$\phi$				
Guaymas	249° 16' 46"28	27° 57' 45"96		17	2	USB
Natal	324° 50' 18"00	-05° 55' 50"00		112	1	Special Op
Ascension	345° 40' 20"72	-07° 57' 19"04		538	3	FPS-16 <sup>(b)</sup> USB
Pretoria and vicinity	28° 20' 53"00	-25° 56' 46"05			1	FPQ-6 <sup>(c)</sup>
Tananarive	47° 18' 09"45	-19° 01' 13"32		1393	3	GRARR <sup>(d)</sup>
Carnarvon	113° 42' 57"88	-24° 53' 50"65		49	3	FPQ-6
	113° 42' 55"06	-24° 54' 14"86		38	3	GRARR
	113° 43' 27"29	-24° 54' 27"33		39	3	USB
Guam	144° 44' 03"89	13° 18' 33"28		86	3	USB
Hawaiian Islands	202° 00' 00"63	21° 31' 26"86		380	1	USB Doppler
	203° 44' 24"11	20° 42' 37"49		3027	1	Baker-Nunn
Gran Canaria	344° 23' 15"00	27° 44' 25"00		22	3	USB

Source 1 - 1969 - Lerch, Fiet al. Geos I Tracking Station Positions on the SAO Standard Earth (G5) NASA TN-D5034

Source 2 - 1966 - Anonymous, Goddard Directory of Tracking Station Locations. Goddard Space Flight Center, Greenbelt, Md. N.A.D. 1927.

Source 3 - Same as 2, but various datums.  
 (a) Also FPQ-6. (H.R. Stanley, private communication)  
 (b) Has MPS-25 (portable version of FPS-16) rather than FPQ-6, (H.R. Stanley, private communication)  
 (c) Has CAPRI (mobile version of FPS-16). (H.S. Stanley, private communication)

## CATEGORY D (Hypothetical Stations)

Name	Location			h(meters)	Source	Type
	$\lambda$	$\phi$				
Puerto Rico 2	293° 00' 00"	18° 15' 00"		0	N.A.	Transponder
Puerto Rico 3	293° 30' 00"	18° 45' 00"		0	N.A.	Tr.
Puerto Rico 4	294° 00' 00"	18° 15' 00"		0	N.A.	Tr.
Jamaica 2	283° 11' 00"	18° 00' 00"		0	N.A.	Tr.
Curacao 2	291° 10' 00"	12° 00' 00"		0	N.A.	Tr.
Bluefields	276° 30' 00"	12° 00' 00"		0	N.A.	Receiver
Chetumal	271° 00' 00"	18° 30' 00"		0	N.A.	Receiver
Nicaragua	274° 30' 00"	11° 00' 00"		1500	N.A.	Receiver

#### 4.3.1.3 Conduct of Experiment (Caribbean)

In the preceding sections the general region of interest has been located, its physical characteristics described, its relation to the satellite's orbit deduced, and the locations of the tracking stations that will tie the orbit to the region's geometry given. With these essential circumstances settled, the verification experiment can be set up. This means (1) specifying how the measurements shall be conducted in particular parts of the general region, (2) stating the additional data and equipment required, (3) noting the logistical problems to be solved, and (4) setting up a schedule.

#### Sub-Regions (Caribbean)

The entire Caribbean region is one selected sub-region.

We require that the altimeter make at least 4 measurements in every 5 km x 5 km square area of the Caribbean, exclusive of portions closer than 10 km to land.\* This will mean a total of approximately  $5 \cdot 10^4$  measurements in the Caribbean as a whole, not counting those extra measurements to be made in proper sub-regions. The 5 km x 5 km size ensures that sea slopes as great as  $1 \cdot 10^{-3}$  will be observed. Based on the known bottom topography of the Caribbean, no slope as great as this is expected to be found. (It should be noted that, as the altimeter is at present constructed, each "measurement" is actually an average value over one second\*\* in time and 10 km x 20 km in area. The average heights over the 5 km squares will have to be recovered by solving a series of simple linear difference equations.)

A higher density of measurements should be made in the following sub-regions (Figure 4-15):

- A - Eastern Caribbean ( $290^\circ$  to  $300^\circ$ )
- B - Misterioso Bank
- C - the Panama North Coast and South Coast
- D - Golfo de Venezuela
- E - Puerto Rico trench

\* Careful attention must be given to the effect of nearby land topography on the returned energy. See Appendix F;

\*\* An average over 0.1 seconds is assumed in most parts of this chapter. The one second value assumed here is a "safe" value.

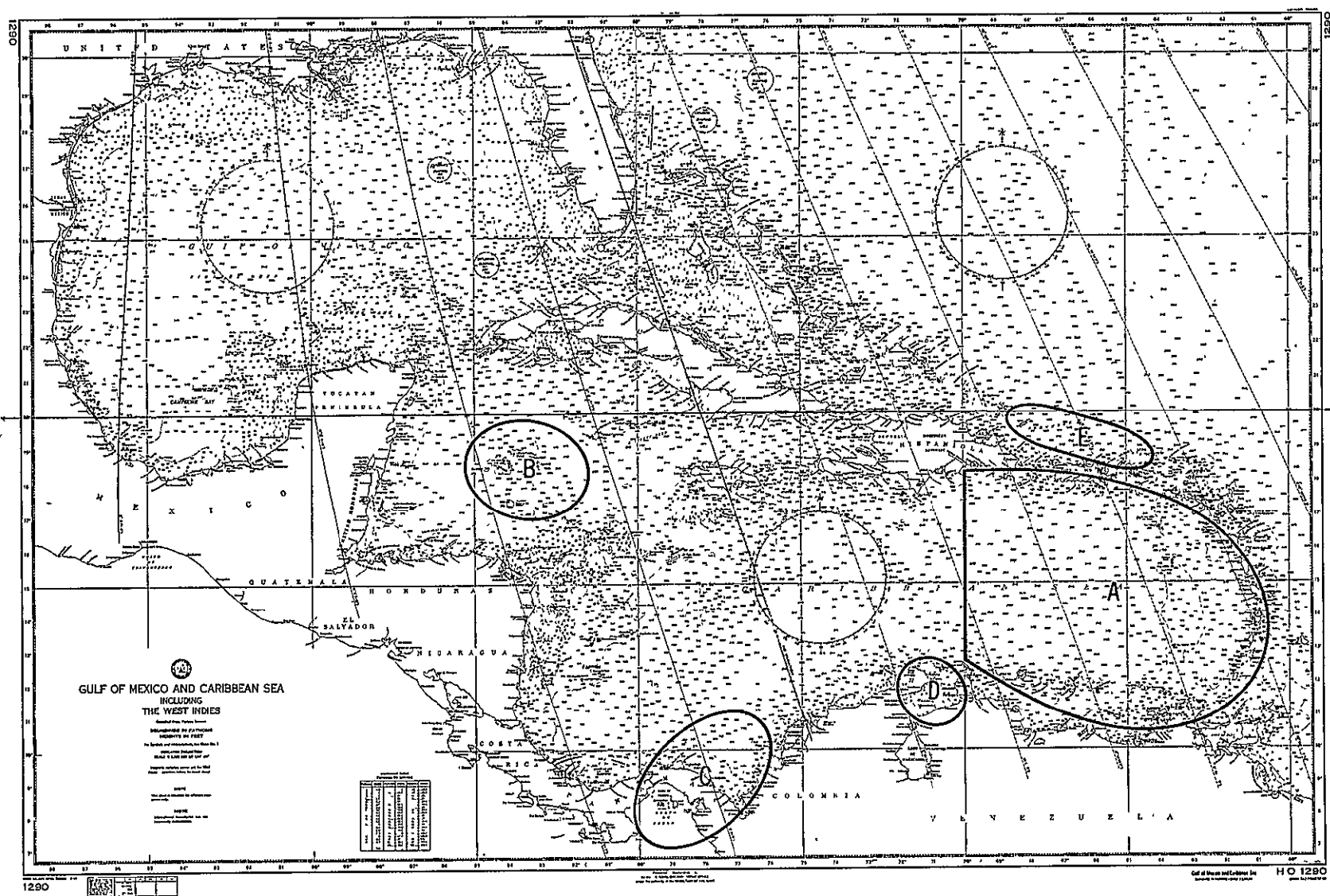


Figure 4-15. Subregions where a Higher Density of Measurements Should be Made

- A Eastern Caribbean
- B Misterioso Bank
- C Panama Coast
- D Gulf of Venezuela
- E Puerto Rico Trench

Whether a higher density is in fact attainable will depend partly on the ability of the GEOS-C altimeter to make measurements (that is, provide measurements to the user) at intervals of less than 1 second of time. It will also depend on the exact orbit into which the altimeter is placed, and to an extent not exactly predictable. Altimeter measurement rate helps determine the number of measurements per unit distance along the surface trace, but this number is also determined by the spacing between adjacent (not consecutive) traces, and the number of measurements per unit distance perpendicular to the trace is of course determined principally by the spacing between adjacent traces (see Figure 4-16). We will consider these regions individually.

1. Eastern Caribbean (290° to 300°)

The principal reason for considering concentration of effort in the eastern Caribbean is the location of tracking stations in relation to the orbit. A reasonable tracking station geometry can be obtained using Grand Turk, Antigua, and a tracking ship (TS) located in the vicinity of Maracaibo. This geometry can be varied by moving the TS to suit the orbit. The TS furthermore can be directly related to the Maracaibo geoid and used for relative accuracy measurements in that region. This also strengthens altimeter locations in the Puerto Rico trench region. The Eastern Caribbean Test Region (ECTR) is then a minimax region; it is the smallest region within which all four categories of the experiment can be covered using tracking stations known to be operating. Addition of optical tracking stations at Curacao, Puerto Rico, Trinidad and Kingston as recommended considerably strengthens the tracking net and makes prolonged reliance on the TS unnecessary. Even more useful would be use of radar stations at Puerto Rico and Trinidad.

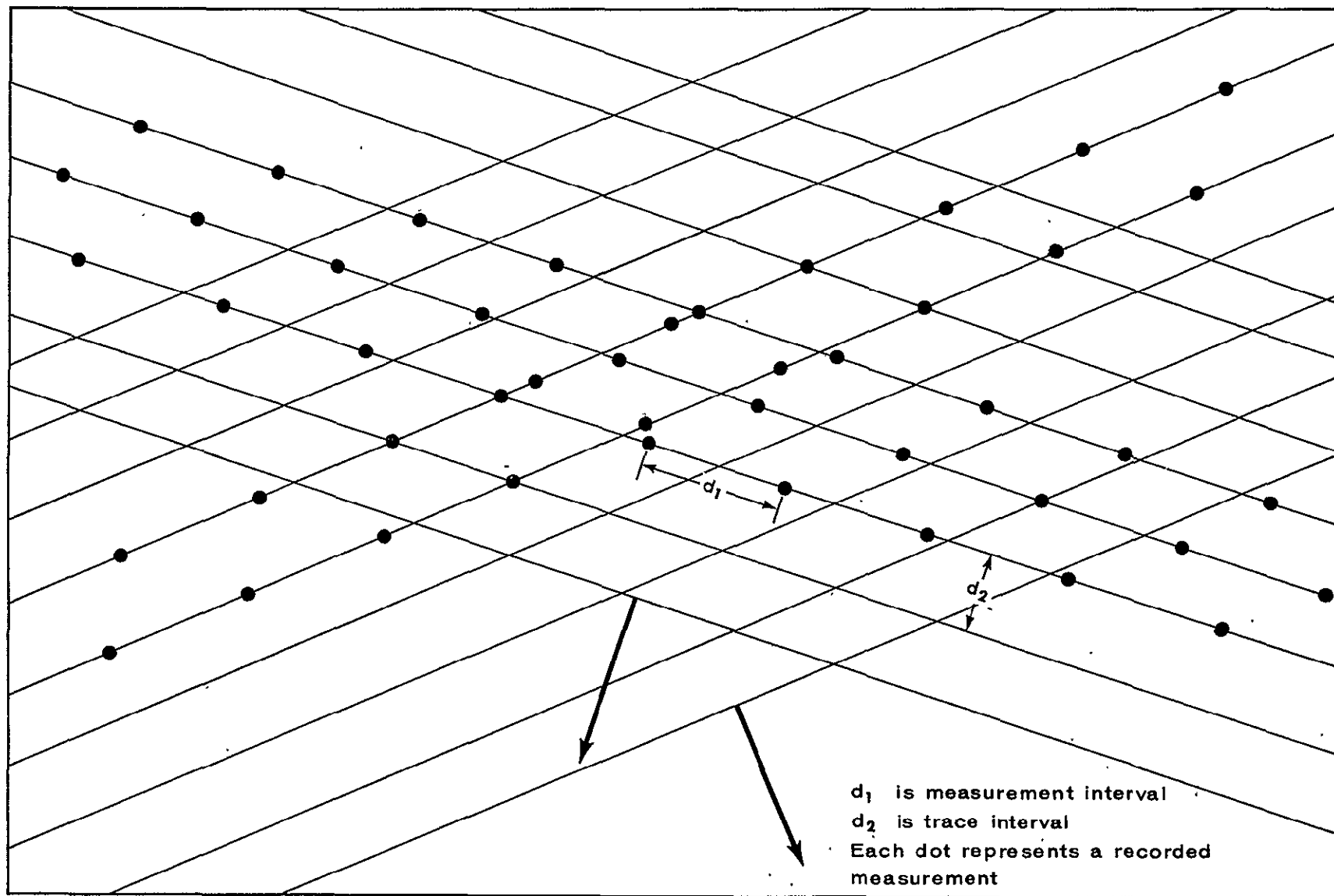


Figure 4-16. Typical Measurement and Trace Intervals

2. Misterioso Bank

Misterioso Bank is located in the western part of the Caribbean about 100 km north of Swan Island and about 600 km west of Jamaica. Its position with respect to radar instruments is not particularly good, although it is well placed in relation to the Homestead, Swan Island and Jamaica stations. The principal reason for singling it out is the steep slope from the Bank to the sea floor; the slope seems to be greater here than at any other place within the Caribbean, with the possible exception of some parts of Bartlett Deep. Furthermore, the slopes around the Bank can be found both in the direction of motion of the altimeter and reflects the topography perpendicular to it. If the geoid reflects the topography in this region as it does in the Puerto Rico trench region,<sup>11, 12</sup> the altimeter will have a geoid variation of 10 m or more within 30 km or less to measure. This may be better than what will be measured above the Trench, since the GEOS-C orbit will be paralleling the Trench most of the time.

3. Panama North and South (Gulf of Panama) Coasts

At present, subregion C is very poorly located with respect to Caribbean region tracking stations, even if all previously active camera stations are included in the tracking network. Nevertheless this region is of particular interest as part of the Caribbean VED for two reasons.

- (1) It is crossed by orbits running approximately along the northern coast of South America, so that the geoid along that coast is best determined using the geoid in Panama as one end.
- (2) The difference in geoid height between the north and south coasts is known to better than 3 cm, while the height difference from spirit leveling is about 20 cm<sup>14</sup>.

The second of these considerations is of particular importance in checking the altimeter for differential accuracy. Since region C will in any case be used for differential tests, the test data can be put to good use strengthening the southern portion of the Caribbean geoid.

#### 4. Golfo de Venezuela

As mentioned in the discussion of the ECTR under A above, a TS should be available in the vicinity of the Gulf of Venezuela for satellite tracking. This will be important in defining orbits passing from the Gulf of Panama to the eastern edge of the Caribbean where the Antigua and Trinidad stations provide data. The geoid in the Gulf of Venezuela is known on a local system, at least<sup>11, 15</sup>, so that inclusion of this region in the special regions merely means that the measurements made there for relative category tests are applied to absolute accuracy determination.

#### 5. Puerto Rico Trench (Brownson Deep)

The Puerto Rico Trench is an intensively studied geological structure<sup>13</sup>. The geoid is known in N-S section from three sets of measurements: pendulum gravity measurements of measurements: pendulum gravity measurements by Worzel<sup>5</sup>, GEON\* measurements by von Arx<sup>12</sup>, and SINS\*\* measurements by Butera et al.<sup>17</sup>. The altimeter will be

\* GEON is the designation of a Gyro Erected Optical Navigation system<sup>16</sup>, a shipborne inertial navigation system.

\*\* SINS is the military designation of a Ship's Inertial Navigation System, a shipborne gyroscopic system originally developed at M.I.T.



moving over the trench almost parallel to the main axis of the trench and hence perpendicularly to the present geoid profiles. Fortunately, the region is just within the  $20^{\circ}$  N latitude limit, so that the region will be very densely covered by the orbit. Tracking geometry is reasonably good and should be improved, for relative category measurements, by use of transponder or other tracking adjuncts on and near Puerto Rico. The optical tracking station at San Juan is of course of very little use in improving height measurements over the trench because of the small zenith angles involved.

The above five subregions are designated for special attention because their geographical location and geophysical characteristics make such attention provide data that are useful in two or more categories at once. This does not mean that no measurements are made in other regions but only that first priority is given to taking measurements in these regions.

#### Additional Data Required (Caribbean)

For tests in the absolute category, we must know satellite location and geoid height at each point at which a comparison with the altimeter measurement is to be made. Information on satellite location will be provided by tracking stations. At the present time, information on radar errors is still not adequate for removal of all systematic errors in the range measurements (see Appendix I). However, this information need not be available before the experiment, since it can be derived as part of the verification experiment. The same is true of the information on tracking station location that is needed. The data reduction procedure will include the tracking station locations as unknowns.

Information on geoid-spheroid separation and mean sea surface height above geoid cannot be derived as part of the final solution without imperiling the validity of the absolute category tests. Geoid-spheroid separation must therefore

be found by properly combining the astrogeodetic version<sup>18</sup>, the gravimetric version of D. Rice<sup>18</sup> running along the chain of islands bounding the Gulf of Mexico and Caribbean on the northeast, and the various satellite geoids. Also, to be accounted for in the solution are the tracking stations in that region whose coordinates with respect to the reference spheroid are known and at which therefore the geoid-spheroid separation is known. Finally, use must be made of the gravity data available in the Caribbean region proper. Quantity and quality of published data or of data available but not published vary considerably from place to place in the Caribbean<sup>18</sup>. It is clear that more gravity data are required, especially between 15° and 20° North and West of the island chain, but more study is needed to make a good estimate of the densification required and the extent to which the densification can be satisfied from existing unpublished data.

At the present time, the American Mediterranean is completely ringed by first-order geodetic control. (The island portion, of course, is put in by HIRAN/SHORAN type surveying). It is not ringed, however, by an astrogeodetic geoid; this geoid stops at present in western Columbia and at Trinidad, nor does it bridge the Yucatan channel as does the geodetic network. Both mainland and island geoids would be improved by geoid profiles across the Yucatan Channel and by a geoid continuation joining Panama with Trinidad. The latter can be achieved at low cost by making zenith camera observations at 40 km intervals along with gravimeter measurements. About 35 stations would be required - a considerable number if an astronomical transit is used, but not if a zenith camera is used. Bridging the gap between the geoid in Cuba and that in Central America presents a more difficult problem. Even at its narrowest, the gap is about 200 km wide; the western end is then on the tip of Yucatan, into which the astrogeodetic geoid has not yet been extended, and the eastern end approaches the shores of Cuba. Once the Panama-Trinidad segment is closed,

a geoid around the entire American Mediterranean is available. Using that boundary is undesirable, since it will mean (1) solving for the geoid over an area twice as large as is needed for the problem; (2) influencing the geoid in the Caribbean by the behavior of the geoid around the Gulf of Mexico. A recommended solution is to extend the geoid on land northward into Yucatan as far as Bahia Chetuman by zenith camera observations, and to make a geoid profile along the edges of the triangle with apices at Jamaica, Chetumal, and Cape Gracias a Dios (Honduras), using von Arx's GEON or SINS<sup>16, 17</sup>.

Salinity, temperature and pressure data are available in densities of 50 measurement points per  $5^{\circ} \times 5^{\circ}$  sector or high except in the far western Caribbean. The far eastern portion has densities of 200-400 measurement points in the same area. STP data off the coast of British Honduras are undoubtedly too few, and there may be too few off the north coast of Panama. In view of the low dynamic relief ( $<0.5\text{m}$ ) of the Caribbean Sea relative to the 1200 mb level<sup>19</sup>, further special measurements to provide uniform measurement density throughout the Caribbean is not justified. Anomalies of the type found at S. Aves Ridge<sup>20</sup> may or may not be common in the region, but they will not affect the anomalous height enough to require special investigation.

If the astrogeodetic geoid completely surrounding the Caribbean region is desirable, this geoid is to function as a boundary condition. Such a geoid can be provided by running a SINS gyroscopic reference survey across the Yucatan Channel. Extension of the astrogeodetic geoid around the South American coast from  $62^{\circ}$  to  $78^{\circ}$  will involve densification of the HIRAN survey net and the observation of additional astronomic positions. For the densification, an ABC type operation should be adequate; for astronomic observation, zenith camera observations are recommended.

The amount of additional data needed on STP in the Caribbean is not known at present. Data for that part of the Caribbean adjacent to the Yucatan peninsula are sparse (see Figure 4-5).

Atmospheric pressure to the nearest 10 millibar along the track of the altimeter is desirable, since this information is needed for correction of the mean sea level computations. The synoptic weather map will be sufficient for this purpose, but further investigation of the statistics of pressure distributions and the effects of these distributions on surface topography is needed.

#### Tracking Stations (Caribbean)

In order to obtain a "fix", i.e., a complete set of location coordinates, for the altimeter at any instant, at least 3 ranging instruments must make observations at that instant. The requirement for simultaneity can be relaxed slightly by using orbital equations for interpolation. The interval between observations is then determined by the amount of random motion accumulated by the satellite between single observations. This matter is investigated further in a following section on error analysis; at this point, we will assume that simultaneity is required; the resulting station distribution needed will be altered after the error analysis if necessary. A simple fix is insufficient to give information on tracking accuracy unless assumptions are made about the orbit. Since we are going to use the orbit for interpolation, we risk creating a mathematical "feed back" by using the orbit for too many things at once. Such feed back can cause errors that are very difficult to either detect or trace, and the tests should be set up so as to minimize the number of assumptions that have to be made. A reasonable check on the "accuracy" is introducing observations from additional stations. Actually, such observations do not improve or check the accuracy but merely check the self-consistency of the tracking system (network). The difference between accuracy and self-consistency in a large system can be considered irrelevant from a practical, if not from a philosophical,

standpoint, and the addition of independent tracking data is therefore made part of the experiment setup. I will, in the following pages, refer to the principle behind this addition as the "redundancy principle". The principle will not be further justified; such justification is properly part of a separate study. In accordance with this principle, it follows that at least 3 ranging stations plus one additional tracking station should be used for each fix. Consulting the list of tracking stations (see Table 4-4 ) and the diagram of station observing areas (see Figure 4-12), it becomes evident that only a very small portion of the 20° zone is simultaneously visible from 4 radar stations, and that the locations of these four stations are such as to give large rms errors in one or two of the altimeter coordinates. The optical tracking stations are more favorably located, but because of weather cannot be depended on for observations more than 30-35% of the time in a particular sector. Furthermore, a good number of the optical tracking stations listed are known to be inactive while others are part of the military SPACETRACK network and are not under NASA direction. To ensure that a redundant number of observations is available for satellite location, four more electronic tracking stations of high accuracy are necessary, and one additional optical tracking station is desirable.

More than this number of electronic tracking stations is not needed for the absolute procedure since the fixes need only be at intervals consistent with the altimeters random walk from its computed location.

Tentatively, we place the electronic tracking stations as follows:

1.     Bakia Chetamal, Br. Honduras
2.     Bluefields, Nicaragua
3.     Curacao, D.W.I.
4.     Jamaica

These four stations and their relation to the radar tracking stations are shown in Figure 4-17. Not shown in the figure is the location of the Apollo ship. This ship will not have any fixed location within the Caribbean, being stationed for best observation at low zenith distances of the altimeter.

In the above discussion, we have referred to the additional "tracking" stations. The term is used to apply to corner-cube reflectors, transponders, of simple receiver-plus-counter sets.

The optical tracking station should be located, for best geometric relation to the other optical stations, in Panama. However, large parts of Panama are almost permanently covered with clouds, and in any case the optical station would be used as support for the electronic tracking stations, not as part of an optical tracking net. The station can therefore be located in Costa Rica, where it is well situated with respect to both Lake Nicaragua and the Gulf of Panama, and where the weather is reasonably good. It is not an essential addition, provided that enough of the present optical tracking network can be used for the altimeter verification experiment. It is therefore not included in Table 4-4.

Table 4-4 gives a list of the tracking stations to be included in the Caribbean net, their type and approximate location. The stations are grouped into four categories: those stations which will provide precise locations within the Caribbean (and Gulf of Mexico) region; those stations in the same region whose observations are used to increase the sampling density; and those stations outside the American Mediterranean whose observations are needed for orbit determination make up Categories A, B, and C respectively; Category D covers seven stations whose exact nature, location, and existence are hypothetical but which are postulated for the purposes of this study. All the postulated stations (Category D) are radar-like but act either as receivers only or as transponders,



Figure 4-17. Location of Electronic Tracking Stations

or simply as reflectors. Further discussion of the possible characteristics of such stations is found below. Three stations close together have been postulated on Puerto Rico. They have been placed there because of the proximity of the Puerto Rico trench and the possible existence there of a (satellite-tracking) camera. They could, considering their nature, have been located in the vicinity of a C- and/or S-band radar also. The Bluefields-Nicaragua and Chetamal stations are postulated (a) as part of the network monitoring the western Caribbean and Gulf of Panama region, and (b) as part of the small cluster of stations (not specifically listed in Table 4-4) on and about Lake Nicaragua for relative height measurement. The Jamaica and Curacao stations belong to both western and eastern Caribbean networks.

The success of the verification experiment will be determined by the number, types, and locations of usable tracking instruments. Which tracking instruments will be usable will depend on many factors not accurately predictable. Particularly uncertain is the number of optical tracking instruments (cameras and lasers) that will be available. This uncertainty about availability is made even more serious by the susceptibility of the stations to loss of observations because of poor weather, the non-professional quality of the tracking effort at some stations, and the heavy drain of flashing lights on available power for the altimeter. Reliance on electronic tracking instrumentation rather than optical should, therefore, be considered essential to the plan.

One way of reducing reliance on optical tracking devices is to place available C- or S-band radars at sites at which the plan otherwise calls for cameras. The extent to which such placement will be possible is not known; it will certainly be very limited.



Where C- and S-band radar tracking facilities are needed, do not exist and cannot be installed, other tracking means must be tried, such as the self-tracking or transponder devices. These in theory can provide the tracking accuracy required. Until they have been completely tested and their performance checked, however, the experiment design cannot consider them as firmly emplaced in the design as more thoroughly tested instruments. There are two electronic tracking devices which must be considered for completing the Caribbean tracking set. One is MISTRAM, a system for tracking of Air Force and Navy rocket missiles at the Atlantic Test Range; the other is SECOR, a system built for the U.S. Army as a geodetic satellite tracker. The principles of operation of these devices are well known and are in any case irrelevant for the most part to the present discussion; only those characteristics of each that are of importance need be mentioned.

MISTRAM stations exist at Valkyrian, Eleuthra, Bermuda, Grand Turk, Antigua, and Trinidad, other locations are not relevant. Only the Valkyrian and Eleuthra stations measure range and range rate; the others work in cooperation with these two.

This station distribution provides at least three stations (Grand Turk, Antigua, Trinidad) well placed for GEOS-C tracking; the Trinidad station is especially valuable. The Bermuda station is of no use to the experiment, the possibility of its relocation on Curacao for this experiment should be explored. MISTRAM's performance has been tested intensively, no testing on satellite tracking has been possible, but simulation tests<sup>22</sup> on a GEOS-C type satellite predict tracking errors (total) of 1-2 meters.

The major drawback to use of MISTRAM is that it requires the installation of a transponder in the satellite. The transponder's weight (8 kg) and volume (6.25 liters) do not present problems; the operating power of 37 watts does, however.

Use of SECOR for filling in vacant spaces in the Caribbean tracking net has several attractive features. First is the mobility of SECOR, which makes it possible to locate a tracking station at any desired site. Second is the probable availability of SECOR for the tracking; the principal geodetic mission of SECOR - providing control in the equatorial belt - will have been practically completed by the time GEOS-C is launched. Relocation of unemployed SECOR stations at Caribbean sites would be a logical and geodetically desirable expedient for tying the SECOR network to western hemisphere datums.

The above advantages of SECOR are balanced by several serious disadvantages. One of these is uncertainty in accuracy of the instrument. While SECOR should be capable of measuring range with s.d. of better than  $\pm 1$  meter, test results known to the present writer do not show that this capability is realized. Comparisons of ranges measured, presumably simultaneously, by radar and SECOR show differences of more than 5 meters<sup>48</sup>. Another disadvantage, possibly connected with the first, is the frequency range (200-500 MHz) in which SECOR operates. The range measurements are markedly affected by ionospheric refractions, and the uncertain accuracy of SECOR makes also uncertain the extent to which the double frequency operation of SECOR is able to correct for refraction.

---

These two drawbacks to SECOR can be removed to a great extent by colocating one of the SECOR stations at a MISTRAM or radar site. Such colocation could even turn the 500 MHz frequency of SECOR to advantage, since it would allow much better evaluation of atmospheric refraction. SECOR, like MISTRAM, requires a transponder in the satellite, but power consumption is considerably lower.

The above considerations lead to the recommendation that MISTRAM be included in the Caribbean tracking net and that the use of SECOR as an alternative to ballistic cameras be investigated. Also recommended is the use of laser ranging instruments instead of ballistic cameras, with planning for inclusion of the French stations in the project.

### Logistics (Caribbean)

The absolute category tests in the Caribbean will consist mostly of tracking the satellite from fixed tracking stations with near-simultaneous measurement of altitude from the satellite. Operation routines should therefore be about the same as that followed for other scientific satellites, in particular previous GEOS series satellites. This routine is well known, reasonably standard, and need not be detailed here. Only the principal exceptions will be noted.

1. Inactive optical-tracking stations called for in the experiment should be put into operation again before GEOS-C launch. Adequate time should be allowed for crew training, camera calibration, and operational checkout.
2. Altimeter data reduction computer programs should be ready (written and checked) long enough before launch to allow immediate use on data.

Some of these programs will involve using altimeter measurements for orbit determination. Until reliable estimates of measurement accuracy are available and the estimates are considered satisfactory, these programs should not be used in the experiment to improve the geoid. At this time an estimated lapse of 8-14 months from launch to use of altitude measurements for geoid and orbit improvement within the experiment does not seem excessive.

3. As a result of analysis of the data produced during the first month, it should be possible to decide which parts of the verification experiment plan have been satisfactorily completed, which require improvement, and so on. Experiment work in certain regions - especially those for verification of differential precision - may be able to be de-emphasized.

4. The altimeter measurements must be scheduled so that the instrument is not turned on while it is over land or outside the designated test regions.
5. The experiment calls for use of a tracking ship within the eastern Caribbean. Placement of this ship for optimum tracking geometry can be scheduled several months in advance, but the desirability of such placement must be weighted against the horizontal and, especially, vertical location errors.
6. Tide variations in the Caribbean are small, being less than 0.6 m in most places<sup>23, 24, 25</sup>. No special scheduling of measurements in relation to tides is necessary.

#### 4.3.1.4. Error Analysis (Caribbean)

The variance of the computed height of the altimeter above IMSL is approximately the sum of the variances of the heights of the altimeter above the spheroid and of the instantaneous mean sea surface above the spheroid. The value is approximate because (1) the component heights involved in computing instantaneous mean sea surface height above the spheroid do not lie on a common straight line with the height of the altimeter above IMSL, and (2) there is considerable correlation between the computed height of the altimeter above the spheroid and the computed height of the instantaneous mean sea surface above the spheroid. The first of these causes has very small effect, fortunately, on the variance; the effect of the second is difficult to estimate but is believed to be small and will not be considered in the analyses. The analysis is therefore broken up into two parts: analysis of the error in location of the altimeter in the spheroidal coordinate system, and analysis of the error in definition of IMSL in that system.

#### Satellite Location Errors (Caribbean)

Satellite (altimeter) location in a spheroidal system of coordinates is defined by two coordinates locating a sub satellite foot point on the spheroid and by a third, height coordinating fixing the altimeter above that point. The standard deviation in the third coordinate is of principal importance to the problem and will be discussed at length; errors in the other two coordinates are also important, however, and will be given adequate attention.

Satellite location in the spheroid coordinate system is computed from (1) tracking instrument locations in that system; (2) tracking instrument measurements; and with (3) assumptions regarding the satellite's motion as a function of time. The satellite location covariance matrix is therefore a function of the variances in tracking instrument location, tracking instrument measurements, and parameters in the satellite equations of motion. The form of this function is determined by the locations of the tracking instruments with respect to each other, by the type of measurement made by each instrument, and by the form of the equations of motion. Because function form is so closely allied with component s.d. size in determining the overall s.d. of satellite height above spheroid, we discuss the form factors--tracking instrument distribution, equations of motion, etc.--first, then the tracking instrument location s.d.'s, and finally the measurement s.d.'s.

#### Satellite Location Errors (Caribbean); Form Factor Effects

The station distribution specified for verification in an absolute frame of reference is such that the altimeter, while it is in one of the proper sub-regions designated above, is observable simultaneously by at least three electronic ranging stations and, in clear weather at night, by at least one optical tracking station. When the satellite is not in one of the proper sub-regions, it is observable simultaneously, under proper conditions, by at least two electronic ranging stations and one optical tracking station. Since, for planning purposes, optical tracking stations cannot be expected to observe the satellite on more than one out of three passes, and then only over a  $10^\circ$  (topocentric) arc unless a Baker-Nunn camera is being used, locations outside the proper sub-regions must rely on orbit theory to provide locations in most instances. An error analysis covering the entire verification experiment is discussed in appendices B and D of this report.

Looking only at the geometric (static or instantaneous) configurations that the satellite and tracking network can assume, we see that the following ones are significant. First (Figure 4-18a), the satellite and surface range tracking stations may be situated near positions that lead to minimum spherical rms error in satellite coordinates. Satellite and stations will be near vertices of a regular tetrahedron. Second (Figure 4-18b), the satellite may be nearly above one of the tracking stations. This will give an oblate error-ellipsoid for the station coordinates, with the minor axis vertical. Third, the satellite nadir may be well outside the triangle formed by the three ranging stations (Figure 4-18c), giving again an oblate spheroid but with the minor axis tilted and all axes larger than in the preceding situations. Corresponding to each of the preceding configurations there are two variations (not pictured) in which the satellite is either considerable higher than in the optimum situation or considerably lower. As the height increases, the equatorial axes of the error ellipsoid increases rapidly in length but the minor axes increase only slightly. As the height decreases from optimum, the spheroid becomes prolate, with the minor axis increasing rapidly in length and with the equatorial axes decreasing to a minimum that is slightly less than the smallest s. d. of the polar axis.

Addition of range-measuring stations to the configuration will result in decreasing the radius of the error-sphere but will not significantly alter the above conclusions. A drastic change in the error pattern occurs, however, if one or more direction-measuring instruments are included in the configuration, especially if the rms error of the direction-measuring instrument is, when converted to linear units, close to that of the ranging instruments. (In the case of GEOS-C, for instance, if we take the range s. d. as  $\pm 5$  meters and the satellite height as 1200 km, so that range varies from 1200 km to 2400 km, the required direction s. d. is about  $0^{\circ}5$  since angular error is approximately

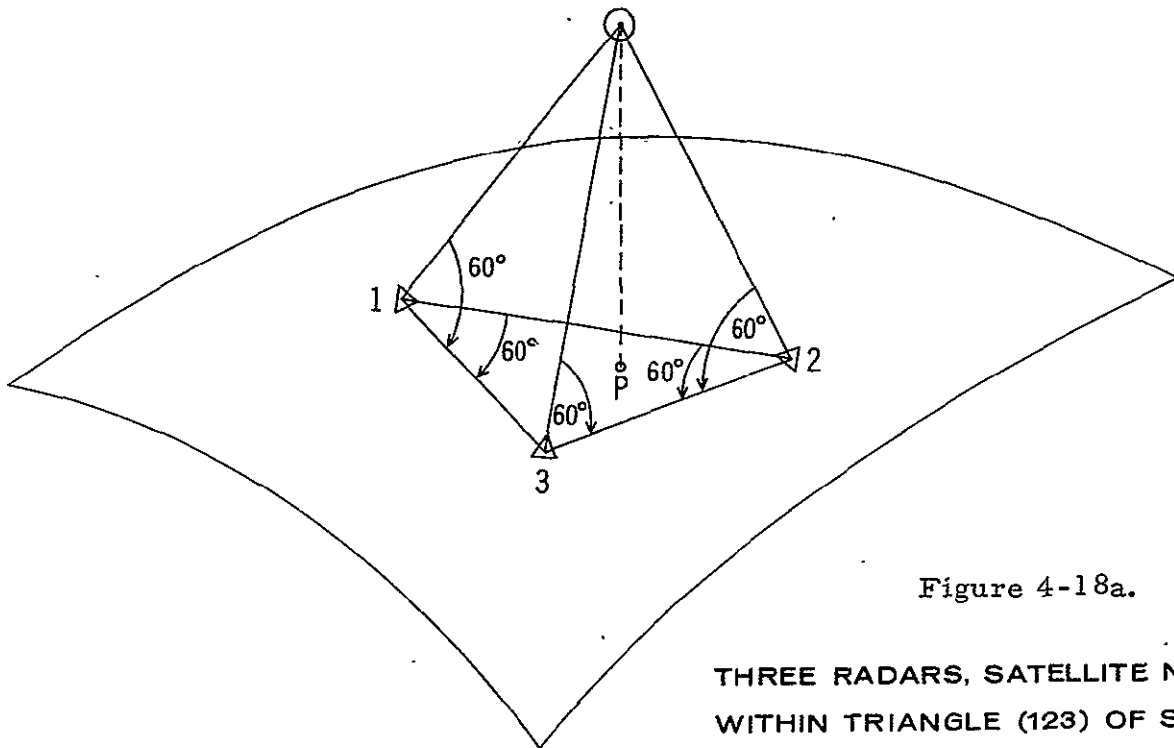


Figure 4-18a.

THREE RADARS, SATELLITE NADIR (P)  
WITHIN TRIANGLE (123) OF STATIONS

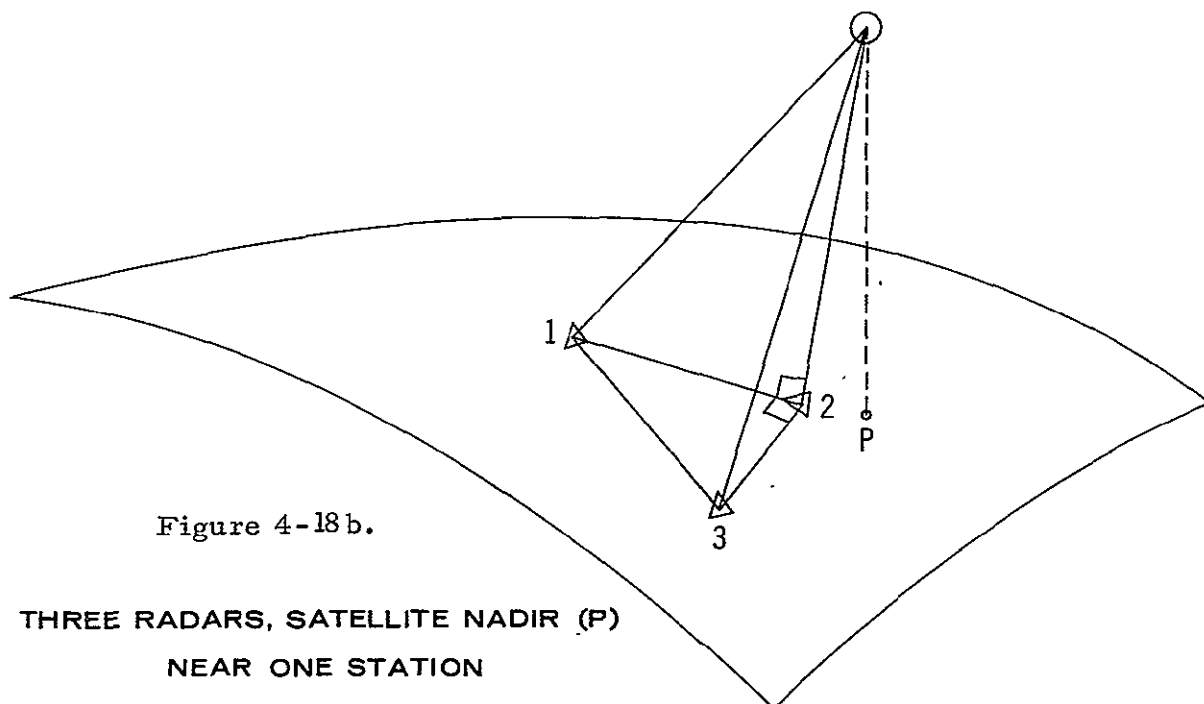


Figure 4-18b.

THREE RADARS, SATELLITE NADIR (P)  
NEAR ONE STATION

Figure 4-18. Geometric Arrangement of Ranging Station Locations

independent of distance.) While  $0''.5$  would be considered large by astronomers, artificial satellite trackers in general cannot average the object's coordinates over a period of minutes or even seconds as astronomers can, so that  $0''.5$  must be considered a small, though not unattainable s.d. for the GEOS-C experiment. Since a s.d. of  $\pm 2$  meters or less for the electronic ranging instrumentation may be possible, a s.d. of  $\pm 0''.2$  in each of right ascension and declination should be looked for. This is not an unreasonable goal, even using present equipment, if conditions are favorable, measurements precise, and if adequate data-reduction procedures are used. While many configurations of satellite direction-measuring instruments (referred to hereafter as cameras for convenience but without prejudice to other types), and range-measuring instruments (referred to hereafter as radars, again for convenience and without prejudice) can be conceived, only a few of these can be operationally realized while showing significant differences in the error ellipsoids. Experience of ESSA and the European Satellite Triangulation Network has shown that, as one would expect, simultaneous observations of a satellite by two cameras is considerably less frequent than observation of a single camera, while simultaneous observation by three cameras is very infrequent. Since even simultaneous observation by two cameras has an information redundancy of 33%, we can dismiss three-camera configurations as unnecessary and improbable. Of the two-camera configurations, we need consider only that in which the satellite and cameras are placed to minimize height s.d. with the satellite at a zenith distance (z.d.) of less than  $60^\circ$ . Below  $60^\circ$  simultaneous observation opportunities decrease rapidly and refraction-caused errors increase. As zenith distance decreases, on the other hand, the height s.d. increases. The two practical situations therefore appear to



be (1) both cameras observing near  $60^\circ$  z.d. and (2) one camera observing near  $60^\circ$  z.d. and the other observing near the zenith. The first of these is shown in Figure 4-18d; the second is not shown but has been subjected to error analysis.

Considering the total milieu within which the experiments will be carried out in the Caribbean (see preceding sections), the most frequent situation involving cameras will be that in which one camera observes simultaneously with two or three radars. (By "simultaneously" here, and elsewhere, is meant at times close enough together that location can be computed for a common time with a s.d. not significantly different from what would have been achieved with true simultaneity. Most camera-radar combinations permit simultaneous observation in this sense; laser-type ranging devices may be exceptions.) Considering again the error characteristics of radars and cameras, we see that in the three-radar, one-camera situation (Figure 4-18e), with the satellite height and radar station separations nearly equal, the camera placement is not critical; the camera information introduces a 67% redundancy and reduces the total rms error correspondingly. In the two-radar, one-camera situation, the redundancy is only 33%. The greatest variance in height will result when the camera is observing at maximum z.d. and the radars are observing nearly right angles to the line of sight of the camera (Figure 4-18f). The principal configurations of camera, radar, and satellite being defined, we proceed to make a numerical estimate of the s.d.'s. associated with the configurations. We do this by selecting radar and/or camera locations from the list (Table 4-5) of possible tracking stations in the Caribbean and contiguous regions to give surface configurations close to those discussed above. The satellite orbit elements  $a$ ,  $e$ ,  $i$  are taken from Appendix M elements  $\omega$  and  $\Omega$  are given a number of values to provide a representative set of longitudes, latitudes and heights for the satellite over the Caribbean, and  $\sigma$  is set arbitrarily equal to zero. Times are selected to give satellite locations at about 20 second intervals (corresponding to about 150 km distance

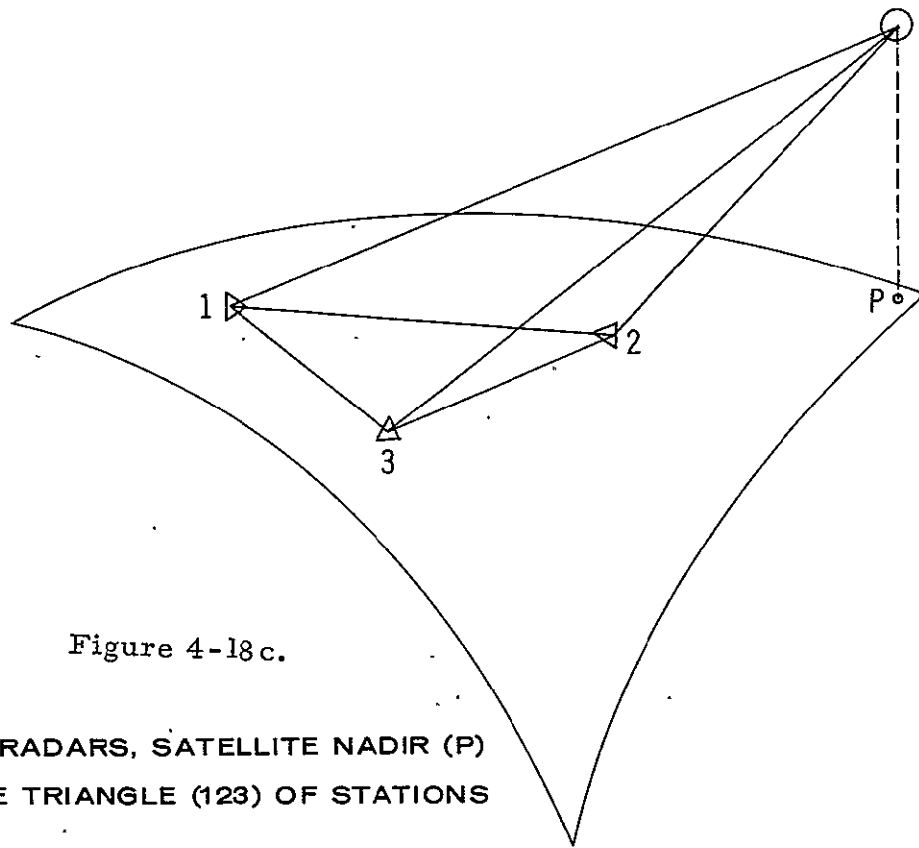


Figure 4-18c.

THREE RADARS, SATELLITE NADIR (P)  
OUTSIDE TRIANGLE (123) OF STATIONS

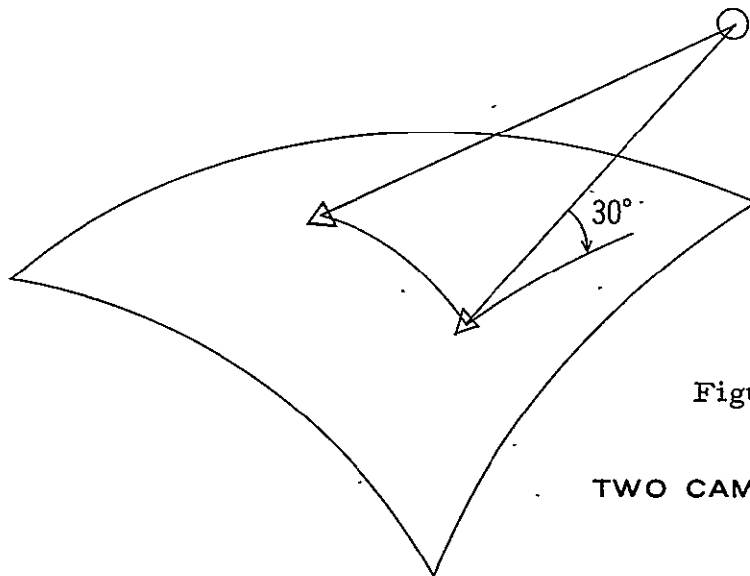


Figure 4-18d.

TWO CAMERA STATIONS

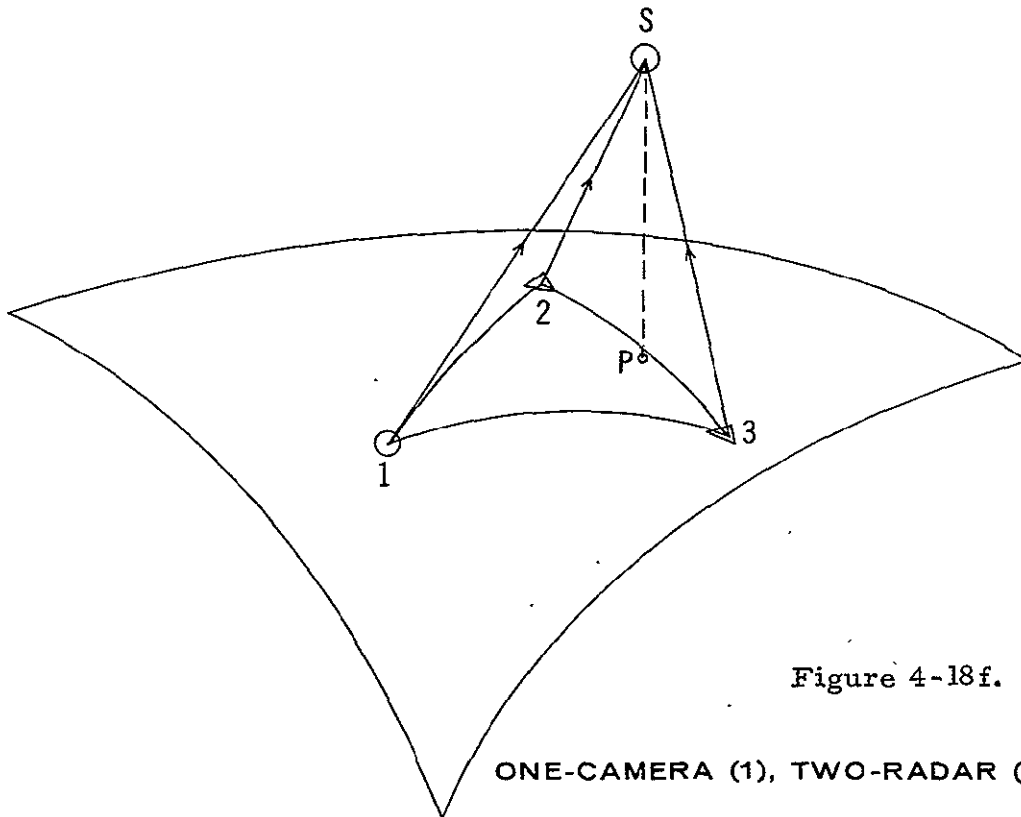
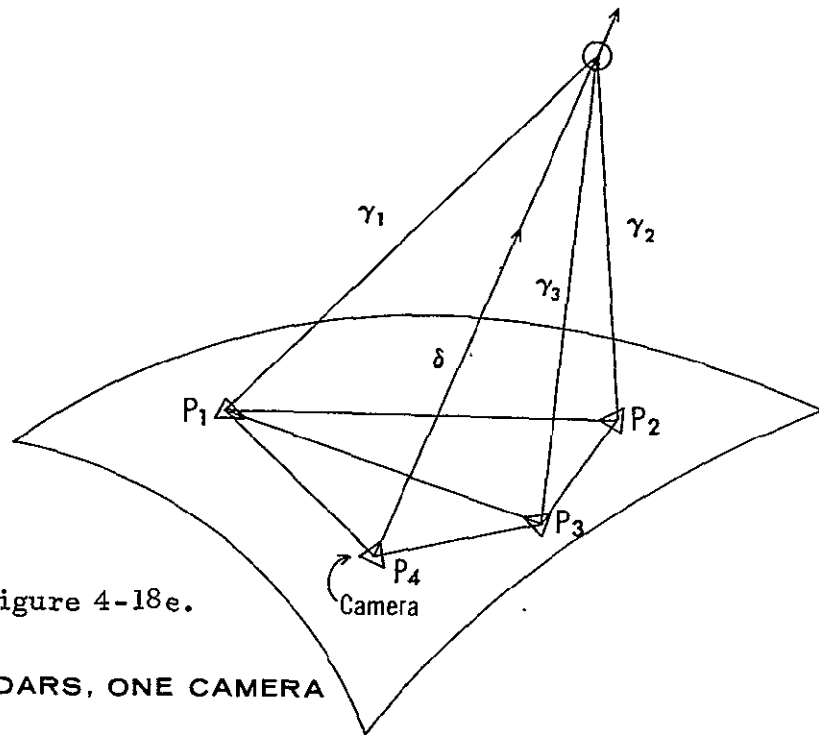


Table 4-5. Tracking Station Locations for the Caribbean

EARTH CONSTANTS									
RA = 6378388.000		E1 = 0.0819918899		E2 = 0.0					
LONGITUDE DDD MM SS.SSS	LATITUDE DDD MM SS.SSS	HEIGHT (METERS)	LONGITUDE (RADIAN)	LATITUDE (RADIAN)	X	Y	Z	Station Name	Station Number
279 24 1.780	28 13 33.980	15.0	4.87645855	0.49263848	918620.0	-5548636.5	2998655.5	CAPE CANAVERAL FPQ	1
279 18 22.930	28 30 28.220	3.0	4.87481576	0.49755565	907102.8	-5535488.1	3026124.4	CAPE CANAVERAL USB	2
279 36 42.690	25 30 24.600	18.0	4.88014755	0.44517822	961816.7	-5679453.1	2729898.4	HOMESTEAD FLA. PC-1000	3
285 29 43.960	24 7 5.520	13.0	4.98283724	0.42094200	1556190.9	-5613138.2	2590277.4	SAN SALVADOR FPS-16	4
273 12 6.440	30 25 17.060	28.0	4.76027073	0.53095369	307469.6	-5496418.0	3210804.9	EGLIN AFB FPS-16	5
262 37 17.920	27 39 11.780	6.0	4.58361238	0.48264065	-726079.4	-5607085.1	2942569.0	CORPUS CHRISTI USB	6
288 52 3.040	21 27 43.680	36.0	5.04168917	0.37458489	1920499.1	-5619715.3	2319132.2	GRAND TURK TPQ-18	7
298 12 23.840	17 8 35.000	42.0	5.20468740	0.29920276	2881682.0	-5372823.0	1868002.8	ANTIGUA FPQ-5	8
298 12 37.410	17 8 51.680	7.0	5.20475319	0.29928363	2881948.2	-5372470.7	1868482.5	ANTIGUA PC-1000	9
291 9 42.550	12 5 21.550	23.0	5.08173240	0.21099843	2251891.9	-5817218.7	1327085.8	CURACAO BAKER-NJNN	10
283 11 26.520	18 4 31.980	485.0	4.94261012	0.31547786	1384224.0	-5905981.0	1966510.0	JAMAICA MOTS 40	11
294 0 22.170	18 15 26.220	58.0	5.13137548	0.31864971	2465154.6	-5535226.7	1985490.0	SAN JUAN MOTS-40	12
298 23 23.670	10 44 32.780	269.0	5.20788635	0.18749093	2980052.6	-5513813.0	1181091.2	TRINIDAD PC-1000	13
276 3 29.870	17 24 16.570	83.0	4.81812621	0.30376762	642558.1	-6054269.4	1895656.1	SWAN ISL PC-1000	14
295 20 46.530	32 20 47.530	21.0	5.15476464	0.56455356	2309039.8	-4874621.5	3393019.8	BERMUDA FPQ-6	15
281 25 14.810	0 37 28.000	3649.0	4.91171920	0.01089861	1263650.8	-6255300.0	-69086.7	QUITO MOTS	16
279 25 23.770	28 28 52.790	14.0	4.87685605	0.49709299	918626.0	-5535018.1	3023547.6	CAPE CANAVERAL FPS-16	17
293 0 0.0	18 15 0.0	0.0	5.11381470	0.31852259	2367653.8	-5577842.8	1984706.2	PUERTO RICO 2 TRANSPONDER	18
293 30 0.0	18 45 0.0	0.0	5.12254135	0.32724923	2409236.5	-5540864.5	2037190.0	PUERTO RICO 3 TRANSPONDER	19
294 0 0.0	18 15 0.0	0.0	5.13126799	0.31852259	2464639.9	-5535672.0	1984706.2	PUERTO RICO 4 TRANSPONDER	20
283 11 0.0	18 0 0.0	0.0	4.94248155	0.31415926	1383950.0	-5908231.0	1958408.4	JAMAICA 2 TRANSPONDER	21
291 10 0.0	12 0 0.0	0.0	5.08181700	0.20943951	2253120.4	-5818930.0	1317417.7	CURACAO 2 TRANSPONDER	22
276 30 0.0	12 0 0.0	0.0	4.82583538	0.20943951	706378.0	-6199800.6	1317417.7	BLUEFIELDS RECEIVER	23
271 0 0.0	18 30 0.0	0.0	4.72984227	0.32288591	105601.4	-6049902.8	2010966.9	CHETUMAL RECEIVER	24
274 30 0.0	11 0 0.0	1500.0	4.79097879	0.19198622	491423.6	-6244129.8	1209306.1	NICARAGUA RECEIVER	25

between nadir points); satellite and station locations are then used to calculate the elements of the geometric structure matrix, and the variances in satellite coordinates computed from the matrix and the variances of station observations and stations locations (see Appendix B).

Table 4-6 gives the tracking station combinations used in the analysis. Some of these combinations contain stations not included in Table 4-5, such stations are assumed to be relay stations (transponders or reflectors) or simple receiver stations. The special sites selected for these stations are given in Table 4-5, Category D. Not all combinations of stations from these categories need be taken; the few combinations given in Table 4-6 give a completely adequate idea of the variances to be expected from any of the practicable combinations. Table 4-7 summarizes the result of the error analyses for the 15 different tracking station combinations.

Table 4-6  
Station Configurations  
(See Table 4-5 for locations)

SET	RADAR			CAMERA
A	San Salvador	Eglin	Corpus Christi	Homestead
B	San Salvador	Grand Turk		Homestead
C		Grand Turk	Antigua	Curacao
D	San Salvador	Grand Turk	Eglin	Jamaica
E	San Salvador	Grand Turk		Swan
F		Grand Turk	Antigua	Jamaica
G	San Salvador	Grand Turk	Antigua	
H	San Salvador	Grand Turk	Antigua	Swan
I		Grand Turk	Antigua	Puerto Rico
J	San Salvador	Grand Turk	Eglin	
K	San Salvador	Grand Turk	Eglin	Jamaica
L		Grand Turk	Antigua	
M		Grand Turk	Antigua	Curacao
N	Curacao	Grand Turk	Antigua	
O	Curacao	Grand Turk	Antigua	Curacao
P	Puerto Rico#2	Puerto Rico#3		Puerto Rico
Q	Puerto Rico#2	Puerto Rico#3	Puerto Rico#4	
R	Puerto Rico#2	Puerto Rico#3	Puerto Rico#4	Puerto Rico

HEIGHT ERROR (in Meters)

Station Type	A *	B	C	D	E	F	G	H	I	J	K	L	M	N	O	P	Q	R
Radar ***	4, 5, 6	4, 7	7, 8	4, 6, 7	4, 7	7, 8	4, 7, 8	4, 7, 8	7, 8	4, 5, 7, 8	4, 5, 7, 8	7, 8, 21	7, 8, 21	7, 8, 21, 22	7, 8, 21, 22	18, 19	18, 19, 20	18, 19, 20
Camera **	3	3	10	11	14	11	-	14	12	-	11	-	10	-	10	12	-	12
Satellite Position ***																		
103	6.2																	
104	5.8			5.9	7.9													
105	5.6	6.3		5.4	8.1													
106	5.5	5.7		5.2	7.8					77.3	4.9	7.8	5.4	7.7	5.4			
107		5.0	6.0		6.7		57.5	6.9	5.7	57.0	4.5	5.2	4.3	5.2	4.3			
108		4.4	5.2		5.4	5.7	39.5	5.5	4.8			4.1	3.7	3.8	3.6			
109		4.6	4.8		5.1	4.9	27.5	4.5	4.3			3.9	3.6	3.2	3.3	4.2	36.1	3.7
110		5.7	4.6			4.3	18.7	4.3	4.2			4.2	3.8	3.3	3.3	3.8	12.2	3.2
111			4.5			4.2	11.2	5.0	4.2			4.8	4.1	4.1	3.7	3.9	16.8	3.2
112			4.7			4.8	5.9	6.4	4.4			5.9	4.7	5.4	4.3	4.5	42.8	3.9
208		6.9		6.0	8.2													
209		6.4		5.7	8.3													
210		5.9		5.5	8.0					92.9	5.2	7.8	5.3	7.3	5.2			
211		5.4	6.3		7.1	6.4	88.9	7.3	5.9	82.3	5.0	7.0	4.5	5.4	4.2			
212		5.4	5.9		6.4	5.9	71.3	6.3	5.1			7.3	4.4	4.3	3.7			
213		6.0	5.7		6.5	5.4	60.4	5.9	4.8			8.0	4.5	4.0	3.6			
214		7.1	5.6			5.1	53.5	5.9	4.6			9.1	4.8	4.3	3.7			
215			5.6			5.2	48.6	6.6	4.7			10.5	5.1	5.2	4.2			
216			5.8			6.0	44.3	7.8	5.0			12.4	5.6	6.8	4.9			
308					8.6													
309			7.5		8.6		250.7	8.7	7.2			13.6	5.9	9.4	5.5			
310			6.7		7.8	6.5	135.8	7.9	5.9			10.3	5.1	6.2	4.4			
311			6.2		6.7	6.0	77.8	6.7	5.0			8.2	4.8	4.4	3.8			
312			5.7		6.5	5.1	44.3	5.6	4.5			6.7	4.5	3.6	3.6			
313			4.9			4.4	21.2	5.1	4.3			5.4	4.3	3.8	3.6			
314			4.5			4.4	5.1	5.8	4.3			5.1	4.3	5.0	4.1			
401																3.8	8.3	3.1
402																3.8	6.6	3.1
403																3.8	6.9	3.1
404																3.8	7.8	3.1
405																8.9	10.6	3.2
406																4.0	16.0	3.2
501																3.8	6.7	3.1
502																3.8	3.9	3.1
503																3.8	4.4	3.1
504																3.8	6.5	3.1
505																3.9	10.5	3.2
506																3.9	13.6	3.2
601																3.8	6.0	3.1
602																3.8	4.1	3.1
603																3.8	4.7	3.1
604																3.9	7.3	3.1
605																3.9	10.6	3.2
606																3.9	14.2	3.2

\* Station Configurations are given in Table 4-6  
 \*\* See Station numbers in Table 4-5  
 \*\*\* See Satellite Positions in Tables A-10 and A-11 (Appendix A)

Table 4-7. Results of Error Analyses for the Caribbean

### Satellite Location Errors (Caribbean); Observation Error Effects

At least three distinct kinds of tracking equipment will be used for observing the altimeter satellite: radar, laser ranging, and camera. Each kind of tracking equipment will be present in several types, each with its own characteristic set of standard deviations. The literature on the standard deviation of a unit observation is voluminous for radar (see e.g., ref. 43-48) and cameras (see e.g., ref. 56-58); literature on laser range errors is scanty but increasing (see, e.g., ref. 59-61). It is not the purpose nor the responsibility of this study to present either a critical analysis of the range and direction errors, nor are the resources available for the study adequate to permit estimation of the effects of these errors in their many possible combinations. The problem of best accounting for measurement errors has therefor been solved by using, for all tracking instrument measurements of a given kind, the same nominal standard deviations regardless of the exact type of instrument, satellite location or velocity, etc. These standard deviations are considered as being reasonable estimates of what the tracking errors are at present in well-run systems. The nominal values for the standard deviations are (in absolute value):

Instrument	Measurement Standard Deviation		
	<u>Systematic</u>	<u>Random</u>	<u>Total</u>
radar	4-4.8 m.	1-2 m.	5 m.
laser	1-1.5 m.	1-1.5 m.	2 m.
camera	0!5	0!8-1!8	1"-2"

### Satellite Location Errors (Caribbean): Station Location Error Effects

The resultant standard deviations in satellite locations given are dependent not only on the observation error standard deviations but also on the errors present in the tracking station location given. A discussion of the difficulties caused by combining errors of the station location type with standard deviations will be found in Appendix H. Such difficulties can be traced to the circumstance that the standard deviations given for satellite locations are in large part measures of scatter of satellite locations while the standard deviations given for station locations are more like error-limit estimates.

In Table 4-8 column 2, the standard deviations for horizontal coordinates of certain of the tracking stations neighboring the Caribbean are listed. Those data, however, were computed on the assumption that the standard deviation increases in accordance with Simmons' formula<sup>26,27</sup>. Ref. 4 notes that the values derived are of doubtful meaning because the quantities used in the formula do not have precise meaning. Using that reference's own estimate of the meanings of the quantities, we get the value given in the third column of Table 4-8. The fourth column gives the values that could be expected if the results of the C&GS satellite survey were used. Since the C&GS stations do not approach any of the VEDS stations except near Antigua, the method of incorporation is not straightforward, as the table would indicate, but must be indirect, i.e., by interpolation via the triangulation network. The final solution would make use not only of C&GS data but also the GEOS tracking data themselves; hence, a self-consistency of  $\pm 2$  meters in horizontal location throughout the Caribbean and Gulf of Mexico tracking network (exclusive, in other words, of stations farther north than Cape Canaveral and farther west than Corpus Christi) should be attainable.

The question of determining the vertical coordinate s.d's. is another kind of problem. Station heights above mean sea level can be assumed to have s.d's. of less than 0.1 meter in the Caribbean and Gulf of Mexico, since these heights have been determined by or (as in the case of Antigua and perhaps other stations) can be determined by spirit levelling. The 0.1-meter



Table 4-8. Standard Deviations of Horizontal Coordinates of Certain Tracking Station Sites Relative to Grand Turk Station\*

Station	S. D. (original)	S. D. (reduced by 67%)	S. D. (with C&GS data)**
Grand Turk	0	0	0
San Salvador	5	2	1
Grand Bahama	8	3	2
C. Canaveral	10	3	2
Antigua	10	3	2
Curacao	15	5	3
Guaymas	23	8	6

\* Based on data in Ref. 28

\*\* B. Chovitz, 1968, private communication

estimate is probably close to a  $3\sigma$  value, so it is certainly a safe  $1-\sigma$  value. Since we intend to provide horizontal coordinates for the stations to  $\pm 2$  meters, we can assume that geodetic distances between stations are known to  $\pm 2$  meters. In view of the small area involved, the corrections to these distances for geoid-above-spheroid can be neglected. Differences between mean sea level and a Caribbean geoid are less than  $0.5 \text{ m}^{19}$  in most places; the error in the difference is estimated, therefore, at less than 0.3 meter.

The most important contribution to the total standard deviation of instrument vertical coordinate error is made by the uncertainty in geoid-spheroid separation. This uncertainty or error can have a standard deviation of much less than 1 m. near the datum point, and can increase to 20-30 m or more at distances of 2000 km or more away. The subject of geoid-spheroid separation errors is extremely complicated. Since it must also be considered in deriving the s.d. in IMSL above spheroid, detailed discussion of the general problem is deferred to the next section. The problem of errors in tracking instrument heights above the spheroid is somewhat different from the more general problem in that these heights can also, and in some cases have been, determined from the satellite observations themselves. The size of the s.d.'s in vertical coordinate varies with the kind of instrument used, method of data reduction used, etc. Baker-Nunn camera locations, for example, have spherical s.d.'s of about  $\pm 12$  m. (ref. 62). Some of the C&GS satellite tracking network stations (optical) in the Caribbean have s.d.'s of about  $\pm 3$  m. in height (ref. 63). Some of the radar stations in the Caribbean region have vertical coordinate s.d.'s of the same order of magnitude (ref. 64). A properly conducted experiment would therefore combine the surface survey information with satellite-tracking derived information to arrive at the finally adopted and used values for satellite location in the spheroidal reference system.

The variances of station location coordinates determined directly from observations of the satellite in range, direction, and even velocity coordinates are basic to the location problem. As long as the satellite locations are going to be derived ultimately by statistically fitting data to short segments of the orbit, the variances derived directly from observations will be much more important than variances resulting from theoretical deficiencies in the orbit. The orbit, in fact, serves primarily as a means of smoothing the observational data. If the tracking stations are located closely enough together, then between fixes the satellite follows a trajectory that is smooth to within the resolving power of the tracking instruments. If the tracking devices were free of systematic errors, the short segment procedure could then be used to find the altimeter accuracy standard deviation or precision standard deviation to any desired degrees of confidence. (This would not be true if a full orbit were used for trajectory fitting, because an orbital trajectory computed from observations over a complete revolution or more contains systematic errors that cannot be removed.) The next step is therefore to modify the results of the preceding analysis of isolated observation errors by applying the orbit equations in such a way as to smooth out the observations.

(Eventually, when altimeters height variances are being computed from actual data, the satellite-above-spheroid variances will be computed in a single step. During the planning stages, the analysis procedure is subdivided into short steps to ensure that no critical details are overlooked.)

The effect of the orbit on satellite location variances is accordingly considered in two parts. First, the variation of a computed orbit from the true orbit is considered. Then the amount of smoothing done by the computed orbit on the satellite coordinates is estimated.

The purpose of the first part is to find over what length of arc a computed orbit (actually, an orbit segment) can be trusted. If the segment were made significantly longer than this without correction from observations, a significant systematic error would be introduced into the satellite altitude by the orbit and, as shown in Appendix H, this error would appear in and could not be removed from the standard deviation of the altimeter measurements as computed. The equations to be used are derived and given in Appendix D. Resources were unfortunately insufficient to permit the computation of representative deviations from data available for various parts of the Caribbean. An estimation method was used which is considerably less realistic, but also considerably easier to perform by hand. This method is reasonably familiar to most people working on satellite dynamics, and an outline is presented here.

The estimation method assumes the existence of pulse or impulse type forces along a typical trajectory in the normal, tangent, and binary directions and of integrating the accelerations over very short segments. Within an orbital period of 110 minutes, the satellite passes through a 16-th degree tessera in 7 minutes. Perturbing accelerations can therefore be considered to be applied over intervals of 7 minutes or less if present-day orbits are considered reliable as far as the 16-th degree harmonics. (Whether orbits are actually reliable to this extent is arguable; see e. g., Ref. 27).

An examination of actual gravity anomalies shows variations of 20 to 40 milligals per 100 km to be common, with variations of 100 milligals over 100 km to be a frequent occurrence in regions of high relief. Taking a value of 200 milligals per 100 km for the gravity perturbation magnitude in the Caribbean, the 100 km corresponds to a wavelength of  $2\pi/400$  and the rate of diminution of the acceleration with height would be about  $(6.4/7.4)^{402}$ , which is close enough to zero to be ignorable. Assuming instead an average acceleration of 50 milligals over the 7 minute interval, the attenuation at satellite height would still be about  $(6.4/7.4)^9$  or one-sixth of sea-level

value. An acceleration of 20 mgal acting for 7 minutes, treated as an impulsive perturbation, produces about 1.5m change in height. This is an order-of-magnitude estimate only, because of (1) the lack of knowledge concerning the surface gravity variations in the Caribbean and (2) the lack of knowledge of the accuracy variances of the gravity field coefficients.

A closer estimate would result by using the equations in Appendix D, with a reasonable estimate of the variance in  $F_N$ ,  $F_T$  and  $F_B$ . For the present work, the value 1.5m can be used if its tentative nature is understood. Hence, a spacing of  $85^s$  or 600 km between fixes would reduce the deviation between true and computed orbit to 0.1 meter. The value of 600 km is taken as the maximum allowable gap between areas of triple coverage (see Figures 4-12(a), 4-12(c) since a distance greater than this will result in the introduction of 0.1m error into the satellite height. Since the above estimates are of the "worst-case" variety, the allowable spacing might be more like 1200 km or greater if more exact calculations were carried out.

With the geometric error estimated and the length of the "no-data" interval established, the last estimate needed is the reduction in satellite height error that can be expected by using a set of orbit equations as a constraint on the observations. The theory required for such estimation is discussed in Appendices D and H, where equations are derived by which the standard deviation of satellite height above the spherical may be computed, given the satellite orbit parameters and the s. d. of the observations. These equations must be applied with great care, as explained in Appendix H, to avoid getting the systematic and random errors confused. They have not been used for computation in this study because of lack of available time. It is not necessary to use them if, as at present, an order-of-magnitude estimate is sufficient.

The explanation of the theory given in Appendix E is enough to show that the results of introducing the orbit as a constraint is equivalent (for short segments) to smoothing out the observations. The analysis of Appendix H shows that systematic errors in the tracking data will remain. Furthermore, the analysis of orbit accuracy in the preceding paragraphs shows that systematic variations of the computed orbit from the theoretical orbit, insofar as they arise from theoretical deficiencies, can be made negligible. Therefore, ignoring the minor corrections that adherence to small-sampling theory would entail, the following conclusions are made:

- (1) over the segment lengths of concern within the Caribbean, simultaneity of observation by different tracking stations is not essential;
- (2) the standard deviation of the satellite height is given approximately by

$$\sqrt{3} \sigma_1 / \sqrt{n}, \quad (4-2)$$

where  $n$  is the number of independent observations on the satellite in a region where the geometric situation gives a standard deviation of  $\sigma_1$ ;

- (3) the standard deviation given above does not take into account the systematic errors in the observations. These errors cannot be removed statistically but must be removed either empirically or by locating the cause of the systematic errors.

In summary, then, the satellite altimeter location can be found, using orbital constraints on its motion over short segments of the orbit and so on, to within 1-2 meters.

All possible corrections are made and to within 2-6 meters if the systematic errors present in ground tracking station instruments are not removed.

## Geoid-Above-Spheroid Separation Errors (Caribbean)

The foregoing discussion estimated the geoid-spheroid separations at the tracking stations. At these stations, the possibility exists of continually reducing the mean square error by forcing agreement between satellite observations and the orbit. No such possibility exists for getting a better geoid at general points in the Caribbean unless the altimeter measurements themselves are used. Such use is, of course, out of the question, at least in the early stages of the experiment. Knowledge of the geoid in the Caribbean must, therefore, be derived from sources other than altimeter data.

There are three major routes to the determination of the geoid-above-spheroid separation: (1) through astrogeodetic measurements, (2) through gravimetric measurements, and (3) through relation to satellite motion. Of these, only the astrogeodetic method rests on a secure theoretical foundation; the other two at present, involve assumptions which are known to be theoretically unsound. The task of evaluating standard deviations for the astrogeodetic method in the Caribbean is not much easier than doing it for the other two, however, because there are insufficient data readily available for exact analysis. For these reasons, a rough estimate only of the s. d. 's is made here; a critical evaluation should be made as part of the final design. The estimation will be carried out here for each of the three methods separately, and the results of combining the methods then estimated.

1. The astrogeodetic method for getting the geoid height  $h_i$  at a point  $P_i$  depends basically on measuring the slope  $s_i$  of geoid with respect to spheroid at a number of points  $P_i$  between  $P_I$  and an initial point  $P_I$  at which the geoid height  $h_I$  is known. To a satisfactory approximation,  $h_i$  is given by:

$$h_i = h_I + \int_{P_I}^{P_i} \tan \zeta \, ds, \quad (4-3)$$

the integral being taken along some path on the spheroid,  $s$  being the distance (on that path) from  $P_1$  to the point where  $\zeta$  is measured. Two major sources of error occur:

- (a) The slopes  $\zeta$  are measured with appreciable errors. On land,  $|\sigma_\zeta|$  is about  $0''.3$  if a good first-order set of observation is made; a  $|\sigma_\zeta|$  of  $0''.1$  is obtainable but the median is probably closer to the former value. Measurements of  $\zeta$  at sea are feasible using gyroscopic reference axes or stabilized platforms, as with the SINS system or the GEON. The s. d. 's are then much greater, the magnitude depending the state of the ocean, the kind of navigation system used, distance from location reference stations, etc. Under favorable conditions,  $|\sigma_\zeta|$  can be assumed to be about  $7''$ ; during an extended cruise in mid-ocean, it could conceivably be much greater. If navigation is by observation on a TRANSIT-type satellite, then it would be fallacious to assume that the navigation s. d. of  $\pm 6''$  can be compounded with the  $\pm 7''$  s. d. with excellent knowledge of location to give  $\pm 9''$  s. d. for  $\zeta$ . A number of  $\zeta$ 's will have been measured between navigation fixes, and these will, therefore, have correlated errors. Considering navigation uncertainties as they now exist, an estimate of  $\pm 20''$  would probably be closer to the truth. Navigation fixes in parts of the Caribbean will be quite good, and  $\pm 7''$  should be obtainable over large regions.
- (b) The second major cause of error in determining  $h_I$  is the discreteness of the measurement intervals.  $\zeta$  is not measured continuously along the curve joining  $P_1$  to  $P_I$  but is measured at  $I$  points along the curve, with intervals  $\Delta S_i$  between points  $P_i$  and  $P_{i+1}$ . The formula employed for determining  $h_I$  is, therefore



$$h_I = h_1 + \sum_{i=1}^{I-1} \tan \zeta_i \Delta S_i \quad (4-4)$$

The error is, therefore

$$\delta h_I = \sum_{P_i}^{P_{i+1}} \int \tan \zeta ds - \tan \zeta_i \Delta S_i \quad ; \quad (4-5)$$

or, if  $\bar{\zeta}_i$  is a suitably chosen value, by

$$\delta h_I = \sum (\tan \bar{\zeta}_i - \tan \zeta_i) \Delta S_i \quad (4-6)$$

The length  $\Delta S_i$  may be as low as 20km or as high as 200km, depending on the epoch of the observations and the topography along the circuit. The difference  $(\tan \bar{\zeta}_i - \tan \zeta_i)$  depends on the topography and geology between  $P_i$  and  $P_{i+1}$ . It can be reduced by using gravimetric measurements between  $P_i$  and  $P_{i+1}$ , but in mountainous regions or regions of great geological inhomogeneity, a very dense set of gravity measurements is required to get deflections to better than 1". An order-of-magnitude estimate can be made for the Caribbean region using 6000km as the distance from  $P_1$  to  $P_I$ , 60km for  $\Delta S_i$  and  $\pm 3''$  for  $\sigma_\zeta$ . The result is  $\pm 9$  meters. The contribution of the measurement s.d.  $\sigma_s$  can be neglected.

No measurements of  $S$  within the Caribbean have been made as yet. Taking  $\pm 7''$  as the s.d. of a GEON or SINS measurement, assuming that measurements are made at intervals of 5km, and that navigation errors are negligible, we come up

with an estimated  $\sigma_h$  of  $\pm 0.7$  m per 100km. This is somewhat better than intercomparison of the SINS, GEON, and gravity-geoid results would indicate for 100km, but is still reasonable. The results obtained by such surveys over extended distances in the Caribbean - getting a profile between British Honduras and Jamaica, for instance - would be poorer because of the greater distance involved as well as because of the greater navigation errors.

2. There are a number of ways of applying gravimetric data to the determination of geoid heights. One is to apply Stoke's formula (or a suitable modification thereof) to the problem using gravity data throughout the world. This method, while theoretically possible, is out of the question for the Caribbean region because of the accuracies required. If we write for the formula to be used,

$$h_1 = \frac{1}{2\pi g_o a_o} \iint \Delta g(\rho, A) \tilde{F}(\rho) d\rho dA \quad (4-7)$$

where  $\tilde{F}(\rho)$  is a suitable weighting function,  $\rho$  is the length from  $P_1$  to  $P$  on the sphere,  $A$  is azimuth, and  $a_o$  and  $g_o$  are average radius and gravity for the spheroid, then the error  $\delta h_1$  is

$$\delta h_1 = \frac{1}{2\pi g_o a_o} \iint_{\Delta S_i} \Delta g(\rho, A) \tilde{F}(\rho) d\rho dA - \Delta g_i \tilde{F}(\rho_i) \Delta S_i \quad (4-8)$$

Or, using the law of the mean, the error  $\delta h_1$  contributed by the difference over the small area  $\Delta S_i$  is

$$\delta h_1 = K [\Delta g(\bar{\rho}_i, \bar{A}_i) \tilde{F}(\bar{\rho}_i) - \Delta g(\rho_i, A_i) \tilde{F}(\rho_i)] \Delta S_i \quad (4-9)$$

These differences become appreciable where gravity data are sparse, even though  $\tilde{F}$  becomes small for large  $\rho$ . The proper

approach is therefore to compute  $h$  not as an "absolute" value but relative to an  $h$  taken as standard within the Caribbean. The formula then becomes, for this difference  $\Delta h$ ,

$$\Delta h_2 = K \iint \Delta g [\tilde{F}(\rho) - \tilde{F}(\rho_1)] d\rho dA \quad (4-10)$$

where the distance  $\rho_1$ , is the distance from the point  $P$  to  $P_i$ . The difference  $\tilde{F}(\rho) - \tilde{F}(\rho_1)$  approaches zero more rapidly than  $\tilde{F}(\rho)$  or  $\tilde{F}(\rho_1)$  if the region over which  $\Delta h_2$  is to be computed is of moderate size.

There are too many unknowns contained in the gravimetric formulae to allow them to be used to derive an unobjectionable estimate of the variance of a geoid height. If we assume that values of gravity are available for all  $1^\circ \times 1^\circ$  tesseræ within a region the size of the Caribbean and if we assume that these values give average values that differ from the true averages  $\Delta g(\bar{\rho}, \bar{A})$  by  $\sigma = \pm 5''$ , then the variance of  $h$  calculated at a point within the region comes to about  $\pm 1$  meter. There are too many questionable assumptions involved in the estimate to allow it to be trusted.

Because gravity values in the Caribbean are sparse, the calculation of geoid heights based on isostatic considerations offer a better chance at present of computing geoid heights than does the straightforward computation using the modified Stokes' formula. If isostasy is assumed throughout a region, a few free air gravity anomalies actually measured can be used in the estimation of gravity anomalies and geoid heights in the region. The method has been used for computation of the geoid along the chain of islands from Florida to Antigua<sup>29</sup>. A standard deviation of  $\pm 1$  to  $\pm 2$  meters is estimated for the geoid heights. If isostasy does not obtain, however, the method will give erroneous answers.

3. The third method of finding the geoid height  $h$  is to go through the following series of equations:

$$\begin{aligned} r_j &= r_j(\vec{X}_s, \vec{X}_j) \\ a_j &= a_j(\vec{X}_s, \vec{X}_j) \\ \delta_j &= \delta_j(\vec{X}_s, \vec{X}_j), \text{ etc.} \end{aligned} \quad (4-11)$$

where  $r_j$ ,  $a_j$ , and  $\delta_j$  are range, right ascension, declination, etc., observations and  $\vec{X}_s$ ,  $\vec{X}_j$  are the satellite and observing station  $j$  vectors, respectively, each  $j$  representing an observation.

$$\vec{X}_s = \iint (\nabla V + \vec{F}) dt^2 \quad (4-12)$$

where  $V$  is the (earth-) gravitational potential and  $\vec{F}$  is the composite vector of nonterrestrial gravitational forces. From (4-11) and (4-12), the constants  $C_n^m$  and  $S_n^m$  in the potential

$$V = \frac{k^2 M}{a_o} \sum_n \frac{a_o}{r}^{n+1} \sum_m P_n^m(\cos \phi') [C_n^m \cos m \bar{\lambda} + S_n^m \sin m \bar{\lambda}] \quad (4-13)$$

are determined, where  $r$ ,  $\phi'$  and  $\bar{\lambda}$  are the satellite coordinates.

$V$  is set equal to some suitable value  $V_o$  that will give the geoid height at the selected datum point. The equation is then solved for  $r$  at longitude  $\lambda$  and latitude  $\phi'$ , and the resulting  $r$  converted to height above the spheroid. This height should be further corrected for the gravitational attraction exerted by matter (mass) outside the reference sphere of radius  $a_o$ .

Because the satellite motion is insensitive to gravity perturbations of short wavelength (except for resonance frequency perturbations), because there are theoretical difficulties in the way of bringing the gravity values down to the surface, and for other more involved

reasons, geoid heights derived in this way are not as trustworthy as heights derived from astrogeodetic data or, for limited areas, from gravimetric data. The reliability of orbit-derived geoids cannot be computed from satellite data alone, since these give merely estimates of the consistency of the geoid relative to the observations that went into the computation of orbit constants.

Comparison of geoids derived by different people gives another method of estimating satellite geoid accuracy, and comparison of satellite geoids with astrogeodetic and gravimetric geoids give still another method. None of the above methods is particularly satisfactory. A comparison of three geoids (Ref. 10, 30, 31) shows differences of up to 15m. A realistic estimate of the s.d. of a given satellite geoid over the whole earth is  $\pm 10$ m. In selected regions, this could be  $\pm 1$  meter.

The preceding discussion has analyzed the errors in geoid-spheroid separation as derived independently by three different methods. An important question to be answered is: what is the standard deviation in geoid-spheroid separation if the best possible values are derived by a combination of the three methods? This question cannot be answered at present. A simple averaging process is definitely not satisfactory. All three methods provide geoids whose heights above the reference spheroid contain large systematic errors. Such errors can be removed only by using an approach that accounts properly for the causes of the systematic errors. Given an adequate amount of gravity data in the Caribbean, a careful fitting together of astrogeodetic, gravimetric, and satellite geoids should enable determination of a single Caribbean geoid in which the systematic error is less than 1 meter with a probability of 67%. This estimate is based on the figures given previously for the s.d.'s of geoid heights computed by the different methods independently, but is obviously not easily justified since no attempts have been made, as far as we can determine, to derive a geoid of this kind for the Caribbean.

(Work done in the past toward combining astrogeodetic, gravimetric and satellite data has been carried out in order to get best values over the entire Earth; the results have been less than optimum over restricted areas.)

#### Errors in Estimation of Instantaneous Mean Sea Surface with Respect to the Geoid (Caribbean)

An estimate is derived here of the amount by which the true instantaneous mean sea surface may differ from the computed IMSL surface. A large number of assumptions must be made, but if Sturges' estimate<sup>19</sup> of 0.5m variation in topography over the Caribbean is anywhere near correct, the errors incurred in estimating these errors should be considerably smaller than this even if the assumptions are not very good. We proceed from geoid to IMSL by the following steps:

Estimate the variance in the height of mean sea level (MSL) above the geoid - i. e., find the difference in mean sea level minus geoid height. The principal contributors to the deviation of mean sea level from the geoid are differences in specific volume at corresponding depths, geostrophic water accumulation, and differential air pressure. Given two adjoining water columns of equal areas, one column will rise to a greater height than the other, ceteris paribus, because of differences in specific volume along the heights of the columns. The following equations apply (Ref. 32 , 33 ).

The error,  $\delta^2 \xi$ , in column height difference,  $\Delta \xi$ , from an error  $\delta^2 \rho$ , in density difference,  $\Delta \rho$ , is:

$$\delta^2 \xi = \int_{z_1}^0 \frac{\Delta \rho}{\rho} dz \quad (4-14)$$

or approximately

$$\delta^2 \xi = \delta^2 \rho \cdot \frac{h}{\rho} \quad (4-15)$$

Since  $\rho \approx 1$ , an error of  $10^{-5}$  on  $\Delta \rho$  over a depth of 2000 meters will cause an error of 0.02m in surface height.

The density difference is a function of temperature and salinity difference; the error in density difference is a function of (1) the number of measurements made per unit area; (2) the rate of change of temperature T and salinity S with horizontal and vertical distance; and (3) the unknown changes in T and S since the measurements were made.

The smallest number of observations available per  $5^\circ \times 5^\circ$  figure in the Caribbean is that for the region just east of Yucatan - a little less than 14 measurements, or a linear measurement density of less than 1 per 100 km. The next greater number of measurements is about 50, or about 1.2 measurements per 100 km.

In the Caribbean, the density at 400 meters depth varies from about  $26.8 \times 10^{-3}$  to  $27.0 \times 10^{-3}$ ; at 1000m depth, it is about 27.8 except near the coast of South America, and at depths of more than 2000 meters, it is practically constant. We, therefore, make a first estimate of s. d. of density as  $\pm 5 \times 10^{-5}$  above 2000 km and  $\pm 0.0$  below that depth. The salinity varies by about  $5 \times 10^{-5}$  over the Caribbean, although at 400m depth, it varies by about  $8 \times 10^{-5}$ .

The density, accordingly, varies by about the same amount (actually about 80% as much, but the difference is insignificant). This agrees with the previous estimate. The variance in column height would then be 0.1 meter over the entire Caribbean (from salinity variation). The variation between adjacent columns 100 km square would be expected to be considerably less.

The density variation with temperature is approximately  $-3 \times 10^{-4}$  per degree centigrade at the same salinity and  $0^{\circ}\text{C}$ . A variance of  $1^{\circ}\text{C}$  in temperature, therefore, corresponds to a variance of less than  $900 \times 10^{-8}$  in density. Over a depth of 2000 km, this results in a variance in column height of 0.6 meters. Temperature uncertainties, therefore, are particularly important. The variations in temperatures are small and predictable, fortunately. At 50m depth, the change in  $t$  is less than  $0.1^{\circ}$  daily and can be well fitted by a sine curve. The annual variation in water temperature in the open ocean at the surface is  $1.7^{\circ}$  between  $20^{\circ}\text{N}$  and  $20^{\circ}\text{S}$ . The variance in temperature, because of unaccountable time variation, is therefore, probably less than  $0.1^{\circ}\text{C}$  at depths greater than 100 meters; the effect of the top 100 meters on height difference is less than 0.01 meter and can be ignored. The big question is, therefore: What is the variation in temperature with horizontal and vertical distance? Measurements by LaFond and LaFond with thermistor chains<sup>21</sup> show a nearly vertical slope of temperature. Other data also indicate slow change horizontally, at least in the open oceans. It is likely that the existing data in the Caribbean are sufficient to allow the temperature at depths greater than 100 meters to be determined with a variance of less than  $0.01^{\circ}\text{C}$ . Investigation of these data have not been sufficient to verify this, however, and it should be checked. The



existence of temperature anomalies in a vertical direction is well known<sup>20, 21</sup>, but the small vertical extent of such anomalies makes their effect negligible.

In summary, then, the uncertainty (standard deviation) in mean sea level caused by specific volume uncertainties is certainly less than 0.6 meters; if the rate of change of temperature with distance is less than 0.1 per 100 km, the uncertainty is less than 0.2 meter.

The geostrophic currents cause water to rise above the equipotential surface. The paper by Sturges<sup>34</sup> indicates that in the Caribbean the height anomaly is less than 0.5m; the uncertainty is assumed, therefore, to be less than 0.3m.

The combined s.d. for determination of MSL height above geoid is, therefore, of the order of 0.3 meters.

2. The next step is to go from mean sea level to that surface which is affected by tides. In the Caribbean, the daily tide amplitude is less than 1m almost everywhere; the uncertainty in tide level can be taken as less than 0.1m (Ref. 23, 24, 25).
3. Finally, the variance of IMSL with respect to the tide-varying surface is required. No data on this are at hand. However, it seems reasonably clear that IMSL and the tide-affected surface do not differ at all except for the water "blown out" of the affected area by the wind. The amount is not known; various estimates<sup>30</sup> gives it as equivalent to between 0.1 and 0.2 meters. Some of this, of course, is the result of vertical pressure, not horizontal.

The varying atmospheric pressure must be accounted for. The height difference in cm caused by a pressure difference  $\Delta p$  in mbar is approximately equal numerically to the pressure difference. An error of 10 mbar in estimating the pressure differences along the altimeter path would, therefore, cause a height error of 10 cm. Such pressure differences must be determined on a day-to-day basis.

In summary, the total standard deviation of IMSL with respect to the geoid is probably less than 0.4 meters.

#### 4.3.2 Hawaiian Islands Region

The Hawaiian Islands region, or more particularly, that part of the Hawaiian Islands region lying in the immediate vicinity of Hawaii and south of  $+20^\circ$ , is a logical choice as a region where absolute (as well as relative and self-consistency) verification procedures can be carried out for several reasons. First, it is one of the few regions within the  $\pm 20^\circ$  zone where there is adequate satellite tracking equipment of all kinds available and a good knowledge of ocean characteristics exists. Secondly, the geodetic framework within which the tracking stations are located is satisfactory as far as horizontal errors are concerned, and may be satisfactory as far as vertical measurements are concerned. Johnston Island has been connected to the Hawaiian chain by several methods, including HIRAN and satellite surveys, and the islands of the chain are also connected through HIRAN traverse as well as by conventional triangulation.

A number of factors make the region less than optimum for VEDS. The horizontal ties, especially between Johnston and the Hawaiian Islands, are weak compared to continental triangulation; the only (unclassified) tie vertically between Johnston and the Islands is through satellite surveys. Furthermore, the orbit carries the altimeter up to the island of Hawaii, but no further, so that all tracking situations will follow the pattern shown earlier in Figure 4-18c or, occasionally, that of Figure 4-18b. Although the latter pattern is satisfactory for altimeter performance verification, it will occur most frequently in the neighborhood of Johnston Island where ocean and geodetic data are least favorable. For these reasons, only measurements in a region close to Hawaii could be expected to be susceptible to verification and these would be largely in the relative and self-consistency categories. Verification in the absolute category may be practicable and should be tried, since it provides an experiment that is independent of those done in the Caribbean.

#### 4.3.2.1 Characteristics (Hawaii)

Figure 4-19, taken from H.O. chart 5800, indicates by a heavy black line the northern limit of the zone of height measurements by the altimeter. Lapan Island is at about  $26^{\circ}$  North and  $171^{\circ}$  West; Hawaii is at  $20^{\circ}$  N and  $155^{\circ}$  W. Figure 4-20 shows the geodetic control for the region and Figure 4-21 shows the satellite geoid<sup>7</sup>. The amount of data on S. T. P for the region available from National Oceanographic Data Center is shown in Figure 4-22<sup>4</sup>. Hogben and Lumb<sup>10</sup> gives no sea-state information on the Central Pacific region. Very general data on the "East Equatorial Pacific" (Table 4-9) are given in Bigelow and Edmundsen<sup>35</sup>. These data, as Bigelow and Edmundsen note, were based on Schumacker's<sup>29</sup> graphic synopsis of world-wide, sailing ship data. Schummacker's data for the Central Pacific do seem to include the Hawaiian Islands region, to judge from his chart. The relevance of these data to the radar altimetry performance, or to radar scattering in general, is uncertain, and it is best for the time being to use them merely to get a feeling for the kind of sea states that may be encountered, without attaching any importance to the numbers themselves.

The question of cloud cover in the Hawaiian Islands - Johnston Island region is different for the verification experiment than it is for ordinary satellite tracking because the experiment will be carried out in a small region in the immediate vicinity of Hawaii. Table 4-10<sup>9</sup> gives the amount of observing time lost at the SAO observing station on Maui because of cloud cover. These data refer to loss of observations on satellites passing at least within  $60^{\circ}$  zenith distance of the observatory and at all azimuths.

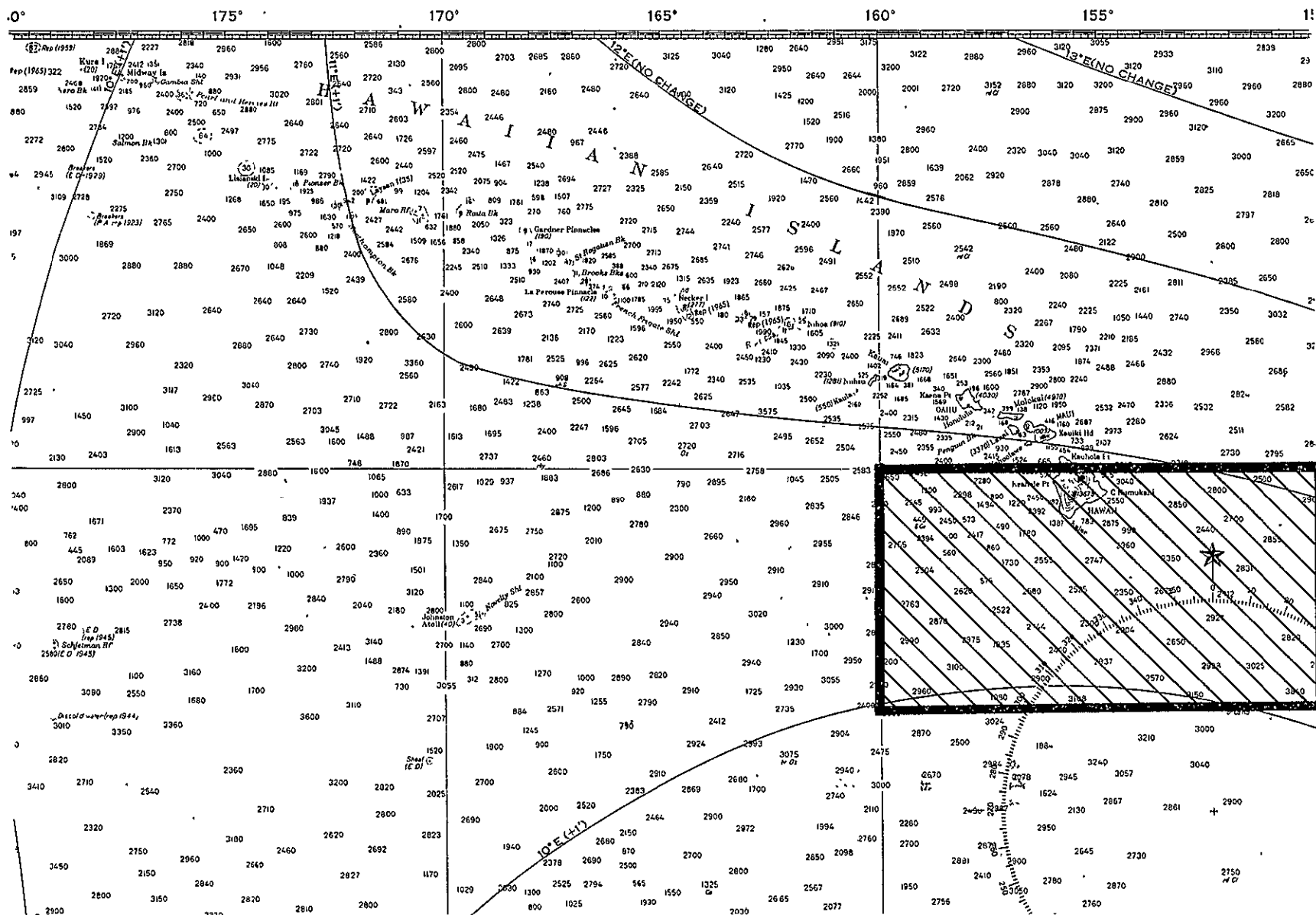


Figure 4-19. Verification Experiment Area (Hawaii)

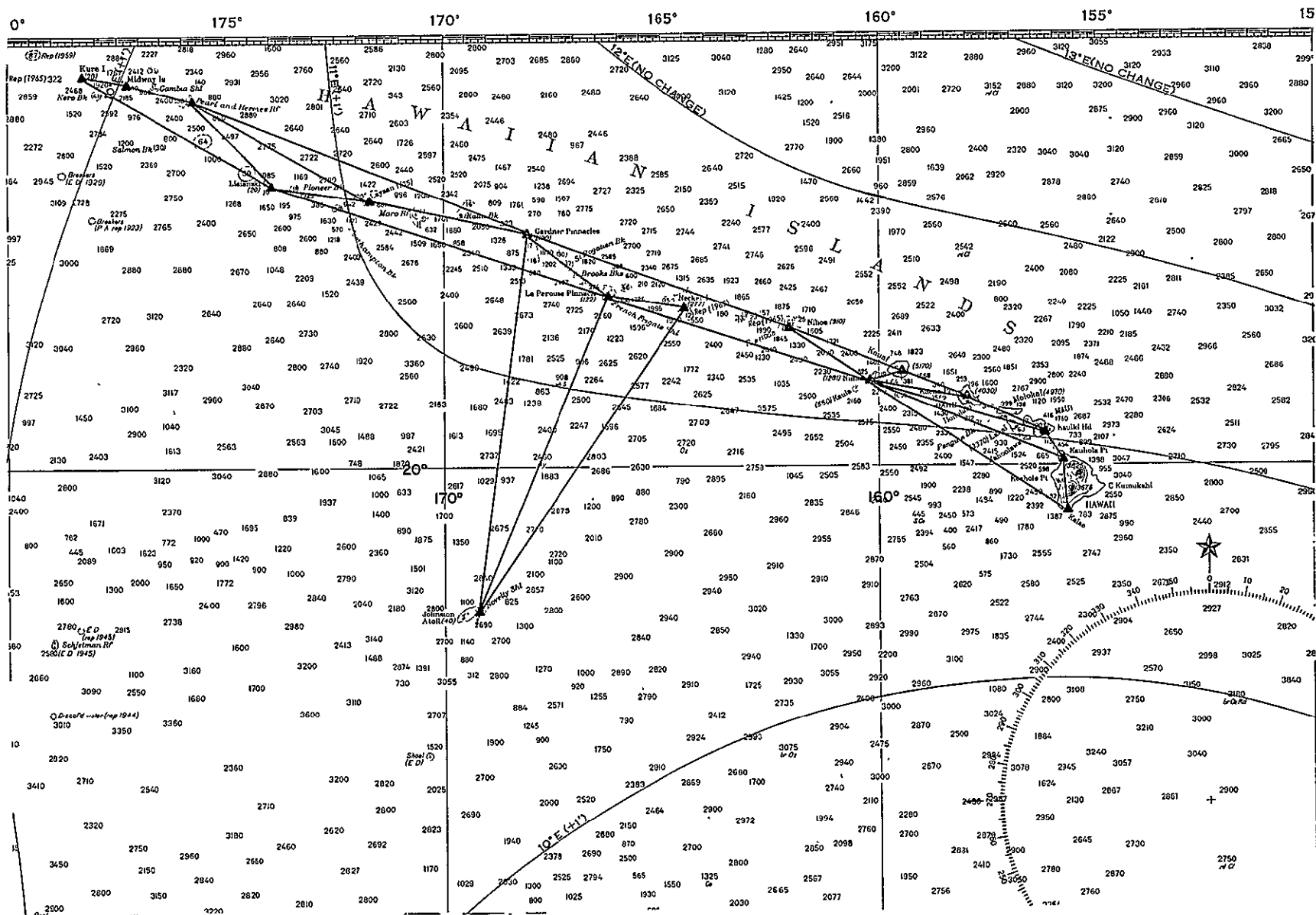


Figure 4-20. Inter-island Geodetic Control (Hawaii)

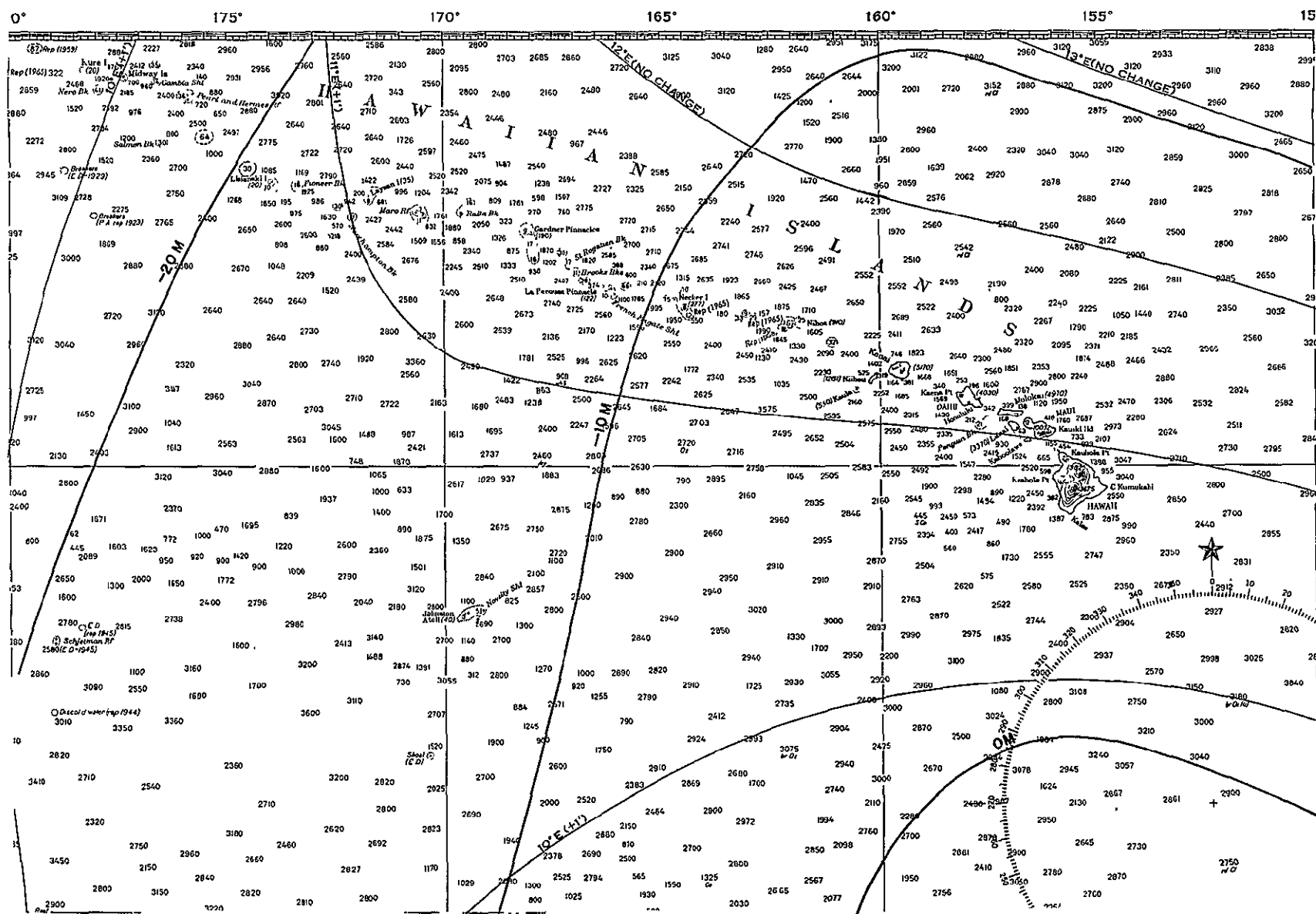


Figure 4-21. Satellite Geoid in Hawaiian Islands Area

21	11	13	77	16	8	55	37	42	91	605	1337	1						1873	1201	1281	351		
125		125		124		123		122		121		120		119		118		117	115		115		
16	14	9	30	16	11	17	212	123	94	349	3008	3721	42					13	95	1426	401	1007	584
58	18	13	22	44	48	47	145	97	44	106	404	2862	1732	22		70	223	265	503	956	160	124	68
090		039		035		037		036		035		034		033		032		031	030		029		
9	13	13	60	506	166	60	9	12	14	9	35	228	810	230		60	119	201	727	1063	161	186	124
1	11	15	27	273	139	56	7	7	3	8	21	17	21	38	45	101	28	14	71	132	116	258	426
054		053		052		051		050		049		048		047		046		045		044		043	
5	20	10	13	66	123	55	11	8		9	15	10	7	30	30	82	52	31	40	59	57	86	409
15	24	10	10	28	13	17	20	17	4	6	13	17	5	10	16	42	27	72	121	188			45
018		017		016		015		014		013		012		011		010		009		008		007	
13	24	18	16	34	19	20	58	24	5	4	13	23	5	7	12	45	34	31	76	27			
18	22	17	6	27	18	14	35	43	10	7	6	23	18	6	7	50	39	65	374	1			
317		316		315		314		313		312		311		310		309		308		307		306	
10	18	9	2	9	11	5	16	18	7		5	3	7	3	3	30	30	27	622	332			
5	14	3	5	7	11	11	16	14	3	4	2	1	14	2	1	20	20	12	48	829	1		
353		352		351		350		349		348		347		346		345		344		343		342	
2	3	3	5	2	7	70	13	7	7	2			2			23	24	1	7	147	268		
3	8	1	1	1	2	6	1	2				1	2			14	3	4	13	17	67		
339		338		337		336		335		334		333		332		331		330		329		328	
5		4		2		2	3		2			1	2	7	1	3	7		7	4	31		

Figure 4-22. Data on S.T.P. in the Verification Experiment Area (Hawaii)  
(Available from National Oceanographic Data Center)



Table 4-9. Wave Height Data For East Equatorial Pacific

Height Range (meters)	From	0	1	1.3	2.3	4	6.5
	To	1	1.3	2.3	4	6.5	-
Frequency (%)		25	35	25	10	5	5

Table 4-10. Cloud-Cover Data For Maui  
(in % of observing time lost)

MONTH	YEAR	
	1962	1963
JAN	23	59
FEB	41	17
MAR	56	70
APR	39	78
MAY	33	52
JUN	5	28
JUL	38	29
AUG	18	23
SEP	20	39
OCT	16	39
NOV	26	32
DEC	33	30

#### 4.3.2.2 Tracking Station Location (Hawaii)

Figure 4-23 shows the locations of the known tracking stations in the Hawaiian Islands - Johnston Island region. The stations are listed in Table 4-11. There are additional radars located on Johnston and Kauai Island, but their locations are necessarily so close to those listed in the table that their inclusion in the error analysis is not worthwhile. As noted earlier, the geometry of the situation is far from optimum. Geos-C does not pass far above the  $20^{\circ}$  latitude line, so that the radars on Kauai do not get a vertical look at it. The Johnston Island radar does, but the Johnston Island radar is not under NASA control.

As emphasized elsewhere in this report, use of the Johnston Island radar does not have the same importance to the verification experiment in its present form that it would have if the experiment extended all through the Hawaiian Islands - Johnston Island region. The variances in the coordinates of the Johnston Island radar with respect to Hawaiian datum need not be materially improved unless the experiment is extended in geographical scope. There is also an AF Baker-Nunn camera on Johnston Island. Its use in the net would not significantly improve location of the altimeter over what is provided by the other tracking stations, and it is therefore omitted from further consideration.

Use of a tracking ship and/or special equipment is recommended and discussed in Section 4.3.2.4 following. Since the tracking ship will not have a fixed location, it need not be further discussed here.



Table 4-11. Tracking Stations in Hawaiian Islands --  
Johnston Island Region

Site Name	Location			Type	Agency
	$\lambda$	$\phi$	H(meters)		
Johnston Island-1	190° 29' 09"5	16° 45' 38"77	8	MPS-25	PMR
Kauai-1	200° 13' 06"10	22° 01' 31"18	13	MPS-25	PMR
Kauai-2	200° 19' 53"96	22° 07' 35"03	1260	FPS-16	NASA
Maui	203° 44' 24"08	20° 42' 37"50	3034	Baker- Nunn	SAO

#### 4.3.2.3 Additional Data Required (Hawaii)

The amount of data already available on the Hawaiian Islands--Johnston Island region is sufficient for carrying out the limited varieties of experiment planned for that region. By restricting the experimental area to that immediately south of Hawaii, the need for knowledge of the geoid anywhere but in that area is eliminated. STP data are adequate in quantity, although a check of their quality is desirable.

Perhaps even more important than the geoid at Johnston Island is the geoid along the Hawaiian Islands from Kallai to Hawaii. Additional useful data may be obtained by running a GEON or SINS instrument from island to island. The tolerance of either device is too large to allow it to improve on the astrogeodetic/gravimetric geoid, but the profile will be invaluable in providing values for the change in the deflection between astro stations. The combination of, e.g., SINS data with conventional data should allow the geoid to be determined to  $\pm 1$  meter referred to the Oahu datum.

Serious consideration should be given to the possibility of running geoid profiles from Johnston Island to Maui and Oahu. Satellite geoids (Figure 4-21, for instance,) show a nearly constant slope between Johnston and the Islands, but the satellite geoids are not with reference to a local (Hawaiian) datum. The geoid profile is not considered essential because the principal contribution of Johnston Island to the verification experiment is to determining the horizontal coordinates of the altitude measurement point, not to height determination. Johnston Island location uncertainties are therefore not critical to the verification experiment unless the region of investigation is extended westward to include the entire region from Johnston Island to Hawaii.

#### 4.3.2.4 Conduct of Experiment (Hawaii)

The following sections specify the major desiderata for conduct of absolute category experiments in the Hawaiian Islands--Johnston Island region.

### Tracking Stations (Hawaii)

The radar tracking stations on Johnston Island and Kauai and the camera station on Maui, listed earlier, are to be used. Without the Maui station, solution for satellite location is useless; the Maui station is essential in the absence of an additional station. Even with the Maui station operating, however, the geometry is far from good. Therefore the plan of operations recommends that an auxiliary tracking station be located on Hawaii.

An alternative to the use of special devices on Hawaii is to use a tracking ship in the region. Observations from the ship will have to be made within a distance from the island that will ensure that the ship's height above the local reference spheroid is known. After verification of the altimeter's performance in the differential category, satellite altimeter readings can be used to gradually extend the geoid from the immediate vicinity of Hawaii to the rest of this region, and the ship location can be related to satellite location (for relative location experiments) rather than to the geoid undulation uncertainties. (One tracking ship is required in the present design for nearly full-time use in the Caribbean; a second ship would have to be available for tracking off Hawaii.) The Hawaiian Islands tracking would require less than 25% the amount of ship's tracking time that the Caribbean phase does, because of the small extent of the region and the gradual extension of tracking effort outward from Hawaii.

Under the conditions of this experiment, the Johnston Island radar does not play a critical role in determining satellite location. Observations from Johnston Island are useful in lowering the variance of the satellite's horizontal coordinates, but are not as effective in providing a small variance for the vertical coordinate. Unless the Maui station cannot be included in the tracking net and complete orbit theory used for finding satellite location, inclusion of Johnston Island radar in the experiment is desirable but not essential. No requirement for extension of this geoid to Johnston Island is known at present, and the question of whether or not to retain the Johnston Island radar to support the Hawaiian Island tracking effort can therefore be decided solely on this basis of convenience at the time of the experiment.

#### Logistics (Hawaii)

All essential data listed for scheduling of observations, etc., in the Caribbean apply to the Hawaii region experiment schedules. Differences in procedure are minor.

#### 4.3.2.5 Error Analysis (Hawaii)

The same kind of error analysis is applicable to the Hawaii region tests that was used for the Caribbean region tests. Analysis is simpler because the region being used is considerably smaller, there are fewer tracking stations, and the datum point is close to the test area. As in the analysis for the Caribbean, the analysis here has three phases: satellite location error, geoid height error, and IMSL height error.

#### Satellite Location Errors (Hawaii)

The geometric errors were investigated first, using three tracking station configurations and six satellite locations with each configuration. One station combination was provided by the radar stations on Johnston and Kauai plus the camera station on Maui. A second was obtained by substituting a ranging station on Hawaii for the camera on Maui, and the third combined all

stations considered. Appendix A lists the satellites and station configurations employed. The geometric analysis (see Appendix B) proceeded as for the Caribbean tests, and the results are tabulated in Table 4-12.

Standard deviations for configurations including all stations (i. e., with the one on Hawaii) are significantly better than those for the other configurations. The question of how far the satellite will deviate from the computed trajectory while traversing the test region is irrelevant in this case, because the satellite can be kept under observation by all stations during its stay in the region. Reference is made to Appendix H for a discussion of the relation between measurement errors and comparison standard errors. Applying the averaging equivalent of the adjustment equation in Appendix B, it appears that there are enough observations available for the test to reduce the random standard deviation to less than 1 meter. As pointed out in Appendix H, the critical item here is not the tracking random standard deviation but the systematic error. The geometry of the test is such that observations are consistently made in one sector of the sky by all instrument, so that biases from this cause can enter. The use of four tracking stations, one of them a camera, should allow estimation of systematic errors to within a meter, even if the Johnston Island station were dropped.

#### Geoid-Spheroid Errors (Hawaii)

The datum point at Oahu West Base is about 500 km, to 700 km. from the test area. An uncertainty of  $\pm 2$  meters in the location of the geoid with respect to the spheroid at the Kauai and Hawaii locations is assigned as a reasonable value. This value may be reducible to below 1 meter using satellite orbits.

#### IMSL - Geoid Errors (Hawaii)

Considering density of oceanographic observations in the region, no difficulty should be encountered in keeping rms error in location of IMSL with respect to geoid below 40 cm.



Table 4-12. Geometric Error in Satellite Height for Ground  
Tracking in Hawaii Area

(RMS Error Relative to Spheroid, in Meters)

Station Configuration*:	26-27-29	26-27-28	26-27-28-29
Satellite* Location			
701	4.9	3.5	3.5
702	5.2	7.3	3.8
703	5.6	4.7	3.8
704	5.9	9.2	4.1
705	6.4	9.3	4.9
706	6.8	13.5	5.2

\* See list of stations and Satellite locations for the Hawaii area in Appendix A.

#### 4.3.3 Marshall Islands

The principal reason for considering the Marshall Islands region as one suitable for verification experiments are the existence of tracking stations on various islands in the group, the excellent geometric relations of the islands to each other, and the existence of a computed geoid (gravity-based, of course) for the region. Against use of the region are its physical remoteness, the lack of accurate geodetic coordinates for most of the islands with respect to each other, and the paucity of ocean data for this region as compared with the amount of data for e.g., the Caribbean. These considerations place the Marshall Islands region a poor third in the list of regions where an absolute frame of reference will be used and probably eliminate it completely as a region where relative frames of reference are used. The Marshall Islands region is well suited for experiments in the self-consistency category, at least in the portions near Kwajalein and Eniwetok. Experiments to determine difference accuracy are probably not suitable, since geoid (MSL) variations are not too well known and tide variations are small (less than a meter).

#### 4.3.4 Lake Maracaibo

Lake Maracaibo is one of the few water bodies of large size within the zone covered by the GEOS-C orbit whose relation to the geoid is well known. It will be traversed about 20 times in an ENE direction and the same number of times in the ESE direction. Use of the region will require less than 7 minutes of altimeter time and will, at 10 measurements per second, provide about 4,000 points on the surface. Since the lake is tied to the geoid in Venezuela, the dense altimeter coverage would allow a thorough check of performance. There are some possible difficulties to using the region, and these are discussed below. One of these is the presence of artificial objects. The lake is in a natural oil basin from which oil is still being extracted, and consequently is cluttered with drilling towers, pump stations, etc. There is also a heavy passenger and freight traffic over the lake. Vessels, drilling installations, etc., may or may not reflect enough radio wave energy back to the altimeter to make a difference.

Another difficulty may be the provision of adequate tracking data, since descending segments of the orbit pass south of all Caribbean tracking stations. This difficulty can be overcome by using the type of instrumentation described in Section 4.3.1.3.

#### 4.3.4.1 Tracking Station Location (Maracaibo)

Only one tracking station--the SAO 36"--camera station at Curacao is in the vicinity of Lake Maracaibo and Gulf of Venezuela. Its coordinates are<sup>28</sup>

Longitude	201° 09' 43" 97
Latitude	12° 05' 26" 31
Height (above MSL)	4.9m

The experiment design for the Caribbean as a whole calls for location of a tracking ship in the immediate vicinity of the Gulf of Venezuela. A combination of tracking ship and camera station gives necessary and sufficient conditions for a fix, but at least one more source of observations should be available for tracking the altimeter on segments of the descending portion of the orbit.

#### 4.3.4.2 Additional Data Required (Maracaibo)

At present, there does not appear to be any need for surface data not otherwise available. Depths in the middle of the lake are about 33m., so that variations in specific volume across the lake will have negligible effect on surface topography. There are large volumes of gravity data in existence<sup>11, 15</sup> that can be used to get geoid-spheroid separations across the Lake and in the Gulf.

#### 4.3.5 Lago De Nicaragua

Because Lago De Nicaragua lies adjacent to the Caribbean test area, is well tied into horizontal and vertical control, and is large enough to serve as a test area, it is considered for use as an area where verification experiments

may be carried out. The following sections describe those characteristics relating to its suitability as a verification test area. Its use is not recommended for verification. Figure 4-24, taken from ACIC chart ONC K-25, edition 2, scale 1:1,000,000 shows the region containing the Lake. Elevations on the map are in feet, contour intervals are 1000 feet.

#### 4.3.5.1 Region Characteristics (Lago De Nicaragua)

Lago De Nicaragua is a fresh water lake about 170 km in its longest dimension and about 65 km in width, with the long axis at an inclination of about  $60^\circ$  to the equator.

It is at an altitude of about 40 meters, although elevations of land points surrounding it and in it rise considerably higher. There are several islands in the lake, but only one of them, Isle de Ometepe, is of great size: about 30 km long on a line running NW to SE and about 8 km wide at its widest, taking up about 2% of the lake area. Satellite paths over the lake will, at the average latitude of the lake, be at an azimuth of about  $60^\circ$  for segments of the ascending phase and about  $120^\circ$  for segments of the descending phase. This is approximately perpendicular to the long axis and at an angle of about  $20^\circ$  to it, respectively. During the two year lifetime of the altimeter, there will therefore be about 40 passes from southwest to northeast and about 15 passes from northwest to southeast.

Cloud cover in the region can be found from Figure 4-9. However, there is considerable variation in cloudiness from one part of Nicaragua to the other, so that microclimatological surveys must be consulted for realistic information about cloud cover over specific land points. Since experiment design does not call for a tracking station per se in the immediate vicinity of the Lake, cloud cover information is irrelevant at present.

The astrogeodetic geoid in the Lago De Nicaragua region is shown in Figure 4-25<sup>2</sup>. Dashed Lines indicate lack of full confidence in contour.



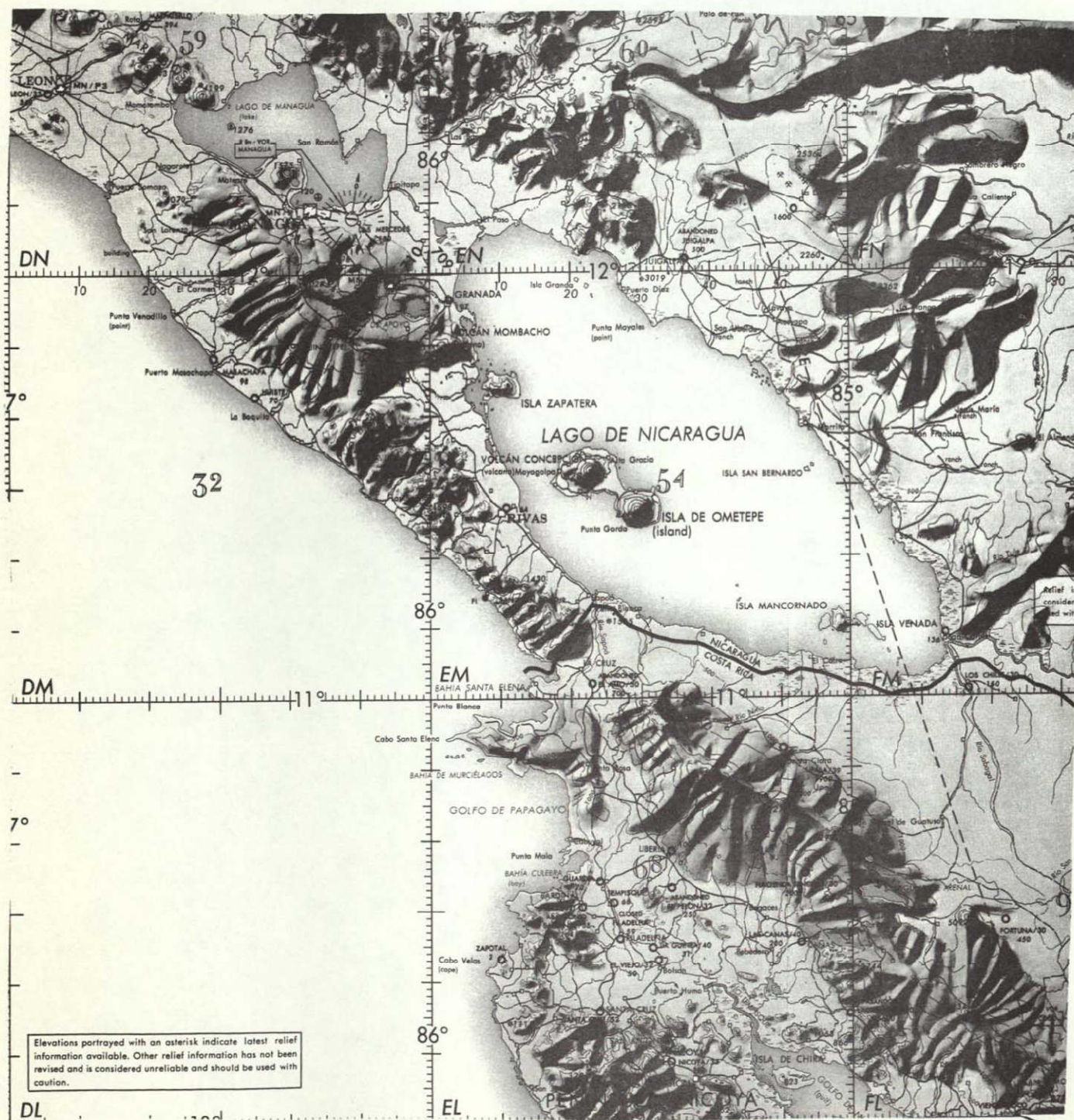


Figure 4-24. Region Containing Lago De Nicaragua



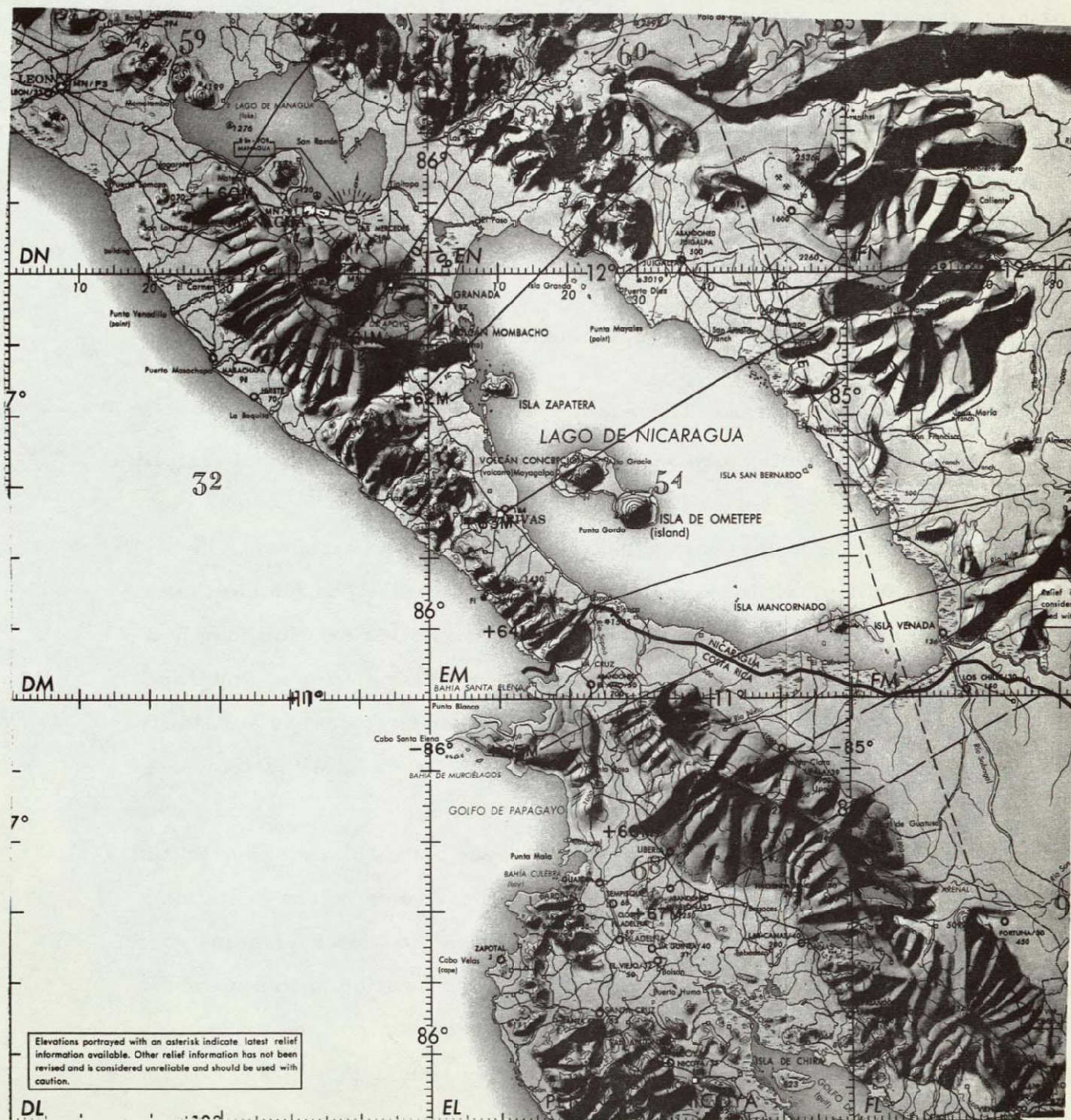


Figure 4-25. Astro Geodetic Geoid Around Lago De Nicaragua



#### 4.3.5.2 Tracking Station Location (Lago De Nicaragua)

There are no known permanent or semi-permanent tracking stations located at present in the Lago De Nicaragua region. The paths of subsatellite points pass, at the eastern end of the Caribbean, between Puerto Rico and Antigua if the path is ascending or passes south of Lake Maracaibo if the path is descending. In either case, the tracking situation is unsatisfactory.

#### 4.3.5.3 Additional Data Required (Lago De Nicaragua)

There is at present a need for additional data to determine if the terrain surrounding the lake would interfere with the transmitted pulses. It appears that the terrain would intercept the wavefront due to the low curvature of the wavefront and the height of the terrain relative to the surface of the lake. (See Appendix F) Lake Nicaragua is therefore not recommended.

#### 4.3.6 Lake Titicaca

Two large lakes--Lake Titicaca in Peru and Lago De Nicaragua in Nicaragua--lie in the Western Hemisphere with the  $20^\circ$  zone covered by the sub-satellite path. Although Lake Titicaca is somewhat the larger of the two, it is considerably farther from the main experimental area (the Caribbean). A satellite at 1000 km. altitude would, given clear weather, be visible to perhaps 5 optical tracking stations, but with good geometric relation to only 2 of them. It would not be within useful range of a radar station at any time. Cloud cover would be an important factor in evaluating the areas suitability. Weather maps<sup>3</sup> show that the mean cloudiness in the Lake Titicaca area varies from about 20% in May to over 90% in September. Cloud cover over the lake are not as important as cloud cover between the lake area and the optical tracking stations. The mean cloudiness in the areas containing the lake and one of the tracking stations other than the one at Arequipa varies between 40% and 90%. The probability of getting a location of the altimeter while it is over or near the lake is therefore extremely low; the probability of getting observations of it even at low elevation is less than 60%. For these reasons, Lake Titicaca is not recommended as an area for verification experimentation. Similar reasons remove other large lake areas in South America from consideration.

#### 4.3.7 Other Regions

The other regions investigated in some detail for their possible use as verification experiment (absolute category) sites were the Persian Gulf, Lake Victoria, Lake Chad, and the Indian Ocean. All of these had to be eliminated because there are not a sufficient number of tracking stations able to provide adequate tracking in these regions. While tracking stations could be placed to give the required measurement density, the cost of providing such tracking would be far out of proportion to the usefulness of the data.

#### 4.4 Critique of Absolute Verification

A test in which the satellite location and ocean surface location are determined independently and in reference frames independent of the satellite, is called for on absolute test. It has the advantage over other kinds of tests that the ocean surface location can be determined without reference to the experiment and the satellite location can nearly be so determined. This makes it useful as a check on methods which compare the altimeter measurements with measurements of the same quantity using some other kind of instrument as a standard. It has the further advantage that, properly designed, it can reduce the systematic errors in the satellite location to a very low figure and even, under certain circumstances, construct the geoid used in its checking.

The principal disadvantage of absolute verification is the difficulty in separating the geoid systematic error from the altimeter error. This is a serious problem, only partly solved by the expedient of using local datums. There is no a priori basis for judging how much of the altimeter variance is contributed by the geoid (other sources of error can be ignored). It appears at present as if the best way of effecting the separation is the obviously painstaking one of analyzing the altimeter measurement residuals to identify certain kinds of residual behavior with geoid variation and other kinds with measurement variation.

Two major areas of testing have been specified: the Caribbean (in which sub-areas were designated), and the Pacific Ocean in the immediate vicinity of Hawaii. The experiments were planned in similar fashion for both areas: track



the altimeter with enough instruments that a redundancy of observations is available for each location; apply equations for short segments of the orbit as conditions on the observations; measure the geoid-spheroid and IMSL-geoid separation independently; compare observed and computed heights and compute the variance of the altimeter measurements.

By providing more than enough independent observations to fix satellite location, systematic errors in that quantity can be virtually eliminated from the computations. The errors can be removed to the extent that the form in which they enter the equations is known; to the extent that the errors cannot be demonstrably eliminated, they do not affect the philosophy of this verification study. The output of the system formed by combining the altimeter plus satellite plus tracker cannot be proven wrong on the basis of any data gathered by the system itself. The operating system is made self-consistent by absorbing the error as a calibration constant. The only way in which the error (if it exists) can be detected is to make independent measures on the system from outside the system. But the outside measure then constitutes a calibration, and the calibration can be used to reduce the error.

If the entire experiment were contained within the Caribbean, it might be somewhat difficult to remove the systematic error in the geoid. But "geoid" measurement in Hawaii (and perhaps on Lago De Nicaragua), provide other independent ways of estimating geoid separation. With systematic errors in satellite location and geoid height removed, the magnitude of the variances in satellite location and geoid height become irrelevant; as shown in Appendix H, the variance of the altimeter measurements can be computed exactly from the variances of the measured and computed quantities.

It is worth noting that the procedure calibrates the tracking systems as part of the adjustment.

Using absolute verification, verification of the accuracy of the altimeter (expressed as a standard deviation) can be carried out. The variance of the altimeter measurements will be found to be:

$$\sigma_m^2 = \varepsilon_g^2 + \tilde{\sigma}_m^2 \quad (4-16)$$

where  $\tilde{\sigma}_m^2$  the variance computed from

$$\tilde{\sigma}_m^2 = \frac{1}{I} \sum_{i=1}^{i=I} (k_{mi} - h_{si} + h_{gi})^2 \quad (4-17)$$

and  $\varepsilon_g^2$  is the square of the smallest systematic error present in the geoid referred to the local geodetic system.

## SECTION 5. RELATIVE VERIFICATION

### 5.1 Summary

The investigation of this approach to verification concludes that a reference altitude accurate to 15 to 25 meters can be predicted with confidence for the C-band equipment now operational on some Apollo ships. With appropriate modification of current equipment, results accurate to 5 to 7 meters can reasonably be expected. With a greater level of effort, accuracy of 2 to 3 meters is achievable.

Errors in relative verification are shown in Table 5-1.

Table 5-1. Relative Verification Error Summary

PERFORMANCE LEVEL	RANGE R	SHIP/ IMSL D	OFF ZENITH ERROR X	PROPA- GATION	H <sub>i</sub>
OPERATIONAL	15-25m*	<2m	2m	1m	15-25m*
CAPABLE	5-7 m	0.3-1m	0.1-0.3 m	1m	5-7 m
FEASIBLE	2-3 m	≤0.3 m	0.1-0.3 m	0.5m	2-3 m

\* AN/FPS-16 Shipboard Radar currently not suitable for zenith tracking

The relative verification method is best performed in a geometric configuration in which the satellite is within 2-1/2° of the zenith of the ranging platform. Additionally, the location should be in a region where a large number of passes can be used. It would also be desirable to carry out the experiment in a region in which other verification methods can be performed, and thus where tracking is available.

In principle, relative verification can be performed wherever a ship can operate within the 20° belt. In practice, multiple passes are most often experienced close to 20° latitude. Furthermore, greatest tracking station

coverage is obtained in the northern regions within the Caribbean indicated in Figure 4-12(b). The Caribbean in the 18° to 20° latitude region, which is within the area of greatest satellite path density (see Figure 6-1), is recommended as the primary location for performance of relative verification.

Relative verification can and should be performed on those relatively infrequent occasions when the satellite passes sufficiently close to the zenith of a land-based tracking station. Their lack of mobility reduces their opportunity for measurement relative to that expected from ships. However, a total of more than 700 opportune passes are available, as follows:

	<u>Latitude*</u>	<u>No. of Passes</u>
Grand Turk	21.4°	200
Kuai	22.1°	100
Tanarive	19°	300
Guam	13.5°	100
Antigua	17°	
Ascension	8°	
Johnston Island	18°	

\* see Figure 6-1

Each laser station could provide up to 300 additional passes, subject to visibility limitations, if located sufficiently close to 20° latitude.

Range measurements are made from a platform, which may be landbased, a ship, a buoy, or an aircraft. A land-based ranging station is most reliable, but provides infrequent opportunities for measurement. A ship is suitable and reliable, and hence is recommended. A buoy could be constructed to serve the purpose, but requires considerable effort. An aircraft is unsuitable if only because its altitude cannot be adequately determined.

Whatever the platform, ranging instrumentation must be available. C-band radar is operational on the Vanguard Apollo tracking ship, and is therefore most suitable. Other alternatives considered are transponders, receivers only, and surface-based synchronized clocks. Radar corner reflectors are shown to be impractical.

The ground support system for relative verification, in addition to providing range information from the platform to the satellite, must provide the zenith angle to the satellite (or its equivalent), platform height above IMSL, and ocean truth information (as for all methods).

The principal advantages of relative verification are:

1. The approach incorporates a direct measurement of the satellite height relative to instantaneous mean sea level.
2. It does not depend upon orbital estimation involving uncertainties in gravitational field and tracking station location.
3. There is no dependence on the geoid relative to the spheroid or IMSL relative to the geoid.
4. The measurement can be performed from a ship in any portion of a large geographical region, within the 18° to 20° belt.

The principal disadvantages of the relative verification are:

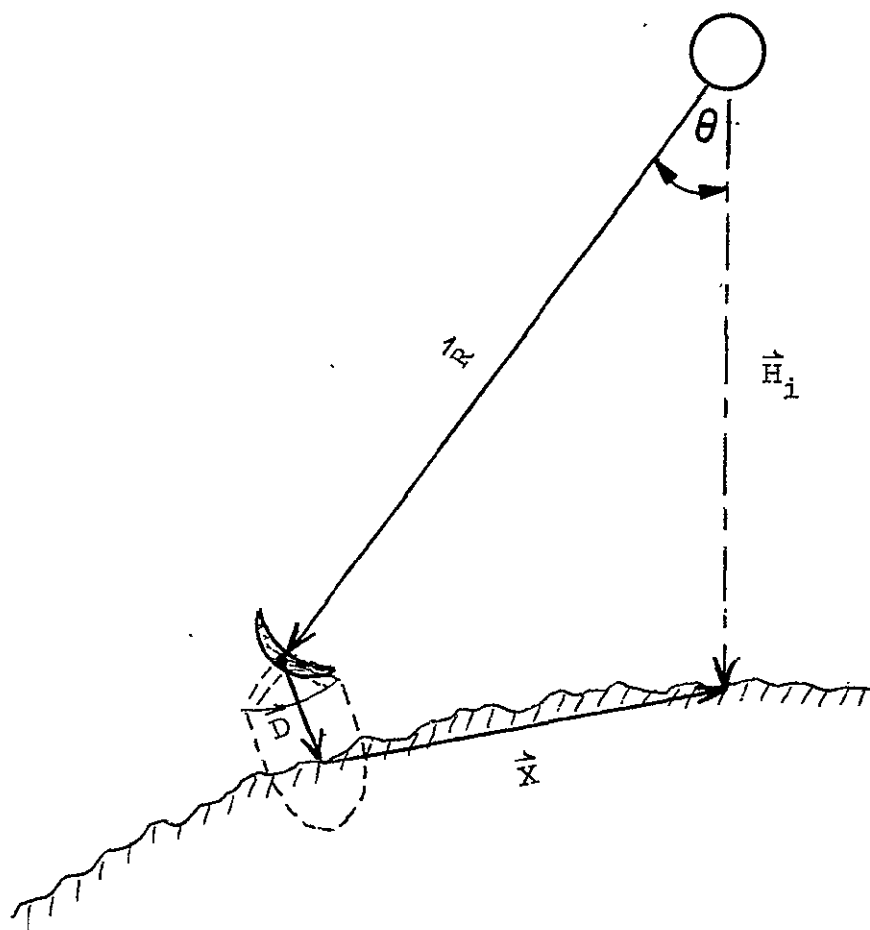
1. The range measurement is limited in accuracy by the capability of a single station in a single (or at best limited) measurement, rather than the statistical improvement of tracking over a large portion of an orbit by a tracking network.
2. For a given tracking facility, the opportunities to make near-zenith measurements (by virtue of satellite position) are relatively few and far between.

## 5.2 Description of Relative Verification

### 5.2.1 Relative Verification Concept

This approach to verification employs an instrumentation system that measures the height of the satellite above a reference point when the satellite is at (or very close to) the zenith of the instrumentation system. (Figure 5-1). The height of this reference point above the instantaneous mean sea level (IMSL) is measured simultaneously. The sum of these measurements is the height of the satellite above instantaneous mean sea level, which provides a reference against which the performance of the satellite altimeter is evaluated.

The Relative Method employs a Range Tracking System, such as a radar, and a system which can measure the height of the reference platform of the Range Tracking System above the instantaneous mean sea level.



$$\vec{H}_i = \vec{R} + \vec{D} + \vec{X}$$

$\vec{R}$  = SLANT RANGE FROM PLATFORM TO SATELLITE

$\vec{D}$  = HEIGHT OF PLATFORM ABOVE IMSL

$\vec{X}$  = PLATFORM TO SUBSATELLITE POINT

Figure 5-1. Relative Verification Geometry.

Figure 5-2 is a block diagram representation of the methodology of a typical relative verification procedure. The satellite tracking system is used to predict satellite location, and provide the zenith angle at the time of measurement. A land-based or ship measurement ranges to the satellite near zenith, and that measurement is corrected for zenith angle. (Ship motion compensation may be required.) A measure of the ship or other station altitude above IMSL is added to the vertical component of range to determine the altitude of the satellite above IMSL for verification purposes.

### 5.3 Geometry

In this section, the Verification geometry is considered, with the objective of establishing the requirements that must be met in the system to provide a verification reference. The geometry of relative verification is shown in Figure 5-1. The verification system is attempting to measure  $H_i$  at the same time and place that the altimeter measures  $H_r$ . The difference of these two measurements  $E(H)$  provides the basis for verifying altimeter performance.

$$E(H) = H_i - H_r \quad (5-1)$$

where

$$H_i \equiv |\vec{H}_i| \text{ and } H_r \equiv |\vec{H}_r| \quad (5-2)$$

The objective of this section of the verification study is to establish how well the verification system can establish  $|\vec{H}_i|$ . Hence the error in verification is given by

$$E(v) = H_i - H_{iv} \quad (5-3)$$

where  $H_{iv} \equiv |\vec{H}_{iv}|$ , and  $\vec{H}_{iv}$  is the estimate of  $\vec{H}_i$  made by the verification system. These quantities are related by the following equation

$$\vec{H}_i = \vec{R} + \vec{D} + \vec{X} \quad (5-4)$$

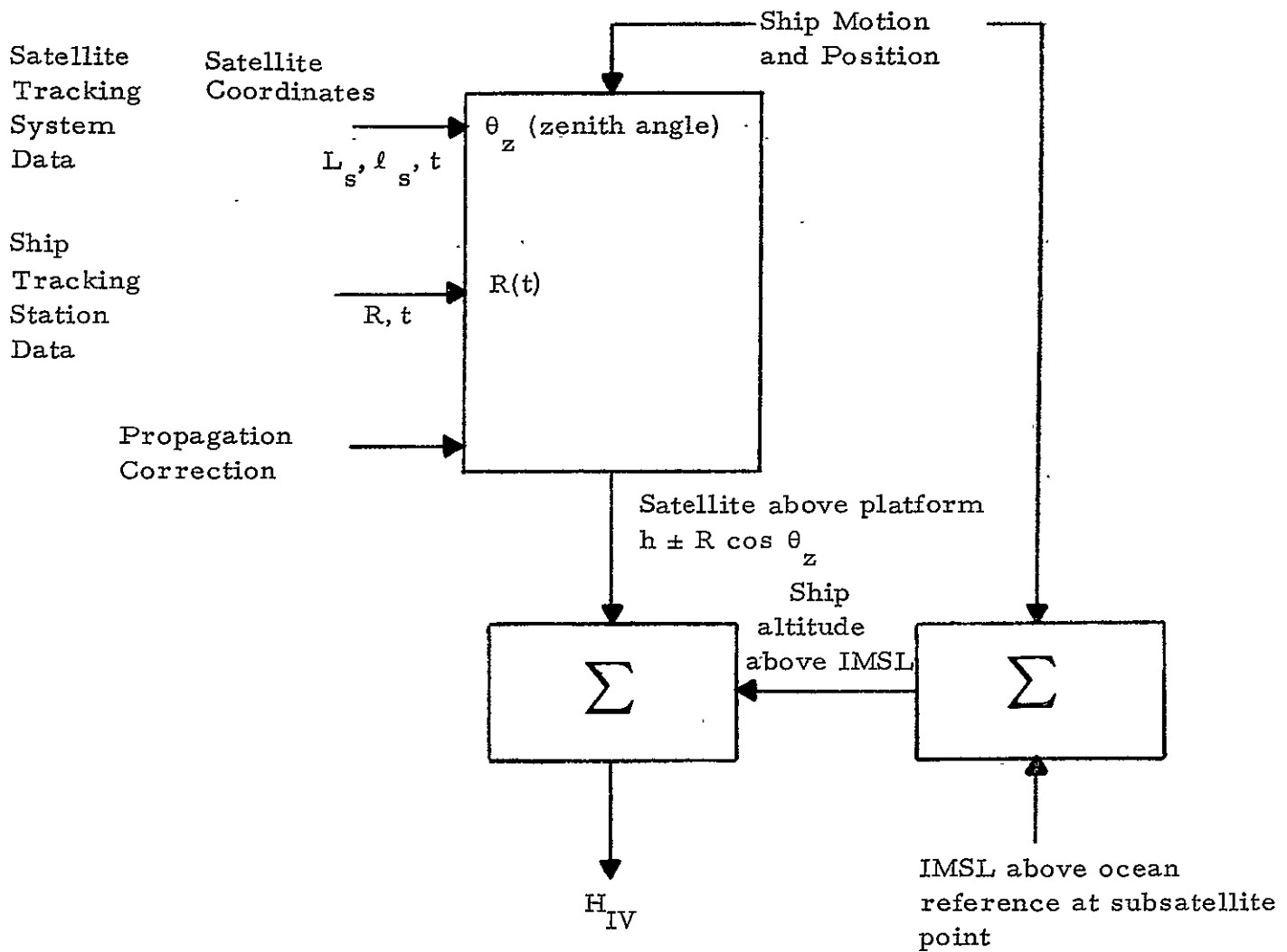


Figure 5-2. Relative Verification Block Diagram



where

- $\vec{R}$  = slant range from the range tracking system to the satellite
- $\vec{D}$  = height of the sensor above its IMSL
- $\vec{X}$  = vector from IMSL at the sensor to the subsatellite point  
IMSL

#### 5.4 Error Analysis

The contribution to the error in verification,  $E(V)$ , due to the error in  $\vec{R}$  results from the error in the magnitude of  $\vec{R}$ , or the error in  $R$ , and from the error in the direction of  $\vec{R}$ , or the zenith tracking angle,  $\theta_z$ . Since the contribution of  $\vec{R}$  to  $\vec{H}_i$  is given by  $R \cos \theta$ , the error in this term is

$$E(R \cos \theta) = dR \cos \theta - R \sin \theta d\theta \quad (5-5)$$

$\theta$  is the angle between  $\vec{R}$  and  $\vec{H}_i$ , and differs from the zenith tracking angle,  $\theta_z$ , by the Earth central angle between the satellite and the tracking station. The first of these two error terms is of the same order as  $dR$ . The second term can also be expressed in terms of  $x$  (where  $x = R \sin \theta$ ):

$$R \sin \theta d\theta = \frac{x dx}{H_i} \quad (5-6)$$

This indicates that the error can be determined equivalently by measurements of  $\theta$  (or, equivalently,  $\theta_z$ ) or by measurements in  $x$ , the distance from the sensor to the subsatellite point.

##### 5.4.1 Errors due to X:

Figure 5-3 shows the numerical value of the error in  $H_i$  due to an error in  $\theta$ , or  $x$ , as a function of  $x$ . The parameter is  $dx$ , the accuracy with which position can be determined by various systems.

$\Theta_z$ : Zenith Angle (for  $H_i = 1100$  KM)

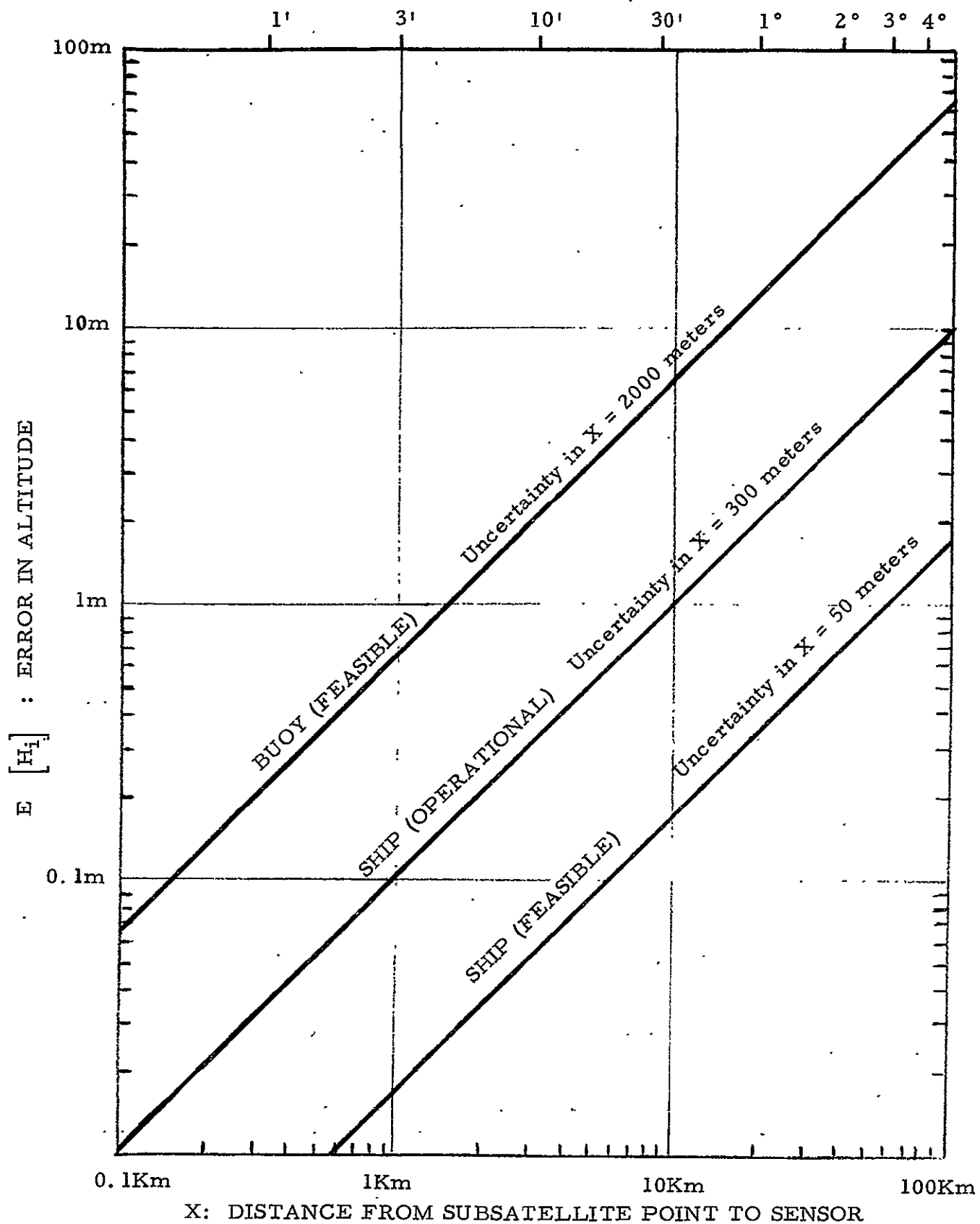


Figure 5-3. Ground Track Error

The measurement of the platform position relative to the subsatellite point can be accomplished by tracking the satellite from known shore stations (which can be readily accomplished to an accuracy of better than 50 m and hence is no problem) and navigating the surface sensor system. This latter function presents a more serious problem. The best available system currently in use provides rms accuracies in horizontal position of from 200 to 400 m; typical is the system available in the Vanguard ships, which integrates SRN-9 (Navigational Computer) with INS (Inertial Navigation System), and which has been evaluated.<sup>68</sup> The horizontal position accuracy could be improved to 60 meters using Differential Omega techniques and limiting observation to ideal propagation conditions.<sup>69</sup> This would require five Omega receivers at shore stations in the Caribbean to correct the Omega fixes taken by the Vanguard ships. Omega equipment is not currently available on the Vanguard ships.

The other approach to establishing  $H_{iv}$  from Range Data would require tracking the satellite in angle from the Apollo ships. Such tracking depends upon knowledge of the local vertical at the tracking ship plus the angular tracking accuracy of ship's radar. The limitation that now bounds this approach is the FPS-16 radar which has an expected error of 0.2 milliradians<sup>70</sup> or about 350 m at 1750 km range. This accuracy could be greatly improved by optical tracking techniques. The rms errors in the optical system, such as a stabilized camera plus that in establishing a local vertical reference should be better than 0.04 milliradians or about 50 m. Such a system would be limited to clear weather tracking.

What does this imply from an operational point of view if 0.5 meter error is allotted to this source? Vanguard ships as currently instrumented can provide the required accuracy for the coordinate system if they were located within 1.3 km from the satellite track. If an upgraded system were to be used, the Vanguard ship could be operated as far as 24 km from the ground track of the satellite and still measure within the 0.5 m error budget for  $H_1$ .

#### 5.4.2 Establishing Instantaneous Mean Sea Level

The direct method depends upon establishing the height of a reference above instantaneous mean sea level. Two approaches can be taken: space averaging and time averaging.

Ergodicity can be assumed; i.e., that time average and horizontal displacement average are interchangeable over a limited distance. An average measurement of the height of the range sensor above instantaneous mean sea level (IMSL) can be performed over an area by measuring the pressure of a deep pressure gage, (i.e., 1000 ft) maintained at an oceanographic isobar. A subsurface buoy<sup>36</sup> that maintain a constant depth, can be equipped with a transponder that indicates the depth of the buoy relative to a ship and the prevailing pressure at that approximate depth. Sonar ranging from the platform on the surface to the deep water buoy will provide a reference accurate to better than 1 ft. A profile of the velocity of sound as a function of depth must be established by a velocity profiling instrument such as a Sing Around Velocimeter<sup>37</sup>. Such instruments measure sound velocity to accuracy of better than 5 parts/million. The subsurface buoy then provides a mean sea level reference for an area of approximately 4000 feet in diameter.

An equivalent reference could be provided at or close to the surface by making a time average of the height of the range sensor above instantaneous mean sea level, using a vertical accelerometer that is maintained upright by an inertial reference unit. Such a system is available on Vanguard's ships. Unfortunately, the averaging computation currently performed are not adequately closely coupled in time base for the correction of radar range data<sup>38</sup> to the desired accuracy of 1 meter. Estimates are that as the system is currently used, errors could be as large as 8-10 meters. However, simple calculation indicates that integration of the PIGA accelerometer output could be configured to control mean sea level smoothing estimate to 0.7 meter over a 20 minute

smoothing interval. Load/Salinity displacement curves are available to establish the metacenter of the Vanguard ship at different fuel loading levels. These are obtainable from the Marine Engineering Department at General Dynamics in Quincy<sup>39</sup>. This result could be translated from the metacenter of the ship to the radar and used to correct radar height data to an accuracy of 1 m<sup>40</sup>, using INS data. The ship system is not currently programmed to accomplish the required level of accuracy so that nominal revision in software and hardware would probably be required. A review of ocean power spectra<sup>41</sup> indicates that energy in waves with period exceeding 5 minutes is less than 0.5 cms<sup>2</sup>. This indicates that the rms of the displacement residual averaged over a 20 minute period would not be as large as 20 cms, which is an acceptable level.

#### 5.4.3 The Measurement System for Range (R)

In this section, the errors that can be expected in the measurement of Range from a station on the ocean surface will be examined. Assuming that Range measurements will be made from the Vanguard Apollo tracking ship, this study will then estimate what might currently be achieved with Vanguard. An estimate is then made of what can be accomplished on the basis of results obtained in the Wallops Island C-band evaluation results. Finally, an outline is presented of what might be done to provide the desired accuracy for the verification system.

##### 5.4.3.1 Current Ranging Capability

Evaluation test results by different groups differ substantially in their conclusion. The best results generated on the basis of a single station indicate that the Vanguard ship as now instrumented can provide a GEOS C tracking accuracy of the order of 6 meters<sup>42</sup>. It is not unreasonable to expect that this system could be upgraded to provide 3 meters accuracy. Several other alternative sets of instrumentation might also provide this accuracy. On the other hand, more pessimistic results of AS-505<sup>43</sup> and AS-506<sup>44</sup> Metric.

tracking performance analysis indicate that Vanguard tracking residual errors are of the order of 10 meters; when ship position are corrected, range bias measurements are accurate to 20 meters. These results are based upon multi-station track fitting. The bias differential between S- and C-band tracking is somewhat larger: of the order of 50 meters. In contrast with these pessimistic results are the results that have been achieved with the FPQ-6 radar and the FPS-16 radar at Wallops Island, which have been differently interpreted by various authors.<sup>45</sup> Mos<sup>46</sup> and Brooks<sup>47</sup> estimate the FPQ-6 to provide better than 2 meters operating with a beacon and 3 meters for skin tracking while the FPS-16 should yield 5 meters accuracy. These results were obtained from comparison of colocated systems of the primary geodetic tracking system. Both AN/FPQ-6 and AN/FPS-16 radars were compared in this exercise. An orbit was generated from the AN/FPS-16 radar and laser results were used to verify the results. The AN/FPS-16 range residuals were referenced to this orbit. A more comprehensive investigation by Leite and Brooks<sup>48</sup> indicates comparable results of 2 meters for short arc analysis of AN/FPQ-6 results and better than 5 meters for long arcs.

Experiments that were conducted in fall of 1969 at Wallops Island indicate that over a 3 month period, the AN/FPS-16 radar maintained a constant bias within two meters relative to the AN/FPQ-6<sup>49, 50</sup>. Further, all the laser tracking systems were within 5 meters bias of the results of the other two systems.

From these results, it is apparent that test data for Vanguard tracking ships do not currently offer sufficient accuracy for the measurement of Range. However, it is expected that the Vanguard system is being sufficiently improved to provide a reference for the experiment, making better use of inherent capability of the system.

Brumberg\* has raised another problem: that of gimbaling limitations that exist on the FPS-16 at zenith. Normally, such limitations primarily effect angular tracking accuracy because of polar gimble lock. An angular accuracy is of secondary importance in this application, specific studies should be conducted to determine what (if any) implications this problem may present for range tracking at zenith.

It should be pointed out that the performance limitations that exist are not inherent physical measurement limitation but rather constraints that have arisen because of the particular constraints on the design and use of the Vanguard System. The only primary physical constraint in range measurement that does not lend itself to compensation are questions relevant to propagation. The results and their implications are summarized here. The expected error is given in Table 5-2.

Table 5-2. Propagation Errors

Region	Frequency (GHz)	Correctable Bias (Meters)	Uncertainty (Meters) ( $1\sigma$ )
Free space	all	-	.3**
Ionosphere	3	1.3	0.30
	7	0.2	0.05
	10	0.1	0.025
Troposphere	3	2.4	0.037
	7	2.4	0.037
	10	2.4	0.037
Total Atmosphere	3	3.7	0.30
	7	2.6	0.062
	10	2.5	0.045

It should be noted that the uncertainty listed for a particular set of readings does not constitute solely a random error, and cannot be reduced by averaging, but includes an unknown bias for that set of data.

\*Personal communication with Paul Brumberg of Goddard Space Flight Center.

\*\*Because of uncertainty in the speed of light.

#### 5.4.4 Possible Alternative Ranging Instrumentation

##### Surface Transponders

The use of transponders on the surface presents an interesting possibility for measuring Range. There are two possibilities in particular that make this alternative of interest:

- The Motorola Arod System
- The design of the altimeter to incorporate its own evaluation system.

A surface transponder would be accessible to have its performance monitored and undergo calibration as required. Discussions with Vega indicate that a marked improvement in performance would be achieved for transponders operated under surface conditions of maintenances and availability, where operating conditions could be closely monitored.

Motorola has designed a precision range tracking system based on surface transponders. The accuracy of this system is expected to be 0.5 meters bias and 0.2 meters rms error at 20,000 kilometers<sup>51</sup>. (For use at a range of 20,000 meters and as a consequence, the weight size and power are excessive for this application.)

A second alternative that could be accomplished at little or no increase in power is to use the altimeter system to perform its own verification. The pulse from the altimeter could be used to actuate the transponder. The transponder would incorporate a precision  $1 \mu$  sec delay to prevent the transponder from interfering with the altimeter range tracking system. The output of the receiver would be gated into a second range discriminator after the altimeter signal finished. The time difference between the altimeter and the verification signal could be used directly for verification. The primary criticism of this approach would be that the only part of the system that was being verified was its interaction with the water surface and the range gate tracker. Many of the instrumentation errors of the altimeter would be common to both systems.



### Surface Corner Reflectors

A corner reflector on the ocean has been suggested for evaluating the altimeter performance. Our study indicates that a corner reflector is not suitable for the verification experiment. The satellite altimeter would measure range to the reflector. The advantage of this approach is that no auxiliary electronic equipment need be required. To obtain a signal of magnitude comparable to that of the ocean surface return\*, the corner reflector\*\* should be approximately 17 meters on an edge. For adequate signal discrimination, the reflector must be larger and of sufficient rigidity and accuracy so that the inside surface was maintained to an accuracy of 1 mm. By standards of current antenna fabrication, this would be extremely difficult. In order not to interfere with the Satellite altitude measurement, the corner reflector would have to be placed at least 5 miles off the satellite track which would greatly increase the accuracy requirements for positioning the reflector. The cross track positioning error should be kept to better than 100 feet, which is well beyond expected navigational tolerances. Surface corner reflectors are therefore not considered suitable.

### Synchronized Clock Systems for Measurement of Range

Satellite altitude could be verified either from the satellite or from the surface, utilizing the altimeter signal and a synchronized clock system. The method is discussed in Appendix P, although not in sufficient detail to make recommendations concerning its use at this time.

---

\* p. 7-11:  $\sigma\sigma_0 = (4 \times 10^7 \text{ m}^2) (10 \text{ dB}) = 4 \times 10^8 \text{ m}^2$  is the radar cross-section.

\*\* Barton, D. Radar System Analysis, Prentice-Hall, 1964; p. 71

## SECTION 6. VERIFICATION OF ALTIMETER PRECISION

This section is divided into two independent parts: section 6.1 on self-consistent verification, and section 6.2 on differential verification. Both these sections are concerned with verification of altimeter precision, involving comparison between altimeter measurements either over the same or nearby locations.

### 6.1 Self-consistent Verification

The self consistency of data that is taken at a given geographical location can be readily used to determine the precision of the altimeter instrument. This technique for verification is significant because it is less sensitive to bias errors in the tracking systems and requires only a determination of change with time of the parameters that contribute to the altitude difference. Variations of this approach can be used at locations where tracking and surface coverage is greatly reduced from that required by other approaches to verification at the expense of only modest deterioration in performance. The method can also be used as an ongoing check to assure that the initially verified performance is maintained throughout the life of the altimeter.

#### 6.1.1 Error Summary

The precision measurements that can be expected by this approach are given in Table 6-1. The errors presented in this table represent what might be expected from this system in a well monitored area such as the Carribean. In such an area the operational level of performance is adequate for 3 meter verification of precision. There would be some degradation if this technique were to be used in a less well monitored area. In order to achieve the operational level of accuracy it has been assumed that the data has been selected to reject such data as is taken when timing synchronization is worse than  $100\ \mu s$ .

#### 6.1.2 Geography

The geographical regions which lend themselves to the self consistency approach to verification are somewhat more extensive than for the absolute or the relative method because of the less stringent data requirements. On the other

Table 6-1. Self-Consistent Verification Error Summary

	Tracking $\sigma_{(m)}$	Ceoid	IMSL	Propagation	$\sigma$ Total
Operational	2-3	-	1 m	1 m	3 m
Capable	1-2	-	1.0 m	1. m	1-2 m
Feasible	< 1	-	.3 m	.3 m	< 1 m

hand, the amount of self consistent verification data that can be garnered from a particular area is very highly latitude dependent. As can be seen from Figure 6-1, the density of suborbital track crossings is thirty times larger at  $20^{\circ}$  than it is at the equator for the planned GEOS C orbit inclination. Hence, regions such as the Carribean, Hawaii, Mozambique, and the region East of Austrailia which meet the dual constraint of being at a latitude of  $20^{\circ}$  and having tracking capabilities particularly lend themselves to this application. The South Pacific, the bulk of the Indian Ocean and the South Atlantic which, because of a paucity of tracking stations do not ideally lend themselves to verification, can also be used if a variant of the self consistency method is used. Two such variants are the loop closure method, & the orbital retrace method.

### 6.1.3 Ground Support System

The supporting system for verification depends upon the level of performance sought.

The operation level of performance can be achieved with the operational C- and S-band tracking systems. Provided that the points chosen to accomplish verification are adequately removed from shore areas to avoid the shore line tidal effects, there is no requirement for surface monitoring to provide the accuracy sought. However, the data must be selected to insure that tracking stations are sychronized to about  $100\mu s$ .

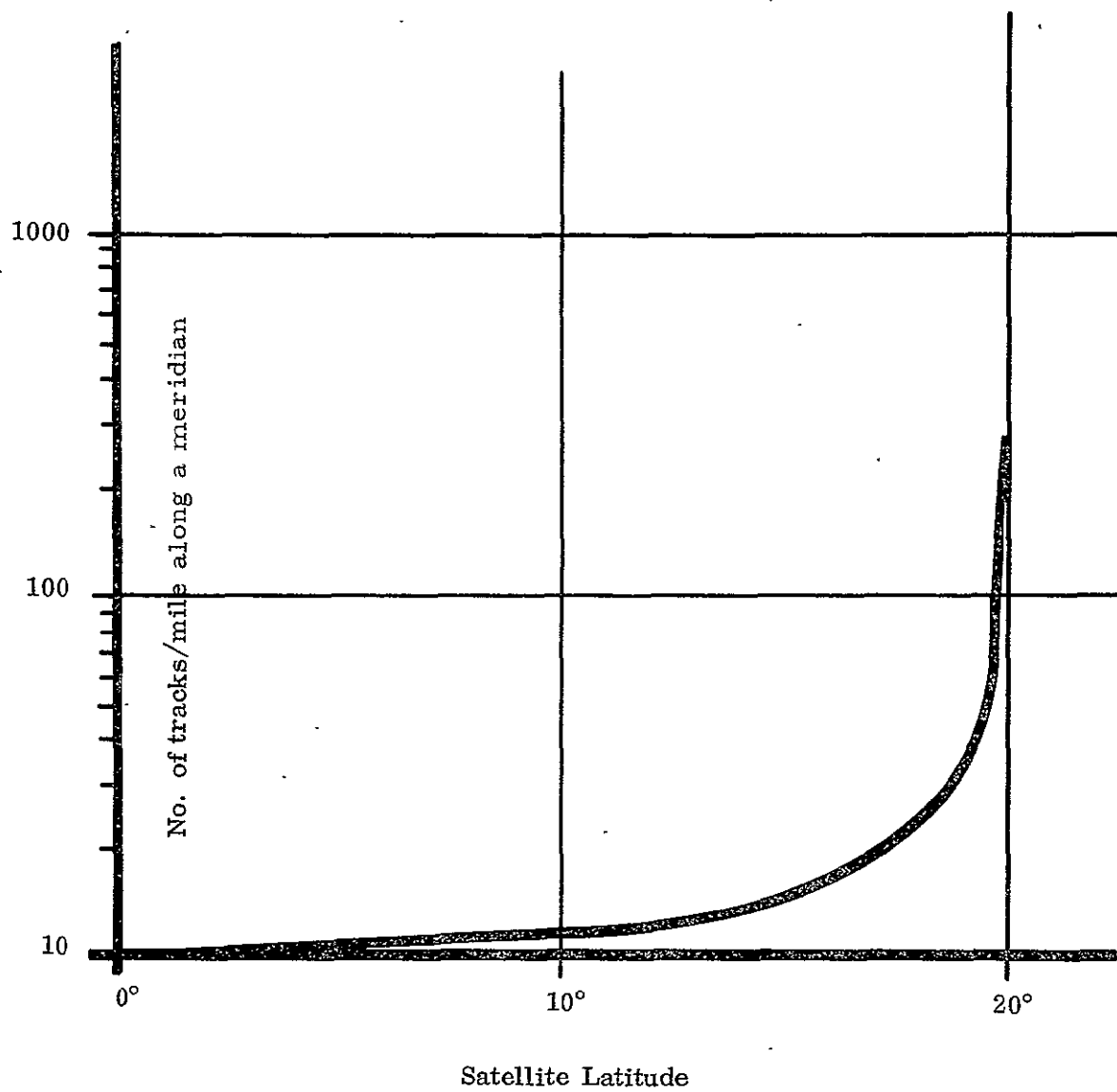


Figure 6-1. Sub-Satellite Tracking Density

The capable level of performance can be achieved by improving the interstation timing synchronizations between tracking sites to 100  $\mu$ s and adding optical tracking stations. Again under open ocean conditions, surface monitoring is not required.

The feasible level of performance requires both upgrading of the tracking network and improvement of the surface monitoring system. In addition to the improvements required for capable, the following additions are required.

- Redesigning of the C-band transponder
- Providing precision movable range tracking units, such as transponders.
- Input of tidal prediction data
- Input of synoptic air pressure data

#### 6.1.4 Data Requirements

Let us next address the question of data required by the self-consistent method.

##### 6.1.4.1 Tracking Data

The tracking data required by the self-consistent method is substantially less than that required for the absolute method, as the requirement for removing the measurement biases is materially reduced. Only tracking data for the two orbits under comparison is required.

##### 6.1.4.2 Surface Data

The surface data requirements for self-consistency is materially reduced in comparison with the absolute method because only the time-dependent part of the measurement enters into the precision computation. As a consequence, the geoid uncertainties can be completely eliminated; and the time variations from temperature and salinity are likely to be negligible. Only the pressure pattern and tides have a time variation that will reflect in this precision measurement. These will only reflect at the feasibility level of measurement. The pressure

pattern can be corrected from synoptic data and the tides from their well established cyclical patterns.

#### 6.1.4.3 Sea State Monitoring

Sea State Monitoring Data requirements will be the same as the data required for the absolute approach as this data tells only the state that is under observation.

#### 6.1.5 Advantages and Disadvantages

The principal advantages of self-consistent verification are:

1. Computationally simple and brief.
2. Requires nominal additional expenditure of effort; no additional hardware demand.
3. Relatively insensitive to errors in tracking system, such as equipment biases propagation errors and tracking station location errors.
4. Requires no knowledge of the geoid.
5. Requires only changes in IMSL, principally tides.
6. Can be used as check on operational performance of the altimeter during its lifetime.

The principal disadvantage of self-consistent verification is:

1. For large crossing angles, is sensitive to (geometric) propagation of errors.

#### 6.1.6 Self Consistency Verification Concept

Self consistency verification is based upon the supposition that at a given geographical position successive altitude measurements that are generated by the altimeter should be consistent. The subsatellite point of each orbit intersects the subsatellite point of every other orbit at two cross-over points. Therefore measurements of altitude and orbital height made at these cross-over points on successive orbits should be self consistent; that is to say, the difference in the altitudes measured by the tracking method should agree with the differences that

are measured by the altimeter. Inasmuch as the same stations in the tracking network are viewing the satellite under essentially the same circumstances on the two orbits, traces that are independent of time which are associated with particular stations should be the same, and as a consequence tend to cancel out in our computation of altitude change. In addition, the uncertainty factors in establishing ISML that are space-dependent rather than time-dependent should also be reduced to negligible magnitude.

Figure 6-2 is an illustration of this method, illustrating a measurement at  $P_i$  on orbit  $i$  and another measurement at the same location, designated  $P_j$  on orbit  $j$ .

The equations governing the self-consistency tests are

$$h_{mi} = h_{si} - h_{oi} \quad (6-1)$$

$$h_{mj} = h_{sj} - h_{oj} \quad (6-2)$$

Then subtracting

$$(h_{mi} - h_{mj}) = (h_{si} - h_{sj}) - (h_{oi} - h_{oj}) \quad (6-3)$$

$$\Delta h_m = \Delta h_s - \Delta h_o \quad (6-4)$$

where it is assumed that, except for tides,

$$\Delta h_o = h_{oi} - h_{oj} = 0 \quad (6-5)$$

It can be shown that the number of crossing points after  $n$  revolutions is given by

$$N = n(n-1), \text{ or for } n \gg 1 \text{ by } N = n^2. \quad (6-6)$$

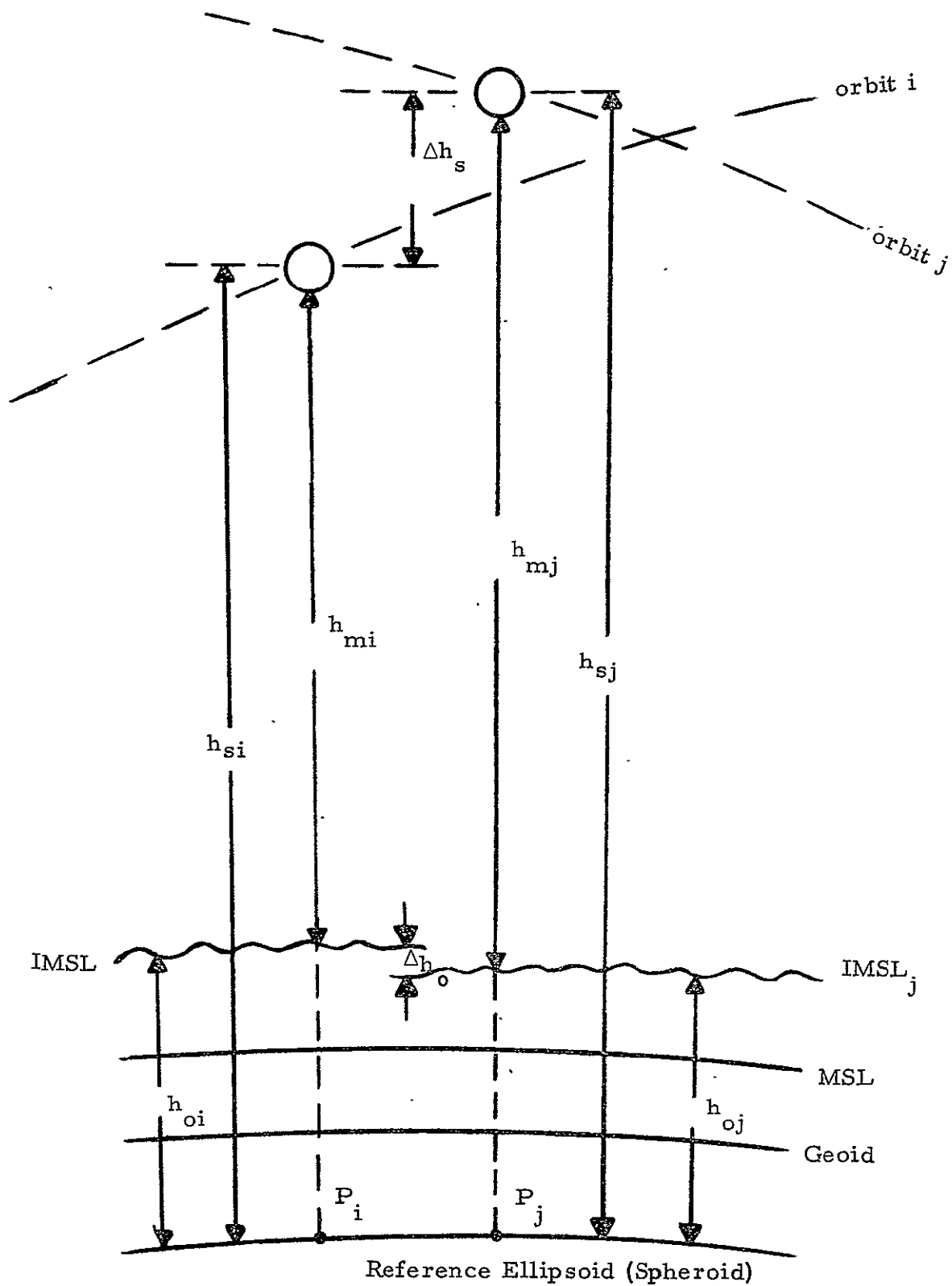


Figure 6-2. Self-consistent Category Test



Assuming a total of 10,000 revolutions, approximately  $10^8$  intersection points are contained within the  $40^\circ$  wide zone about the equator, so that the average density is 6000 intersections per square degree. Obviously, the actual density will be about six times as great near the zone boundaries and about one sixth as great near the equator. This can be seen from Figure 6-1 where the density of satellite tracks is plotted as a function of latitude.

#### 6.1.7 Error Analysis

The self consistency method is based upon equations 6-4 and three assumptions. Equation 6-4 is a mathematical identity whose terms are measured by different techniques. The errors then arise from the degree to which these assumptions are true. These assumptions are:

1. That the satellite on the  $i$ th and  $j$ th orbit are being tracked by the same set of tracking systems under essentially the same conditions so that the errors in the determination of altitude difference at the cross-over point cancel out. This is more nearly so for orbits crossing near  $20^\circ$  latitude.
2. That points  $i$  and  $j$  correspond geographically.
3. That the height of the surface being measured (IMSL) is independent of time, except for tides.

Let us examine the errors that arise from these assumptions:

##### Assumption 1

The errors that result from Assumption 1 are shown in Table 6-2, resulting in the first column of figures in Table 6-1.

##### Assumptions 2 and 3

The errors that result from Assumptions 2 and 3 are shown in Table 6-3 and explained in Section 4.3.1.4 and/or the accompanying notes.

Table 6-2. Tracking Errors in Self-Consistent Verification

Cause of Error	Magnitude of Errors			Source of Information
	Operational	Capable	Feasible	
Bias - Station Height and Location	2	0.5	0.1	Note 1
RMS Random Error	1	>0.1	>0.1	Table 4-1
RMS Propagation Error	1	0.5	0.5	
Tracking System Drift	2	0.5	0.5	Note 2
Timing Synchronization	0.2	0.02	0.02	Note 3

Note 1:

Tracking Station height and satellite location errors propagate into the computation of the altitude of the  $i^{\text{th}}$  and  $j^{\text{th}}$  orbit in exactly the same way, particularly for orbit crossings close to  $20^\circ$  latitude. The expected error in height difference is less than 10% of the assumed error in tracking station height.

Note 2:

Tracking System Drift - This error results from drift characteristics in the transponder, the radar delay uncertainty and timing reference. The current transponder has repeatability to better than 2 meters<sup>50</sup>. The transponder could be redesigned to provide a repeatability of 0.5 m.

Note 3:

Timing Synchronization between Ground Tracking Stations is critical to this method. The error coefficient is 3 meters/millisecond. It is assumed that when timing synchronization error exceeds 1 millisecond, the data will be rejected. Errors of this magnitude can be determined best later.

Table 6-3. Errors that Result from Location Difference and Time Difference  
Between Points i and j

$x$  = position displacement

Cause of Error	Magnitude of Error	
$\frac{\partial h_s}{\partial x}$ (1)	max 0.03 meters/meter (2)	
$\frac{\partial h_o}{\partial x}$ (1) $\left\{ \begin{array}{l} \text{Geoid} \\ \text{IMSL} \end{array} \right.$	$>1 \times 10^{-3}$ meters/meter $1 \times 10^{-4}$ meters/meter	
$\frac{\partial h_o}{\partial t}$ $\left\{ \begin{array}{l} \text{Geoid} \\ \text{T/S Pattern} \\ \text{Tides} \\ \text{Pressure} \end{array} \right.$	Insignificant Insignificant 0.3 m 0.3 m	

(1) Points i and j correspond geographically

(2) The ellipticity of the orbit results in an error in satellite altitude if either the epoch of the satellite or the position of the satellite is uncertain for an orbit that has a height differential of 200 miles. This value will vary from 0 to 0.03 meters/meter.

#### 6.1.8 Variants of the Self Consistent Method

There are two powerful variants of the simple self-consistent method:

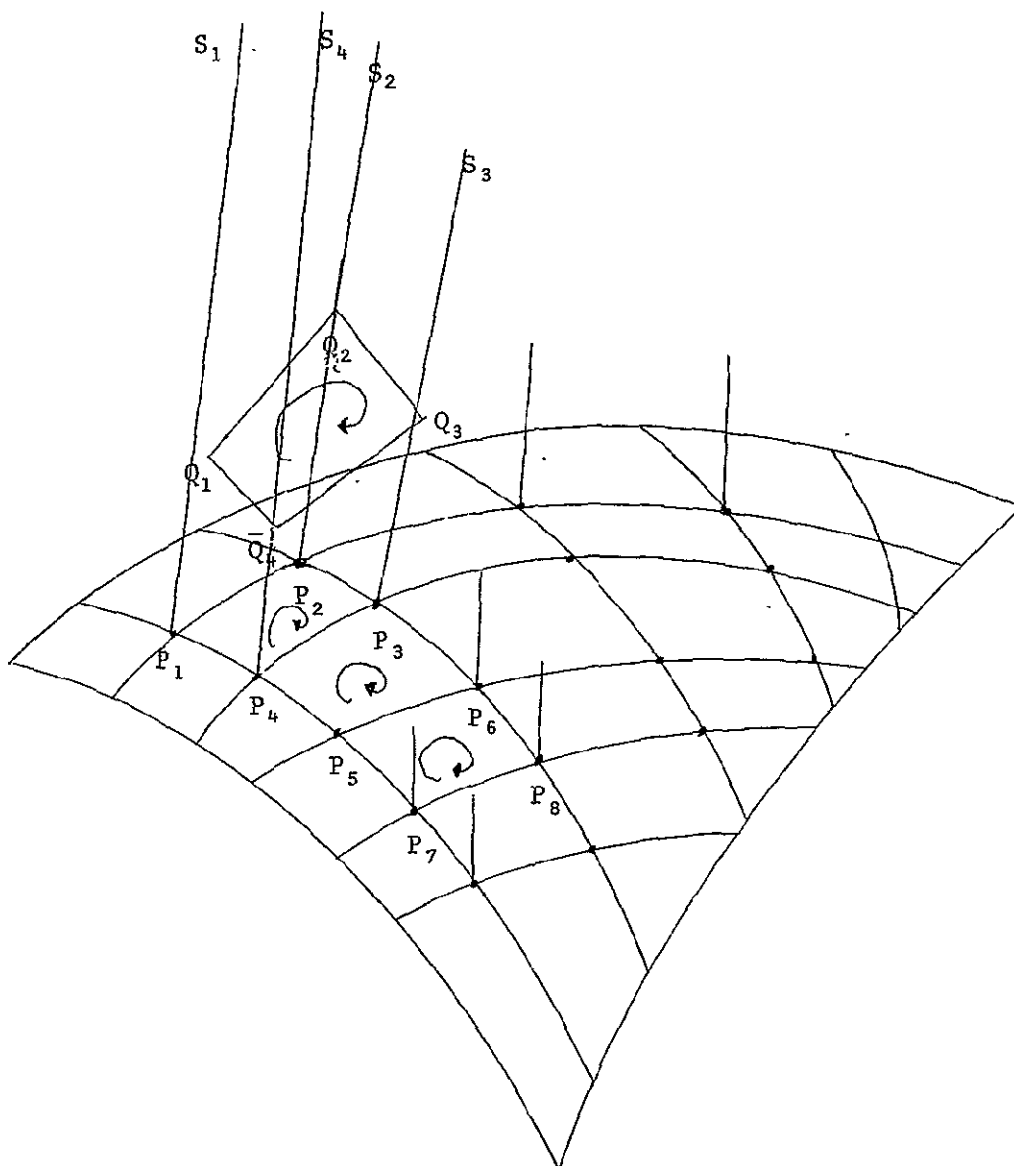
- The closed loop method
- The retrace method.

These methods have three significant advantages over the simple single point approach:

- The errors that result from errors in position measurement cancel out, if the geometry remains constant.
- The time dependence of IMSL cancels out under some circumstances
- These methods reduce the dependence of the satellite altimeter system on surface tracking stations to an extent that it can be a useful survey instrument.

The closed loop method is based upon three or more orbits whose subsatellite traces intersect at three or more points on the surface and enclose a small region on the surface, Figure 6-3. The density of occurrence of such loops is high in the region between  $15^{\circ}$  and  $20^{\circ}$  latitude. The reason that this method yields an improved error performance is that the errors which result from position uncertainties are canceled out because the difference in altitude between the ends of the leg is relatively insensitive to small translations of the leg along its own path.

The retrace method is based upon two orbits whose subsatellite traces follow very nearly the same ground track (see Figure 6-4). Such orbits will measure essentially the same surface topography. It can be simply shown that in the region close to  $20^{\circ}$  over the two-year life of the satellite that pairs of orbits will have subsatellite traces that do not depart from each other by more than 150 meters for distances well in excess of 600 miles. Such orbits can be



- $P_i$  - points on MSL surface  
 $Q_i$  - corresponding points on MSL surface  
 $S_i$  - points occupied by altimeter at first passage over  $P_i$

Figure 6-3. The Path-Intersection Grid

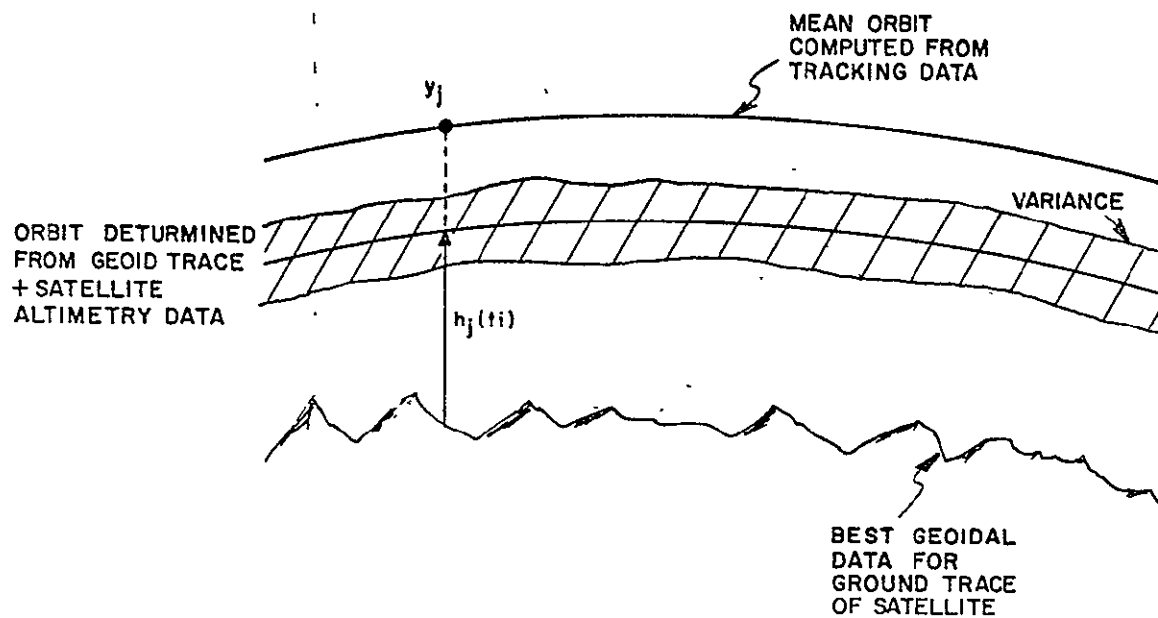


Figure 6-4. Measurement of Altimeter Repeatability By Multiple Passes on Same Ground Trace

used to make a direct comparison of the surface topography. With this technique the orbital characteristics can be corrected over the complete satellite revolution. Trenches and other topographic features which represent harmonics well above those that influence the orbital dynamics can be compared to establish the precision of the instrument.

## 6.2 Differential Verification

### 6.2.1 Summary

Differential verification compares the change in altimeter readings over a short segment of an orbit with independently determined changes in satellite orbit and changes in IMSL over the same orbit segment. This approach requires knowledge of changes in IMSL over the interval of measurement and hence of topography, or the geoid. The geoid need not be known in an absolute sense. Similarly, tracking requirements are reduced to knowledge of changes in altitude rather than accurate orbital tracking.

This method provides a high precision measurement of satellite altitude, and has high accuracy in application to measuring the slope of the geoid. It is insensitive to errors in absolute location of the satellite, and to errors in the location of mean sea level. On the other hand, there are limited areas of applicability, and the verification information on the altimeter is limited to precision rather than accuracy.

Figure 6-5 suggests the experimental concept of differential verification. Figure 3-1 is helpful in relating various quantities of interest.

Figure 6-6 is a block diagram representation of the methodology of a typical differential verification procedure. A tracking network provides information on the change in satellite altitude (relative to an Earth-fixed coordinate system) between two satellite readings. Using knowledge of the geoid at the

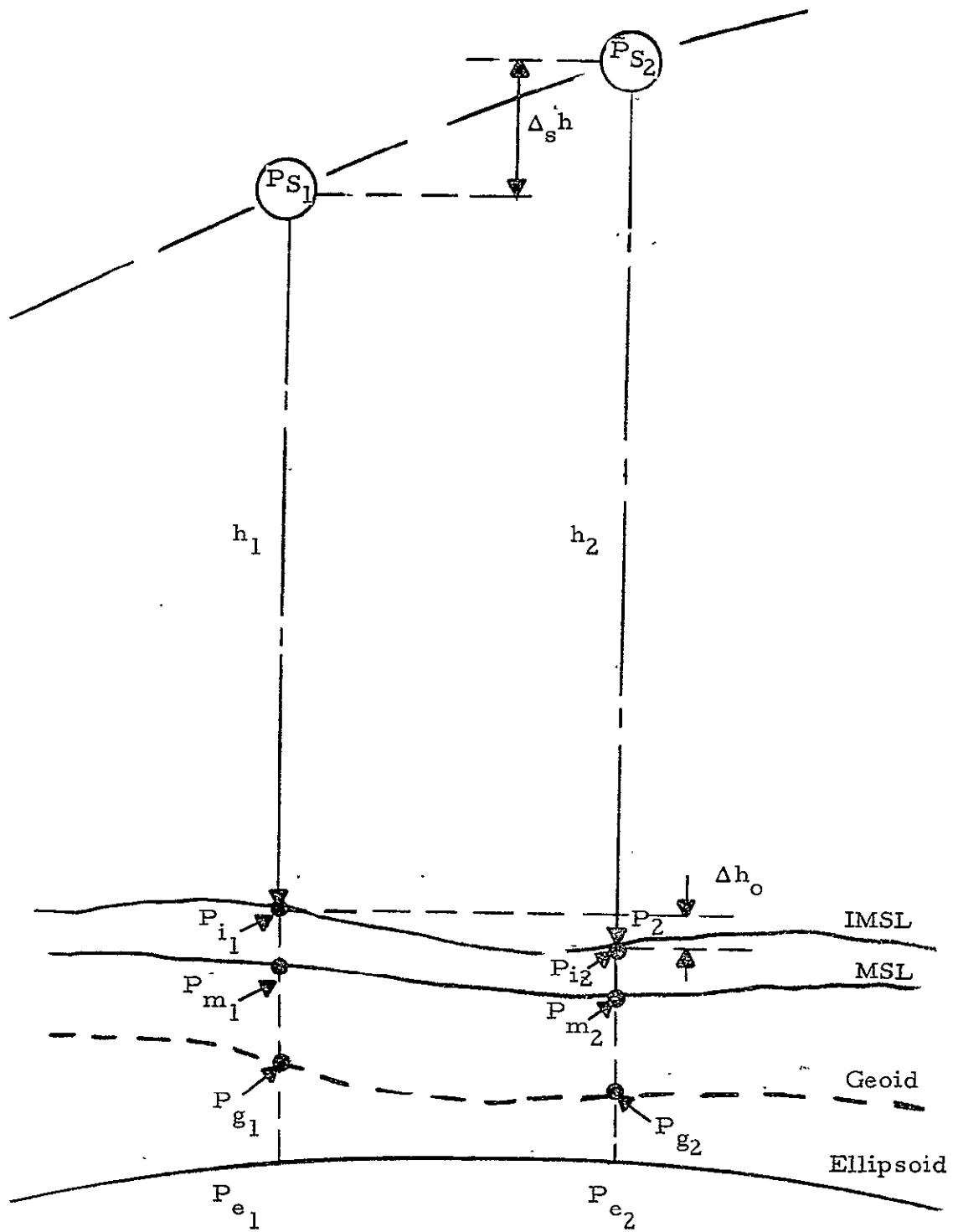


Figure 6-5. Differential Verification



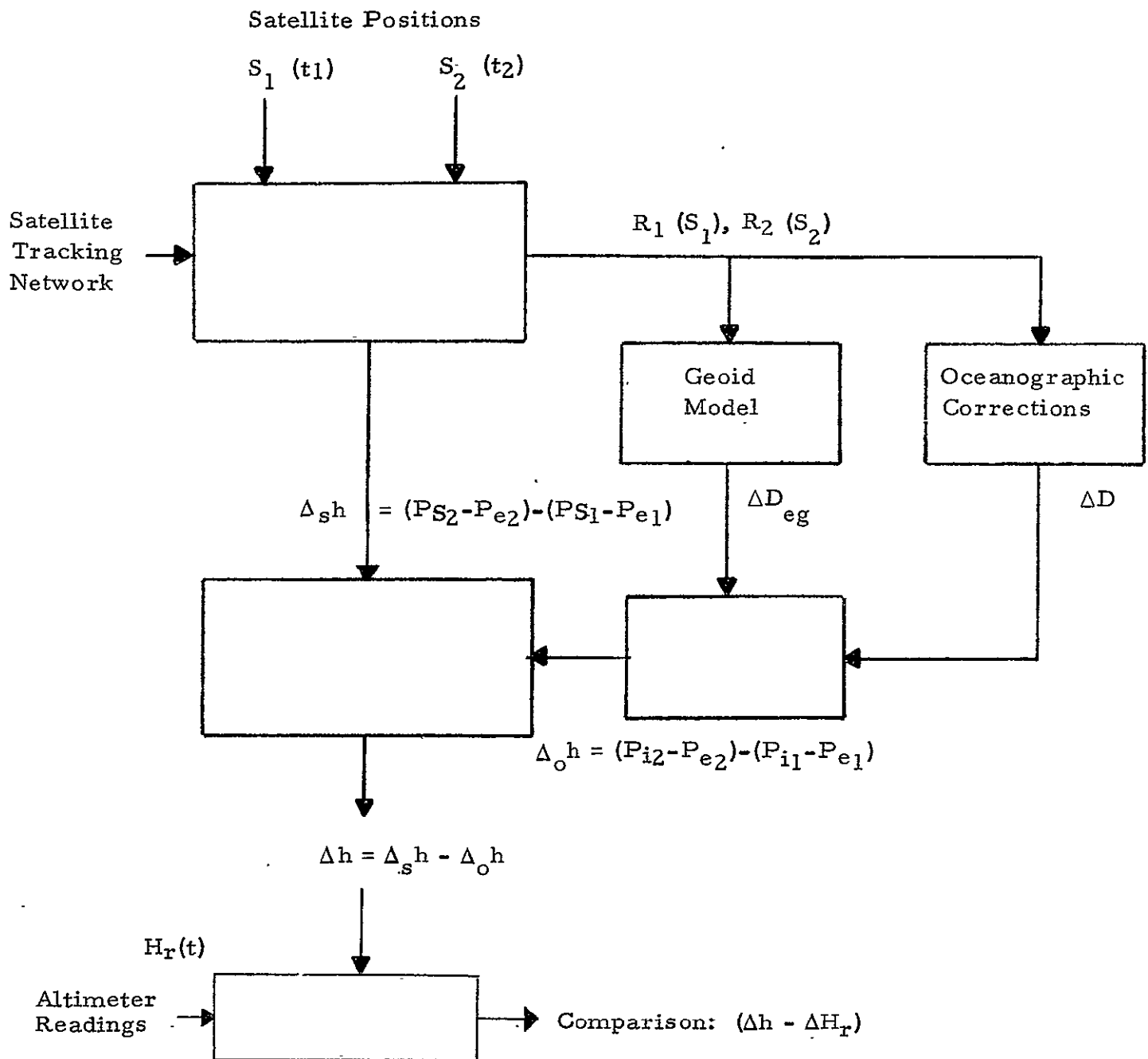


Figure 6-6. Differential Verification Block Diagram

subsatellite points, and local oceanographic corrections, the difference in IMSL at the two subsatellite points can be determined. The changes in the two ends of the altimeter ranging points are combined to provide the verification determination of the net altitude change in differential verification.

The summary of errors in differential verification, shown in Table 6-4, indicates that current procedures and equipment can verify differences in altimeter readings to 3 meters, with 1 to 2 meters achievable with minor modifications, and better than one meter ultimately expected.

Table 6-4. Differential Verification Error Summary

	Tracking: $\Delta$ Propagation	Tracking $\sigma$	Sea Surface		$\sigma$ Total
			$\Delta$ Deg Geoid	$\Delta$ IMSL	
Operational	.5-1m	2-3m	1 m	.5-1m	3m
Capable	.5m	1-2m	.7m	.3-.5m	1-2m
Feasible	.3m	< 1m	.5m	.3m	< 1m

The "operational" category refers to currently available systems, including instrumentation, personnel and currently available reporting activities. A total rms error of 3 meters is expected under these currently available conditions.

With some effort, the operational conditions can be upgraded by (a) improving tracking accuracy - mainly through timing to at least 100 micro-seconds for all stations - thereby reducing the largest error source; (b) reduction in geoid slope error by examination and reduction of existing geoid and gravity survey data; (c) improved knowledge of changes in IMSL through increased geographical and/or temporal density of surface data in the measurement region. The total rms error could thereby be reduced to 1 - 2 meters for this "capable" category.

With considerable effort, a "feasible" category can be obtained for reducing the rms errors for the GEOS-C verification experiment to less than 1 meter.

This involves upgrading operational features as follows:

- (a) Propagation error reduction through increased local meteorological data, such as that obtained from rockets;
- (b) improved tracking accuracy through greater care in taking and processing data, station procedures, and selection of specific test locations;
- (c) additional geoid slope data through local surveys at test locations
- (d) additional ocean surface data through instrumentation at test areas.

The principal advantages of the differential verification are:

1. Performance can be almost anywhere; in areas with no geoidal changes, results indicate drift in the altimeter system.
2. Errors in the tracking system, such as equipment biases and propagation errors, are practically cancelled out.
3. Station location errors are not critical; changes in position are more significant than the positions themselves.
4. Errors in the determination of IMSL (including changes in the geoid elevation, and in oceanographic corrections) are reduced significantly by being concerned with the change between two points, and canceling out dependence on a tracking station network, or an ellipsoidal coordinate system.
5. Only local changes in geoid topography need be known; surveys need not be known over extended areas.

The principal disadvantages of the differential verification are:

1. Ability to measure topographic changes can be determined in limited areas where topographical features undergo substantial changes in elevation over short distances, such as at the Puerto Rico Trench (Brownson Deep) and on the two sides of Panama (at selected times).

2. It does not verify accuracy, but precision or changes in altitude.
3. Abnormal gross changes in altimeter operation or readings are not checked, and would not normally be noticed. Bias cannot be detected.

#### 6.2.2 Support Data

The support data necessary for implementation of differential verification include:

- (a) Tracking data, particularly for changes in the tracking height relative to the geoid;
- (b) Geoid slope data, which is a much less stringent requirement than absolute location of the geoid relative to the spheroid;
- (c) Changes in IMSL relative to the geoid over the track length, which is a less stringent requirement than the IMSL itself;
- (d) Changes in propagation errors over the track (which are also usually small);
- (e) and ocean truth monitoring, which is required to about the same degree for all verification methods.

#### 6.2.3 Geography

The regions considered most suitable for differential category tests are as follows: There is a group of specific locations where there are known to be substantial changes in the IMSL (or geoid): (a) Puerto Rico Trench; (b) Offshore on either side of the Isthmus of Panama.

In addition, there are other locations which have not been specified, to be determined on the basis of the following criteria: (a) location in the Caribbean below  $20^{\circ}$ . (Possibly also near Hawaii, also below  $20^{\circ}$ .) (b) In region where tracking is favorable, based on station locations; (c) availability of geoid data through gravity survey, etc.); (d) availability of ocean surface data; (e) availability of atmospheric (including meteorological) data. The last three imply that this is a "busy" or "interesting" area, or else that one is willing to compensate for the

absence of data. Determination of specific locations based on these criteria is a recommended objective for further study.

#### 6.2.4 Theory

A differential test of the altimeter is a test in which the height difference between two surface points  $P_1$  and  $P_2$  is found by comparison of the difference computed from altimeter heights above these points with a height difference arrived at by measurements at the surface. Figure 6-7 shows the geometric relationships existing between the points concerned, and the following relations are evident: Heights measured at the surface are with respect to the sea surface first, with respect to the geoid by immediate consequence, and with respect to the reference spheroid by further computation. Since differential tests are by definition and preference made entirely within local geodetic systems, the reference surface ( $P_e$ ) can be made to pass through  $P_g$ , without prejudice to the experiment. In its passage from  $P_{S1}$  to  $P_{S2}$  the altimeter height above the spheroid therefore changes from  $P_{S1} P_{e1} = P_{S1} P_{g1}$  to  $P_{S2} P_{e2}$ , or by an amount  $\Delta_{sh}$ . The surface height difference measured with respect to the geoid by standard techniques such as spirit leveling, etc., gives the quantity,

$$\Delta D = \Delta(P_i P_g) \quad (6-7)$$

In making the test, the various heights must be reconciled. This involves the following computations (see Figure 3-8):

1. Determine  $\Delta_{sh}$ , the change in height of the satellite above the reference surface (ellipsoid). Only short segments of the orbit are used, with a considerable number of fixes on the satellite along at least one portion of the segment; this reduces location standard deviations below that for a singled fix.
2. Resolve  $\Delta_{sh}$  into its components along  $H_1$  (or  $h_1$ ) or  $H_2$  (or  $h_2$ ).
3. Resolve  $(D + D_{eg})$  into components along  $H_1$  (or  $h_1$ ) or  $H_2$  (or  $h_2$ ) for the values at  $P_{S1}$  and  $P_{S2}$ .

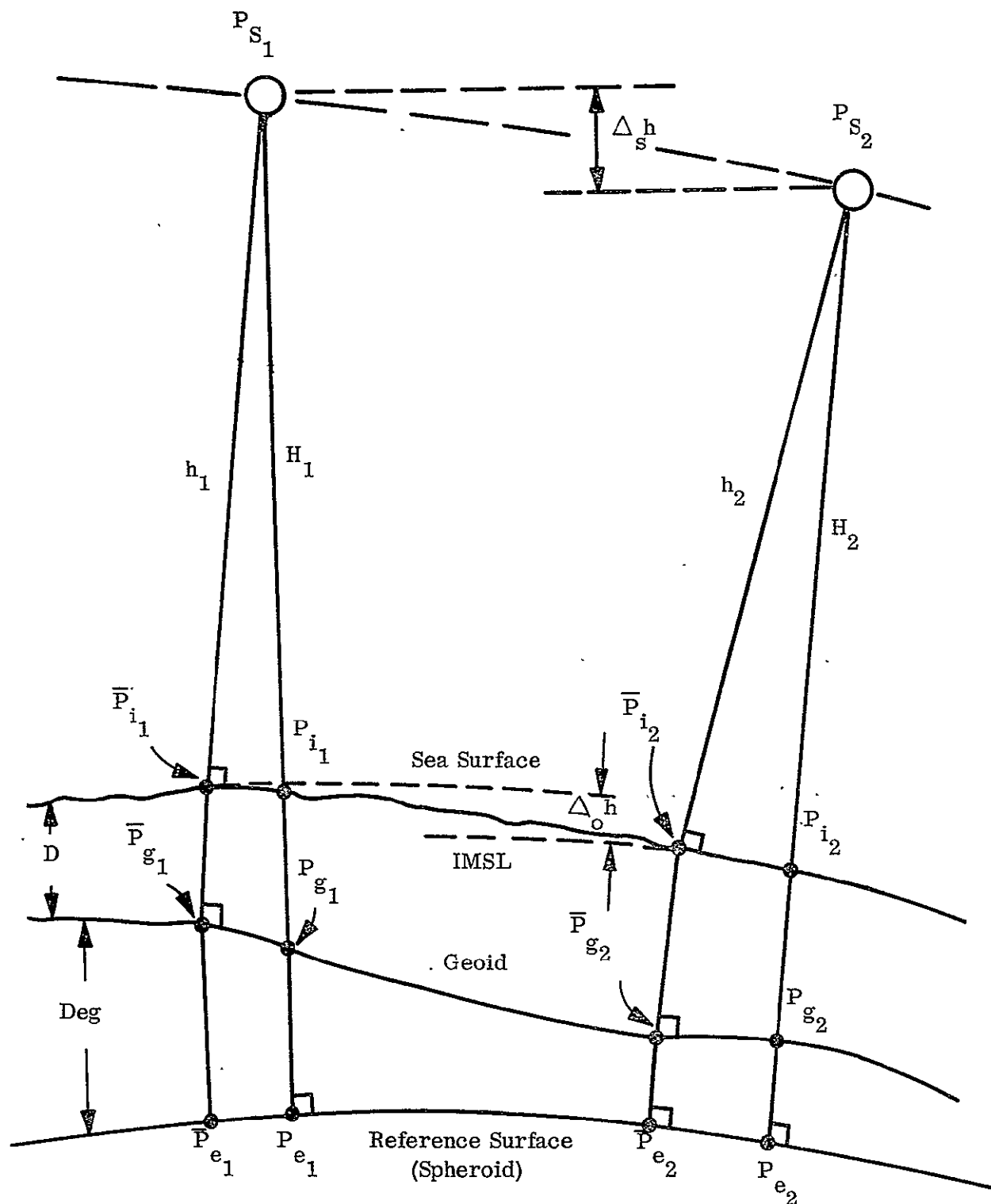


Figure 6-7. Geometric Relations Between Heights in Differential Verification

4. Determine  $\Delta_{oh}$ , the difference between the values of  $(D + D_{eg})$  at  $P_{s1}$  and at  $P_{s2}$ .
5. Determine  $\Delta h = (\Delta_{sh} - \Delta_{oh})$
6. Compare with  $(H_{r2} - H_{r1})$ , the difference in altimeter readings from  $P_{s1}$  to  $P_{s2}$ .

#### 6.2.5 Error Analysis

There is a negligible error involved in determining the position of the satellite relative to the geoid by  $(P_s \bar{P}_i) + (\bar{P}_i \bar{P}_g)$  rather than by  $(P_s P_g)$ , as shown in Figure 6-7. This can be seen by assuming a difference between sea slope and geoid slope of  $1:10^4$  as a worst case, which for a satellite height of 2000 km makes an error of about 10 mm.

The error between  $(\bar{P}_g \bar{P}_e)$  and  $(P_g P_e)$  can be found by assuming the difference between the geoid slope and spheroid slope to be  $1:10^3$  as the worst case, which, for a satellite height of 2000 km, makes an error of less than 1 meter. A 1-meter error is too great to be allowed if an alternative is available. Such an alternative is available because we know the geoid slope approximately in the area, which can provide a correction to the measured height. Since the geoid height itself is not used, the correction does not imperil the validity of the test. The correction can, in theory, be obtained from the altimeter measurements themselves by taking (satellite) height differences corrected for  $\Delta_{sh}$  close together and computing the geoid slope (which is for our purpose close enough to IMSL slope).

Assuming that the experiment is not performed in localities with special effects such as bores, etc., the maximum rate of change of IMSL (relative to the geoid) can be assumed to be less than 0.3 mm per second (during which the satellite travels approximately 7 km).

Over a time interval of 300 seconds, an error of less than 0.1 meter will be incurred if we are ignorant of the geoid at the second point with respect to the first. 0.1 meter is negligible as far as the problem of verification is

concerned. A time interval of 300 seconds is equivalent to a horizontal distance between points of over 2100 km - a distance greater than any we shall assume for application of the differential verification method. In order to avoid having to cope with too many uncertain quantities, we will assume that points  $P_1$  and  $P_2$  are less than 1000 km apart.

Passing from  $P_{S_1}$  to  $P_{S_2}$ , the altimeter changes its height above the spheroid by an amount  $\Delta_s h$ . The height of the instantaneous mean sea level (IMSL) above the spheroid changes by an amount  $\Delta_o h$ . The altimeter changes its height above IMSL approximately by this amount:

$$\Delta h \equiv \Delta_s h - \Delta_o h \quad (6-8)$$

The term approximately is used because the quantity  $\Delta h$  is not exactly the change in height of the altimeter above the IMSL. For most regions the difference is insignificant. If the local deflection is 100" and the satellite is at 2000 km altitude, the difference between  $h$  and the true altitude is 0.5 m. At least part of this error can be removed by computation using an estimated value of the local deflection. The quantity  $\Delta h$  can, therefore, be computed from the measured  $\Delta h$  and from the computed  $\Delta_s h$ , which is obtained either from the orbit or from tracking data directly.

The error theory applicable to differential measurements is essentially the same as that given for the absolute category of experiments (particularly 4.3.1.4) and in the relevant appendices. The main difference is that the errors we are concerned with are those in the increments rather than in the total quantities. The important difference errors are those in satellite locations, geoidal height, and IMSL. We consider the errors in that order.

#### A. Satellite Location Error

The error  $\Delta^2 h_s$  in difference of satellite height,  $\Delta_s h$ , arises from (1) orbit errors and (2) tracking errors. In the first category, we have

$$\Delta_s h \text{ (from orbit)} = \frac{dH_e}{ds} \Delta s \quad (6-9)$$



where  $\Delta s$  is the distance between  $P_{S1}$  and  $P_{S2}$ . The error  $\Delta^2 h_s$  is therefore

$$\Delta^2 h_s = \Delta \cdot \Delta_s h = \Delta \cdot \frac{dH}{ds} \Delta s \quad (6-10)$$

Only short segments of the orbit are used. The segments are determined from observations whose s.d. in range is estimated<sup>48</sup> at 6m; of which 5m are assumed to be systematic and 3 m are assumed to be random. The estimates are liberal. Using the same arguments as in Section 4, we find that

$$\frac{dh}{ds} = \frac{\partial h_s}{\partial r_1} \frac{dr_1}{ds} + \frac{\partial h_s}{\partial r_2} \frac{dr_2}{ds} + \dots \quad (6-11)$$

where  $r_1, r_2$ , are the ranges measured from starting (or with suitable modification, right ascension, declination, etc.). The error  $\Delta^2 h_s$  is therefore

$$\Delta^2 h_s = \Delta s \sum_j \frac{\partial h_s}{\partial r_j} \Delta \frac{dr_j}{ds} \quad (6-12)$$

and

$$\sigma^2_{\Delta sh} = \frac{\partial h}{\partial r_j} \sum_{\Delta r} \frac{\partial h}{\partial r_j}^T \quad (6-13)$$

where  $\sum_{\Delta r}$  is the variance matrix of the set  $\left\{ \frac{dr_j}{ds} \right\}$ . Writing

$$\frac{d\Delta r_j}{ds} = \Delta \frac{dr_j}{ds}, \quad (6-14)$$

the constant part of the systematic error in  $r_j$  drops out. Because we are using an orbit segment to constrain the  $h_i$ , the variance in  $\Delta_s h$  is taken to be  $n^{-1/2}$  times the variance in  $r_j$  (the random portion), where  $n$  is the number of observations used in deriving the segment (this approximation is good enough for the present purpose). The s.d. in  $\Delta_s h$  over a segment 3000 km long is therefore about 0.3 m. We will ignore the contribution of systematic, non-constant errors in  $r_j$  because, while definite information on the nature and magnitude of such errors is lacking, information available says that the errors are considerably smaller than the constant errors<sup>48</sup>. These considerations lead to the conclusion that over an orbital segment controlled by observations along its length, the variance of  $h_i$  differences,  $\Delta_s h$ , is 0.1 m plus the variance caused by deviation of the true orbit from the computed orbit segment. For lack of exact data on the Caribbean gravitational effects, we use the estimate that an acceleration of 200 mgal at the surface, acting over a horizontal distance of 1500 km on a satellite at 1000 km altitude, will affect the height of the satellite by less than 0.1 meter over this distance. This amount is negligible; the effect of the error in direction of gravity at satellite height is also negligible. The standard deviation of  $h_s$  is therefore estimated to be less (in absolute value, of course) than 0.3 m over a 1000 km distance.

#### B. Geoid Location Error

Since we are limiting the distances  $s$  between points  $P_{S_1}$  and  $P_{S_2}$  to 1000 km, satellite geoids are of no use for getting geoid height differences. Only gravimetric and astrogeodetic data are of value for good height difference computation. Using either kind of data, we can put the error at  $P_{S_1}$  equal to zero. The error at the other end can then be estimated using the formulae given in Section 4. Geoid height difference errors from astrogeodetic observations turn out to be 0.8 meters per 50 km interval, assuming that the variation of geoid slope,  $\xi$ , between stations introduces an average error of 10 times the error in  $\xi$  at a single station, taken to be 0.3". A 1000 km distance would therefore cause a height uncertainty of less than 4 meters. This can be reduced to less than 1.5 meters by halving the distance between stations, and can of course be reduced still farther by using gravimetric data to interpolate between stations.

The above estimates are for geoid variations on land or along a coast. Using GEON or SINS for finding  $\xi$  in open ocean, the error in  $\xi$  at a single station is at least 6" but the variation in  $\xi$  between stations would remain the same as before. In this case the interval between measurements will have to be reduced to 10 km in order to reduce the error in  $\xi$  to 1.5 meters. Data on the s.d.'s (accuracy) of SINS and GEON measurements are not available; the only data on this point refer to the differences between GEON, SINS and gravimetric geoid profiles. SINS and GEON heights agree to within 2 meters (ref. 17), GEON and gravimetric heights agree to within 4 meters, or with about 2 m variation. The s.d. of the gravimetric profile itself is not known.

The s.d. of geoid height differences derived from gravimetric data will not be estimated here because (1) too many unknown factors are involved to make any estimate believable, and (2) gravimetric profiles will not be used anyway.

### C. Error in IMSL with Respect to Geoid

This subject is covered in Section 4.3.1.4. The errors in IMSL difference along coastal waters are certainly less than 10 cm and can be ignored; in the open ocean they are less than 40 cm and can be ignored.

The principal contribution to the standard deviation,  $\sigma_{\Delta h_o}$ , of the height difference are satellite location s.d., estimated at less than 0.3 m, and the standard deviation  $\sigma_{\Delta h_j}$ , estimated at less than 4 meters for a worst case and at less than 1.5 m for reasonable cases. If possible we would wish to reduce the geoid height difference s.d. to a value comparable to that for the satellite height difference s.d. The easiest way to do this is to make the interval between the points  $P_1$  and  $P_2$  small. The regions selected in test areas should have the available test points separated by less than 100 km. A worst-case standard deviation is less than 1 m for these cases, and the s.d. can be reduced farther if data are available.

Another source of uncertainty is pressure variation, which can cause amplitude variations over a long period of 0.5 m<sup>30</sup>. Synoptic weather data can be used to compute the amount of variation, however, and an uncertainty of less than 0.2 m is expected.

### Summary

The error analysis for differential verification indicates that satellite height (above spheroid) differential introduces an rms error of 0.3 meters, Geoid height differential introduces about 1.5 meters, and the height differential in IMSL is negligible. The total rms error is thus about 1.6 meters.

Differential verification is therefore suitable for measurement of altimeter precision.

### 6.2.6 Regions of Experimentation

The region considered for carrying out the tests in the differential category of tests are:

1. The Caribbean Sea;
2. Lake Nicaragua;
3. Gulf of Panama plus Northern Coast of Panama;
4. Puerto Rico Trench

These are considered individually.

#### 6.2.6.1 Differential Measurements Over the Caribbean

The theory given in the preceding paragraphs, and the error analysis given in the following, both show that in order to be sure of keeping the standard deviation of the comparison difference to within  $\pm 1$  meter, the distance between points  $P_{S_1}$  and  $P_{S_2}$  must be less than 100 km. This requirement makes impossible measurement of height differences over the entire Caribbean. Instead, point pairs  $P_1 - P_2$  must be chosen within short distances of each other in offshore regions, or may be chosen in open ocean regions where large IMSL differences

can be expected. Selection of offshore point pairs must be made in such a way that reliable, measurable differences exist. Considering the small tidal variations in the Caribbean, most such differences will amount to no more than 30-40 meters and then must exist over time, not distance, intervals.

There are a few regions in the Caribbean where large variations of IMSL with distance can be expected. One of these is just north of Swan Island, at the edges of Mysterioso Bank. No astrogeodetic measurements are known for this region, but a large number of unclassified gravity data exist that should be convertible to geoid profiles. These same data could be explored for the existence of suitable regions elsewhere in the Caribbean.

#### 6.2.6.2 Differential Measurements in the Lake Nicaragua Region

Consideration was given to measuring the height difference between Lake Nicaragua and the Pacific Ocean to the west, and between Lake Nicaragua and the Caribbean to the east. Spirit leveling extends both ways from Lake Nicaragua, and the height difference of about 35 meters is, therefore, known to better than  $\pm 10$  cm. Tracking instrumentation in the region is practically non-existent at present.

Use of the Lake Nicaragua region would have the advantage that it could eventually provide a tie between the geoid in Central America and the geoid in the West Indies.

Closer examination of topographical maps indicate that the mountains in and near Lake Nicaragua interfere with altitude measurements, thus making this region unsuitable for such verification measurements.

#### 6.2.6.3 Differential Measurements in the Gulf of Panama - Panama North Coast Region

The difference between mean sea level at Balboa and mean sea level at Cristobal is about 20 cm, according to leveling work done in the 1930's. This is insufficient, by itself, for testing the altimeter. The range in tides is quite

different at the two places, being about 4 meters at Balboa and 1 meter at Cristobal. The difference of up to 5 meters is measurable by the altimeter, and the small range in this at Cristobal compared to that at Balboa makes possible the use of height differences from measurements on a single pass, without need to worry about correlation of heights on the two sides.

#### 6.2.6.4 Differential Measurements in the Puerto Rico Trench Region

The Puerto Rico Trench, or Brownson Deep, lies to the north of Puerto Rico and is outside the Caribbean Sea proper. It is included here because it does lie within the  $20^{\circ}$  zone and its profile (south to north) has been measured gravimetrically by GEON, and by SINS. Half of the passes of the altimeter over the trench will unfortunately be parallel to the long axis of the trench; the other half, on the ascending portion of the orbit, will be at an angle of about  $60^{\circ}$  to the existing profiles. The geodetic situation is sufficiently advantageous that every effort should be made to process the altimeter data for recovery of the trench profile. This should be checked against geodetic data obtained using (one or more of) the techniques described in Section 4 (p. 4-64).

#### 6.2.6.5 Differential Measurements East of the Caribbean

A particular region east of the Lesser Antilles has been suggested by Mr. Talwani as a possible site for differential measurements due to relatively large changes in geoid heights, apparently unaccompanied by a corresponding trench or ridge. Further study would be required to confirm its suitability for verification, particularly with regard to its proximity to tracking and telemetry stations.

## SECTION 7. DESIGN DATA (INCLUDING DISCUSSION OF VEDS RADAR ALTIMETER MODELS)

In addition to the main objective of verifying the performance of the satellite altimeter, the experiment has the second objective of deriving empirical design data to assist in the development of higher performance altimeters for use in the 1970's, such as SEA SAT-A. It is this second objective which this section addresses. To gain perspective on the effects of design data on the altimeter, this section includes the discussion of the VEDS altimeter models.

For the development of high accuracy altimeters, it will be important to understand the interaction of the electromagnetic radiation with the ocean surface at near-normal incidence, where there is currently inadequate data. Most studies of radar-ocean interaction have involved large incident angles. Even in those cases concerned with near-normal incidence, geometric features of the experiment generally reduce the near-normal angular resolution, thereby limiting the applicability of results to satellite altimetry. For example, at satellite altitude of 1000 km, a 50 nanosecond pulse has a footprint corresponding to an angle of about 1/2 degree on the ocean surface (see Fig. 7-1), whereas at aircraft altitude of 4.6 km (15,000 feet), a pulse of the same length subtends an angle of 6.5°, or more than ten times as large.

In addition to the angular resolution, the rate of area coverage is much greater from a satellite. In the example cited earlier, the ratio is greater than 200. The satellite "sees" waves with wavelengths about 15 times that seen from the aircraft. The effect on the returns from the satellite relative to that of the aircraft is at present estimated on the basis of theory, but unverified experimentally. Extrapolation of experimental results from the aircraft to experiments at satellite altitudes thus entails some risk, and cannot satisfactorily substitute alone for satellite measurements. On the other hand, satellite experiments may be correlated with data from aircraft experiments in order to validate the applicability of additional results from the aircraft experiment.

The main reason for being concerned with design data is that a satellite altimeter has never before been flown and tested; when the altimeter is finally tested, the tests will be much more meaningful when design data are obtained,

both in the sense of validation of the instrument, and in terms of the additional design know-how for the more accurate altimeters needed for the SEA SAT satellites.

The first part of this section develops a radar altimeter model for the verification portion of VEDS. This model is adequate for purposes of planning the verification portion of the experiment.

The second part considers the impact of the design data requirements on the radar altimeter model, and the third part develops a modified model of the radar altimeter which would be applicable to both altimetry and design data. The modifications would have substantial impact on altimeter design requirements, but do not significantly affect the verification portion of the study. The areas of design most affected are the size, weight, and power requirements.

The fourth part deals with the implications of pulse compression. The fifth part covers the telemetry capability required for GEOS-C.

## 7.1 Radar Altimeter Model - For Verification Only

### 7.1.1 General Description

Although the final specifications for the GEOS-C radar altimeter are not yet available, and the GEOS-C radar altimeter has not yet been designed, the basic operation of the altimeter can be described sufficiently for purposes of the VEDS program.

The satellite is expected to be placed in a near-circular orbit, with an inclination of about  $20^\circ$  to the equator. The nominal orbital altitude is expected to be about 1000 kilometers, with heights ranging from 600 to 850 nautical miles ( $1.1 \times 10^6$  to  $1.6 \times 10^6$  meters). The altimeter is assumed to be a range tracking pulse radar, with its antenna fixed to the satellite to point down at the earth's surface. The satellite attitude would be within two degrees of the normal to the earth's surface, with the radar beam looking straight down, as shown in Figure 7-1.

Altitude measurements would be made over the ocean surface with an accuracy of 5 meters. The altimeter would be programmed or controlled to initiate operation when the satellite reaches a position over the ocean, and terminate operation when the satellite is to pass over a land mass. Operation will be restricted to conserve satellite power, which must be shared by all of the equipments housed within the satellite.



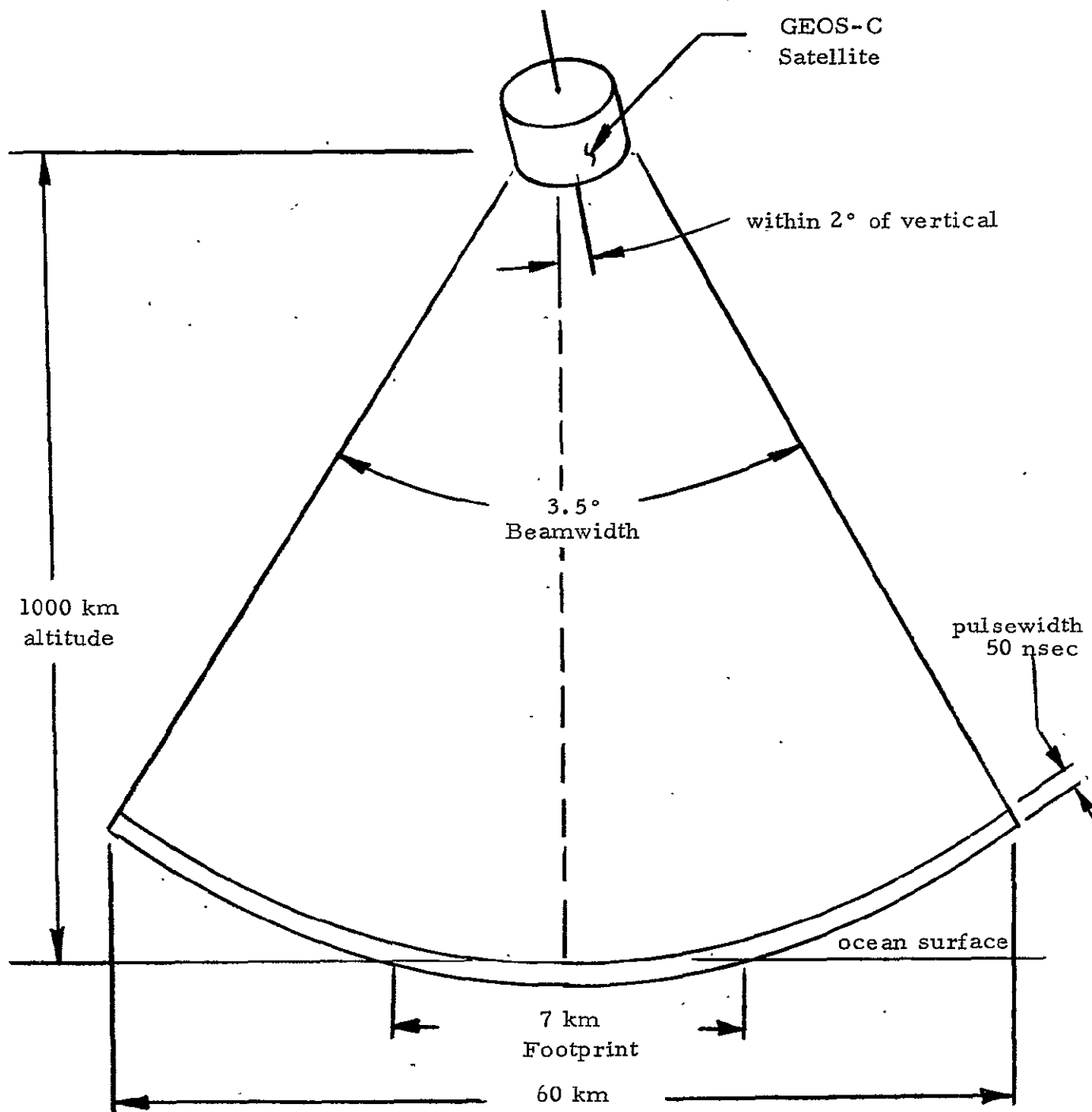


Figure 7-1. Radar Altimeter Operation

A simplified block diagram of the radar altimeter is shown in Figure 7-2. The transmitter will generate pulses of X-band radiation which will be directed by the transmit/receive switch to the antenna. The antenna will beam the pulses toward the earth's surface. The echoes from the surface will be received by the antenna, and diverted to the receiver by the transmit/receive switch. These signals will be amplified and detected in the receiver. The range tracker will track the leading edge of the received echo; the time difference between the time of transmission and the reception of the echo leading edge is a measure of the satellite height above the ocean surface. The timing generator will provide timing pulses to the transmitter, receiver, and tracking circuits. The timing reference will be supplied from the satellite, accurate to about one part in  $10^{11}$ .

The radar altimeter may operate with an ambiguous pulse repetition frequency. That is, the time of travel of the pulse from the satellite to the ocean surface and back may exceed the time between pulse transmissions. Under these conditions, the tracker range measurement, which is the time from the most recent transmission to the leading edge of the echo, must be added to an integral number of interpulse periods to get the true ranging time. The ambiguity in the number of pulse periods to be added can be resolved from a knowledge of the approximate orbit of the satellite.

If the satellite orbit is eccentric with apogee and perigee of 850 and 600 nautical miles respectively, and a period of 100 minutes, the maximum altitude rate will be about 250 meters per second. The time at which each altitude measurement is made must be known within about one millisecond, to keep the error in altitude measurement due to orbit eccentricity (and thus altitude rate) well below one meter.

#### 7.1.2 Expected Radar Altimeter Characteristics

Since the GEOS-C radar altimeter has not yet been designed, its characteristics have been assumed for the VEDS study. Parameters have been taken from many sources, within and without the Raytheon Company, and represent state-of-the-art values.

The major physical and system parameters are given in Table 7-1.

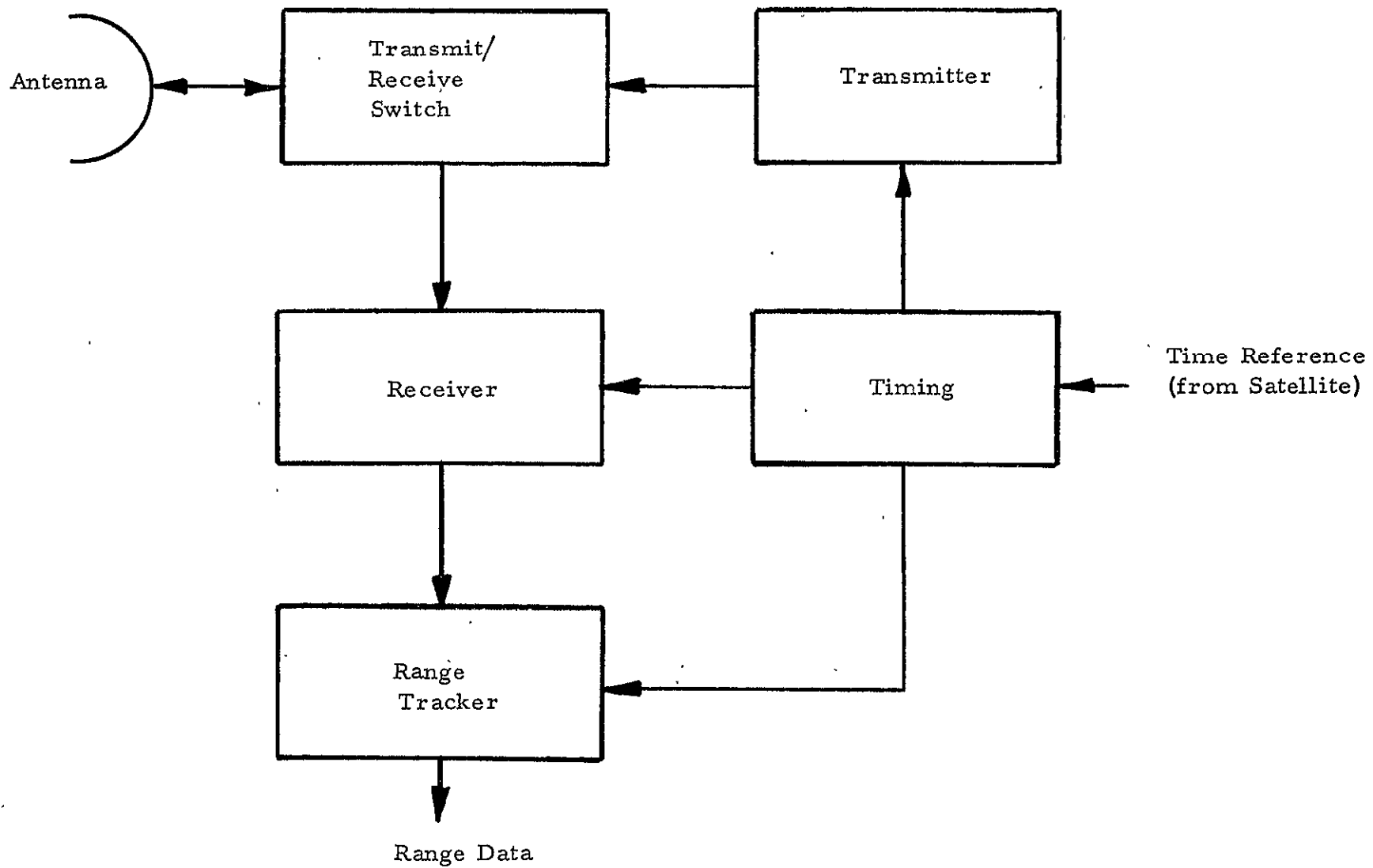


Figure 7-2. Radar Altimeter Model Simplified Block Diagram

Table 7-1. VEDS Radar Altimeter Characteristics

Weight of Electronics	20 lbs
Size of Electronics	9 x 6 x 11.5 inches
Weight of Antenna	5 lbs
Size of Antenna	2 feet in diameter
Transmitter Tube Life	200 - 500 hours
Prime Power	25 watts
Spacecraft Attitude Excursion	2°
Readout Resolution	1 meter
Altitude Accuracy	5 meters
Minimum Altitude Ambiguity	1000 meters

The size and weight given in the table are the values that are expected to be available for the altimeter. The space at the bottom of the satellite will permit the use of a 2-foot diameter antenna without interference with other satellite-borne equipment. The tube life of 200 to 500 hours is based upon the use of a magnetron transmitter. Longer lifetimes would be available if a TWT were used as the output tube, but more volume, weight and power would be needed for a TWT transmitter.

The prime power, 25 watts, is the amount expected to be available for the altimeter. Spacecraft attitude will be held within 2 degrees of normal. The altitude measurements from the altimeter will have an accuracy of 5 meters, and the readout resolution will be 1 meter. Because of the long ranging time, about 7 milliseconds for a height of  $10^6$  meters, it may be desirable to use an ambiguous pulse repetition frequency, and resolve the measurement ambiguity from a knowledge of the satellite orbit. The minimum ambiguity is specified as 1000 meters, to insure that the ambiguity can be resolved.

Typical radar altimeter transmission characteristics are presented in Table 7-2.

Table 7-2. VEDS Radar Altimeter Transmission Characteristics

Altimeter Frequency	X-band
Pulse Length	50 nanoseconds
Peak Power	5 kilowatts
Pulse Repetition Frequency	1 kilohertz

It is assumed that the altimeter will operate at X band, since this represents a good compromise between the antenna gain and beamwidth values that can be provided. A high gain value will increase the altimeter sensitivity. However, the antenna beamwidth must be kept wide enough to maintain operation as the satellite attitude varies. In addition, there is a wide variety of tubes and components available at X-band, and they are of lighter weight than similar components for lower frequencies. The values for pulse length, peak power and prf have been selected to provide high range accuracy, with low peak power and enough average power for adequate sensitivity. Peak power must be kept low to limit interference within the satellite, and to keep the altimeter transmitter size and weight within bounds.

#### 7.1.2.1 The Echo Shape

Figure 7-1 shows a sketch of the satellite and the radar pulse intercepting the earth's surface. The received echo on the average will have a shape similar to that shown in Figure 7-3. The signal will rise linearly over a time period ( $t_1-t_2$ ), equal to the radar pulse length. The signal level will then remain almost constant and then drop off slowly as the echo is received from the edges of the beam. The total pulse width will be several microseconds long, for the VEDS parameters. The time interval between the pulse transmission and the  $t_1-t_2$  portion of the echo represents the desired altitude measurement. A leading edge tracker will be used to track this initial portion of the pulse.

#### 7.1.2.2 Range Ambiguities

The use of an ambiguous pulse repetition frequency rather than an unambiguous pulse repetition frequency increases the average radiated power of the altimeter, and thus its measurement accuracy, for a peak power limited system. Several pulses will be "in flight" in the ranging space from the satellite to the ocean surface and back to the satellite. Since the altimeter cannot relate

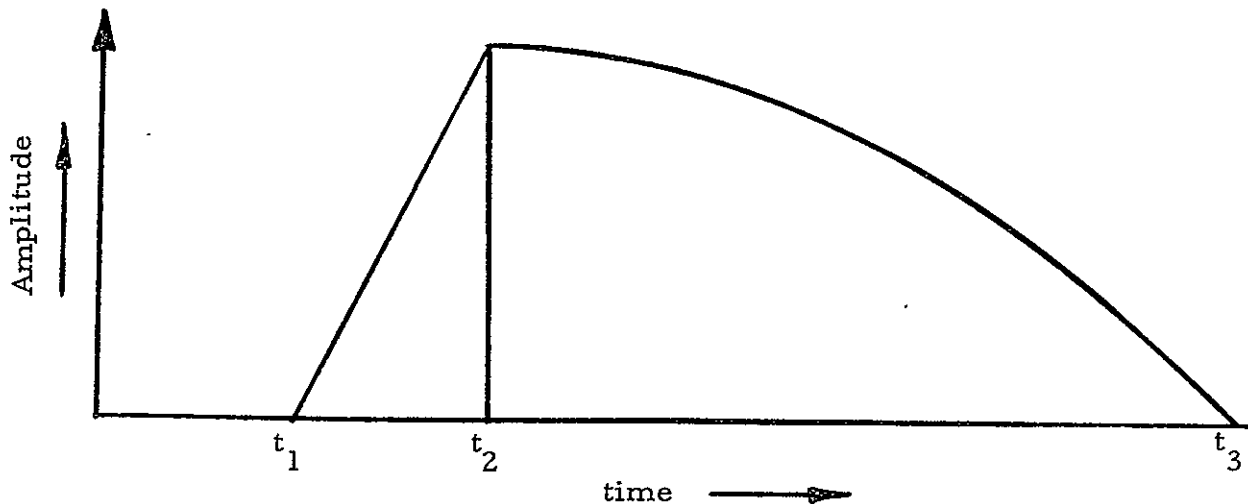


Figure 7-3. The Echo Waveform .

received pulses to their original transmission times, it will measure the interval from the most recent transmission time to the leading edge of the next received waveform, as shown in Figure 7-4. The actual ranging time is calculated by adding to this measured interval an appropriate number of interpulse periods, determined from independent orbital data.

#### 7.1.2.3 Signal Integration

With a satellite period of about 100 minutes, and an observed surface area 7 kilometers in diameter for a 50 nanosecond pulse width, each spot on the surface will be viewed for about one second. Thus an output data rate of one second will permit processing all of the collected information for each surface resolution cell.

A one second integration time would be about optimum, since one altitude value would be provided for each location of the ocean surface. A longer integration time would average readings over more than one resolvable area, and thus degrade the attainable measurement accuracy. Shorter integration times could be used if the redundant altitude measurements were relayed to the surface, where readings for each resolvable area could be averaged on the ground. It is conceivable that the raw data in the tracker could be of some use and could be relayed to earth. If data is to be sent more frequently than once per second, the data rates would be increased.

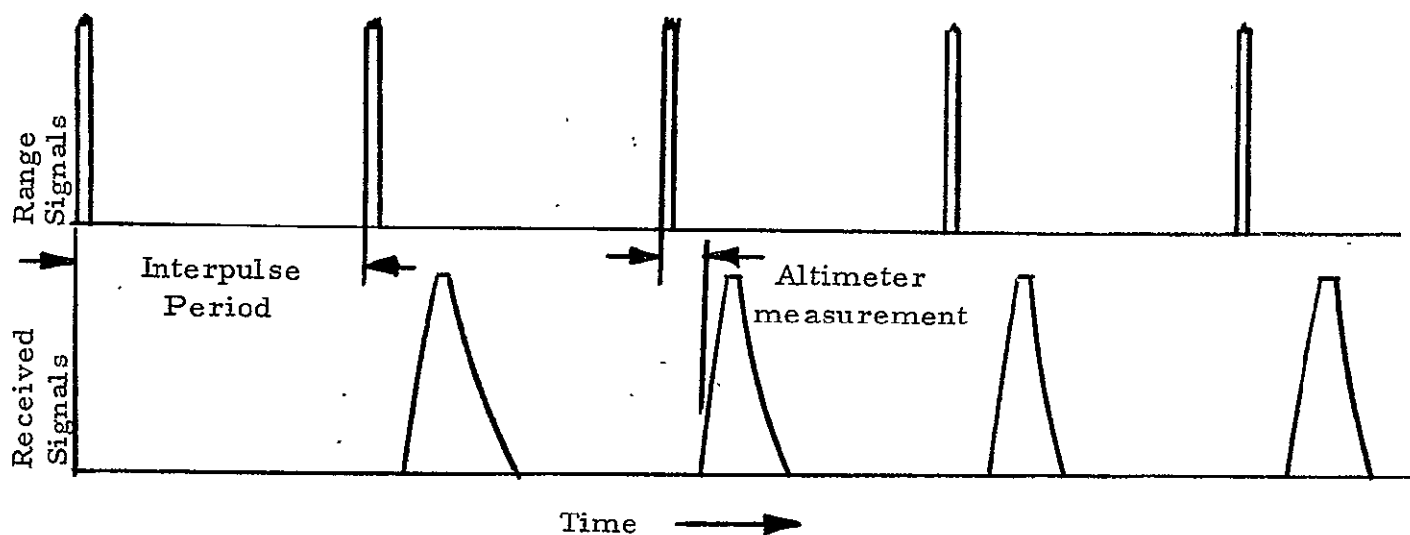


Figure 7-4. Time Relationships Between Transmitted and Received Pulses and the Time Interval Measured by the Altimeter

#### 7.1.2.4 Atmospheric Effects

Range errors due to the atmosphere and ionosphere can be compensated to within a fraction of a meter, as discussed in Appendix Q. However, clouds, fog and precipitation can produce two other effects. The altimeter signal will be attenuated by scattering in passing through the atmosphere, and may be reflected at an interlayer boundary. Neither of these effects should interface with altimeter operation except when extremely heavy rainfall is present.

If rainfall fills the 3.5 degree beamwidth to a height of 6000 feet above the surface, that is, a storm 30 nautical miles in diameter and the rainfall rate is heavy (16 mm per hour), the signal attenuation will be only 1.2 dB. The backscatter level will be  $2 \times 10^5$  square meters. For a 50 nanosecond pulse and a poor surface reflectivity of +5 dB, the radar cross section of a 7 kilometer diameter circle is  $10^8$  square meters, 27 dB above the rain cloud backscatter level. Only rainfall rates in excess of 16 mm per hour will degrade the altimeter operation.

#### 7.1.3 Detailed Description of the VEDS Radar Altimeter Model

Figure 7-5 shows a detailed block diagram of the radar altimeter. The transmitter, driven by the modulator and high voltage power supply will generate an RF pulse that will be radiated by the antenna. The received echo will be

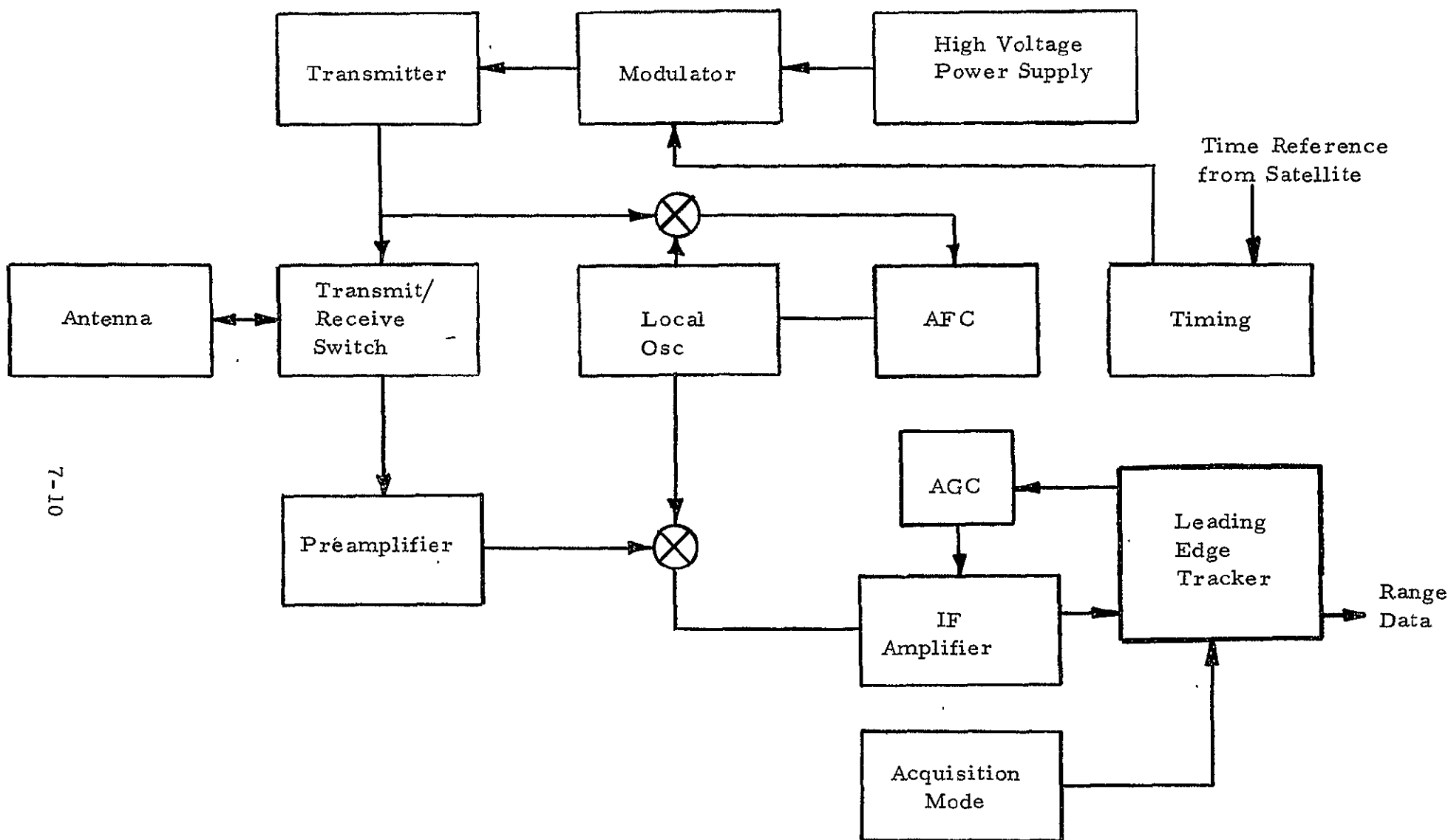


Figure 7-5. Detailed Block Diagram of the VEDS Radar Altimeter Model



directed by the transmit/receive switch to a preamplifier and a mixer, where it will be converted to an intermediate frequency. An AFC circuit will hold the local oscillator on frequency. The output of the IF will go to the leading edge tracker when the received signal will be tracked, and a gated AGC generated to maintain the level of the signal from the IF amplifier.

#### 7.1.3.1 Altimeter Parameters

The assumed parameters of the altimeter (for satellite attitude of  $\pm 2^\circ$ ) are:

Peak Power ( $P_T$ )	5 kilowatts
Antenna Diameter	2 feet
Antenna Beamwidth	3.5 degrees
Antenna Gain (G)	33 dB
Wavelength ( $\lambda$ )	3 cm
Pulse Length	50 nanoseconds
Signal Bandwidth (B)	20 MHz
Noise Figure (F)	5 dB
System Loss (L)	2 dB
Altimeter Altitude (R)	$10^6$ meters
Target Area ( $\sigma$ )	$4 \times 10^7 \text{ m}^2$ (7 km diameter circle)
Backscatter Coefficient ( $\sigma_0$ )	+10 dB
Altitude Ambiguity	1000 meters
Pulse Repetition Frequency (PRF)	1 KHz

#### 7.1.3.2 Radar Range Equation

The values tabulated above can be substituted into the radar range equation to provide the single pulse signal-to-noise ratio.

$$S = \frac{P_T G^2 \lambda \sigma \sigma_0}{(4\pi)^3 R^4 KTBFL} \quad (7-1)$$

where S is the single pulse signal to noise ratio, K is Boltzmann's constant,  $1.37 \times 10^{-23}$  joules per  $^\circ\text{K}$ , T is the reference temperature  $290^\circ\text{K}$ , and the other parameters are defined above. With these values, the single pulse signal-to-noise

ratio, will be equal to +9.5 dB. Of course, the tracker will provide a substantial amount of post detection integration, further improving the smoothed signal-to-noise-ratio. This signal level is adequate for accurate tracking.

Since the illuminated ground area increases directly with altitude, the received signal power varies inversely as the cube of altitude. A change in altitude from 600 to 850 nm will cause a 4.5 dB decrease in signal level.

#### 7.1.4 Altimeter Data Output

There will be three types of data telemetered from the altimeter. First will be the altitude measurements. Second, time measurements to identify the time of measurement of altitude. And third, the performance of the altimeter will be monitored. In addition, the raw data from the GEOS-C altimeter will require processing on the ground to put it into useful form.

##### 7.1.4.1 Altitude Measurements

Altitude has a maximum value of perhaps 2000 kilometers, and a resolution of 1 meter. This would require a 21 bit word. In practice, fewer bits would be needed with an ambiguous prf, or, with an unambiguous prf, a fixed value could be subtracted from the reading and only the increment transmitted.

##### 7.1.4.2 Timing

Due to the high altitude rate that could exist with an eccentric orbit, the altitude measurements must be made accurate in time to 1 millisecond. If time is to be designated to this accuracy out of 24 hours, 27 bits will be needed. However, although the measurements would be timed to this accuracy, it will be possible to report time each minute using many fewer bits, to identify a sequence of altitude measurements.

##### 7.1.4.3 Performance Monitoring

To check on altimeter operation, it will be desirable to monitor several parameters of the unit. For example, the following could be monitored:

- a. Input Voltage
- b. High Voltage Power Supply Voltage
- c. Transmitter Current
- d. Receiver Noise Level

- e. AGC Level
- f. Signal Level (output)
- g. Range Servo Error
- h. Transmitter Temperature
- i. Receiver Temperature

Each of these could be monitored with about 4 bits accuracy.

#### 7.1.4.4 Altimeter Data Rate

If the altitude data is sent once per second and the timing and performance data once per minute, the combined data rate would be about 22 bits per second, only slightly more than the rate for the altitude measurements themselves.

With altitude measurements made at a rate of 10 per second, and the timing data sent 10 times per minute, the combined rate would be about 220 bits per second. The higher data rate, while desirable, may be limited by the capacity of the telemetry link.

With a prf of 1000 Hz, the maximum ranging interval would be  $1.5 \times 10^5$  meters, and 19 bits of data would be needed for an altitude measurement. With timing indicated to one second out of a day, 17 bits would suffice. The use of these reduced word sizes would lead to slight reductions in the total data rates.

#### 7.1.4.5 Processing of the Altimeter Data at Ground Stations

The raw data from the GEOS-C altimeter will require processing at the ground to put it into useful form. Calibration will be needed to compensate for known or determinable errors in the measurement, such as fixed time delay errors in the tracking circuits and refraction errors. There may also be calibration errors that depend upon surface conditions such as sea state or the presence of severe storms with unusually high rainfall rates. The stability of the satellite clock should be checked periodically, time measurements synchronized with the ground, and corrections made for known errors in timing or synchronization. And, of course, the altitude measurements must be corrected to eliminate the effect of orbital parameters, as well as surface and environmental effects that will cause the altitude measurements to deviate from those which the altimeter is supposed to measure.

## 7.2 Collection of Design Data for SEA SAT-A

It should be feasible to obtain data from GEOS-C to aid in the design of SEA SAT-A, if added weight size and power consumption will be permissible beyond that needed for the altimeter itself. In addition, higher communications capacity will be needed to handle the increased data flow, and the altimeter will need some extra data storage and processing capacity.

### 7.2.1 Purpose

For the development of high accuracy altimeters it will be important to establish the precise shape of the leading edge of the echo waveform, under a variety of ocean surface conditions. Presently available data on backscatter measurements at near normal incidence indicate a wide scatter for the backscatter coefficient. Additional data is now being collected. Backscatter measurements are being made over a range of frequencies from 0.4 to 8.9 GHz by NRL's Wave Propagation Branch. A NASA/Raytheon program\* is in progress that includes flying an altimeter experiment in an aircraft to measure radar backscatter levels and waveforms at altitudes up to 18,000 feet. These measurements are expected to investigate the return pulse shape, and to provide some information on backscatter vs angle under various ocean conditions. However, these measurements are limited by the geometric constraints, and by the limited nature of the experimental equipment employed. They were intended to provide information useful in the design of future radar altimeters, including that for GEOS-C.

For SEA SAT-A, more precise waveform information at satellite altitude is needed. The signal processor is sensitive to the waveform shape, particularly that of the leading edge; hence an understanding of the shape under various ocean conditions will have an influence on the SEA SAT-A processor design. Waveforms should be obtained under various ocean surface conditions, and also with a variety of values of equipment parameters.

### 7.2.2 Data Collection

Two types of data are needed as a minimum: the shape of the leading edge of the echo, and the backscatter coefficient.

#### 7.2.2.1 Echo Waveform Data

For GEOS-C to provide echo waveform data for use in the design of advanced altimeters, three additional capabilities must be added to its altimeter. First, a

\* Space Geodesy Aircraft Experiment NASA-1932, 1970

waveform sampling device is needed; second, data storage will be needed to hold the samples until they are transmitted to the ground; and third, the data transmission rates to and from the ground must be adequate to provide the increased capacity needed, or an alternate mode defined.

#### Waveform Sampler

This device will periodically sample the echo waveform, and convert the samples into a series of binary words giving the amplitude of the waveform at a series of points in time. The sampler will consist of a device to select a series of measurements along the waveform and an analog to digital converter to measure the voltages at the selected times.

Since the waveform sampler will operate on single pulses, it should be feasible to sample pulses with arbitrary spacing. This will permit determination of the time over which the echo is decorrelated, and changes its shape.

#### Sampling Rate

The sampling rate could be as high as the altimeter pulse repetition frequency - 1000 pulses per second - or as low as desired. The upper limit will impose a heavy burden on the data link, and on the storage capacity within the altimeter, and will also provide for more data than will be necessary for this function. For example, with a 100 minute orbit, and 1000 samples per second, 6 million samples could be taken each orbit. A more reasonable sampling rate would provide several samples, perhaps 10, for each resolved area on the surface. Since the resolved area changes each second for a 50 nanosecond pulse width, this would mean a sampling rate of 10 per second. It would be desirable to relate the echo waveforms to ocean surface conditions, and sampling may be limited to ocean areas where we have a knowledge of wind, sea state, tidal, and storm conditions. If waveforms are collected only for those ocean areas where surface conditions are known, the average sampling rate over the orbit would be much lower than 10 per second.

#### Number of Measurements for Each Sample

The average echo waveform is expected to consist of an almost linear ramp, one transmitted pulse length in duration, followed by a slowly decaying amplitude, whose duration will depend upon the altimeter antenna beamwidth, and the variation of backscatter coefficient with viewing angle. With a 50 nanosecond pulse, and a

3.5 degree beamwidth, the rise time will be about 50 nanoseconds long and the decay will last for a few, (1 to 2) microseconds. In collecting data for SEA SAT-A, we will be concerned with the ramp and the effect of ocean surface conditions on the waveform. Our measurements, then will be concentrated around the ramp itself.

The present state-of-the-art of sampling and hold circuits can provide sampling times of a few nanoseconds. However, power consumption, circuit complexity, and size and weight will increase with very short sampling times. Some compromise will be needed to select an adequate sampling time so that the needed hardware will fit within the satellite. If we sample from 25 nanoseconds before the ramp to 25 nanoseconds after, using a 10 nanosecond sampling gate, then we will collect 10 measurements for each sampled waveform. It would be desirable to collect more points. The waveform is expected to contain data about ocean surface conditions, and the quality of the waveform reproduction on the ground will determine its usefulness.

#### Amplitude Measurement Accuracy

The accuracy with which each measurement should be made, should be sufficient so as not to degrade the signal to noise ratio of the echo waveform. With the signal-to-noise ratio at the top of the ramp at 10 dB, six bit sampling, to 2% should be adequate, even with a square law detector. If high signal to noise ratios are expected, the number of bits in each measurement should be increased, to take advantage of the higher quality of the data.

#### Data Storage

With six bit measurements, and 10 measurements per sample, each waveform will be described by a 60 bit word. These sixty bits are collected in a very short time, possibly within a pulse repetition interval. They must be stored for transmission to the ground. If data are to be collected over areas where data links are not available, the entire series of waveforms must be stored, along with timing and signal to noise measurements. It is more likely that waveforms will be collected over instrumented areas so that surface measurements are also available. In this case, the data storage capacity need only be sufficient to store data that the transmission system capacity cannot accept. For example, with a transmission capacity of 600 bits per second, ten waveforms per second could be transmitted, and needed storage would be limited to a 60 bit word.

If the transmission rate were lower, say 100 bits per second, then the storage must be adequate to store the extra 500 bits for each second of time for which data is collected.

#### Data Transmission Rates

As noted above, a 600 bit per second rate would be needed to transmit waveforms at a 10 sample per second rate, where each sample waveform consists of ten 6 bit measurements. In addition, a 27 bit timing word and 40 bits of performance monitoring should be transmitted periodically, perhaps for each one minute of data. As noted above, storage and transmission rates are interdependent, and both influence the experiment design.

The most demanding analog to digital (A-to-D) converter requirements are those for the waveform sampling. For that application, ten 6-bit words must be formed in less than one pulse interval.

Buffers will be needed with the capacity to store data between transmissions. If the sequence of data is repeated each minute, then one minute of data must be buffered to be assembled for transmission.

#### 7.2.2.2 Backscatter Coefficient Measurement

The backscatter coefficient can be computed from a knowledge of the altimeter parameters and the amplitude of the peak echo. In sampling the echo waveform a partial measurement will have been made of the peak echo size. To complete the measurement the AGC level must also be monitored. With these two values, the AGC level, and the amplitude of the echo at its peak, it will be possible to calculate the backscatter coefficient.

#### 7.2.3 Correlation Time

An important design parameter for altimetry is the correlation time between pulses; i.e., the time interval between pulses for two successive pulses to be decorrelated. This sets an upper limit on the pulse repetition frequency (prf). It also has statistical implications which relate to time constants of the altimeter system. The method for determining correlation time will be to obtain pulse shape data on successive pulses which are paired an interval  $t_0$  apart, where  $t_0$  is the inverse of the prf. As the prf is increased, and  $t_0$  decreases, one would expect greater correlation.

#### 7.2.4 Monitoring Conditions

Waveform shape, correlation time and backscatter coefficient are of interest in themselves, particularly in the absence of any data at all. In designing the experiment, however, one must consider the conditions under which they should be monitored. One set of conditions involves various ocean surface conditions. These are not pre-programmable, but they are predictable to some extent. Clearly, for this purpose, availability of advance forecasting would be helpful in deciding which areas should be given higher priority. The probability of obtaining various ocean conditions (sea states) is available from several sources (e.g. Reference 10). In addition, some real time measurement of ocean surface conditions will be required.

Another parameter of interest is altitude. The GEOS-C satellite is expected (for purposes of this study) to vary in altitude between 600 nmi (1100 km) and 850 nmi (1575 km); this is a factor of 1.4, which significantly affects the geometry of the problem. Accordingly, it would be of interest to compare results at the extremes of altitude, all other things being equal.

Ideally, a designer would like to twiddle knobs and change a variety of parameters while his prototype instrument is performing.. Perhaps a great variety of equipment parameters could be varied on command, but this tends to be expensive in many ways. As a minimum, it would be of interest to determine the effect of different pulse widths on the return signal. This should be coupled with different pulse power levels. The results of different pulse widths would provide specific design information on which pulse width seems to perform best, and would also provide improved understanding of how the electro-magnetic energy interacts with the ocean surface. We would expect to find different signal-to-noise ratios, and slightly different pulse shapes. The determination of when to change pulse width is open to several options. The change could be pre-programmed on a time basis, such as 25% of each day's available operation could be allotted to each of four different pulse widths. Or, there could be a "normal" pulse width most of the time, with occasional periods when another pulse width would be used. Or, the pulse width could be changed by command, or programmed by command, depending on other considerations. Inasmuch as experience with the GEOS-B satellite indicates considerable time constraints on operation of the satellite, it would seem advisable to program by command, based on criteria prepared well in advance,



and up-to-date history of satellite use. Four pulse lengths are recommended: 20, 50, 100 and 200 nanoseconds. The minimum pulse length is determined primarily by expected limitations on detection of return signal.

The processor to be used in the GEOS-C altimeter has not been designed. There are undoubtedly some design parameters within the processor which could be varied, and the results of which would be an understanding of methods of improving the processor design. While processor design has not been studied within the context of the Verification Experiment Design Study, introducing capability to change processor parameters should be considered.

### 7.3 Radar Altimeter Model - Incorporating Design Data Capability

The radar altimeter for GEOS-C will have two functions. First, it is to measure altitude accurately, to 5 meters, from its location in orbit to the instantaneous mean sea level of the ocean surface. Second, it is to provide data to aid in the development of altimeters of higher accuracy.

This second altimeter function will significantly affect the altimeter design. The data to be collected by GEOS-C will be echo waveform shapes for different transmitter pulse lengths, and backscatter coefficient measurements. Thus the transmitter must be capable of generating several pulse widths. We have selected four values: 20, 50, 100, and 200 nanoseconds. To make ten measurements over a time period of twice the pulse width, the receiver bandwidth must be widened to 250 MHz for the 20 nanosecond width, 100 for the 50, 50 for the 100, and 25 for the 200. The normal tracking bandwidth using a 50 nanosecond pulse would be 20 MHz. This bandwidth increase will degrade the single pulse signal to noise ratio in the waveform sampling channel compared to that needed for tracking alone. Since a 5 KW transmitter pulse would be adequate with a 50 nanosecond pulse width, and a 20 MHz signal bandwidth, a power increase of 11 dB is needed to provide the same signal to noise ratio in a channel with a 250 MHz bandwidth. This increase in power level could be attained either by increasing the transmitted pulse length using pulse compression, or by increasing the transmitted peak power. For the purpose of defining the altimeter characteristics for VEDS, either approach is acceptable. A peak transmitter power of 50 KW would be suitable for meeting these requirements. The average transmitter power would be held constant with pulse width changes by varying the transmitter pulse repetition rate.

GEOS-C design data, in addition to directly answering some design questions for SEA SAT-A will be used to establish correlation at satellite altitude with data from the NASA/Raytheon Aircraft Experiment Program at aircraft altitude. This will validate extrapolation of Aircraft Experiment data, greatly increasing the number and scope of its applicable relationships.

#### 7.3.1 Model Characteristics

The VEDS radar altimeter model with provisions for collecting design data is assumed to have the following characteristics:

Operating Frequency:	X band
Antenna Diameter:	2 feet
Antenna Beamwidth:	3.5 degrees
Peak Transmitter Power:	50 kilowatts (could be reduced significantly if pulse compression were used)
Transmitter Pulse Lengths:	20, 50, 100, and 200 nanoseconds
Pulse Repetition Frequency:	variable with pulse length from 500 to 5000 Hz to keep the average transmitted power at 0.5 watt
Transmitter Tube Life:	200 - 500 hours
Average Prime Power:	42 watts for altimeter operation alone 57 watts to collect design data and altitude measurements
System Accuracy:	5 meters, rms
Resolution of Output Data:	1 meter
Data Processor:	
Type of Tracker:	leading edge
Integration Time:	0.1 to 1.0 sec
Waveform sampling:	
Rate:	10 waveforms per second

Samples:	10 amplitude measurements per waveform, over a time span of twice the pulse width*
Sampling Accuracy:	6 bit amplitude measurement
Bandwidth Requirements:	250 MHz for 20 nanosecond pulse width 100 MHz for 50 nanosecond pulse width 50 MHz for 100 nanosecond pulse width 25 MHz for 200 nanosecond pulse width
Backscatter Measurement:	
AGC Measurement:	6 bits per single measurement
Peak Signal Measurement:	6 bits per single measurement

### 7.3.2 GEOS-C Radar Altimeter Measurements

There are two categories of measurements that will be provided by the GEOS-C radar altimeter - those measuring altitude, and those to be used in the design of higher accuracy altimeters.

#### 7.3.3 Altitude Measurements

The satellite is expected to be at a nominal altitude of  $10^6$  meters, with a possible range of 600 to 850 nautical miles ( $1.1 \times 10^6$  to  $1.6 \times 10^6$  meters). Measurement to  $2 \times 10^6$  meters, unambiguously, with 1 meter resolution will require a 21 bit word. Due to the high altitude rate with the 600 by 850 nautical mile orbit, each altitude measurement would need a time tag accurate to 1 millisecond. Twenty-seven bits are needed to designate time to this accuracy out of 24 hours. The altitude measurement rate would be one per second corresponding roughly to the time of observation of a single surface resolution cell.

Not every altitude measurement needs to be relayed with a 21 bit word or to be identified with a time tag. Each time tag could identify a block of altitude measurements, so that the time would be identified once for each minute of data. The altitude measurement could be ambiguous, with the ambiguity resolved by knowledge of the satellite orbit; with 1000 meter ambiguity, 10 bits should suffice for each altitude measurement.

---

\*This does not preclude consideration of other alternative samplings, such as trailing edge, or simply a larger time span; these could be performed for some selected tests.

In addition to the altitude data, the operation of the altimeter would be monitored, by measuring parameters such as the input voltage, the high voltage supply, transmitter current, receiver noise level, signal level, AGC level, tracker error, and transmitter and receiver temperatures. These measurements should require about 40 bits of data, and could be monitored once each minute. Only the altimeter performance monitoring would use analog data.

The maximum total simultaneous data rate for altimetry and monitoring would be:

Altitude Measurement:	21 bits per second
Timing:	27 bits per minute
Monitoring:	40 bits per minute
Total:	22 bits per second

If the measurement rate were increased to 10 per second, the total data rate would increase to about 220 bits per second.

#### 7.3.4 Design Data Measurements

A minimum of two types of data are recommended to be collected - echo waveform shapes and backscatter coefficient measurements. The echo shapes would be sampled for relaying to ground stations. Ten waveforms would be sent each second, with each sampled 10 times in a time span of twice the pulse width centered about the leading edge of the echo as shown in Figure 7-6. Each measurement would be made with 6 bit accuracy to provide reasonable accuracy in reproducing the waveform and enough dynamic range to allow for noise on the echo. Each waveform will be represented by a 60 bit word, and with 10 waveforms collected each second, the waveform data rate will be 600 bits per second.

To measure backscatter coefficient, both the AGC level, and the peak echo amplitude would be measured, each with 6 bit accuracy. With an AGC time constant of about one second, the AGC level could be sampled three times per second. Peak amplitude measurements could be made 30 times per second for a combined data rate of about 200 bits per second.

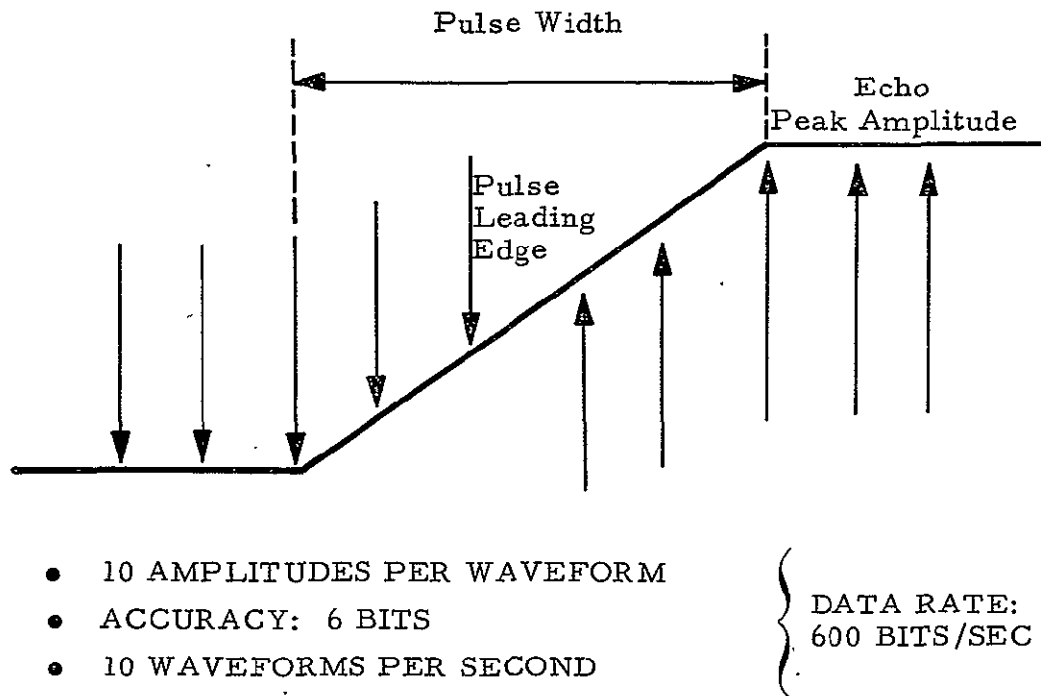


Figure 7-6. Echo Waveform Measurement

Thus the total data rate for design data would be:

Echo Waveform:	600 bits per second
Backscatter Coefficient:	200 bits per second
Total	800 bits per second

#### 7.3.5 Size, Weight and Power Requirements

There are options available in the design of the altimeter that permit trading off performance against size, weight and power. For example, a basic altimeter could be designed using a magnetron transmitter to provide about 500 hours of lifetime. This lifetime could be extended to about 2000 hours if a traveling wave tube amplifier were used. However, the travelling wave tube requires more volume, weight, and power. The addition of the capability to collect design data will add further to the size, weight and power consumption of the altimeter.

Table 7-3 contains estimates of the volume, weight and power consumption of three versions of the altimeter.

Table 7-3. Estimated Physical Parameters of Optional Altimeter Designs

	Basic Altimeter		Altimeter to Collect Design Data (TWT)	
	Magnetron	TWT	Altimeter Mode	Design Data Mode
Volume (in <sup>3</sup> )	620	1140	1200	1200
Electronic Weight (lbs)	20	34	40 <sup>(1)</sup>	40 <sup>(1)</sup>
Antenna Weight (lbs)	5	5	5	5
Power (watts)	25	42	42	57 <sup>(1)</sup>
Maximum Output Data Rate (bits/sec) <sup>(2)</sup>	220	220	220	1020

(1) Recent efforts indicate that A-to-D converter state of the art design can reduce Design Data requirements to about 36 lbs and 45 watts.

(2) 10 altitude measurements per second.

Although a detailed analysis has not been carried out of the size, weight and power consumption of the components of the altimeter, it does appear reasonable to assume that a basic altimeter using a magnetron transmitter can be designed to meet the constraints listed in the table. Replacing the magnetron with a TWT transmitter will lead to the increases shown. The TWT is a larger and heavier tube, less efficient in operation, and requires more filament power. To arrive at the weight of an altimeter capable of collecting design data, the added space and power requirements have been based upon values for an experimental, high performance A/D converter typical of the type needed to sample waveform data.

#### 7.4 Implications of Pulse Compression in the Altimeter

The use of pulse compression in the altimeter is completely analogous to generating a higher peak power level, so far as altimeter performance is concerned, except for three effects - the generation of range sidelobes, the effect of doppler on range measurement, and the effect if the target area changes within a transmitted pulse length. With proper design, the use of pulse compression should pose no fundamental problems.

Range sidelobes are generated in the process of compressing one long pulse into a short one. Their amplitude can be controlled much as the sidelobes of an antenna can be shaped. For the altimeter, it should suffice to specify a range sidelobe level that will not affect the range measurement. This could be done by setting the sidelobe level requirement so that the largest sidelobe will be below noise level.

In compressing a dispersed pulse, it is passed through a filter with a time delay that is a function of frequency. The doppler shift of the received signal due to the satellite altitude rate will cause a range error that must be calibrated, and corrected. This should be a small error, and will be a function of the pulse compression parameters.

System performance could be affected if the target, the ocean surface, were to change shape within the time period of the transmitted pulse. To have an effect, the motion would have to be a fraction of a wavelength within a pulse width. For this application, the vertical velocity of elements of the echo surface would have to be

$$v = \frac{.01\lambda}{\tau} = \frac{(.01)(3 \times 10^{-2})}{10^{-6}} = 300 \text{ meters per second}, \quad (7-2)$$

assuming the minimum detectable change is one percent of a wavelength, and the transmitted pulse width is one microsecond. Thus the velocity of the ocean surface would have to be about Mach 1 to have an effect. This is not a likely situation.

Within the tolerance of a first order estimate, the volume, weight and power in Table 7-3 for the "Altimeter to Collect Design Data" apply to a pulse compression system. Such a system would significantly reduce the 50 KW transmitter peak power, the reduction depending on the selected pulse compression ratio.

### 7.5 Telemetry Capability

From the analysis in sections 7.3.3 and 7.3.4, the maximum telemetry down link capacity required is 822 bits per second for an altimeter operating at a measurement rate of 1 per second, and 1020 bits per second for a measurement rate of 10 per second. NASA's STADAN (Space Tracking and Data Acquisition Network) facilities can provide the capacity for the maximum rate of 1020 bits per second on a single channel.<sup>52</sup> The STADAN network coverage includes the entire Caribbean area, as well as other portions of the satellite orbit, including possibly Hawaii. Reference 52 compares the STADAN system with the USB (Unified S-Band), including considerations of data rate availability, compatibility with analog/digital data, coverage, etc. These considerations were not considered critical for purposes of this study.

## SECTION 8. EXPERIMENT INTEGRATION CONSIDERATIONS

### 8.1 Introduction

The assemblage of all the available information into a neat little package for VEDS is not a simple step-by-step process. In fact, the main purpose of the Verification Experiment Design Study was to demonstrate feasibility of the experiment, and to indicate methods of performing the experiment. This section indicates some of the major considerations that enter into an integrated experiment, mainly to indicate their impact on the experiment, and to suggest either methods of handling the considerations or what must be done in order to handle them. The list is by no means complete, since many system problems are indicated throughout the report. In most cases the amount of concern depends strongly on decisions which have not yet been firmly established. The discussions attempt to indicate the basis for decisions.

### 8.2 Design Data and Verification

This section considers the interrelationship between the Design Data portion of the experiment and the Verification portion of the experiment, both in terms of their impact on each other and in terms of their competition with regard to the GEOS-C satellite.

In principle, the Design Data portion has very little to do with the Verification portion. Verification requires transmission of altitude and time information to the ground stations. The Design Data equipment need not function in order to perform altimetry; however, the altimeter must be functioning in order to obtain design data. This is necessary for two reasons: (a) the design data depends on the return signal from the altimeter for its data, and (b) the design data requires timing information (the time of the return pulse) to enable sampling to start at



the relevant time. This is the extent of the direct impact of the two portions of the experiment upon each other.

With regard to the GEOS-C satellite, the design data portion involves additional equipment, with added weight\* and volume.

Power is a consideration, since the design data power requirement\* makes the equipment package exceed the assumed power allocation of 25 watts. Storage is not required for on-line transmission of information. But if design data and altimeter data are both required in areas where on-line transmission cannot be performed, then they compete for the storage allocation, if any. Telemetry need not be a problem, since our study indicates that adequate telemetry can be made available. With on-board storage, data collection in remote areas would probably create a demand for higher telemetry rates.

### 8.3 Storage and Telemetry

Storage and telemetry are interrelated in that if all available telemetry channels are filled, and data are being developed at a rate in excess of the telemetry capacity, then storage must accommodate the excess data (beyond the telemetry capacity) until such time as the data can be telemetered (while no additional data are being developed). This could occur if the altimeter data rate were very large, and/or if the design data rate were very large, relative to the telemetry rate, or if alternating methods were not used.

---

\* Recent efforts indicate that A-to-D converter state of the art design can reduce Design Data requirements to about 36 lbs and 45 watts (last column in Table 7-3).

Data rate for the altimeter alone, when sampling ten times per second, is about 220 bits per second. Increasing the sampling rate would increase the bit rate approximately in the same proportion.

The data rate for the design data, when sampling 10 waveforms per second each in ten places is about 600 bits per second; when sampling for backscatter coefficient 30 times per second, the data rate is about 200 bits per second. Both these would change approximately in proportion to the change in sampling rate.

The total of the aforementioned data rates is 1020 bits per second, which is well within capabilities of current telemetry capabilities.

In the absence of on-board storage, there is no question that there is no point in operating anywhere in the absence of a live telemetry link. If there is some on-board storage, then several advantages are offered:

1. There is the opportunity to obtain both altimetry data and design data over remote regions under environmental conditions which have low probability in the regions where tracking stations are located; this would improve the opportunities for making measurements (such as design data) under these otherwise rare circumstances.
2. There is the opportunity to obtain geodetic information in regions not involved in the verification procedure. Although the accuracy specifications for the GEOS-C altimeter do not meet many, if not most, geodetic requirements, they do satisfy some; and should be used for that purpose if possible. In fact, precision rather than accuracy is adequate for many geodetic requirements, which should extend the applicability of altimeter results to geodesy.

3. In view of the expense involved in the GEOS-C program, it is important to extract as much useful data from the program as possible. On-board storage would ensure that all available telemetry links were kept busy at least to the extent of the storage capacity. Thus, even if reliability were only fair, an inexpensive (in terms of size, weight, power as well as dollars) large-capacity storage device may be a worthwhile risk.

The orbital period is in the order of 100 minutes or 6000 seconds. If all the Earth were ocean, then at 1020 bits per second, a complete revolution could be stored in about 6 million bits. STADAN with about 4,000 bits/sec (using all available channels) would take about 25 minutes to telemeter that much information. USB, with 51.2 kHz (approximately bits per second) would require about 120 seconds (2 minutes). The storage requirement is obviously much less, since (a) the Earth is not all ocean, even in the 20° belt; (b) during transmission, which takes place twice during many of the orbits, the stored data is removed, thereby enabling the same storage to be used more than once per orbital revolution; (c) not all areas on the ocean are of interest.

One can readily justify some modest amount of on-board storage, such as 10,000 bits, or 1000 bits, or even 100 bits. With such storage available, one could take altimeter readings at lower rates, such as 2 per second (about 45 bits/sec), and obtain more than 20 seconds worth of data in 1000 bits. Design data could be taken at a different time, and for a smaller number of samples. These limited amounts of storage would still provide useful design data, and possibly useful geodetic data. They are needed for data acquisition, not due to transmission constraints.

As pointed out in earlier sections, verification can be performed primarily in the Caribbean. Existing telemetry channels are adequate to meet the bit rate requirement for live data transmission, both for verification and for design data requirements. Additional verification or design data out of the range of the telemetry network would require some on-board storage, the quantity depending on how much such data can be justified. Even with very limited on-board storage, selected readings can be made in remote regions and telemetered at the next convenient telemetry station.

#### 8.4 Time and Timing

Time is an essential ingredient in measurement, and particularly when the measurement is sensitive to small changes in time. The meaningful data from the altimeter consists of pairs of numbers indicating altitude and the corresponding time; lengths of the order of a meter are significant, and the time it takes light to travel one meter is about 3 nanoseconds. Thus timing of the order in nanoseconds is significant. It takes about 4 milliseconds for electromagnetic radiation to travel a distance of about 1100 km (600 nmi). This time must, of course, be entered in all ranging calculations as a correction. However, the accepted value of the velocity of light has a standard deviation, or uncertainty, of about  $1.3 \times 10^6$ , corresponding to an uncertainty of about .37 meter in 1100 km. This uncertainty in the velocity of light is a scaling factor that applies equally to all measurements and represents the limit of current technology. It will therefore not be considered further.

Timing has an effect on the calculation of satellite position in orbit. Consider, for example, that the path (orbit minus time) is known precisely from tracking. Since the satellite velocity is typically 7 km/sec along the orbit, an error of 1 millisecond in time would produce a tracking error of 7 m. Additionally, the altitude rate of the satellite is typically 100 meters/sec; a timing error of 1 millisecond would then correspond to an altitude error of .1 meters. This is in addition to an altitude error by virtue of the tracking along the orbit, which can be of the same order of magnitude as the track error itself - i.e.,

about 7 meters for each millisecond. Errors due to timing must be smaller than 0.1 millisecond in order to reduce satellite altitude error due to timing to less than about 1 meter.

It is thus essential to have accurate correlation of altimeter height measurements with time. This has implications for the stability of the altimeter clock and for the data rate. It is pointed out in Appendix P that synchronization between satellite clock and ground station would probably be required every 2 days in order to maintain an error of less than 3 nanoseconds (1 meter) in transit time of the ranging signal. Even if synchronization were a daily requirement, it could be met, at least in principle. (Of course, there are other considerations between feasibility and deployment.) Once synchronized, time signals are largely unnecessary for a day or two. Alternatively, the satellite could be scheduled to send out a timing signal at regular time intervals, such as every 10 seconds; during that time interval, the satellite will have travelled about 70 km, which is a convenient tracking distance. The timing signal is perfectly suitable for a crude time-check, while the short-term increment can be either programmed or incrementally number tagged. Programming is adequate, providing the number of readings in the interval is not so large as to cause a loss of count, and providing the probability of an error is sufficiently low that large blocks of data will not be lost due to lack of synchronization.

Timing is also essential to the collection of design data. The pulse length of 50 nanoseconds (corresponding to a range of 25 feet, or about 8 meters) and the sampling schedule on the pulse for design data introduces the requirement that the start of the return signal (ramp) be known to the order of 10 or 20 nanoseconds; otherwise, sampling must be extended at either end of the signal in order to be sure to include the significant portions of the ramp. (10 to 20 nanoseconds corresponds to 1-1/2 to 3 meters in altitude.)

The on-board clock is assumed to have a stability of about  $1:10^{11}$ . This is adequate stability over a few minute of time, or for any single pass. Hence the clock stability will satisfy the requirements for the collection of design data. It is then up to the altimeter design to provide circuit stability which will enable the design data circuits to sample at the right time.

Timing considerations appear in several portions of this study. Appendix C provides information on frequency and time standards. Appendix P is concerned with synchronization of the satellite clock with surface receivers in order to triangulate on the altimeter signal. In addition, each time distances to accuracies of the order of one meter or less are measured with time signals (ranging), all the problems of timing and clocks come to mind. It is not our purpose here to review in detail the techniques of precision timing, but rather to remind the casual reader of the pitfalls which may arise in experiments which appear conceptually simple. It should also be recognized that equipment performance in the laboratory is often difficult to obtain in the field under conditions of limited control.

In summary, time is a constant source of worry in any precision experiment such as this. Technology is capable of dealing with many of the timing problems, and there are no fundamental problems which cannot be dealt with adequately, at least in principle. Timing must be built into the planning of the experiment, in order to ensure the integrity of experimental results.

#### 8.5 Power, Weight and Volume\*

Setting aside volume for the moment, the specifications on altimeter weight is 25 lbs, and on power is 25 watts average, 5 kilowatts peak. The altimeter designed only for altitude measurements can readily meet these specifications. The addition of design data requirements raises the weight to about 40 lbs, and the power to 42 watts for altimeter operation, and 57 for design data requirements. These are first order estimates.

---

\* See footnote, P. 8-2

Volume is probably not a problem, since earlier discussions on space availability indicated that there was a high probability that some space could be made available, if necessary, to meet excess requirements over that nominally allotted the altimeter. Power is probably the most serious gating item.

The power constraint simply stated as 25 watts average is somewhat inadequately expressed, since the power system has its own problems. First of all, the source of power is an array of solar panels, which (for 20° inclination) does not collect solar energy during a portion of each orbit. The storage batteries of GEOS-B had 3 storage batteries with a total capacity of about 490 watt-hours, but whose schedule must be carefully monitored to prevent excessive discharge; similar constraints are likely on GEOS-C. The power schedule of the altimeter and telemetry system must be scheduled compatibly with other power demands. Of particular concern are demands for high power for short periods of time, such as for the transponder (25 to 30 watts during interrogation) and the optical batteries (whose beacons draw about 670 watt-seconds per flash). It has been estimated that a power drain of about 1200 watt-minutes would be reasonable<sup>37</sup>. This would correspond to availability of 42 watts for altimetry data over 28% of the orbit, or 57 watts for design data (including altimetry) over 21% of the orbit. These constraints are certainly not a problem as far as verification is concerned and appear reasonable from the point of view of design data. (assuming that large portions of the ocean are probably uninteresting most of the time).

In summary, the power constraint is reasonable. The large power (in excess of specifications) called for in the design data portion is probably tolerable by the system with proper scheduling. Weight may be a problem from the point

of view of weight distribution within the satellite and of payload. Volume is probably not a real constraint.

#### 8.6 Ocean Truth & Atmospherics

Two aspects of the ocean have a large impact on the VEDS results: the description of the ocean surface, and the location of IMSL.

Ocean Truth, a description of the ocean surface, is necessary both in verifying altimeter measurements and in developing design data; in both cases, it is important to know the conditions of the sea surface on which the measurements were made. The condition of the ocean is characterized by many parameters. A description of the parameters, as well as a review of current methods of measuring them, is given in Appendix O.

Our investigation indicates that instrumentation for the measurement of ocean descriptors is relatively primitive, is more often than not custom-made, and is usually quite expensive. In the hostile ocean environment, it is usually difficult to collect good data.

Despite the difficulty in obtaining satisfactory ocean truth information, every attempt should be made to plan and implement a realistic program for attaining ocean truth, both for altimeter verification and for design data.

An adjunct to the measurement of ocean truth is the determination of the atmospheric environment; the effects on radar are mainly in the troposphere and in the ionosphere. These are discussed in Appendix Q. For purposes of VEDS, atmospheric environment can be adequately measured, but some additional work will be needed to relate particular altimeter measurements in time and space to the corresponding atmospheric conditions.

#### 8.7 Instantaneous Mean Sea Level (IMSL)

IMSL is a critical parameter in VEDS because it is the location of the surface to which the satellite altimeter measures. In verification, it is



therefore necessary to be able to locate it. Section 4.3.1.4 and Appendixes R and S discuss the location of IMSL.

In the case of Absolute Verification, where IMSL is calculated, the calculation involves a number of assumptions which, while they have reasonable scientific basis, cannot be assigned a high degree of confidence. This is due to the many uncertainties involved in the assumptions, in the paucity of detailed data which is directly and reliably applicable to the specific calculation of IMSL, and to the general uncertainties in the data themselves.

In the case of Relative Verification, the location of IMSL is determined locally by direct observation. In calm waters this would present no problem, since the distance from a shipborne radar (for example) to a calm surface would be readily measurable. In more turbulent waters, the problem becomes more complicated due primarily to the difficulty of locating IMSL.

#### 8.8 Software and Data Handling

Each time a new instrument has been introduced into the National Geodetic Satellite Program, new software has been required for reducing the data. The radar altimeter will be no exception. New software will be required, not only for use in connection with the Verification Experiment, but for use in preprocessing the data so that it can be used by Principal Investigators who will be using the measurements for their own studies in various scientific fields.

The sources of data in the GEOS-C Radar Altimeter Experiment are:

1. Satellite and its radar
2. Participating tracking stations
3. Various sources of environmental data
  - a. Oceanographic
  - b. Atmospheric and Meteorological
  - c. Tropospheric
  - d. Ionospheric

The measurement rates under consideration for the GEOS-C radar altimeter are 1 to 10 measurement per second. By the time the altimeter has operated several hundred hours, several million measurements will have been telemetered to the ground. Moreover, millions of bits of data on ocean conditions, atmospheric conditions, ionospheric conditions, and tracking station observations will have to be correlated with the altimeter measurements. This is necessary to correct for refractivity error in the altimetry data, to be able to relate the conditions of the ocean with the satellite altimeter measurements, to provide the geodetic position of the measurements, and to relate the orbit to the IMSL surface so that the verification experiment and geodetic and oceanographic analyses can be carried out.

It will be essential to have the software for the Verification Experiment completely ready at the time the satellite is launched. In this way it will be possible to conduct Verification studies and analyses early in the life of the satellite and learn what its capability and accuracy are quickly before going on to experiments of a scientific nature.

It will also be important to have documentation prepared for providing the Principal Investigators with a complete description of all the preprocessing that is done to the data prior to their receiving it.

A data handling plan should be prepared, based on an experiment design plan, and should trace the data flow through the system. It should include data acquisition, format, processing, programs, analysis, results, etc. It should contain built-in checks for gross errors, and occasional readouts to permit monitoring. Provision for calibration should be part of the system. The location of human decisions should be included, and the criteria and decision required should be specified.

In order to provide effective data handling, it is necessary to have a good understanding of the expected results, including format, density of output, and evaluation. Advanced planning is essential to economic extraction of the full value from the data.

A quote from a report<sup>53</sup> entitled Preprocessing Electronic Satellite Observations illustrates this point:

"One of the purposes of the National Geodetic Satellite Program is to store the data obtained from geodetic satellites in a central location, where it may be utilized by qualified personnel involved in geodetic research. In accordance with this purpose, the Geodetic Satellites Data Service (GSDS) was established within the National Space Science Center at Greenbelt, Maryland. A large amount of data has now been obtained by the various agencies involved in the National Geodetic Satellite Program, and is deposited in the GSDS. However, difficulty has been experienced in the utilization of this data because of an insufficient knowledge of the preprocessing procedures and the corrections applied to the data before submission to the GSDS."

#### 8.8.1 Software Recommendation

It is recommended that efforts be started toward the objective of having the necessary software available concurrently with the launch of GEOS-C early in 1972.

It is further recommended that the software required for Verification and the software for preprocessing the data for later use by Scientific investigators be prepared jointly as a single project.

Specifically, the following steps are recommended:

1. Describe the data the satellite and the altimeter will generate.  
This included the media on which the data will be recorded on the ground, the types of data, amounts, timing, format, etc.
2. Describe the data that will be available from the tracking stations and the preprocessing software that exists and which could be utilized to preprocess the data prior to its delivery to the scientific investigators.

3. Describe the data that will be available from the various sources of environmental data, the media, the format, etc.
4. Present these descriptions to the scientific investigators. After the scientific investigators have reviewed these, have them provide their assessment of their needs for data and the preprocessing they want done before the data is delivered to them.
5. Compare what the scientific investigators want with what will be available and determine what new preprocessor software is needed.
6. After defining the new preprocessor software requirements, prepare a functional specification for the software.
7. Upon approval of the functional specification, design the preprocessor software. This would include the development of the appropriate editing, smoothing and compaction algorithms. Document the design of the preprocessor software.
8. Design a Data Reduction Operations System. This would include the development of a plan for implementing the system.

#### 8.9 Experiment Integration

It is apparent that the performance of the experiment will be very sensitive to experiment constraints. Among the decisions having substantial influence on the experiment will be the following:

1. The question of whether design data will be included at all. (The preliminary design considerations used in this study may be superseded by technological developmental improvements, such as the more compact A-to-D converters noted recently.)
2. The question of whether there will be on-board storage. (This determines whether any data will be taken out of range of a telemetry station.)

3. The question of priority in GEOS-C power and telemetry scheduling.
4. The question of whether to plan for a 500-hour use of the altimeter, or some other number.

Regardless of the answers to the above, one of the objectives of the experiment is to obtain the most useful information from the data. It is therefore important to try to take advantage of all the data available. Several ways of utilizing the data have been proposed. An outline of a static error analysis is presented in Appendix B, and an outline of a dynamic error analysis is presented in Appendix D. These can be guides to the effective use of all available data.

The appendices referred to above are concerned primarily with the tracking problem which involves minimizing errors in tracking as well as improving tracking station location. The latter is a fall-out of the experiment, and can be used subsequently to improving tracking. Other aspects of the problem of experiment integration await other decisions. For example: What mix should there be of the four different approaches to verification? In particular, the relative method requires zenith tracking as the satellite passes overhead. Clearly this will not be performed often; and while it is being performed, it is perfectly compatible to simultaneously perform absolute, differential and self-consistent verification simultaneously. In large measure, these methods use portions of the same data, and in one sense they represent different ways of looking at the data.

It is not likely that the verification experiment will be completely optimized. It is likely that as the answers to the outstanding questions are formed, decisions will be made which direct the experiment. But such direction is beyond the scope of this study.

## APPENDICES

- APPENDIX A. LIST OF TRACKING STATIONS
  - APPENDIX B. MATHEMATICAL BASIS FOR GEOMETRIC ERROR ANALYSIS
  - APPENDIX C. CHARACTERISTICS OF FREQUENCY AND TIME STANDARDS
  - APPENDIX D. MATHEMATICAL BASIS FOR ANALYSIS OF ERROR IN SATELLITE LOCATIONS (DYNAMICAL SITUATIONS)
  - APPENDIX E. EFFECT OF ORBITAL CONSTRAINTS ON LOCATION ERRORS
  - APPENDIX F. INFLUENCE OF LAND TOPOGRAPHY ON RETURN PULSE
  - APPENDIX G. VERIFICATION METHOD USING PATH INTERSECTIONS
  - APPENDIX H. NOTE ON RELATIONS BETWEEN STANDARD DEVIATIONS INVOLVED IN THE VERIFICATION EXPERIMENT
  - APPENDIX I. NOTES ON BIASES, SHORT-PERIOD VARIATIONS, AND OTHER COMMON CONCEPTS
  - APPENDIX J. REMOVAL OF EFFECTS OF CERTAIN TYPES OF SYSTEMATIC ERRORS FROM OBSERVATIONS
  - APPENDIX K. PURPOSE AND ORGANIZATION OF ERROR ANALYSIS
  - APPENDIX L. CONFIDENCE LIMITS FOR THE STANDARD DEVIATION OF THE ALTIMETER HEIGHT
  - APPENDIX M. CONSTRAINTS ON VEDS
  - APPENDIX N. TERMINOLOGY AND DEFINITIONS
  - APPENDIX O. OCEAN SURFACE CONDITIONS (OCEAN TRUTH)
  - APPENDIX P. SURFACE VERIFICATION OF ALTITUDE UTILIZING ALTIMETER SIGNAL
  - APPENDIX Q. TROPOSPHERIC AND IONOSPHERIC EFFECTS
  - APPENDIX R. CONTRIBUTIONS TO MEAN SEA LEVEL IN THE OPEN OCEAN
  - APPENDIX S. THE FIGURE OF THE SEA: AN ESTIMATE OF ERROR
- GENERAL REFERENCES

# APPENDIX A

## LIST OF TRACKING STATIONS

C-Band Radars:

Table A-1.

FPS - 16

MPS - 25\*

MPS - 26\*\*

Site Name	Coordinates		
	$\lambda^\circ$	$\phi^\circ$	h(meters)(c)
Cape Canavaral (Kennedy)	279.4	28.5	14
Ely, Nevada (MPS-19c)	244.9	39.3	-
Grand Bahama (a)	281.6	36.6	14
San Salvador(b)	285.5	24.1	5
Puerto Rico(b)	-	-	-
Bermuda	295.3	32.3	18
Gran Canaria**	344.4	27.7	35
Anclote, Fla.	-	-	-
Pretoria*	28.3	-25.9	1626
Woomera	136.8	-30.8	151
Green River, Utah	-	-	-
Kauai*	200.3	22.1	1140
Kauai	200.3	22.1	1155
Pt. Arguello	239.4	34.6	646
San Nicolas, Calif.	-	-	-
White Sands	253.6	32.3	1232
Blanding, Utah*	-	-	-
Eglin AFB	273.2	30.4	28
Cape San Blas, Fla.	-	-	-
Wallops Island	284.5	37.5	10
Tananarive	-	-	-
Johnston Island*	190.5	16.8	6.8
Edwards AFB, Calif.	-	-	-

- Sources: (1) Goddard Directory of Tracking Station Locations NASA/Goddard, 1966.
- (2) Geodetic Satellite Observation Station Directory NASA/Goddard, 1969
- (3) Geonautics Memorandum, 30 January 1969, subject J184 Task 7-4 (from G. E. Graham).
- (4) "Listing of Range and Space Flight Tracking and Data Acquisition Equipment of the DOD and NASA", by the Space Flight Ground Environmental Panel of the Aeronautics and Astronautics Coordinating Board, July 1967.
- (a) Converted for AN/FPS-13
- (b) Not active.
- (c) Heights are with respect to North American Datum, 1927, for points on that datum, and above MSL for other points.

Table A-2.

C-Band Radars:

FPQ-6

TPQ-18\*

Site Name	<u>Coordinates</u>			Source
	$\lambda^\circ$	$\phi^\circ$	h(meters)(c)	
Patrick AFB	279.4	28.2	15	1, 2
Merritt Isl., Fla. *	279.3	28.4	12	1, 2
Grand Bahama*	281.7	26.6	12	1, 2
Grand Turk*	288.9	21.4	28	1, 2
Antigua	298.2	17.2	58	1, 2
Bermuda	295.3	32.3	19	1, 2
Ascension*	345.6	-08.0	143	1, 2
Carnarvon	113.7	-24.9	62	1, 2
Vandenberg AFT*	239.4	34.7	102	1, 2
Wallops Island	284.5	37.8	13	3
Canton Island	188.6	-2.5	0	-

- Sources: (1) Goddard Directory of Tracking Station Locations NASA/Goddard 1966.
- (2) Geonautics Memorandum, 30 January 1969, subject J184 Task 7-4 (from G. E. Graham).
- (3) Geodetic Satellites Observation Station Directory NASA/Goddard, 1969.
- (4) Heights are with respect to North American Datum, 1927, for points on that datum, and above MSL for other points.



Table A-3.

USB - 30 ft.

XMT 2.09 - 2.12 Gc/s

USB - 85 ft. Antenna\*

RCV 2.27 - 2.3 Gc/s

Site Name	<u>Coordinates</u>		
	$\lambda^\circ$	$\phi^\circ$	h(meters)(c)
Merritt Isl., Fla.	279.3	28.5	10
Grand Bahama	281.8	26.6	18
Bermuda	295.3	32.3	21
Antigua	344.4	17.0	28
Gran Canaria*	345.7	27.7	40
Ascension	355.8	-07.9	562
Madrid*	113.7	40.5	825
Carnarvon	144.7	-25.9	58
Guam	149.0	13.3	127
Canberra*	200.3	-35.6	1148
Kauai	243.1	22.1	1150
Mojave*	249.3	35.3	965
Guaymas	262.6	27.9	19
Corpus Christi	-	27.7	10
Johannesburg	-	-	-

- Sources: (1) Goddard Directory of Tracking Station Locations, 1966.  
 (2) Geonautics Memorandum, 30 January 1969, subject J184 Task 7-4 (from G. E. Graham).  
 (3) Heights are with respect to North American Datum, 1927, for points on that datum, and above MSL for other points.

Table A-4.

GRARR

Site Name	<u>Coordinates</u>		
	$\lambda^\circ$	$\phi^\circ$	h(meters)(2)
Fairbanks	212.5	65.0	371
Rosman	277.1	35.2	876
Santiago	289.3	-33.2	695
Tananarive	47.3	-19.0	1385
Carnarvon	113.7	-24.9	51

Sources: (1) Goddard Directory of Tracking Station Locations, NASA/Goddard 1966.

(2) Heights are with respect to North American Datum, 1927, for points on that datum, and above MSL for other points.

Table A-5.MOTS

Site Name	<u>Coordinates</u>		
	$\lambda^\circ$	$\phi^\circ$	h(meters)(3)
Ft. Myers, Fla.	278.1	26.5	20
Quito	281.4	- 0.6	3555
Lima	282.8	-11.8	155
Santiago	289.3	-33.1	920
Johannesburg	27.7	-25.8	1530
Tannanarive	47.3	-19.0	1375
Woomera	136.9	31.4	152
Blossom Pt.	282.9	38.4	5
Mojave, Cal.	243.1	35.3	905
St. Johns, Newf.	307.3	47.7	60
College, Alaska	212.1	64.9	160
E. Grand Forks, Minn.	262.0	48.0	255
Winkfield, Eng.	359.3	51.4	60
Rosman, N. C.	277.1	35.2	915
Orroral, Australia	148.9	-35.6	932

Sources: (1) Goddard Directory of Tracking Station Locations, 1966.

(2) Geodetic Satellite Observation Station Directory, 1969.

(3) Heights are with respect to North American Datum, 1927, for points on that datum, and above MSL for other points.

Table A-6.

USAF PC-1000\*

Site Name	<u>Coordinates</u>		
	$\lambda^\circ$	$\phi^\circ$	
Semmes, Ala.	271.7	30.8	80
Homestead, Fla.	279.6	25.5	20
Jupiter, Fla.	279.9	27.0	25
Grand Turk, Bahamas	288.8	21.4	8
Antigua	298.2	17.1	7
Curacao	291.1	12.6	25
Trinidad	298.4	10.7	270
Swan Island	276.1	17.4	85
Greenville, Miss.	269.0	33.5	45
Stoneville, Miss.	269.1	33.4	44
Colorado Springs	255.1	39.0	2191
Pago Pago	189.3	-14.3	5
Natal, Brazil	324.8	- 5.9	31
Paramaribo	304.8	5.5	17
Hunter AFB, Ga.	278.8	32.0	15
Quito, Ecuador	281.6	- 0.1	2663
Aberdeen, Md.	283.9	39.5	6
Kindley AFB, Bermuda	295.3	32.4	25

Sources: (1) NASA TN D-5034 (1969).

(2) Geodetic Satellite Observation Station Directory NASA/Goddard 1969.

(3) Heights are with respect to North American Datum, 1927, for points on that datum, and above MSL for other points.

\* The above locations have been occupied by PC-1000 cameras. These sites may not be occupied at present.

Table A-7.

Special Optical Cameras (MOTS 40 and PTH 100<sup>1</sup>)

Site Name	<u>Coordinates</u>			
	$\lambda^\circ$	$\phi^\circ$	h(meters)(4)	Source
Edinburg, Texas	261.7	26.4	65	1, 2
San Juan, P. R.	294.0	18.25	60	1, 2
Jupiter, Fla. (4 cameras)	279.8	27.0	25	2
Kingston, Jamaica	283.2	18.1	485	1, 2
Bermuda	295.3	32.3	20	1, 2
E. Grand Forks, Minn.	263.0	48.0	250	1, 2*
Columbia, Mo.	267.8	38.9	270	1, 2
Denver, Colorado	255.4	39.6	1800	1, 2
Sudbury, Ont.	279.0	46.5	275	1, 2
Greenbelt, Md.** (2 cameras)	283.1	39.0	55	1, 2
Clarksville, Ind.	274.3	38.4	190	2
Wallops Island**	284.5	37.8	4	3
Carnarvon, Australia**	113.7	-24.9	39	3

Sources: (1) Goddard Directory of Tracking Station Locations, 1966  
 (2) NASA TN D-5034 (1969)  
 (3) Reference 50  
 (4) Heights are with respect to North American Datum, 1927, for points on that datum, and above MSL for other points.

\* Station is at E. Grand Forks, Minn., Ref. 2 site name refers to location of U. of N. Dakota.

\*\* PTH 100 Camera

Note: The above stations have been in operation. A majority are probably no longer active.

Table A-8.

TRANET

Site Name	<u>Coordinates</u>		
	$\lambda^\circ$	$\phi^\circ$	h(meters)(2)
Smithfield, Australia	138.7	-34.7	40
San Miguel, Phil.	120.1	15.0	10
Tafuna	189.2	-14.3	5
South Point, Hawaii	202.0	21.5	380
Sao Jose Dos Campos, BR.	314.1	-23.2	605
Mahe, Seychelles	55.5	- 4.7	595
Misawa	141.3	40.7	20
Thule			
Las Cruces	253.2	32.3	1200
APL, Howard Co., Md.			
Stoneville, Miss.	269.1	33.4	44

Sources: (1) NASA TN D-5034 (1969).

(2) Heights are with respect to North American Datum, 1927, for points on that datum, and above MSL for other points.

Note: Stations without coordinates are not considered for experiment.

Table A-9.

SAO Tracking Net (Baker-Nunn and Special Cameras)

Site Name	<u>Coordinates</u>		
	$\lambda^\circ$	$\phi^\circ$	h(meters)(4)
Mt. Hopkins, Ariz.	249.1	31.7	2348
*Jupiter, Fla.	279.9	27.0	13
*Curacao	291.1	12.1	7
Arequipa	288.5	-16.5	2457
Olifantsfontein	28.3	-25.9	1560
*Villa Dolores	294.9	-31.9	598
Comodoro Rivadavia	292.4	-45.9	200
Maui	203.7	20.7	3034
Mirny, Antarctica	93.0	-66.5	200
Woomera	136.9	-31.4	141
Helsinki	24.9	60.1	40
Dodaira	139.2	36.0	910
Naini Tal	79.5	29.3	1925
Addis Ababa	39.0	8.7	1923
San Fernando	353.8	36.5	26
Natal	324.8	- 5.9	42
Dionysos	23.9	38.1	400
Oslo	10.8	60.2	576
Johnston Island (USAF)	190.5	16.7	5
Cold Lake Alberta	249.9	54.7	702
Edwards AFB	242.1	34.9	760

Sources: (1) Goodard Directory of Tracking Station Locations, 1966.

(2) Geodetic Satellite Observation Station Directory NASA/Goddard 1969.

(3) Weiffenbach, G. (private comm.)

(4) Heights are with respect to North American Datum, 1927, for points on that datum, and above MSL for other points.

\* Special Cameras

Table A-10. Satellite Positions for the Caribbean

Satellite Position (Caribbean)	X	Y	Z	Lat	Long	height (m)
101	-699751.93	-7264917.44	2653434.34	19.979	-95.502	1387524.17
102	-302738.41	-7301450.13	2659622.45	19.999	-92.374	1398270.42
103	94960.06	-7319252.92	2657652.85	19.955	-89.257	1409012.04
104	492298.47	-7318365.44	2647565.14	19.847	-86.152	1419716.37
105	888242.34	-7298874.25	2629423.27	19.678	-83.061	1430351.11
106	1281770.21	-7260911.65	2603314.96	19.447	-79.989	1440884.45
107	1671876.09	-7204654.53	2569351.04	19.157	-76.935	1451285.13
108	2057571.65	-7130323.08	2527664.73	18.809	-73.904	1461522.54
109	2437888.37	-7038179.42	2478410.95	18.404	-70.895	1471566.78
110	2811879.50	-6928526.26	2421765.50	17.946	-67.911	1481388.75
111	3178621.96	-6801705.43	2357924.28	17.436	-64.952	1490960.21
112	3537218.03	-6658096.45	2287102.41	16.875	-62.020	1500253.83
113	3886796.95	-6498115.03	2209533.43	16.268	-59.115	1509243.30
114	4226516.45	-6322211.60	2125468.34	15.615	-56.237	1517903.31
115	4555564.08	-6130869.76	2035174.77	14.920	-53.386	1526209.68
201	-2122796.85	-6964262.51	2649674.76	19.998	-106.952	1369385.56
202	-1740724.83	-7082035.96	2647305.19	19.951	-103.809	1380064.23
203	-1354269.77	-7181479.76	2636758.42	19.840	-100.679	1390794.27
204	-964471.78	-7262414.43	2618100.61	19.665	-97.565	1401542.59
205	-572369.86	-7324709.76	2591422.37	19.429	-94.468	1412276.30
206	-178999.14	-7368284.28	2556838.08	19.132	-91.392	1422962.84
207	214611.86	-7393104.55	2514485.14	18.776	-88.337	1433570.05
208	607443.75	-7399184.31	2464523.22	18.364	-85.307	1444066.29
209	998488.73	-7386583.64	2407133.36	17.897	-82.302	1454420.47
210	1386752.88	-7355407.88	2342517.18	17.378	-79.323	1464602.21
211	1771258.38	-7305806.64	2270895.90	16.809	-76.372	1474581.82
212	2151045.50	-7237972.60	2192509.46	16.192	-73.449	1484330.47
213	2525174.61	-7152140.36	2107615.56	15.529	-70.554	1493820.20
214	2892727.92	-7048585.19	2016488.67	14.824	-67.687	1503023.97
215	3252811.20	-6927621.75	1919419.08	14.079	-64.848	1511915.76
216	3604555.35	-6789602.80	1816711.89	13.297	-62.036	1520470.62
217	3947117.86	-6634917.85	1708686.01	12.480	-59.252	1528664.69
218	4279684.17	-6463991.87	1595673.17	11.631	-56.492	1536475.26
219	4601468.95	-6277283.87	1478016.93	10.752	-53.757	1543880.82
220	4911717.23	-6075285.59	1356071.66	9.847	-51.045	1550861.11
301	-1622134.01	-7361663.56	848622.63	6.423	-102.426	1207491.62
302	-1241550.83	-7418851.24	989914.50	7.497	-99.500	1208491.00
303	-857305.01	-7455071.21	1127937.01	8.548	-96.560	1210109.91
304	-470473.56	-7470247.95	1262236.75	9.572	-93.604	1212342.63
305	-82140.30	-7464371.48	1392374.15	10.566	-90.630	1215181.28
306	306607.97	-7437497.04	1517925.23	11.526	-87.639	1218615.86
307	694685.45	-7389744.60	1638483.22	12.448	-84.630	1222634.32
308	1081011.12	-7321297.94	1753660.09	13.331	-81.601	1227222.58
309	1464512.61	-7232403.57	1863087.98	14.170	-78.553	1232364.61
310	1844129.87	-7123369.27	1966420.49	14.962	-75.486	1238042.55
311	2218818.76	-6994562.47	2063333.90	15.705	-72.400	1244236.72
312	2587554.52	-6846408.28	2153528.22	16.396	-69.296	1250925.76
313	2949335.12	-6679387.42	2236728.10	17.032	-66.176	1258086.75
314	3303184.38	-6494033.84	2312683.69	17.611	-63.040	1265695.23
315	3648154.96	-6290932.23	2381171.24	18.130	-59.890	1273725.40
316	3983331.14	-6070715.35	2441993.71	18.589	-56.729	1282150.17
317	4307831.41	-5834061.19	2494981.13	18.985	-53.558	1290941.32
318	4620810.84	-5581690.09	2539990.90	19.317	-50.380	1300069.58
319	4921463.27	-5314361.68	2576907.93	19.584	-47.198	1309504.78
320	5209023.23	-5032871.85	2605644.70	19.786	-44.015	1319215.94



Table A-11. Fictitious Satellite Positions Over Puerto Rico

EARTH CONSTANTS								Satellite Position (Caribbean)
RA = 6378388.000		EI = 0.0		E2 = 0.0				
LONGITUDE DDD MM SS.SSS	LATITUDE DDD MM SS.SSS	HEIGHT (METERS)	LONGITUDE (RADIAN)	LATITUDE (RADIAN)	X	Y	Z	
- 67 6 0.0	18 46 0.0	1490960.0	1.17111593	0.32754012	2899357.3	-6863740.1	2531686.5	401
- 66 37 0.0	18 44 0.0	1490960.0	1.16268017	0.32695835	2957738.4	-6840388.7	2527351.3	402
- 66 6 0.0	18 42 0.0	1490960.0	1.15366263	0.32637657	3019895.9	-6814782.5	2523015.2	403
- 65 42 0.0	18 35 0.0	1490960.0	1.14668132	0.32434035	3069505.9	-6798201.9	2507832.2	404
- 65 15 0.0	18 34 0.0	1490960.0	1.13882734	0.32404946	3123108.9	-6774546.9	2505662.3	405
- 64 32 0.0	18 32 0.0	1490960.0	1.12631914	0.32346769	3208226.0	-6736268.4	2501322.0	406
- 67 10 0.0	18 32 0.0	1490960.0	1.17227948	0.32346769	2895345.9	-6876554.2	2501322.0	501
- 66 38 0.0	18 28 0.0	1490960.0	1.16297106	0.32230413	2960381.8	-6851972.7	2492638.7	502
- 66 8 0.0	18 25 0.0	1490960.0	1.15424441	0.32143147	3020942.0	-6827864.6	2486124.1	503
- 65 45 0.0	18 20 0.0	1490960.0	1.14755398	0.31997703	3068037.3	-6810790.2	2475262.1	504
- 65 12 0.0	18 17 0.0	1490960.0	1.13795467	0.31910436	3134178.7	-6782984.1	2468742.5	505
- 64 48 0.0	18 10 0.0	1490960.0	1.13097335	0.31706815	3183589.8	-6765472.7	2453522.6	506
- 67 10 0.0	18 15 0.0	1490960.0	1.17227948	0.31852259	2900110.4	-6887870.1	2464395.0	601
- 66 45 0.0	18 10 0.0	1490960.0	1.16500727	0.31706815	2951535.1	-6869884.0	2453522.6	602
- 66 12 0.0	18 6 0.0	1490960.0	1.15540796	0.31590459	3018494.2	-6843842.6	2444820.9	603
- 65 45 0.0	18 4 0.0	1490960.0	1.14755398	0.31532282	3072735.7	-6821220.2	2440468.9	604
- 65 17 0.0	18 0 0.0	1490960.0	1.13940911	0.31415926	3129376.3	-6798542.1	2431762.3	605
- 64 50 0.0	17 55 0.0	1490960.0	1.13155513	0.31270482	3184175.5	-6776948.5	2420874.4	606

Table A-12. Tracking Station Locations for the Caribbean

EARTH CONSTANTS									
RA = 6378388.000		EI = 0.0819918899		E2 = 0.0					
LONGITUDE DDD MM SS.SSS	LATITUDE DDD MM SS.SSS	HEIGHT (METERS)	LONGITUDE (RADIAN)	LATITUDE (RADIAN)	X	Y	Z	Station Name	Station Number
279 24 1.780	28 13 33.980	15.0	4.87645855	0.49263848	918620.0	-5548636.6	2998655.5	CAPE CANAVERAL FPQ	1
279 18 22.930	28 30 28.220	3.0	4.87481576	0.49755565	907102.8	-5535488.1	3026124.4	CAPE CANAVERAL USB	2
279 36 42.690	25 30 24.600	18.0	4.88014755	0.44517822	961816.7	-5679453.1	2729898.4	HOMESTEAD FLA. PC-1000	3
285 29 43.960	24 7 5.520	13.0	4.98283724	0.42094200	1556190.9	-5613138.2	2590277.4	SAN SALVADOR FPS-16	4
273 12 6.440	30 25 17.060	28.0	4.76827073	0.53095369	307469.6	-5496418.0	3210804.9	EGLIN AFB FPS-16	5
262 37 17.920	27 39 11.780	6.0	4.58361238	0.48264065	-726079.4	-5607085.1	2942569.0	CORPUS CHRISTI USB	6
288 52 3.040	21 27 43.680	36.0	5.04168917	0.37458489	1920499.1	-5619715.3	2319132.2	GRAND TURK TPQ-18	7
298 12 23.840	17 8 35.000	42.0	5.20468740	0.29920276	2881682.0	-5372823.0	1868002.8	ANTIGUA FPQ-6	8
298 12 37.410	17 8 51.680	7.0	5.20475319	0.29928363	2881948.2	-5372470.7	1868482.5	ANTIGUA PC-1000	9
291 9 42.550	12 5 21.550	23.0	5.08173240	0.21099843	2251891.9	-5817218.7	1327085.8	CURACAO BAKER-MUNN	10
283 11 26.520	18 4 31.980	485.0	4.94261012	0.31547786	1384224.0	-5905981.0	1966510.0	JAMAICA MOTS 40	11
294 0 22.170	18 15 26.220	58.0	5.13137548	0.31864971	2465154.6	-5535226.7	1985490.0	SAN JUAN MOTS-40	12
298 23 23.670	10 44 32.780	269.0	5.20788635	0.18749093	2980052.6	-5513813.0	1181091.2	TRINIDAD PC-1000	13
276 3 29.870	17 24 16.570	83.0	4.81812621	0.30376762	642558.1	-6054269.4	1895656.1	SWAN ISL PC-1000	14
295 20 46.530	32 20 47.530	21.0	5.15476464	0.56455356	2309039.8	-4874621.5	3393019.8	BERMUDA FPQ-6	15
281 25 14.810	0 37 28.000	3649.0	4.91171920	0.01089861	1263650.8	-6255300.0	-69086.7	QUITO MOTS	16
279 25 23.770	28 28 52.790	14.0	4.87685605	0.49709299	918626.0	-5535018.1	3023547.6	CAPE CANAVERAL FPS-16	17
293 0 0.0	18 15 0.0	0.0	5.11381470	0.31852259	2367653.8	-5577842.8	1984706.2	PUERTO RICO 2 TRANSPONDER	18
293 30 0.0	18 45 0.0	0.0	5.12254135	0.32724923	2409236.5	-5540864.6	2037190.0	PUERTO RICO 3 TRANSPONDER	19
294 0 0.0	18 15 0.0	0.0	5.13126799	0.31852259	2464639.9	-5535672.0	1984706.2	PUERTO RICO 4 TRANSPONDER	20
283 11 0.0	18 0 0.0	0.0	4.94248155	0.31415926	1383950.0	-5908231.0	1958408.4	JAMAICA 2 TRANSPONDER	21
291 10 0.0	12 0 0.0	0.0	5.08181700	0.20943951	2253120.4	-5818930.0	1317417.7	CURACAO 2 TRANSPONDER	22
276 30 0.0	12 0 0.0	0.0	4.82583538	0.20943951	706378.0	-6199800.6	1317417.7	BLUEFIELDS RECEIVER	23
271 0 0.0	18 30 0.0	0.0	4.72984227	0.32288591	105601.4	-6049902.8	2010966.9	CHETUMAL RECEIVER	24
274 30 0.0	11 0 0.0	1500.0	4.79092879	0.19198622	491423.6	-6244129.8	1209306.1	NICARAGUA RECEIVER	25

Table A-13. List of Stations for the Hawaii Area

EARTH CONSTANTS											
RA =		6378388.000		E1 =		0.0819918899		E2 =		0.0	
LONGITUDE DDD MM SS.SSS	LATITUDE DDD MM SS.SSS	HEIGHT (METERS)	LONGITUDE (RADIANS)	LATITUDE (RADIANS)	X	Y	Z	Station Name	Station/ Satellite Position		
190 29 9.500	16 45 38.770	8.0	3.32460739	0.29253061	-6007106.1	-1111830.1	1827523.3	JOHNSTON ISLAND MPS-25 RADAR	26		
200 19 53.960	22 7 35.030	1260.0	3.49644698	0.38617848	-5544265.2	-2054369.0	2387889.4	KAUAI-2 FPS-16	27		
205 0 0.0	19 30 0.0	4000.0	3.57792496	0.34033920	-5454665.1	-2543552.1	2116963.9	HAWAII FPS-16	28		
203 44 24.080	20 42 37.500	3034.0	3.55593420	0.36146496	-5466258.6	-2404075.2	2242535.6	MAUI BAKER-NUNN	29		
200 0 0.0	20 0 0.0	1490960.0	3.49065850	0.34906585	-6951025.1	-2529966.2	2677662.3	HAWAII SATELLITE POSITION	701		
200 0 0.0	17 0 0.0	1490960.0	3.49065850	0.29670597	-7073299.7	-2574470.5	2288770.3	HAWAII SATELLITE POSITION	702		
205 0 0.0	20 0 0.0	1490960.0	3.57792496	0.34906585	-6704073.3	-3126160.7	2677662.3	HAWAII SATELLITE POSITION	703		
205 0 0.0	17 0 0.0	1490960.0	3.57792496	0.29670597	-6822003.8	-3181152.6	2288770.3	HAWAII SATELLITE POSITION	704		
210 0 0.0	20 0 0.0	1490960.0	3.66519142	0.34906585	-6406099.4	-3698563.2	2677662.3	HAWAII SATELLITE POSITION	705		
210 0 0.0	17 0 0.0	1490960.0	3.66519142	0.29670597	-6518788.3	-3763624.1	2288770.3	HAWAII SATELLITE POSITION	706		
/E											

/6

## APPENDIX B

### MATHEMATICAL BASIS FOR GEOMETRIC ERROR ANALYSIS

An error analysis is developed for a static geometric configuration in which range and angle measurements are made on a satellite with no consideration of satellite dynamics. The effects of satellite dynamics on the error analysis is considered in Appendix D.

In analyzing geometric (static) tracking errors, we consider a tracking network made up of  $n_r$  range-measurement stations and  $n_d$  direction measuring stations. The range-measuring and direction-measuring stations are located at points  $P_i (\lambda_i, \phi_i, h_i)$  with longitude  $\lambda_i$ , latitude  $\phi_i$ , and height  $h_i$  above a standard ellipsoid (see Figure B-1); the coordinates have associated standard deviations  $\sigma_{i\lambda}$ ,  $\sigma_{i\phi}$  and  $\sigma_{ih}$  or, in matrix notation,  $\Sigma_{ij}$  with  $\Sigma_{ij}^2$  denoting the covariance matrix. Range measurements  $r_i$  from station  $i$  to the satellite have associated standard deviations  $\sigma_{ir}$ ; right ascension ( $\alpha_i$ ) and declination ( $\delta_i$ ) measurements have standard deviations  $\sigma_{i\alpha}$  and  $\sigma_{i\delta}$  respectively. For convenience, we designate the matrix of standard deviations for the observations as a whole by  $\Sigma_Q$  and the covariance matrix by  $\Sigma_Q^2$ . The standard deviations and covariance matrices of the satellite coordinates  $x_{s1}$ ,  $x_{s2}$ ,  $x_{s3}$  (where 1, 2, 3 denote x, y, z, respectively) are denoted by  $\Sigma_s$  and  $\Sigma_s^2$  respectively.

The observations  $r_i$ ,  $\alpha_i$ ,  $\delta_i$ , the station locations  $\lambda_i$ ,  $\phi_i$ ,  $h_i$ , and the satellite location  $\lambda_s$ ,  $\phi_s$ ,  $h_s$  are related by the equations

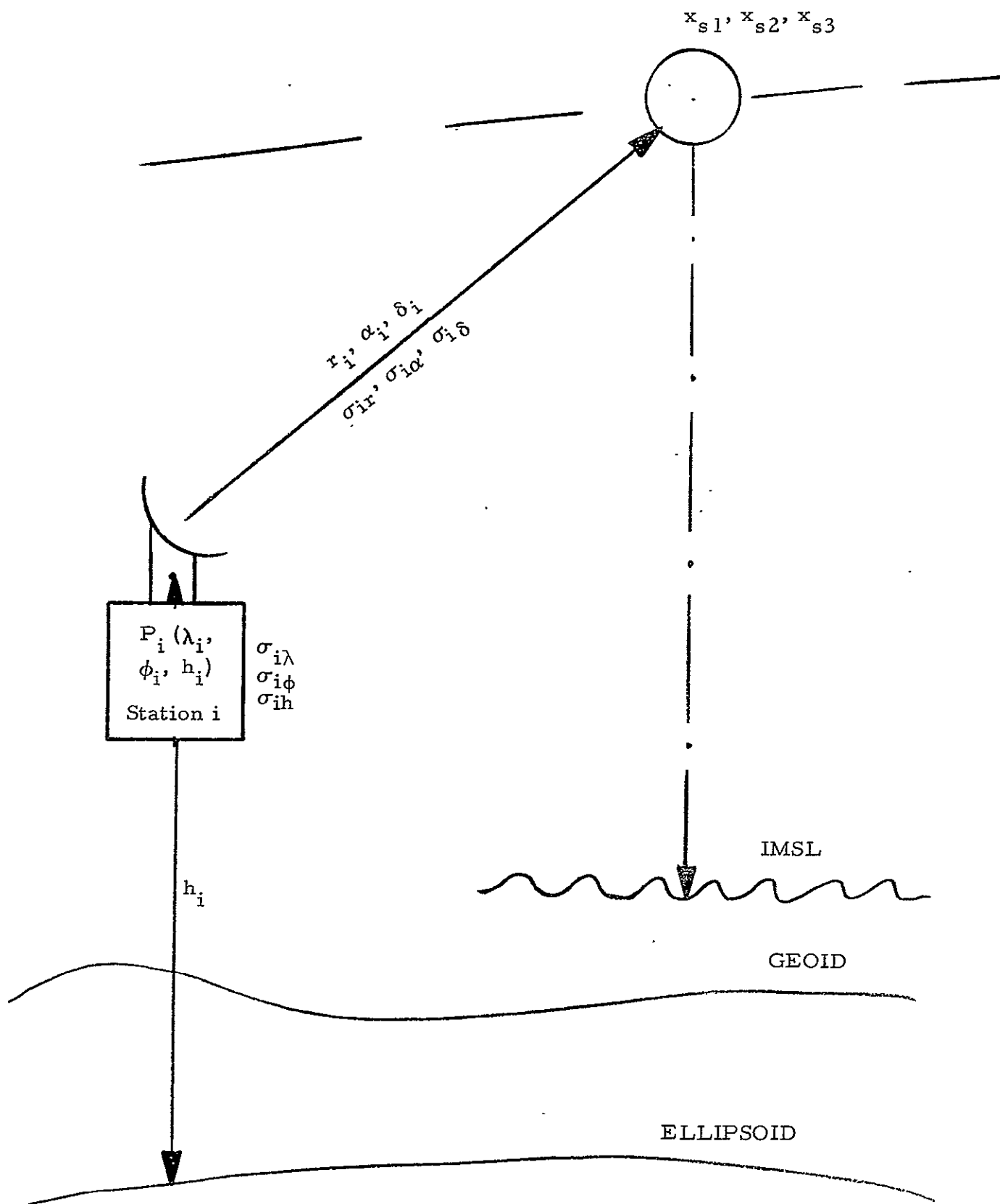


Figure B-1

$$\left. \begin{aligned} r_i^2 &= \sum_{j=1}^3 (x_{sj} - x_{ij})^2 \\ \cos^2 \alpha_i &= \sum_{k=1}^2 (x_{sk} - x_{ik})^2 / \sum_{j=1}^3 (x_{sj} - x_{ik})^2 \\ \sin^2 \delta_i &= (x_{s3} - x_{i3})^2 / \sum_{j=1}^3 (x_{sj} - x_{ik})^2 \end{aligned} \right\} \quad (1)$$

In these equations, the space-fixed rectangular coordinates  $x_{ij}$ ,  $x_{sj}$  are obtained from the geodetic coordinates  $\lambda_i$ ,  $\phi_i$ ,  $h_i$  of the station and  $\lambda_s$ ,  $\phi_s$ ,  $h_s$  of the satellite through the equations (for each station  $i$  and satellite location  $s$ ):

$$\begin{bmatrix} x_1 \\ x_2 \\ x_3 \end{bmatrix} = (N + h) \begin{bmatrix} \cos \phi \cos \theta \\ \cos \phi \sin \theta \\ \sin \phi \end{bmatrix} - \begin{bmatrix} 0 & 0 & 0 \\ 0 & 0 & 0 \\ 0 & 0 & Ne^2 \end{bmatrix} \begin{bmatrix} \cos \phi \cos \theta \\ \cos \phi \sin \theta \\ \sin \theta \end{bmatrix} \quad (2)$$

$N$  is the radius of curvature in the prime vertical,  $\theta$  is the angle

$$\theta = \alpha - \omega t - \alpha_G$$

where  $\omega$  is the rate of rotation of the earth,  $t$  the time elapsed since epoch,  $e$  is the eccentricity and  $\alpha_G$  the right ascension of Greenwich at epoch.

The above equations non-linear in  $x_{ij}$ ,  $x_{sj}$ , are exchanged in the usual way, for equations linear in the corrections  $\Delta r_i$ ,  $\Delta a_i$ ,  $\Delta \delta_i$ ,  $\Delta x_{ij}$ ,  $\Delta x_{sj}$ , to give (in matrix form) the equation

$$[Q] = [A_{ij}] [\Delta x_{sj}] + [B_{ij}] [\Delta x_{ij}] \quad (3)$$

The matrix  $[\Delta Q]$  is defined as

$$\begin{bmatrix} \Delta r_1 \\ \vdots \\ \Delta r_6 \\ \Delta a_7 \\ \Delta \delta_7 \\ \Delta a_8 \\ \Delta \delta_8 \\ \Delta a_9 \\ \Delta \delta_9 \end{bmatrix} \quad (4)$$

where the  $\Delta r_i$ 's are defined as the observed measurements minus computed values of radar range, and the  $\Delta a_i$  and  $\Delta \delta_i$  are defined as the observed measurements minus computed values of the right ascension and declination, respectively, of the satellite from a camera station.

In a straightforward manner, this equation is converted to the homogeneous equation

$$\begin{bmatrix} \vdots \\ I \\ \vdots \end{bmatrix} - B \quad [\Delta Q] = [A] [\Delta x_{sj}] \quad (5)$$

or, for short

$$[C] [\Delta Q] = [A] [\Delta x] \quad (6)$$

The covariance matrix  $\left[ \sum_s^2 \right]$  is therefore given by  $\left[ \sum_s^2 \right] =$

$$\left\{ [A]^T [A] \right\}^{-1} [A]^T [C] \left[ \sum_Q^2 \right] [C]^T [A] \left\{ [A]^T [A] \right\}^{-T}; \quad (7)$$

and the covariance matrix  $\left[ \sum_g^2 \right]$ , which contains the standard deviation,  $\sigma_h$ , of the altitude, is given by

$$\left[ \sum_g^2 \right] = [D] \left[ \sum_s^2 \right] [D]^T \quad (8)$$

where  $[D]$  is the inverse of the Jacobian of equation (2).

The computer program embodying these error equations provides space for data from nine tracking stations - six radar and three camera stations - for a total of twelve observations per satellite position. Weighting matrices are not used; their use would have entailed extended justification of the weights used, and the results would have been little more reliable than they are without weighting. A number of assumptions were made to simplify the programming; they relate to the transformation of variances from a rotating to a non-rotating frame of reference and do not affect the results of the error analysis.

The preceding pages give the equations used for computing the standard deviations of the satellite location from the standard deviations of the observations and the observing station locations. These equations apply to static, (instantaneous) situations only.



## APPENDIX C

### CHARACTERISTICS OF FREQUENCY AND TIME STANDARDS

Cited here, as examples of frequency-standard performance, are the specifications for (a) the Rohde-Schwarz XSR rubidium frequency standard, (b) the H/P crystal oscillator standard, and (c) the H/P cesium frequency standard. These specifications are given in Table C-1. Rohde-Schwarz specifications are traditionally conservative, sometime excessively so; H/P specifications are optimistic but reasonable.

For further background information, the reader is referred to the Proceedings of the IEEE, February 1966,<sup>27</sup> or some of the 1967-69 issues of the periodical Frequency.

Table C-1. Frequency Standard Specification

	Rohde/Schwarz XSR	H/P XTAL 106A/B	H/P Cesium 5061A
Frequency Variation			
Long-term	$\pm 6 \cdot 10^{-11}$	$\leq 9 \cdot 10^{-9}$ (2)	$\pm 1 \cdot 10^{-11}$ (1)
Short-term (3)			
1 ms	$< 3 \cdot 10^{-9}$	$8 \cdot 10^{-10}$	$5 \cdot 10^{-10}$
10 ms	$< 3 \cdot 10^{-10}$	$1.9 \cdot 10^{-10}$	$10^{-10}$
1 s	$< 6 \cdot 10^{-12}$	$1.9 \cdot 10^{-11}$	$7 \cdot 10^{-12}$ (4)
Frequencies Generated (Mc/S)	0.1 1 5	0.1 1 5	0.1 1 5
Clock Output	N.A.	N.A.	N.A.
Jitter (10)	N.A.	N.A.	$2 \times 10^{-8}$ S
Perturbation Effects			
Air Pressure	$\leq 1 \cdot 10^{-12}$ / 100 mutg	Not Known	Not Known
Temperature/°C	$\leq 1 \cdot 10^{-12}$	$8 \cdot 10^{-10}$	$< 5 \cdot 10^{-12}$
Magnetic Field/gauss	$< 1 \cdot 10^{-11}$	N.K.	$< 2.5 \cdot 10^{-12}$ (5)
Voltage/volt	$< 2 \cdot 10^{-12}$	$< 4 \cdot 10^{-12}$	$< 1 \cdot 10^{-11}$ (6)
Reference	(7)	(8)	(9)

## NOTES TO TABLE C-1

1. The cesium frequency standard is a primary standard, and consequently has, properly speaking, no long-term frequency variation. The figure given is therefore in the nature of a performance guarantee.
2. Crystal oscillators of the commercial variety usually have their "long-term" frequency stabilities given for 24-hour periods. The figure given here is calculated from the H/P specification assuming random variation over a 1 year interval. Since at least part of the specified long-term stability is drift, and therefore predictable to some extent, the actual frequency stability is probably much lower than that given (lower numerically).
3. For use as a ranging instrument, we are interested in  $df/dt$ , or in  $\Delta f/\Delta t$  for  $\Delta t \rightarrow 0$ . Hence the "short-term" variations gotten by averaging are not really significant for our problem.
4. Estimated from H/P chart, ref.
5. Estimated from 2-gauss field value.
6. Estimated from 8-volt range value.
7. 1969-Anonymous ATOMIC FREQUENCY STANDARD XSR - Data Sheet, Rohde & Schwarz, Munchen.
8. 1968 - Anonymous H/P REFERENCE CATALOG - 1969, Hewlett-Packard Co., Palo Alto. pp. 648-651.
9. 1968 - Same as Ref. 8, pp. 643-645.

10. Jitter, as here understood, is the rms variation (in seconds) between times of emission of successive pulses. It is not enough that the frequencies remain constant; a random variation of 20 n sec. in pulse transmission interval is equivalent to a 6-meter variation in computed distance. Such variation is of no importance in measuring range differences; it is very important in measuring range. Commercial, ready-made counters can measure time intervals to 10 n sec., custom-made counters should be able to measure to 5 n sec. or even 1 n sec. Such measurement accuracy is of no use for range measurement unless the emitted pulse comes out at intervals  $t_i \pm 5$  n sec. or better, where  $t_i$  is the assumed interval.

## APPENDIX D

### MATHEMATICAL BASIS FOR ANALYSIS OF ERROR IN SATELLITE LOCATIONS (DYNAMICAL SITUATIONS)

An Earth satellite follows a two-dimensional path imbedded in four-dimensional space. The two-dimensional path is called a trajectory. The one dimensional timeless portion of a trajectory is called a path. The actual trajectory of a satellite differs from the trajectory computed observation of the satellite. The following pages derived simple equations for estimating the scatter of computed satellite locations about actual locations.

In designing an experiment in which at least partial dependence is to be placed on a theoretical orbit, we will want to know how far to trust that orbit (set of equations). That is, we will want some estimate of the accuracy variance associated with the theoretical orbit. The following equations are used to find an expression for the variance matrix of the quantities.

$$\Delta x = x_{\text{true}} - x_{\text{computed}}$$

$$\Delta y = y_{\text{true}} - y_{\text{computed}}$$

$$\Delta z = z_{\text{true}} - z_{\text{computed}}$$

In the process of deriving the final equations, a number of assumptions have had to be made to keep the mathematical effort within the bounds of this study. The most suspect of these assumptions is the one that permits a simple transition from perturbation error to perturbation variance.

The assumption is certainly effective, and it appears at present to be sufficiently plausible to allow its introduction.

We start with the usual perturbations in their Gaussian form<sup>54</sup>, but slightly changed from the usual form given in most works. The symbols  $a$ ,  $e$ ,  $i$ ,  $\tilde{\omega}$ ,  $\Omega$  and  $\sigma$  have their usual meanings;  $F_N$  is the perturbing force in the direction of the radius vector to the orbit point (positive outwards),  $F_T$  is the perturbing force in the (momentary) orbital plane and perpendicular (positive in the direction of motion) to the radius vector, and  $F_B$  is the perturbing force in the direction  $\vec{F}_N \times \vec{F}_T$ .  $V$  is the true anomaly,  $E$  is the eccentric anomaly,  $n$  the mean motion,  $r$  the radius vector, and  $p = a(1-e^2)$  the semi-latus rectum. Then

$$\frac{da}{dt} = \frac{2e \sin V}{n(1-e^2)^{1/2}} F_N + \frac{2a(1-e^2)^{1/2}}{nr} F_T$$

$$\frac{de}{dt} = \frac{(1-e^2)^{1/2} \sin V}{na} F_N + \frac{(1-e^2)^{1/2} (\cos E + \cos V)}{na} F_T$$

$$\frac{di}{dt} = \frac{r}{a^2} \frac{\cos(\omega+V)}{n(1-e^2)^{1/2}} F_B$$

$$\begin{aligned} \frac{d\tilde{\omega}}{dt} = & - \frac{(1-e^2)^{1/2}}{nae} \cos V F_N + \left( \frac{r}{p} + 1 \right) \sin V \frac{(1-e^2)^{1/2}}{nae} F_T \\ & + \frac{r}{a} \frac{\tan \frac{i}{2} \sin(\omega+V)}{na(1-e^2)^{1/2}} F_B \end{aligned}$$

$$\frac{d\Omega}{dt} = \frac{r}{a^2} \frac{\csc i \sin(\omega+V)}{n(1-e^2)^{1/2}} F_B$$

$$\begin{aligned} \frac{d\epsilon}{dt} = & \left[ - \frac{2r}{na^2} + \frac{e(1-e^2)^{1/2} \cos V}{na[1+(1-e^2)^{1/2}]} \right] F_N \\ & + \left[ \left( \frac{r}{p} + 1 \right) \frac{(1-e^2)^{1/2} \sin V}{nae} \right] F_T \\ & + \left\{ \frac{r}{a} \left[ \frac{e^2}{1+(1-e^2)^{1/2}} + (1-e^2)^{1/2} \right] \frac{\tan \frac{i}{2} \sin(\omega+V)}{na(1-e^2)^{1/2}} \right\} F_B \end{aligned}$$

Defining

$$\eta \equiv (1-e^2)^{\frac{1}{2}}$$

and using the relations

$$r = a\eta^2/(1+e \cos V)$$

$$\tilde{\omega} \equiv \Omega + \omega$$

$$\varepsilon \equiv \text{mean longitude at epoch} = \sigma + \tilde{\omega}$$

we get the equations

$$\frac{da}{dt} = \frac{2e}{n\eta} \sin V F_N + \frac{2}{n\eta} (1 + e \cos V) F_T$$

$$\frac{de}{dt} = \frac{\eta \sin V}{na} F_N + \frac{\eta}{na} (\cos E + \cos V) F_T$$

$$\frac{di}{dt} = \frac{\eta \cos(V+\omega)}{na(1+e \cos V)} F_B$$

$$\begin{aligned} \frac{d\omega}{dt} = & -\frac{\eta}{nae} \cos V F_N + \frac{\eta \sin V}{nae} \left( \frac{2 + e \cos V}{1 + e \cos V} \right) F_T \\ & - \frac{\cos i}{\sin i} \frac{\eta \sin(V+\omega)}{na(1+e \cos V)} F_B \end{aligned}$$

$$\frac{d\Omega}{dt} = \frac{\eta \sin(V+\omega)}{na \sin i (1+e \cos V)} F_B$$

$$\begin{aligned} \frac{d\sigma}{dt} = & \frac{\eta}{na} \left[ \frac{\cos V}{e} - \frac{2\eta}{1 + e \cos V} - \frac{e \cos V}{1 + \eta} \right] F_N \\ & + \frac{\eta}{na} \frac{\sin(V+\omega)}{(1+e \cos V)} \left( \frac{1-\cos i}{\sin i} \right) F_B \end{aligned}$$

These equations are linear in the perturbing forces  $F_T$ ,  $F_N$ , and  $F_B$ , and can be abbreviated to

$$\begin{aligned}
 \frac{da}{dt} &= a_{11} F_T + a_{12} F_N + a_{13} F_B \\
 \frac{de}{dt} &= a_{21} F_T + a_{22} F_N + a_{23} F_B \\
 \frac{di}{dt} &= a_{31} F_T + a_{32} F_N + a_{33} F_B \\
 \frac{d\omega}{dt} &= a_{41} F_T + a_{42} F_N + a_{43} F_B \\
 \frac{d\Omega}{dt} &= a_{51} F_T + a_{52} F_N + a_{53} F_B \\
 \frac{d\sigma}{dt} &= a_{61} F_T + a_{62} F_N + a_{63} F_B,
 \end{aligned}
 \tag{D-1}$$

or in matrix form,

$$[dq/dt] = [a_{ij}] [F_j],$$

where

$$[dq/dt] \equiv [da/dt, de/dt, di/dt, d\omega/dt, d\Omega/dt, d\sigma/dt]^T$$

and

$$[F_j] \equiv \begin{bmatrix} F_T \\ F_N \\ F_B \end{bmatrix}$$

We define the perturbing force  $[F_j]$  as the difference between the actual force acting on the satellite and the theoretical force obtained from the best satellite tracking-data derived constants defining the Earth's gravity field,



atmosphere, and radiation environment, and the luni-solar gravity field. This definition of  $[F_j]$  is not very useful, since the work involved in finding the "best" set of constants would take more time and money than the problem can justify. If we change the definition by using, instead of "the best", the phrase "a set of commonly-used", we get a useful definition but one whose application to our problem can be criticized because we should be using the best orbit. Fortunately, we are concerned only with orbital segments less than 10,000 km. and mostly about 5,000 km. long, and it can be shown that for such short segments the differences between various orbits are insignificant. One way of showing this is to compare an analytic orbit with an orbit of a few terms fitted to the same observations. We have done this with a set of 3rd degree polynomials, fitting these to fictitious observations computed from an analytic orbit; for segments of 1000 km. length the empirical and analytic orbits differed by less than two meters. Therefore we can probably safely assume that over short segments analytic orbits fitted to observations over these segments will differ, in their predictions, less from each other than from the true orbits. The actual errors  $\Delta q_i$  accumulated in the elements  $q_i$  between times  $t_1$  and  $t_2$  are derived from equations (D-1) by integrating each equation with respect to time over the interval  $t_2 - t_1$ .

$$\Delta q_i = \int_{t_1}^{t_2} (a_{i_1} F_T + a_{i_2} F_N + a_{i_3} F_B) dt$$

The forces  $F_T$ ,  $F_N$ ,  $F_B$  are functions of the satellite coordinates and therefore functions of time. They could, if we were interested in  $\Delta q_i$ , be represented as a small number of terms of a Fourier series fitted to actual or guessed-at gravity differences:

$$F_T = R_e \left[ \sum A_T e^{-ikt} \right]$$

with similar formulae for  $F_N$  and  $F_B$ . 27

The present problem concerns, not  $\Delta q_i$ , but  $\sigma_{qi}$ , the standard deviation in the  $\Delta q_i$ . We therefore need not the  $F_T$ ,  $F_N$ ,  $F_B$ , but their standard deviations  $\sigma_T$ ,  $\sigma_N$ ,  $\sigma_B$  or, generally the covariance matrix  $\Sigma_F^2$ . The elements of  $\Sigma_F^2$  are also functions of time, but we can reasonably expect that they will change less rapidly than the  $F$ 's themselves since they are average values, not the values themselves. Assuming for the moment, therefore, that  $\Sigma_F^2$  is constant over the short arc segments we are interested in, and substituting for the  $F$ 's their average errors, we find that

$$\begin{aligned}\Delta q_i &= \int_{t_1}^{t_2} [A] [F] dt \\ \Sigma_q^2 &= \int_{t_1}^{t_2} [A] \Sigma_F^2 [A]^T dt \\ &= [B] \Sigma_F^2 [B]^T\end{aligned}$$

where

$$[B] = \int_{t_1}^{t_2} [A] dt.$$

This step is, as earlier remarked, open to criticism, but is taken as an expedient measure to avoid the following further and more complicated steps:

- (a) express the variations  $F_N$ ,  $F_T$ ,  $F_B$  as linear Fourier series in  $V$  or  $t$  as the independent variable;
- (b) integrate each term of the form

$$a_i [K_{jn} \cos(nV) + L_{jn} \sin(nV)], \text{ etc.}$$

- (c) combine terms.

There does not seem to be the need for such a complicated procedure for the simple situation we are trying to analyze.

We integrate these equations with respect to the true anomaly  $V$  by using the equations

$$\frac{dt}{dV} = \left(\frac{r}{a}\right)^2 (n\eta)^{-1}$$

$$\left(\frac{r}{a}\right) = \frac{\eta^2}{(1+e \cos V)}$$

and integrating. The individual integrands, denoted by  $\tilde{a}_{ij}$ , are

$$\tilde{a}_{11} = 2e \sin V (1 + e \cos V)^{-2} (\eta/n)^2$$

$$\tilde{a}_{12} = 2(1 + e \cos V)^{-1} (\eta/n)^2$$

$$\tilde{a}_{13} = 0$$

$$\tilde{a}_{21} = (1 + e \cos V)^{-2} (\eta^4/n^2 a)$$

$$\tilde{a}_{22} = \frac{\eta^4}{n^2 a} \left[ \frac{1}{1+e \cos V} - \frac{\eta^2}{(1+e \cos V)^3} \right]$$

$$\tilde{a}_{23} = 0$$

$$\tilde{a}_{31} = 0$$

$$\tilde{a}_{32} = 0$$

$$\tilde{a}_{33} = \frac{\eta^4 \cos(V+\omega)}{n^2 a (1+e \cos V)^3}$$

$$\tilde{a}_{41} = - \frac{\eta^4}{n^2 a e} \frac{\cos V}{(1+e \cos V)^2}$$

$$\tilde{a}_{42} = \frac{\eta^4}{n^2 a e} \sin V \left[ \frac{1}{(1+e \cos V)^2} + \frac{1}{(1+e \cos V)^3} \right]$$

$$\tilde{a}_{43} = - \frac{\eta^4}{n^2 a} \cot i \frac{\sin(V+\omega)}{(1+e \cos V)^3}$$

$$\tilde{a}_{51} = 0$$

$$\tilde{a}_{52} = 0$$

$$\tilde{a}_{53} = \frac{\eta^4}{n^2 a} \csc i \frac{\sin(V+\omega)}{(1+e \cos V)^3}$$

$$\tilde{a}_{61} = \frac{2 \eta^4}{n^2 a e} \left[ \frac{\eta \cos V}{(1+e \cos V)^2} - \frac{2\eta e}{(1+e \cos V)^3} \right]$$

$$\tilde{a}_{62} = 0$$

$$\tilde{a}_{63} = \frac{\eta^4}{n^2 a} \left( \frac{1+\cos i}{\sin i} \right) \left( \frac{\sin(V+\omega)}{(1+e \cos V)^3} \right)$$

The integrands occurring in these equations are easily, if not quickly, integrated, and the intermediate steps leading to the elements  $b_{ij}$  of [B] are therefore left out. In order to conserve space, I give the indefinite integrals; each expression is to be evaluated twice; once for  $\cos V(t_1)$ , and once for  $\cos V(t_2)$ , and the first result subtracted from the second. (Considerable computing time is saved by evaluating common factors only once, of course). The same integrals occur again and again in the  $b_{ij}$ , and the following notation is therefore used.

$$q \equiv (e + x)/(1 + ex)$$

$$I_1 \equiv - [\arcsin(q)]/\sqrt{1-e^2}$$

$$I_2 \equiv (1-e^2)^{-1} \left( I_1 - e \sqrt{\frac{1-q^2}{1-e^2}} \right)$$

$$I_3 \equiv (1-e^2)^{-2} \left[ \frac{I_1}{2} - 2e \sqrt{\frac{1-q^2}{1-e^2}} + q \sqrt{\frac{1-q^2}{1-e^2}} \right]$$

Then we have

$$b_{11} = 2 \left( \frac{\eta}{n} \right)^2 (1 + ex)^{-1}$$

$$b_{12} = -2 \left( \frac{\eta}{n} \right)^2 I_1$$

$$b_{13} = 0$$

$$b_{21} = - \left( \frac{\eta^4}{n^2 a} \right) I_2$$

$$b_{22} = - \left( \frac{\eta^4}{n^2 a} \right) [I_1 - \eta^2 I_3]$$

$$b_{23} = 0$$

$$b_{31} = 0$$

$$b_{32} = 0$$

$$b_{33} = - \frac{\eta^4}{n^2 a} \frac{\cos \omega}{e} (I_2 + I_3) + \frac{\sin \omega}{2e(1+ex)^2}$$

$$b_{41} = \frac{\eta^4}{n^2 ae} \left[ I_1 - \frac{I_2}{e} \right]$$

$$b_{42} = \frac{\eta^4}{n^2 ae^2 (1+ex)} \left[ \frac{3+2ex}{2(1+ex)} \right]$$

$$b_{43} = \frac{\eta^4 \cot i}{n^2 ae} \left[ \frac{\cos \omega}{2(1+ex)^2} - \sin \omega (I_2 + I_3) \right]$$

$$b_{51} = 0$$

$$b_{52} = 0$$

$$b_{53} = \frac{\eta^4 \csc i}{n^2 a e} \left[ \frac{\cos \omega}{2(1+ex)^2} - \sin \omega (I_2 + I_3) \right]$$

$$b_{61} = - \frac{2\eta^5}{n^2 a e} \left[ \frac{1}{\eta e} (I_2 + I_3) - 2eI_3 \right]$$

$$b_{62} = 0$$

$$b_{63} = - \frac{\eta^4}{n^2 a} \left( \frac{1+\cos i}{\sin i} \right) \left[ - \frac{\cos \omega}{2e(1+ex)^2} + \sin \omega I_3 \right]$$

More useful than the element variances are the variances in location referred to the moving trihedron with origin at the satellite. Again, because the orbit is of low eccentricity, we can use the variances in the direction of  $F_N$ ,  $F_T$ , and  $F_B$  instead. To the accuracy we need for calculation of variance, we can take the variance in  $r$ , the variance in  $\omega + \sigma$ , and the variance in a suitable function of  $i$ ,  $\Omega$  and  $V$ . Then we have

$$[\Sigma_L^2] = [A_L] [\Sigma_a^2] [A_L]^T$$

where  $[\Sigma_L^2]$  is the covariance matrix for the errors  $\Delta r$ ,  $(\Delta\omega + \Delta\sigma)$  and the error  $\Delta T$  in the transverse direction,  $[\Sigma_a^2]$  is the covariance matrix of the elements, and the matrix  $[A]$  has the elements as follows

$$\begin{array}{lll}
a_{11} = \frac{r}{a} & a_{12} = -\frac{2e}{1-e^2} + \frac{\cos V}{1+e \cos V} & a_{13} = 0 \\
a_{14} = \frac{e \sin V}{1+e \cos V} & a_{15} = \frac{e \sin V}{1+e \cos V} & a_{16} = 0 \\
a_{21} = 0 & a_{22} = 0 & a_{23} = 0 \\
a_{24} = r & a_{25} = 0 & a_{26} = r \\
a_{31} = 0 & a_{32} = 0 & a_{33} = r \sin(\omega+V) \\
a_{34} = 0 & a_{35} = r \sin i \sin(\omega+V) & a_{36} = 0.
\end{array}$$

The preceding pages derived simple equations for estimating the variance of actual measured satellite locations compared with locations computed from a theoretical orbit.

## APPENDIX E

### EFFECT OF ORBITAL CONSTRAINTS ON LOCATION ERRORS

The equations derived in Appendix B are free from any assumptions regarding the orbital motion of the satellite. They therefore are very useful for studying the effects of various satellite-and-tracking-station configurations and for getting "order-of-magnitude" estimates of satellite locations, but are not as useful for making close estimates of satellite location. For fine work, the equations must be modified to take into account the correlation between locations that the orbit equations introduce. It is of course not necessary to introduce into the variance analysis an orbit complete with tesseral harmonics up to degree and order 20, luni-solar perturbation, atmospheric drag, and so on. We are dealing with arc segments less than 300 km long which are fitted individually to the tracking data. This effectively eliminates the need for considering secular and long-period perturbations. In fact, it is sufficient to approximate the segment, for our purposes, by a low-degree power series or harmonic series. A set of third-degree polynomial equations has been found to give satellite locations that differ by less than 1 meter from those provided by a complete orbit, when fitted to the same tracking data, over a 1800 km segment, so that our approximation is reasonable. We therefore repeat the observation equations of Appendix B.

$$\Delta Y = A \Delta X \quad (1)$$

where  $\Delta Y$  is the observation matrix,  $\Delta X$  the matrix of satellite location errors, and  $A$  the coefficient matrix. To this (matrix) equation we add the condition equation

$$C = B \cdot \Delta X \quad (2)$$



where the matrices B and C are not yet defined. One way of handling the conditions would be to require that the coordinates lie on the path described by the orbit. This would require eliminating the time from the equations for the coordinates. Since in general the path (time-independent space curve) is better determined than the orbit, such a condition would be realistic. Because the approximation of orbits by sets of 3<sup>rd</sup> degree polynomials has been successful in keeping the rms error in all three coordinates down to better than one fifth of the radar tracking  $\sigma$ , restricting the condition to the satellite path would not be worth while. We therefore use the time-dependent equations

$$[X] = [1 \ t \ t^2 \ t^3 \ t^4] [D] \quad (4)$$

where  $[D]$  is the set of constants  $\ell_{ij}$  defining the orbit segment. With the condition equations in this form, we can substitute directly for  $\Delta X$  in (1) and drop equation (2), so that

$$\Delta Y = A \cdot T \cdot L \quad (5)$$

where L consists of the elements  $\Delta \ell_{ij}$  and T is the matrix

$$[1 \ t_i \ t_i^2 \ t_i^3 \ t_i^4]. \quad (6)$$

The covariance matrix for  $\Delta L$  is then

$$\Sigma_L^2 = (T^T A^T A T)^{-1} T^T A^T \Sigma_Y^2 A T (T^T A^T A T)^{-T}, \quad (7)$$

with the covariance matrix for X being

$$\Sigma_X^2 = T \Sigma_L^2 T^T. \quad (8)$$

## APPENDIX F

### INFLUENCE OF LAND TOPOGRAPHY ON RETURN PULSE

The pulse emitted by the altimeter is assumed to have a duration of 50 nsec. If the altimeter were designed so that it pays no attention to energy returned more than 50 nsec. after energy from an emitted pulse starts to return, then an altimeter 1100 km. above a flat surface would receive and make use of energy scattered from a circular area about 6 km. in radius. If the area were occupied entirely by water, the surface could be considered spherical on the average even if the surface were rough. If the area were occupied partly by land, a flat or spherical surface would fit poorly because the land surface would project above the average water level, but would not be visible below water level, to the radar. In fact, any land outside the area which were high enough to reflect energy back to the altimeter during the 50 nsec. interval that the altimeter was paying attention to returned energy would cause the altimeter to measure an incorrect altitude. The following table shows the land heights  $h$ (in meters), which at the given distances  $d$  (in km.) would return energy to the altimeter during the 50 nsec. interval.

<u>Distance <math>d</math> (km)</u> <u>From Footpoint</u>	<u>Height <math>h</math> (meters)</u> <u>of Land</u>
10	30
15	85
20	165
30	400
40	700
50	1100
75	2500
100	4500

Setting a limit of 15 km. as the smallest allowable distance from altimeter footpoint to land would therefore safeguard against interference from land-caused echoes unless the coast were lined with exceptionally high trees or cliffs or there were high mountains close inland.

The situation is not quite as simple, however, as one might think from the above discussion. Any bit of land returning energy during the 50 nsec. interval would affect the shape of the returned-energy versus time at any instant by an amount proportional to the ratio of the land area to the total area that would be returning energy at that instant if that area were at the same distance from the altimeter as the land. If the altimeter were able to distinguish 100 different levels of energy, then the land would have to occupy 0.1% or more of the total area to be distinguishable. This statement must be modified somewhat, since it assumes that the equivalent scattering cross section ( $\sigma_0$ ) of land is the same as that of water. It will have to be modified further because of radio noise; e.g., part of the energy that the altimeter interprets as echo actually originates within the receiver or leaks in or is scattered into the receiver from other sources than the emitted pulse. These considerations lead to the conclusion that the effects of land on the signal are not calculable from land height alone (which would greatly exaggerate the effects) but must be calculated, if the matter is important, using land height, land area, land scattering cross section, noise level in the receiver, and energy level resolution. Earth curvature need not be taken into account, obviously, since at 1100 km. altimeter height the pulse's wave front recedes from a flat surface more than six times as fast as an average spherical earth surface does.

# APPENDIX G VERIFICATION METHOD USING PATH INTERSECTIONS

An interesting way of looking at the self-consistency data has been suggested, considering the heights above path-intersection points as being related thru loop-closure equations. As shown in Figure G-1, the points  $P_i$  on the reference surface lie at the intersection of projections of the satellite paths onto the reference surface. At every  $P_i$  three independent heights are identified: the height  $h_{oi}$  of  $Q_i$  above  $p_i$ , the MSL surface above the reference surface; and two heights  $h_{si}$  of  $S_i$  above  $P_i$ , the altimeter above the reference surface. From this viewpoint, the height differences  $(h_{o,i+1} - h_{o,i})$  around any closed circuit, and in particular about a circuit around an elementary 4-point cell, must sum up to zero and hence, if satellite heights  $h_{si}$  are reduced to the common value of some one height  $h_{sl}$  at which  $h_{oi}$  is known, we find that the changes in the altitude  $(h_{si} - h_{oi})$  must sum to zero around any circuit (or must sum to the same value over any two paths between a given pair of points).

We write  $h_{mi}$  for the measured altitude above point  $Q_i$ . Above a given point  $P_i$  we therefore have

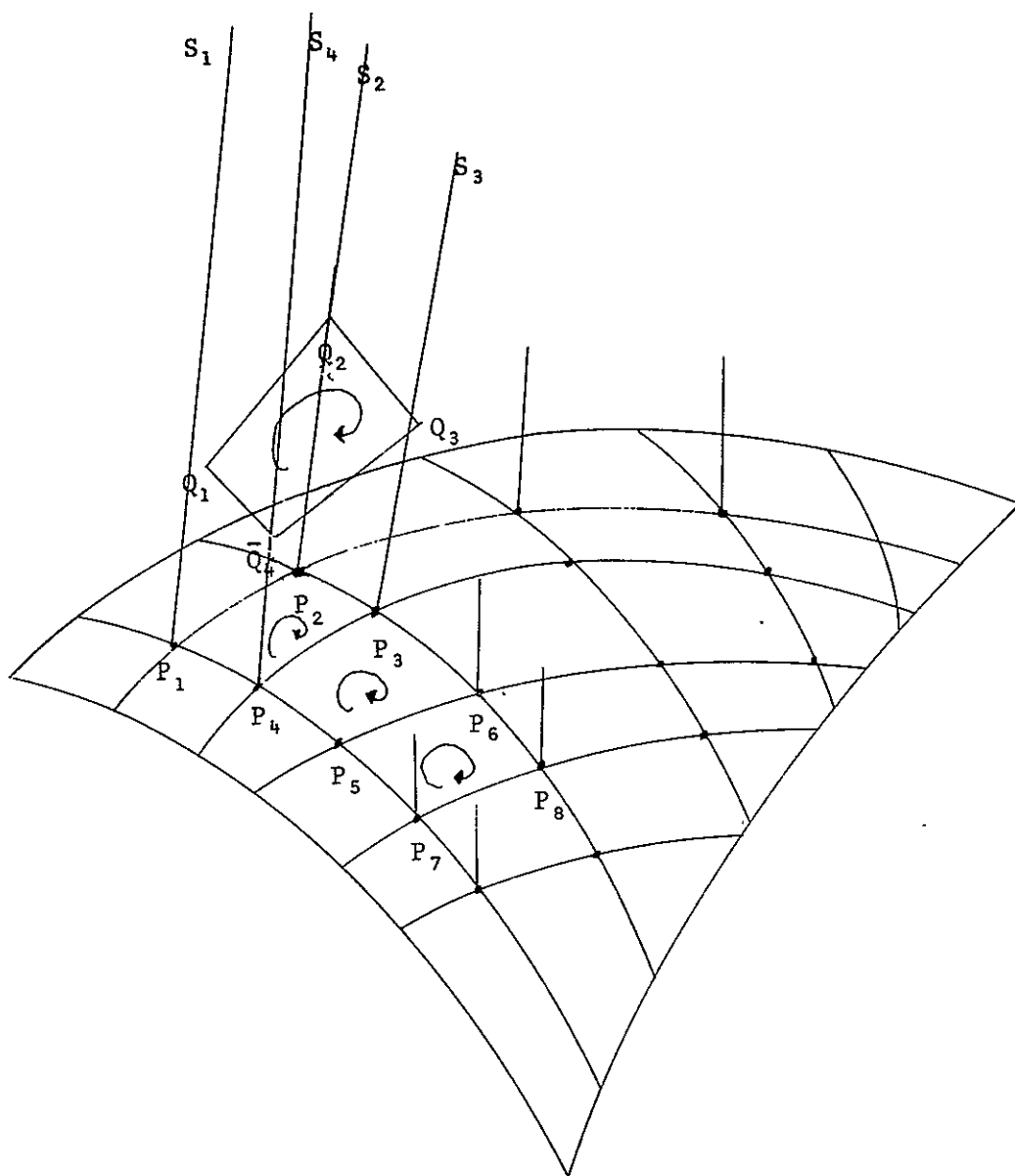
$$h_{mi1} = h_{si1} - h_{oi1} \tag{G-1}$$

$$h_{mi2} = h_{si2} - h_{oi2}$$

for the two measurements denoted by the subscripts 1 and 2.

We write

$$\bar{h}_{mi2} = h_{mi2} - (h_{si2} - h_{sl}), \tag{G-2}$$



$P_i$  - points on MSL surface

$Q_i$  - corresponding points on MSL surface

$S_i$  - points occupied by altimeter at first passage  
over  $P_i$

Figure G-1. The Path-Intersection Grid

which refers the second altitude of a pair above  $P_i$  to a common equalaltitude surface thru the point  $S_1$ .

It is easy to show that any circuit ( $P_{i_1} P_{i_2} \dots P_{i_k}$ ) can be expressed as a finite sum of circuits about elementary 4-point circuits, which I will call cells. The set of cells therefore forms a basis for the space consisting of circuits in the reference plane, and the closure condition for the problem is therefore exactly (completely and sufficiently) expressed by the set of closure conditions for the cells. Letting

$$\Delta h_{mi} \equiv h_{m, i_2} - h_{m, i_1} \quad (G-3)$$

be the difference between altitudes at two successive (clockwise) points of a cell, we have

$$0 = \Delta h_{mi} + \Delta h_{mj} + \Delta h_{mk} + \Delta h_{ml} \quad (G-4)$$

Equation G-4 plus a sufficient number of given altitudes, then constitute a description of the experiment. (In a gross sense; there are of course many details to be attended to, but these do not affect the main line of the argument).

This viewpoint is mentioned here because it provides a different and possibly, in some cases, a more useful way of writing the equations for self-consistency tests. The equations are different only in their appearance; mathematically, they are exactly equivalent to those given in the main part of the memorandum. A rapid topological verification is gotten by noting that if we sum over all cells, we are left with a single closed circuit around the boundary of the cell simplex.

This means that if the equation G-4 imposes rigorous conditions on the  $h_{mi}$ , the value of  $h_{mi}$  at any point within the simplex is determined by the

altitudes along the boundary and by equation G-4. But all altitudes are measured independently of all other altitudes; we can change any one  $h_{mi}$  or  $h_{oi}$  without changing the other  $h_{mi}$ 's or  $h_{oi}$ 's either in the interior or on the boundary.

Algebraically, to show the equivalence of this formulation with the self-consistency formulation (SCF), given in the main part of the study, we have to show that either formulation can be derived from the other. The algebra involved is so simple that it will merely be outlined. If there are  $N$  cells in the simplex, there are  $2N + 2$  points. Since there are  $N$  independent equations of the type G-4,  $N + 2$  altitudes are required. Going from SCF to the present formulation merely means taking  $N + 2$  pairs of the  $h_{mi}$  in G-4 as given, and writing the remaining equations in the form

$$\begin{aligned} h_{mi} &= h_{mi} + (h_{m,i+1} - h_{mi}) + (h_{m,i+2} - h_{m,i+1}) \\ &+ (h_{m,i+3} - h_{m,i+2}) \\ &+ (h_{m,i} - h_{m,i+3}) \end{aligned} \quad (G-5)$$

with

$$h_{oi_1} = h_{oi_2}. \quad (G-6)$$

Going from CMF to SCF merely unwinds the development in the other direction and I need not write it down.

Two points should be noted. First, in order to get by with only  $N + 2$  given altitudes, we must have given also the values of the quantities in G-4. If those values are not given, the full  $2N + 2$  altitudes must be known. The equations G-4 in that case cannot function as condition equations. But as pointed out earlier, the  $\Delta h$ 's in our problem are not independently known. If the  $h_{oi}$  are independently known and the  $h_{si}$  by definition are known, we are merely back at the problem of verification by an absolute method.

## APPENDIX H

### NOTE ON RELATIONS BETWEEN STANDARD DEVIATIONS INVOLVED IN THE VERIFICATION EXPERIMENT

We have set up four categories for classifying the types of procedures used in verifying altimeter performance: absolute, relative, self-consistent, and differential. In each of these categories, the measured altitude  $h_{mi}$  is compared with another quantity, given or calculated or measured, to determine the scatter of the measured altitude about a true value (giving an accuracy standard deviation) or about an average value (giving a precision standard deviation). (For convenience, we assume a Gaussian distribution; questions of number of samples, etc., are irrelevant to the present argument.) Unfortunately, while what we want from the Verification Experiment are the standard deviations mentioned, what we will get is something different because in no case do we have "true" values available for comparison. In every case, we must compare the  $h_{mi}$  with values which themselves contain errors, and these errors may or may not be known. This note explains the difficulties that must be removed in order to go from  $\tilde{\sigma}_m$ , the standard deviation of  $h_{mi}$  calculated from available data, to  $\sigma_m$ , the standard deviation of  $h_{mi}$  given the true altitude (see Figure H-1).

First, note that although we have available  $I$  altitude measurements  $h_{mi}$  measured above  $J$  points  $P_j$  on the reference ellipsoid, we have at the most two heights at each  $P_j$ , so that a particular ocean-above-ellipsoid height  $h_{oi}$  is measured only twice and, furthermore, from two different altitudes. Any questions as to the altimeter's precision -- i. e., ability to consistently give the same answer when measuring the same thing -- can be answered only by inference and not by direct computation. At every point,  $P_k$  above which two measurements  $h_{m_1}$  and  $h_{m_2}$  have been made, we have



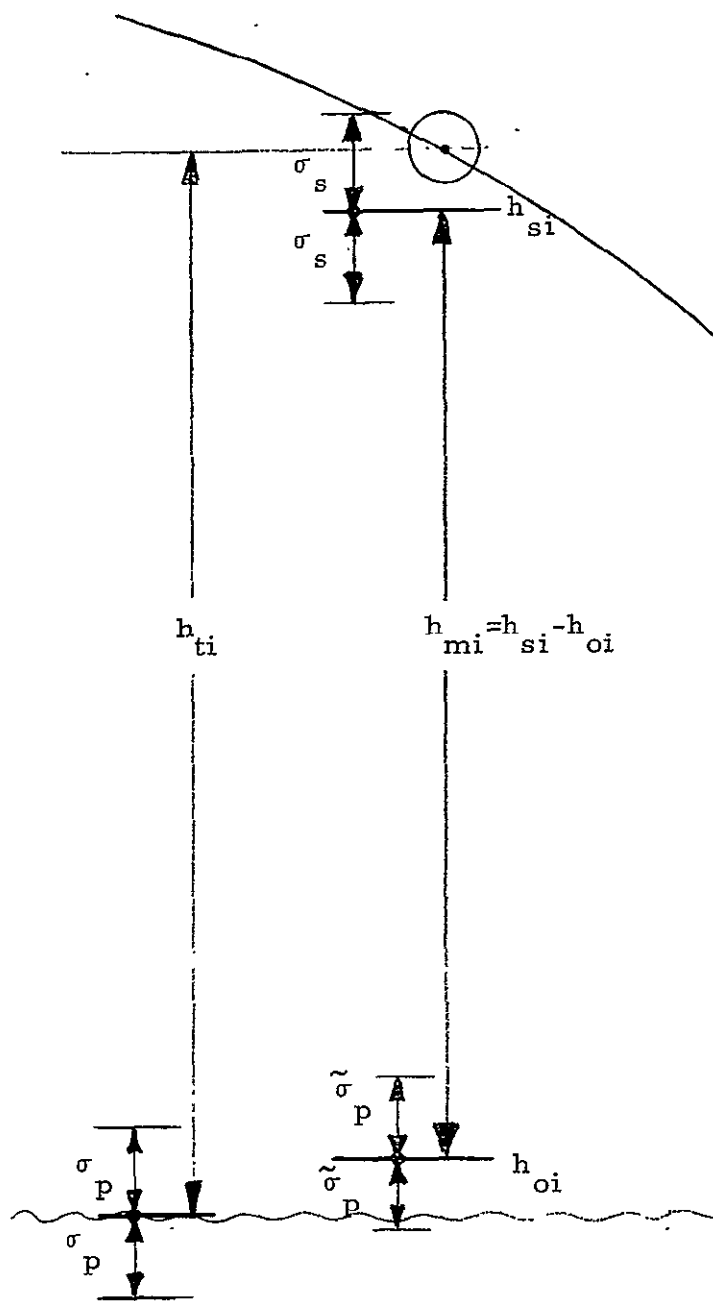


Figure H-1.

$$h_{m_1} = h_{s_1} - h_{o_1} \quad (1)$$

and

$$h_{m_2} = h_{s_2} - h_{o_2} \quad (2)$$

with the condition

$$h_{o_1} = h_{o_2} \quad (3)$$

Here,  $h_o$  and  $h_s$  refer to ocean and satellite heights, respectively, above the ellipsoid reference surface and the subscripts 1 and 2 refer to the order of measurement. Had both measurements been made from a height  $h_{s_1}$ , or if the difference  $\Delta h_{s_k} = h_{s_2} - h_{s_1}$  were known exactly, we could get a precision s.d.  $\sigma_p$  for  $h_{m_i}$  over the grid of points  $P_k$  from

$$\sigma_K^2 = \frac{\sum_k (h_{m_{2k}} - \Delta h_{s_k} - h_{m_{1k}})^2}{2(2K-1)} \quad (4)$$

where  $k = 1$  to  $K$ . Obviously, this  $\sigma_p$  is the same for all the points  $P_k$  if the uncertainty in  $\Delta h_{s_k}$  is the same but not otherwise. Furthermore, it is misleading to the extent that we are uncertain of what  $\Delta h_{s_k}$  may be. A bit of algebra shows that the difference between  $\sigma_P^2$ , the variance about the true value, and  $\tilde{\sigma}_P^2$ , the calculated variance, is given by

$$\sigma_P^2 - \tilde{\sigma}_P^2 = \frac{K}{2K-1} \frac{\sigma_s^2}{2} + \sigma_s \sigma_P \quad (5)$$

where  $\sigma_s$  is the standard deviation of  $h_{s_k}$ . This equation shows that the true precision s.d. of the altimeter can be computed if we know the s.d. of  $h_{s_k}$ . Again, we find an unfortunate obstacle to achieving our objective  $\sigma_P^2$ ; the  $\sigma_s^2$  in (5) is the accuracy variance of satellite height above reference surface; what orbit computations give is closer to a precision variance. What to do about this difference requires more attention than can be devoted here, and we merely note the fact and pass on to the second case where we seek the accuracy s.d. of  $h_{m_i}$ .

Let  $h_{mi}$  be the measured satellite height above the sea surface at point  $P_i$ , and let  $\sigma_m$  be the standard deviation of  $h_{mi}$ . Note first that

$$\sigma_m = \sqrt{\frac{\sum_i (h_{mi} - h_{ti})^2}{I}} \quad (6)$$

where  $h_{ti}$  is the true value, and second that of necessity the sum is taken over  $i$  and therefore applies to observations made at different points. The problem would have been much simpler could we have compared  $h_{mi}$ 's made at a single point, but for a given  $i$ , there is only one  $j \neq i$  for which  $P_j = P_i$ . The number could be increased by generalizing the concept of "point" appropriately, but we will not discuss the results.

Let  $h_{si}$  be the given "height" of satellite above the reference surface at  $P_i$ , and  $\sigma_{si}$  the standard deviation of  $h_{si}$ . Let  $h_{oi}$  be the height of the sea surface above the reference surface at  $P_i$  and let  $\sigma_{oi}$  be the s. d. of  $h_{oi}$ . We write, also

$$\epsilon_{mi}, \epsilon_{si} \text{ and } \epsilon_{oi} \quad (7)$$

for the corrections to  $h_{mi}$ ,  $h_{si}$  and  $h_{oi}$  respectively, and separate each of these corrections into two parts; a constant correction and a random variable correction, denoting the former by the subscript 1 and the latter by the subscript 2.

The two quantities in which we are most interested are the accuracy standard deviation  $\sigma_m$  and the precision standard deviation  $\bar{\sigma}_{ti}$ . Consider first  $\sigma_m$ .

We write

$$\begin{aligned} h_{ti} &= h_{mi} + \epsilon_{1m} + \epsilon_{2mi} \\ s_{ti} &= h_{si} + \epsilon_{1s} + \epsilon_{2si} \\ o_{ti} &= h_{oi} + \epsilon_{1o} + \epsilon_{2oi} \end{aligned} \quad (8)$$

so that

$$h_{mi} - h_{ti} = \epsilon_{1m} + \epsilon_{2mi} . \quad (9)$$

Since

$$h_{ti} = s_{ti} - o_{ti} , \quad (10)$$

we have also

$$\begin{aligned} h_{mi} - h_{ti} &= h_{mi} - s_{ti} - o_{ti} \\ &= h_{mi} - h_{si} + h_{oi} - (\epsilon_{1s} + \epsilon_{2si}) + (\epsilon_{1o} + \epsilon_{2oi}) . \end{aligned} \quad (11)$$

A bit of simple algebra then shows that the difference  $\Delta$  between the variance  $\sigma_m^2$  for which we are looking and the variance  $\tilde{\sigma}_m^2$  that we compute by

$$\tilde{\sigma}_m^2 = \frac{\sum_i [h_{mi} - (h_{si} - h_{oi})]^2}{I} \quad (12)$$

is given by

$$\begin{aligned} \sigma_m^2 - \tilde{\sigma}_m^2 &= \Delta^2 \\ &= (\epsilon_{1o} - \epsilon_{1s})^2 + \sigma_{2o}^2 + \sigma_{2s}^2 \\ &\quad + (\epsilon_{1o} - \epsilon_{1s}) \bar{\epsilon}_d + \frac{2 \sum_i (\epsilon_{2oi} - \epsilon_{2si}) \epsilon_{di}}{I} . \end{aligned} \quad (13)$$

Here  $\sigma_{2o}^2$  and  $\sigma_{2s}^2$  are the variances of the  $\epsilon_{2oi}$  and  $\epsilon_{2si}$  respectively, and

$$\begin{aligned} \bar{\epsilon}_d &= \sum_i \epsilon_{di} / I \\ \epsilon_{di} &= (h_{mi} - h_{si} + h_{oi}) . \end{aligned} \quad (14)$$

In this equation, only  $\tilde{\sigma}_m^2$ ,  $\epsilon_{di}$  and  $\bar{\epsilon}_d$  can be considered known.  $\sigma_m^2$  is what we are looking for; the quantities  $(\epsilon_{1o} - \epsilon_{1s})$ ,  $\sigma_{2o}^2$  and  $\sigma_{2s}^2$  may be found from given information about the standard deviations of the satellite location, sea surface, geoid, etc., or they may not. The question can be devised only by

finding out how the given s. d. 's are related to those in the equation. Consider first the relation of  $\epsilon_{1s}$  and  $\sigma_{2s}$  to the standard deviation  $\bar{\sigma}_{si}$  of a satellite height above ellipsoid that is given as input.  $\bar{\sigma}_{si}$  does not correspond to  $\sigma_{si}$ ,  $\sigma_{2s}$  or  $\epsilon_{1s}$ . It is computed from the covariance matrix for the orbital elements, and gravity field constants. These in turn are computed from the covariance matrix of the observations and tracking coordinates. Complete analysis of the relation is outside the bounds of this study; it is enough here to note that for I (the number of observations) large, and for a well-derived orbit (and I do not go into the definition of "well-derived"),  $\bar{\sigma}_{si}$  should be close to  $\sigma_{2s}$ . If the equations for  $h_{si}$  and  $\bar{\sigma}_{si}$  will be a function more of the amount of unresolved "constant" error in the tracking data than of the deficiencies in the orbit itself.

The relation of  $h_{1o}$  and  $\sigma_{2o}$  to the standard deviation  $\bar{\sigma}_{oi}$  given as input is much more complicated even than the relations of satellite height just discussed.  $h_{oi}$  is the sum of several parts; height of geoid above spheroid, height of mean sea level above geoid, and height of IMSL above MSL. The last two of these have small variances compared to the variance of the geoid-spheroid separation and will be ignored in this appendix. The variance of the geoid-spheroid separation will then be considered to make up the whole of  $\sigma_{oi}^2$ .

There are three basic ways of finding  $h_{oi}$  at present:

1. from astrogeodetic measurements;
2. from gravimetric measurements; and
3. from satellite motion measurement.

Other methods are for the most part combinations of these. Taking these in order, we find that the standard deviations they give for  $h_{oi}$  are related as follows to the quantities in equation (13) above.

The s.d. of  $h_{oi}$  derived by astrogeodetic techniques depends on the s.d.'s of the geodetic coordinates of the intermediate points  $P_j$  ( $j < i$ ), the s.d.'s of the measured deflections  $\xi_j$  and  $\eta_j$ , and on the (unknown) values of  $\xi$  and  $\eta$  between  $P_j$  and  $P_{j+1}$ . In regions where deflections do not vary rapidly, as, e.g., in geologically uniform plains areas, the s.d.'s build up slowly with distance, a value of  $\pm 1.5$  m over 2000 km being not unreasonable. In regions where deflections vary rapidly, the build-up will be much greater, and a s.d. of  $\pm 15$ -20 m, in the same distance could be expected. This number can be reduced by gravimetric interpolation, by identification of astro-geodetic points with points whose geoid-spheroid separation were determined geometrically, etc.

2. The s.d. of  $h_{oi}$  derived by gravimetric techniques depends on the s.d. of the gravity measurements, the density and number of measurements, the equations used, and the location of the point at which  $h_{oi}$  is being computed. If we use a global concept, finding  $h_{oi}$  from gravity values over the entire world, evaluation of the s.d. of  $h_{oi}$  would involve the equation

$$\sigma_{h_{oi}}^2 = K^2 [F] [\Sigma_{\Delta g}^2] [F]^T \quad (15)$$

where  $K^2$  is a constant,  $[\Sigma_{\Delta g}^2]$  is the covariance matrix of the gravity anomalies, and  $[F]$  is the area weighting function appropriate to finding  $h_{oi}$ . In the VED, however, we limit our attention to a small area and are concerned not with  $h_{oi}$  referred to a best globally-fitted sphere but with  $h_{oi}$  referred to a sphere best-fitted to the Caribbean region. This means that we need

$$\sigma_{\Delta h_o}^2 = \langle (h_{oi} - h_{oo})^2 \rangle, \quad (16)$$

which means a reduction of  $\epsilon_{10}$ , since we eliminate a large block of dubious material from the computation.

3. The s. d. of  $h_{oi}$  derived from tracking data by way of orbit theory depends for the most part of the s. d. 's of the tracking data used as input. If we look at the basic equation

$$V_o = V(\lambda_i, \phi_i, h_{oi}, C_n^m, S_n^m). \quad (17)$$

We see that the variance of  $h_{oi}$  is determined by the variances of the coefficients  $C_n^m, S_n^m$  of the harmonic expansion of the potential  $V$  ( $V_o$  is suitably selected value). There are only a few coefficients available -- perhaps 200 if we strain the credibility gap. Hence, the variance of  $h_{oi}$  will be slowly changing function of  $\lambda$  and  $\phi$  and furthermore, the error it measures will be reasonably constant over great distances, or in the jargon, will be highly correlated.

In summary, the accuracy s. d. of the altimeter measurements can be derived from the s. d. relative to geoid and/or satellite heights above the spheroid if the systematic and random errors of these heights are known (or can be reduced to negligible quantities). The magnitudes of these errors in relation to the required altitude s. d. are then irrelevant. In the VE, the required knowledge of the errors is not available to begin with, and it is part of the design task to set up the experiment so that those errors which are present are either made innocuous or are determined as part of the experiment. Discussion of this aspect of the VED does not belong in this appendix.

## APPENDIX I

### NOTES ON BIASES, SHORT-PERIOD VARIATIONS, AND OTHER COMMON CONCEPTS

Nothing is really constant except by definition. Hence when, in comparing an observable with its theoretical value, we distinguish between a constant part of the difference and a varying part, we do so with the knowledge that the division is artificial. A more realistic nomenclature might be to call the variations long-period and short-period, with long-period variations being those that we cannot get rid of by averaging over the time interval for which we have data. Short-period variations, if they are random, can be given meaningful scatter-measures such as r. m. s. error, standard deviation, etc. Long-period variations can be, and frequently are, given scatter measures, but the meaning is then quite different from what it is for the scatter measures of short-period variables. At present, custom does not provide different symbols for the scatter measures of long-period versus short-period variables. The user of s. d.'s etc., must therefore be very careful in distinguishing between them, especially if they are provided by someone else, and the only sure way of distinguishing is to study the nature of the parent variables.

Another division of errors is into systematic and non-systematic (random) errors. While these terms are sometimes used as synonyms for constant and short-period errors, respectively, such use is erroneous. Systematic errors are those which can be expressed as functions of the independent variables of the problem, non-systematic errors are, of course, those which, because they occur randomly, cannot be expressed as functions of the independent variables. In one sense there are no non-systematic errors on the microscopic scale; events are considered random when our theory is inadequate to deal with them. One can usually remove systematic errors by



introducing enough empirical terms into the theory to account for them. This is quite permissible for applications of theory but gives no insight into the causes of the errors. Ad Hoc approaches are good for the short run, not for the long haul.

The term "bias" has no widely-accepted meaning. It is used impartially for constant error, long-period error, long period systematic error, and for systematic error. It is also used by some workers as a synonym for, or measure of skewness. Perhaps its most widespread use is as a vague descriptor of any error that cannot be clearly identified as random.

Note carefully that the binary divisions discussed above are not clear-cut dichotomies but merely convenient separations. A given error "variable" may fall into one, both, or neither of the two binary divisions. The important thing in error theory is not how we classify the errors but how we handle them.

## APPENDIX J

### REMOVAL OF EFFECTS OF CERTAIN TYPES OF SYSTEMATIC ERRORS FROM OBSERVATIONS

Let  $\{Q_i\}$  be a set of I observations on a set of corresponding quantities  $\{q_i\}$ . The  $q_i$  are assumed unknown and unknowable. The differences  $\{\delta q_i\} \equiv \{Q_i - q_i\}$  are called residuals; they are the errors in the observations. We assume that the  $\delta q_i$  can be separated into two parts,  $\delta q_{1i}$  and  $\delta q_{2i}$ , such that

$$\delta q_i = \delta q_{1i} + \delta q_{2i} \quad (1)$$

and

$$\lim_{I \rightarrow \infty} \sum_{i=1}^I \delta q_{2i} = 0 \quad (2)$$

The  $\delta q_{1i}$  are systematic errors; we assume that they are slowly\_varying with respect to the  $\delta q_{2i}$ .

Suppose that the  $q_i$  are not independent but are related by J condition equations

$$0 = f_k(q_1, \dots, q_I), \quad j = 1 \text{ to } J \quad (3)$$

so that

$$-\Delta j = f_j(Q_1, \dots, Q_I) \quad (4)$$

where  $\Delta j$  is the discrepancy resulting from substituing  $Q_i$  for  $q_i$ .

Then

$$\begin{aligned}
 0 &= f_j(\{Q_j\}) \\
 &+ \sum_i \frac{\partial f_j}{\partial q_{1i}} \delta q_{1i} + \sum_i \frac{\partial f_j}{\partial q_{2i}} \delta q_{2i} \\
 &+ \text{higher order terms}
 \end{aligned} \tag{5}$$

or

$$\Delta j = \sum_i \frac{\partial f_j}{\partial q_{1i}} \delta q_{1i} + \sum_i \frac{\partial f_j}{\partial q_{2i}} \delta q_{2i} \tag{6}$$

If the  $\delta q_{1i}$  are systematic errors, they can be considered constant over suitable chosen sub-sets of  $i$ . Using the usual least-squares procedures, we can determine the  $\delta q_{1i}$  along with the satellite coordinates, but not the  $\delta q_{2i}$ . The condition equations then become

$$\Delta j = \sum_i \frac{\partial f_j}{\partial q_{1i}} \delta q_{1i} \tag{7}$$

and the systematic errors  $\delta q_{1i}$  that are found will have variances determined by the way the random perturbations

$$\frac{\partial f_j}{\partial q_{2i}} \delta q_{2i} \tag{8}$$

enter the problem.

If, as seems to be the case with the electronic tracking instruments, the systematic errors  $\delta q_{1i}$  are large compared to the random errors  $\delta q_{2i}$ , the equations (7) can be solved directly for the  $\delta q_{1i}$ . In the tracking problem, these equations will involve the observations from only 4 or 5 stations at a time, but the standard deviations in the station locations must be accounted for in the solution.

## APPENDIX K

### PURPOSE AND ORGANIZATION OF ERROR ANALYSIS

#### Error Analysis

The error analysis serve two purposes. First, it shows the way in which station coordinate errors, tracking errors, altimeter orbit errors, etc., combine to give a final altitude error; hence, they can be used to guide changes in the experiment set up, the tracking station arrangements, etc., being adjusted to minimize the altitude error. Secondly, it serves to demonstrate that the set up finally arrived at does indeed allow the altitude to be found (independently of the altimeter measurements) to the accuracy required for verification. Since design of the experiment set up is partly an art involving many trials and almost as many errors, the design procedure is best served by error analysis consisting of separate and individually applicable portions, each of which describes the effect of a different part of the set up. Three types of error analyses are distinguished for convenience. Type I, which is concerned with the effect of the geometry on the Height error; Type II, which is concerned with the effect of theory deficiencies on the Height error; and Type III, which is concerned with the effect of imposing constraints on the altimeter location.

#### Error Analysis - Type I

This analysis studies the effect of station arrangement, station location error, tracking measurement, and tracking measurement error on satellite coordinate error. It is completely geometric in nature and does not involve the satellite orbit. The orbit enters only as a convenience in preparing input data.

From given orbit elements and a set of times, and from a given set of station coordinates, sets of satellite coordinates are computed. These coordinates, together with tracking station coordinates, are used to compute the elements of the observation coefficient matrix  $[a_{ij}]$  or  $[A]$ . The equations are given in Appendix B.

### Error Analysis - Type II

The most important deficiency in theory is the inadequacy of the theory to describe the orbit of the altimeter. There is no way of removing this deficiency in the reduction; in practice, the multiplication of observations reduces the effect of theoretical insufficiencies. Although the deficiency cannot be removed, its effect can be estimated, and the mathematics is given in Appendix D.

### Error Analysis - Type III

Two kinds of constraints appear in the theory. One is the type applied to the solution for the ocean surface heights  $h_{oj}$ . Knowledge of the surface and of the geoid in particular itself is unsatisfactory, but knowledge of limits on allowable slopes is quite good. The good condition inequalities, therefore, are in their original form,

$$S_1 < \partial h_o / \partial x < S_2$$

$$S_3 < \partial h_o / \partial x < S_4$$

where the  $S_i$  are constants and, for practical work,  $S_1 = S_3$  and  $S_2 = S_4$ . For computation, the inequalities are turned into equations by adding nuisance variables.

The second type of constraints is that placed on the heights  $h_{sj}$  of the satellite above the reference surface by requiring that the satellite coordinates  $X_{si}$  satisfy the equations of the orbit. The mathematics for imposing this condition are given in Appendix E.

APPENDIX L  
CONFIDENCE LIMITS FOR THE STANDARD DEVIATION OF  
THE ALTIMETER HEIGHT

$$\Delta h_i = h_{li} - h_{ci} \quad i = 1 \text{ to } N$$

$$\sigma^2_{\Delta h} = \sigma^2_{h_l} + \sigma^2_{h_c} \quad \sigma_{h_l h_c} = \sigma_{h_{li} h_{ij}} = \sigma_{h_{ci} h_{cj}} = 0 \quad i \neq j$$

Errors in  $h_{ci}$  are  $N(0, \sigma^2_{h_c})$  where  $\sigma^2_{h_c}$  is known.

Errors in  $h_{ij}$  are  $N(0, \sigma^2_{h_l})$  where  $\sigma^2_{h_l} \leq \sigma^2_{oo}$  is a specification

$$s^2_{\Delta h} = \frac{1}{N-1} \sum_{i=1}^N (\Delta h_i - \bar{\Delta h})^2$$

$$\bar{\Delta h} = \frac{1}{N} \sum_{i=1}^N \Delta h_i$$

How large must N be so that probability requirements for the following statements are met:

$$E(\Delta h) = 0$$

$$\sigma^2_{h_l} \leq \sigma^2_{oo}$$

The quantity  $t = \bar{\Delta h} / s_{\Delta h} \sqrt{N}$  is distributed as Student's  $t$  with  $(N-1)$  degrees of freedom, the hypothesis being  $E(\Delta h) = 0$ . The  $(1-\alpha) = \gamma$  confidence interval is

$$(\bar{\Delta h} - t_{N-1; 1-\alpha/2} \frac{s_{\Delta h}}{\sqrt{N}}) \leq \delta h \leq (\bar{\Delta h} + t_{N-1; 1-\alpha/2} \frac{s_{\Delta h}}{\sqrt{N}})$$

Figure L-1<sup>55</sup> can be used to determine sample sizes so that the  $(1-\alpha) = \gamma$  confidence interval will be shorter than  $L$  where  $L$  is a multiple of the unknown  $\sigma\Delta h$ . The length of the interval is  $2t_{N-1;1-\alpha/2} (s\Delta h/\sqrt{N})$ .

- b. Assume that if  $\sigma^2\Delta h \leq \sigma^2_{oo} + \sigma^2_{hc}$  then  $\sigma^2_{h_1} \leq \sigma^2_{oo}$ . The quantity  $(s^2\Delta h/\sqrt{N-1})/(\sigma^2\Delta h)$  is distributed as chi-square with  $(N-1)$  degrees of freedom. The  $(1-\alpha)$  confidence interval is

$$\frac{(N-1) s^2\Delta h}{\chi^2_{N-\chi; \chi-\alpha/2}} \leq \sigma^2\Delta h \leq \frac{(N-\chi) s^2\Delta h}{\chi^2_{N-\chi; \alpha/2}}$$

Figure L-2<sup>55</sup> can be used to determine sample size so that the hypothesis  $H_0$  can be tested against the alternate hypothesis  $H_1$ .

$$H_0 : \sigma^2\Delta h = \sigma^2_{oo} + \sigma^2_{hc}$$

$$H_1 : \sigma^2\Delta h > \sigma^2_{oo} + \sigma^2_{hc}$$

### Example

1. Let  $\gamma = 0.99$  or  $\alpha = 0.01$ .

Determine  $N$  so that we can be 90% sure that the  $\gamma$  confidence interval is less than  $0.75 \sigma\Delta h$ . From Figure L-1  $N \sim 60$ .

2. Let  $\alpha = 0.005$

Determine  $N$  so that the test is performed with a power 0.95 and so that the ratio

$$R = \frac{\sigma\Delta h}{\sqrt{\sigma^2_{oo} + \sigma^2_{hc}}} \leq 1.4. \text{ From Figure L-4 } N \sim 75.$$

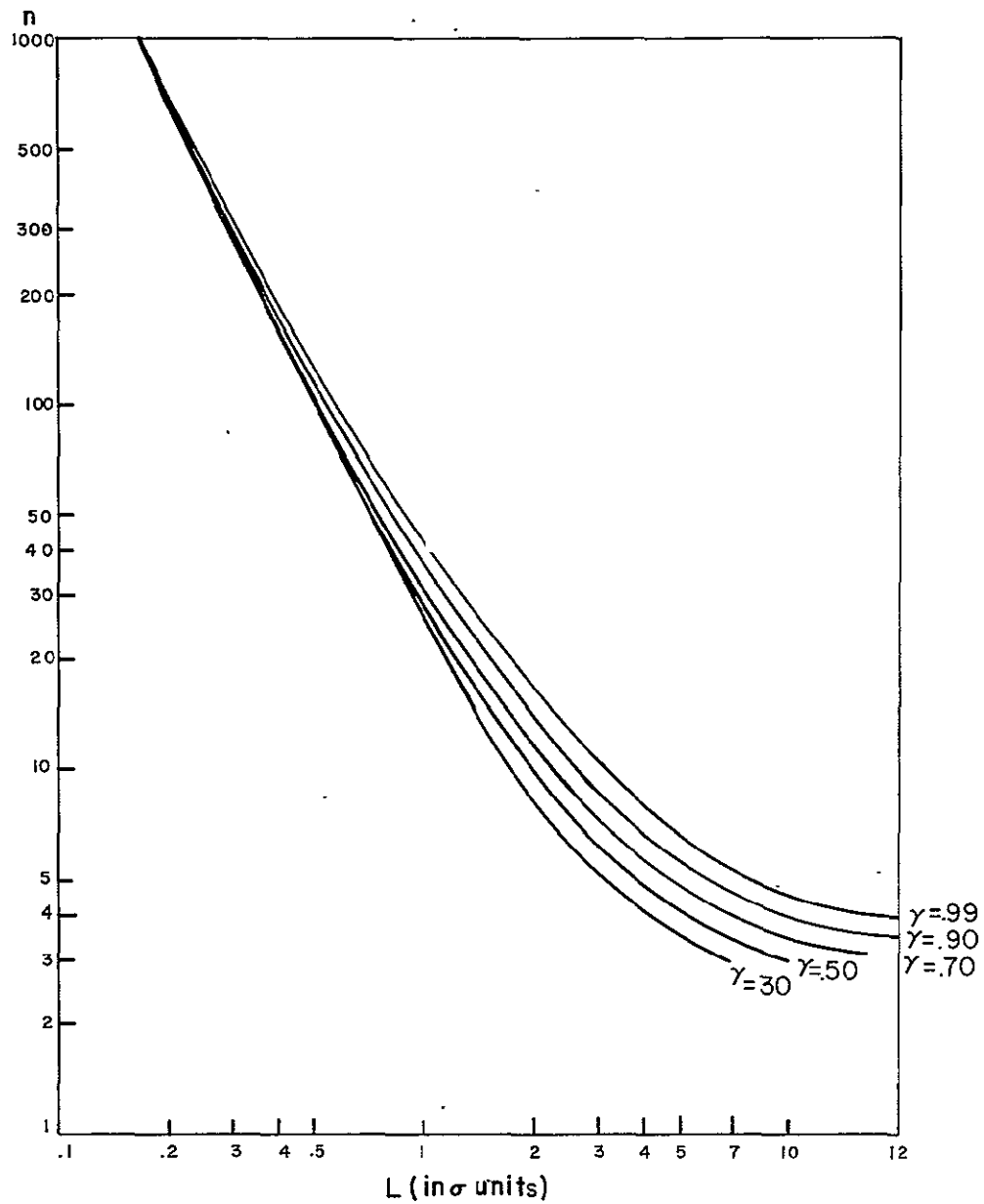


Figure L-1. Graphs of sample size required to insure with a given probability  $\gamma$  that a confidence interval for the mean with confidence coefficient .99 will be shorter than  $L$ .



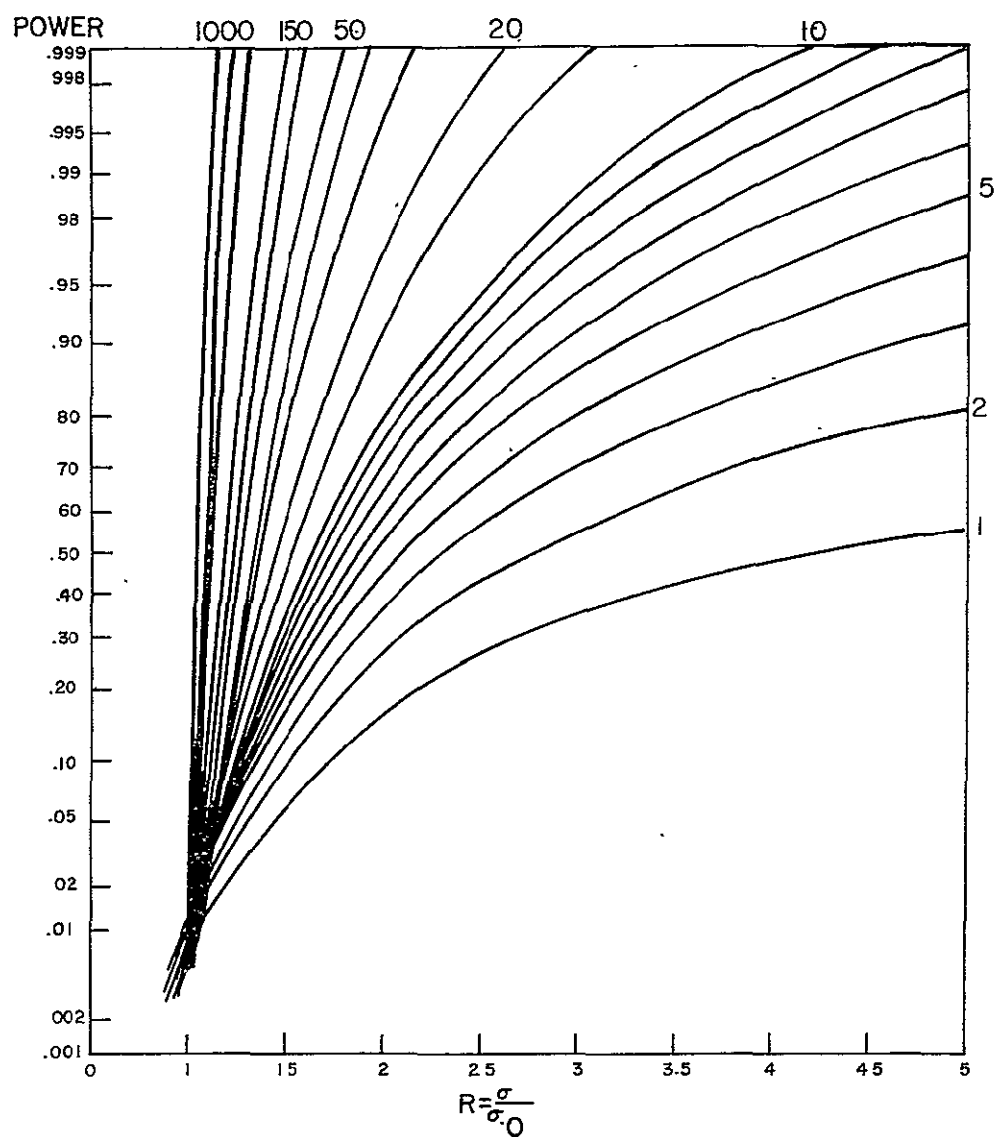


Figure L-2. Power curves for testing  $H_0: \sigma^2 = \sigma_0^2$  against  $\sigma^2 > \sigma_0^2$  at 0.005 significance level.  $H_1:$

$\alpha$  is the Type I error, i. e., the probability of rejecting a perfectly good hypothesis.  $\beta$  is the Type II error, i. e., the probability of failing to reject a false hypothesis. Power =  $1-\beta$ .

## APPENDIX M

### CONSTRAINTS ON VEDS

This section enumerates the explicit constraints on VEDS, as well as many of the implicit constraints embodied in the scope of this document.

#### M-1 Explicit Constraints on VEDS

The constraints enumerated below were reviewed with and approved by Mr. J. D. Rosenberg of NASA as a basis for this study.

##### M-1.1 Satellite Orbital Parameters

Apogee	850 nautical miles	(1575 km)
Perigee	600 nautical miles	(1100 km)
Inclination	20 degrees	

##### M-1.2 Satellite Attitude

Maintained within 2° of the normal (to the Reference Ellipsoid) at least 90% of the time.

Attitude angles known in retrospect for all times to within 1°.

Attitude angle rate "small"; less than 1/3 degree per minute (of time) at least 95% of the time.

##### M-1.3 Satellite Lifetime

Useful satellite lifetime during which the Verification Experiment may be performed is two (2) years.

##### M-1.4 Satellite Power Availability for Radar Altimeter

Average prime power available to radar altimeter: 25 watts;

Maximum peak power into antenna by radar altimeter: 5 kilowatts;

Assume no schedule problem in power availability to radar altimeter\*.

---

\* The power schedule may preclude use of the radar altimeter concurrently with the flashing beacon. This will restrict camera tracking to portions of the track during which the satellite altimeter is not ranging, and will require closer examination of the power schedule.

#### M-1.5 Satellite Data Storage Available to Radar Altimeter

Assume short-term processing storage is always available. Consider no available long-term storage.

Consider some long-term storage, such as tape recorder, as an alternative.

#### M-1.6 Communications and Tracking

Assume availability of the existing tracking nets.

Assume access to primary on-board instrumentation as necessary.

Assume availability of Apollo Tracking ships, with possibility of strategically placing one ship for limited time.

Assume limited equipment in addition to existing equipment at stations.

#### M-1.7 Primary On-Board Instrumentation

Doppler Beacon

Laser Reflectors

Flashing Lights

C-Band Transponder

Goddard Range and Range Rate

Unified S-Band

RADAR ALTIMETER

#### M-1.8 Clock

Assume availability of best classical clock flyable; of the order of  $10^{11}$  stability.

#### M-1.9 Space and Weight

Assume no problem for the present.

This item may be re-opened, if necessary.

#### M-1.10 Satellite Housekeeping

Assume none will interfere with radar altimeter during its operation, and during verification.

#### M-1.11 Other On-Board Experiments

Assume none will interfere with radar altimeter during its operation, and during verification.

#### M-1.12 Radar Altimeter Specs Assumed for GEOS-C, for VERIFICATION EXPERIMENT DESIGN STUDY

ACCURACY	$\pm 5$ meters;
PRECISION	$\pm 5$ meters;
RESOLUTION	1 meter;
USEFUL LIFETIME	200 to 500 hours;
FREQUENCY	X Band; 8 to 10 GHz

#### M-2 Experiment Scope and Implicit Constraints on VEDS

The experiment is to find out whether or not the given satellite altimeter can, from heights of 1100 km to 1575 km above the surface, measure these height to  $\pm 5$  meters rms error. It is explicitly assumed that the altimeter manufacturer claims that the heights are measured from the altimeter to a surface called instantaneous mean sea level. It is implied that the  $\pm 5$  meters (or better) should be obtained regardless of the state of agitation of the ocean surface and that the 1100 km lower height limit is not a limit on the altimeter, which should retain the  $\pm 5$  meter error down to 200 km or lower, but is a limit on the experiment's capabilities. The scope of the experiment is actually much narrower than the above description allows, due to constraints imposed upon the experiment, as summarized in the previous section.

While most of the obvious constraints on VEDS have been enumerated earlier, several constraints which have substantial impact are explored individually and in greater detail, as of the initiation of this study.

#### M-2.1 Time

Time is the one variable that controls the scope of all projects. The verification project is limited by the

- (1) useful life of the altimeter, and the
- (2) useful life of the verification experiment results.

The first of these facts is dependent upon among other things, the lifetime of the altimeter power supply and of the power supplies of associated equipment in the satellite. This lifetime has been set at 2 years, so that the field measurement phase of verification experiment must be completed within two years after the date of launch.

The second factor has not yet been given a numerical value. We can assume, of course, that results must be available before design and construction of a successor altimeter such as SEA SAT-A is unchangeably under way. Also since VEDS also has the responsibility for getting data useful in designing a successor altimeter, these data should be coming out well before design is fixed. The following are judged to be reasonably expensive of the time requirement:

- (1) the experiment shall have at least tentative values for the altimeter rms error within 4 months of the launch date;

(2) it shall have reasonably good values for rms error under different conditions within 2 years of the date of launch and shall have accumulated all needed or possible satellite dependent data by that time; and

(3) it shall have final values on altimeter performance within 2.5 years of the launch date.

#### M-2.2 Equipment

The equipment to be used will be dictated not only by what is available and allowed, but by the time within which the experiment must be carried out, the volume of data we can usefully handle, the areas in which we can work, etc. This section will be concerned with the availability and allowed aspects.

The amount of equipment required will include, in addition to the satellite and its launching equipment, a certain amount of tracking equipment to tell where the satellite was known to be; computing equipment to tell, from the tracking data, where the satellite was between observations, telemetry (communications) equipment to get altimetry data from the satellite to the ground, more computing equipment to reduce the altimetry data, and more communications equipment for use in coordinating tracking, altimetry, and computing effort.

In addition, it will be necessary to put into the field non-satellite associated equipment to independently establish the IMSL. This may involve use of at least one hydrographic survey ship equipped for measuring gravity, ocean depths, and salinity, temperature and pressure variables. Location of the survey ship with respect to established tracking stations will require certain equipment. This will be of standard types and will include a set of HYDRODIST or AUTOTAPE. At least one high-altitude (10 km to 20 km) flying airplane

equipped with a precision wide angle mapping camera and radar altimeter may be required, to check sea state in the altimeter spot. Finally, a certain amount of miscellaneous equipment such as measuring engines, automatic plotters, clocks, etc., will be needed. Such items will not be detailed here.

Primary concern is with the tracking equipment. All NASA and NASA-supported tracking stations will be assumed available for tracking, and all will be assumed to be allowed for contributing data to the orbit determination. Figure M-1 shows the stations involved, their types and their locations. Appendix A gives the station coordinates to 0.0, which is adequate for planning. Not all these stations will be used for precise, orbit-independent, fixing of altimeter position, however. Some will be unable to track the satellite because it will be invisible (or near enough as makes no difference) to them; others will be located where no geodetically significant altitudes are to be measured, and some will not be used because they cannot fix the satellite location accurately enough. In particular, we can eliminate from consideration because of area requirements, all tracking stations above  $+25^\circ$  (N) or below  $-25^\circ$  (S). Because they are not in geodetically useful areas, we can probably ignore some stations such as A10, 9006, A5, and M9. Because of their large instantaneous measurement r.m.s. errors, we will eliminate the MINITRACK stations and TRANET stations.

In addition to the stations shown in Figure M-1 and M-2, we assume that those USAF PC-1000 camera stations in geodetically useful areas may be asked to cooperate at specific times. Status of the U.S.C. & G.S. net at time of verification is not known, but we will assume that at least three stations will be available for tracking in North or Central America at some time.

### M-2.3 Geographical Regions

The orbit of the altimeter is scheduled at present to have an inclination of about  $20^\circ$ . Only regions within latitudes  $+20^\circ$  and  $-20^\circ$  on the Earth are therefore open to the verification experiment. Furthermore, only water areas



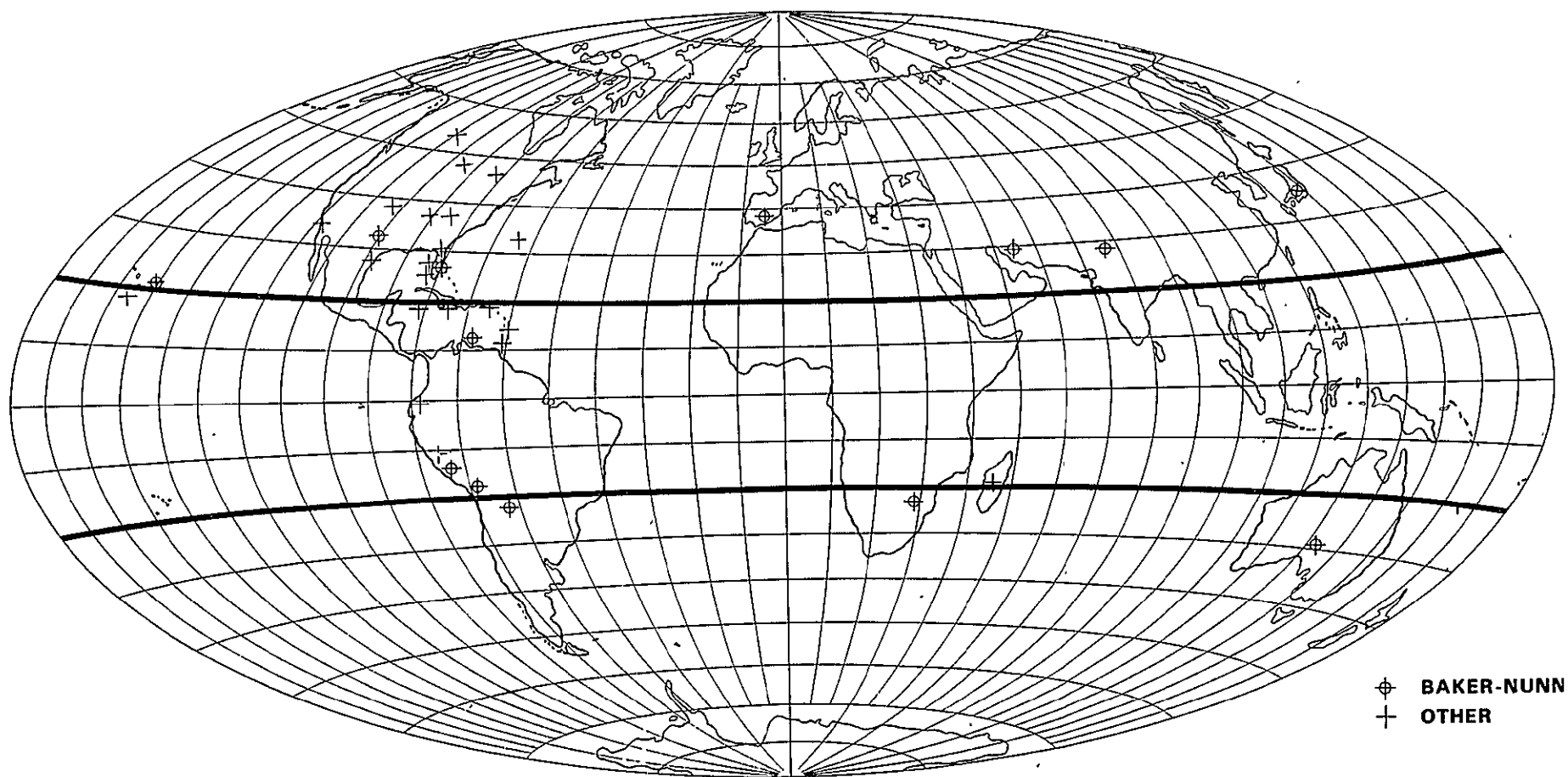


Figure M1. Optical Tracking Stations

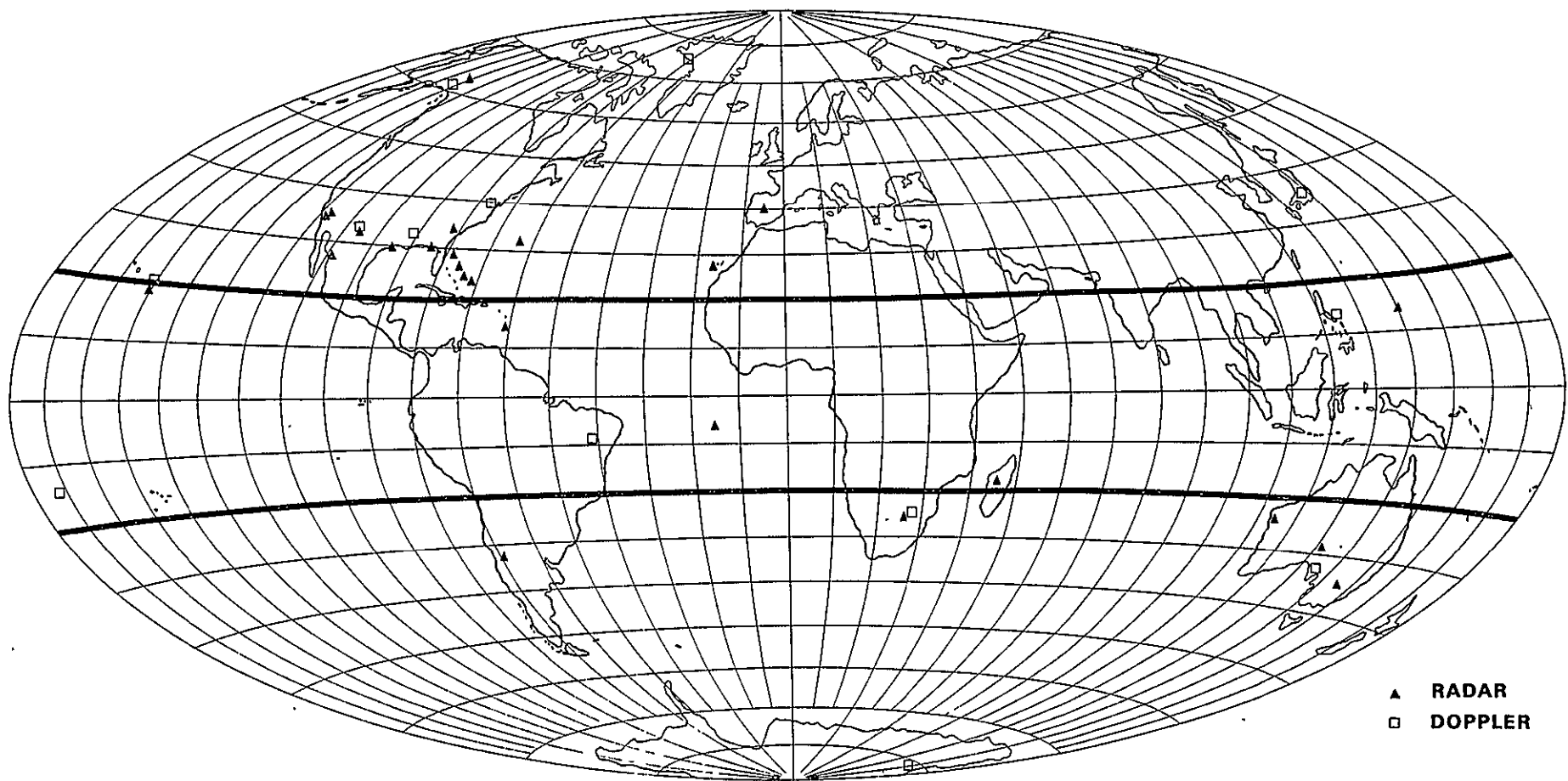


Figure M2. Electronic Tracking Stations

need be considered; political and engineering considerations eliminate experiments over land areas. This effectively limits the areas to Lake Nicaragua and Lake Victoria, to large bays like Lake Maricaibo, and to open oceans.

A further restriction on the regions open to the experiment is set by the requirement that only those regions be used where there is sufficient geodetic information to allow verification. This restriction is not as severe as it seems because very little geodetic information is needed to verify some aspects of altimeter performance. In fact, we can identify at least four categories of verification, only one of which induces a strong regional limitation. Here, however, the monetary efficiency restriction must be noted. Having selected an area of well known geodetic characteristics, we should carry out in that same area all other verification experiments that require appreciably more money to be spent unless there are essential aspects of the altimeter's performance that cannot be verified by experiment in that area. Since experiments in the absolute and relative categories are the ones needing most money to be carried out, we can conclude that these should be co-located, and that the experiments in the last two categories may be carried out anywhere circumstances allow except for those parts of the two experiments that will require special equipment (such as new tidal stations, aircraft flights, and so on).

An additional consideration in the selection of experimental regions is the availability of sufficient oceanographic and geographic information to determine instantaneous sea level where necessary, either from available data or by use of additional measurements.

#### M-2.4 Additional Equipment

Not shown in Figures M-1 and M-2 are the ships used by NASA as mobile tracking stations. At least one of these ships can be expected to be available to the experiment where the experiment is carried out in accessible waters. Exact time and numbers of ships must be left indefinite at present.

In addition to the tracking equipment discussed above, there is considerable optical tracking equipment in operation as part of the European Satellite Triangulation Network. The instruments in this network have varying accuracies, but with careful use should be able to get directions to  $\pm 0.5''$  to  $\pm 1.0''$ . Where appropriate (i. e., in the few cases that the camera stations can see the satellite), cooperation from the countries using these cameras might be obtained.

#### M-2.5 Orbit

The orbital elements  $a$ ,  $e$ ,  $i$ ,  $\Omega$ ,  $\omega$ ,  $\tau$  suffice to determine the location of the altimeter at a given time  $t$ .  $a$  is the semi-major axis of an ellipse,  $e$  the eccentricity of that ellipse, and  $i$  the inclination of the plane of that ellipse to the equatorial plane.  $\Omega$  is the right ascension of the intersection of the ellipse plane with the equatorial plane,  $\omega$  the angle from the line of nodes to the line of apsides (at perigee), and  $\tau$  is the time at which the true anomaly of the satellite is zero.

The most important restriction is imposed by the inclination  $i$ , since it limits the altimeter to making measurements over the zone between latitudes  $+i$  and  $-i$ ; here,  $i = 20^\circ$ .

The next most important restriction is that placed by  $a$  and  $e$  conjointly. The semi-major axis is approximately 7,780 km and  $e$ , the eccentricity, is about 0.025. This will cause the altimeter to bob up and down between altitudes of about 1150 km to 1600 km (neglecting the flattening of the earth). At a  $60^\circ$  zenith distance limit for useful observations, the satellite carrying the altimeter can be tracked out to distances (projected on the earth) of less than 1200 km at minimum altitude and of less than 1700 km at maximum altitude--say about 1500 km average.

The line of nodes at  $20^\circ$  inclination will regress at the rate of about  $5^\circ$  per day. As far as the altimeter is concerned this merely increases the spacing between successive tracks by about  $0.4^\circ$ , an amount that can be

ignored in preliminary planning. More important is the motion of the line of apsides.. at  $20^\circ$  inclination of the orbital plate, the line of apsides (connecting extremes of altitude) progresses at the rate of about  $0.1^\circ$  per revolution or  $2.4^\circ$  per day. The altimeter will therefore maintain minimum altitude over the Caribbean, for example, for only 4-5 days at a time, or for 16-20 days in 2 years. Approximately these same values apply to times during which the altimeter will have minimum height over the Hawaiian Islands-Johnston Islands area and over the Marshall Island. Unless the orbital elements are selected with great care, the altimeter will pass over Lakes Chad, Maracaibo, and Nicaragua less than 30 times (each) during a two year period, for example, for a total of less than 400 individual measurements.

The element  $\tau$  is of importance only in its relation to the weather to be expected at the tracking stations. The altimeter and electronic tracking devices will work satisfactorily in most kinds of weather except electrical storms; optical equipment such as cameras and lasers will work satisfactorily only in clear weather. The time of launch should therefore be selected to put the altimeter in its most favorable position with respect to optical tracking stations during seasons that are usually clear. If the launch time, and hence  $\tau$ , cannot be controlled, the observing schedules must be drawn up with the given  $\tau$  and  $\Omega$  in mind.

## APPENDIX N

### TERMINOLOGY & DEFINITIONS

Many terms used in this report have not before been used with precisely the denotations given them in this report or have not before been given precise denotations. The most frequently used terms are therefore defined below; other terms with special meanings are defined at the place of their first use.

#### 1. Distance and Related Terms

Distance is the length of a geodesic between two points. For the purposes of this report, the satellite altimeter is assumed to be a geometric point and all tracking stations are assumed to be points. The distance from the altimeter to a tracking station will occasionally be referred to as a range; the distance from the altimeter to the altimeter footpoint on a given surface will be called the height. (A footpoint is that point at which a perpendicular from the altimeter intersects the given surface. We assume one and only one footpoint for each location of the altimeter and each given surface). Unless otherwise stated, distances between ground points will be distance calculated on the International Spheroid between the footpoints of the ground points. Also unless otherwise stated, the distances are distances in vacuum; i. e. refraction effects have been taken into account where necessary.

#### 2. Measurement

An altimeter distance measurement (or measurement) is a number given to the experimenter and purporting to be the altimeter height. It must be accompanied by a specification of a time corresponding to the measurement. The construction of the altimeter system to be used in the experiment is such that the measurement will not be the same as any actual height of the altimeter above a real surface. In determining height, the altimeter system produces a number which is the result of averaging and manipulating in a complex fashion

a large number of observations. Neither the averaging process nor the measurement technique had been fully specified at the time of this study. It was assumed that the measured height would be the measured height of the altimeter above a surface called instantaneous mean sea level, defined below. (Measured height is not the number sent from the satellite as "height" but is the result of applying a number of calibration corrections to the telemetered "height" number. The nature and validity of the calibration corrections are not the concern of the experimenter in his role as verifier of the altimeter performance; they are of concern to him only insofar as he is expected not only to verify performance but also to show performance may be improved.)

### 3. Sea Level

Sea level is the height of the sea at a given longitude and latitude at a given instant. It is synonymous with "sea height" and a host of other terms. Sea level is measured with respect to a reference surface associated with North American Datum 1927. (NAD 1927 specifies the Clarke 1866 spheroid. In following sections of the report locations and computations are assumed to be made on the International Spheroid or Reference Ellipsoid rather than the Clarke; transformation from one spheroid to the other as necessary is assumed.) The set of all sea levels at a given instant of time defines the sea surface at that instant (defined as the Momentary Sea Surface,  $A_s$ ). To avoid complicated explanations and procedures on minor matters, this study will concern itself only with continuous sea surfaces, and will not consider spray, surface mist or fog, foam, etc.

### 4. Momentary Sea Surface

The Momentary Sea Surface, is a real-world concept of the figure of the ocean surface "frozen" at a given instant of time over an area. (Distractions such as air-sea interface and air pockets will be neglected for purposes of this study.)

## 5. Instantaneous Mean Sea Level

Instantaneous mean sea level (IMSL) at a given instant is defined only for a given area of sea surface. It is the height of that surface whose (constant) height above the International Spheroid (see above) is ocean level at that instant within that area. Stated slightly differently, the IMSL is defined as the momentary sea surface averaged over a specified area, subsequently defined as the footprint. (The averaging is performed by selecting an ellipsoid, from the same family as the reference ellipsoid, for which the volume of water above that ellipsoid is equal to the volume of air below, over the footprint area.) It is presumed that the IMSL is not sensitive to the precise size of the footprint, and does not change significantly from one area to the neighboring area. In following sections we shall frequently assume that IMSL within an area differs by an insignificant amount from the height found by averaging, over a few minutes or time, the heights at a few points widely spaced throughout the area. The time period must be short to avoid significant contributions from the tide or seiches; the wide spacing is desirable to ensure that persistent differences in wave pattern between various parts of the area will not bias the IMSL.

Radar altimeter measurements are averages of measurements made over a 1-second interval. During this interval the altimeter has moved a distance of about 7.5 km parallel to the spheroid and up to 500 meters perpendicularly to it (in altitude). The ocean surface probed by the altimeter, (i. e., which contributes to the measurement process) is called the footprint, and is in an area about 10 km wide and 20 km long.

## 6. Mean Sea Level

Mean sea level is the average value of sea level, at a given longitude and latitude, over a specified period of time. No matter what period of time is taken for the averaging, it will be found that second average over another equal but non-overlapping period will have a different value from the first. If



we specify the time interval to be 20 years, so that it includes the saros, we find that all major tidal, tsunami, meteorological, and wind-wave effects average out. Mean sea levels in successive 20-year periods will then differ by only a few millimeters, in the open oceans at least. These persistent differences may be caused by changes in water volume, water mass, current changes, etc.

## 7. Altimeter

The altimeter is used in more than one sense. In the narrow sense, it refers to the radar hardware system on-board the satellite, including the antenna and on-board data processing, but excluding other satellite subsystems such as telemetry, storage or the clock; ground support equipment is excluded. In the broader sense, it includes all related hardware and software, including ground tracking systems and ground-based computers.

In any event, the output of the altimeter consists of pairs of numbers of altitude and associated time. The altitude is a measure of the distance from the satellite to the IMSL, and the time is the instant at which the altitude is applicable. These pairs of numbers are the ones to be verified.

Whether the term altimeter, or altimeter system, or satellite altimeter, etc., is intended in the narrow or in the broader sense is determined by the context in which it is used. For purposes of describing the radar, the altimeter is described in the narrow sense, while for purposes of verification the altimeter (or altimeter system) is thought of in the broader sense.

## 8. Geoid

The geoid is here defined as that equipotential surface which has a height of zero meters at the Meade's ranch, Kansas, monument. This definition makes the geoid inaccessible at the point where it is defined, but does relate the geoid to the same physical point as that used in defining NAD 1970.

## 9. Convention and Geometry

As a matter of convention, the following symbols are adopted (see Figure N-1): P designates points, and A designates areas; the subscripts specify the particular point or area. Unless otherwise specified, all areas A will be defined with dimensions of the order of the size of the radar footprint area, centered about a point designated as P, where A and P have the same subscript.

(In general, H is used for a height or Satellite-to-Earth measurement, while D is used for distances of less than 100 meters.)

The fundamental reference for all positions is the Reference Ellipsoid. This is the International Reference Ellipsoid of 1930, an acceptable reference for geodetic data as well as for tracking data.

$P_s$  is defined as the instantaneous position of the satellite, which changes with time.

$P_e$  is a point on the Reference Ellipsoid corresponding to  $P_s$ , such that  $P_s$  lies on the normal (perpendicular to the Reference Ellipsoid) which passes through  $P_e$ . The distance between  $P_s$  and  $P_e$  is defined as the Height of the satellite, a vector quantity with magnitude  $H_e$ .

$P_g$  is a point on the Geoid lying on the normal (to the Reference Ellipsoid) passing through  $P_e$ .

MSL is Mean Sea Level, not further defined at this time. (Oceanographers would refer to this as climatological sea level.)  $P_m$  is a point on MSL lying on the normal through  $P_e$ .

$A_s$  is the momentary sea surface (described earlier) of size the order of the footprint about the normal to the Reference Ellipsoid;  $A_s$  is the rough "picture" of the real ocean.

$P_i$  is defined as the intercept of the height vector with the instantaneous sea level. The intercept of the height vector with  $A_i$  is designated  $P_i$ . The distance from  $P_s$  to  $P_i$  is called  $H_i$ . It is assumed (and discussed subsequently) that the radar tries to measure  $H_i$ .

$R$  is defined as the radar uncorrected (or uncalibrated) range reading. This is the best radar estimate of the ocean surface location in the absence of calibration; it is raw data.  $P_r$  is the point a distance  $R$  from  $P_s$  along the height vector.

$C$  is defined as the radar calibration correction, resulting from correlation between the radar ranging values  $R$  and other information about the real world.

$H_r$  is the best radar measurement of  $H_i$  ( $P_i$ ) after calibration correction  $C$ .

$E_r$  is the residual radar error, or uncertainty in the radar measurement  $H_r$ .

$P_{iv}$  is the verification experiment measurement of  $P_i$ ; i. e., it presupposes that  $P_i$  cannot be determined precisely, even for verification purposes.

$E_v$  is the residual verification error, or the uncertainty in the verification experiment measurement  $P_{iv}$ .

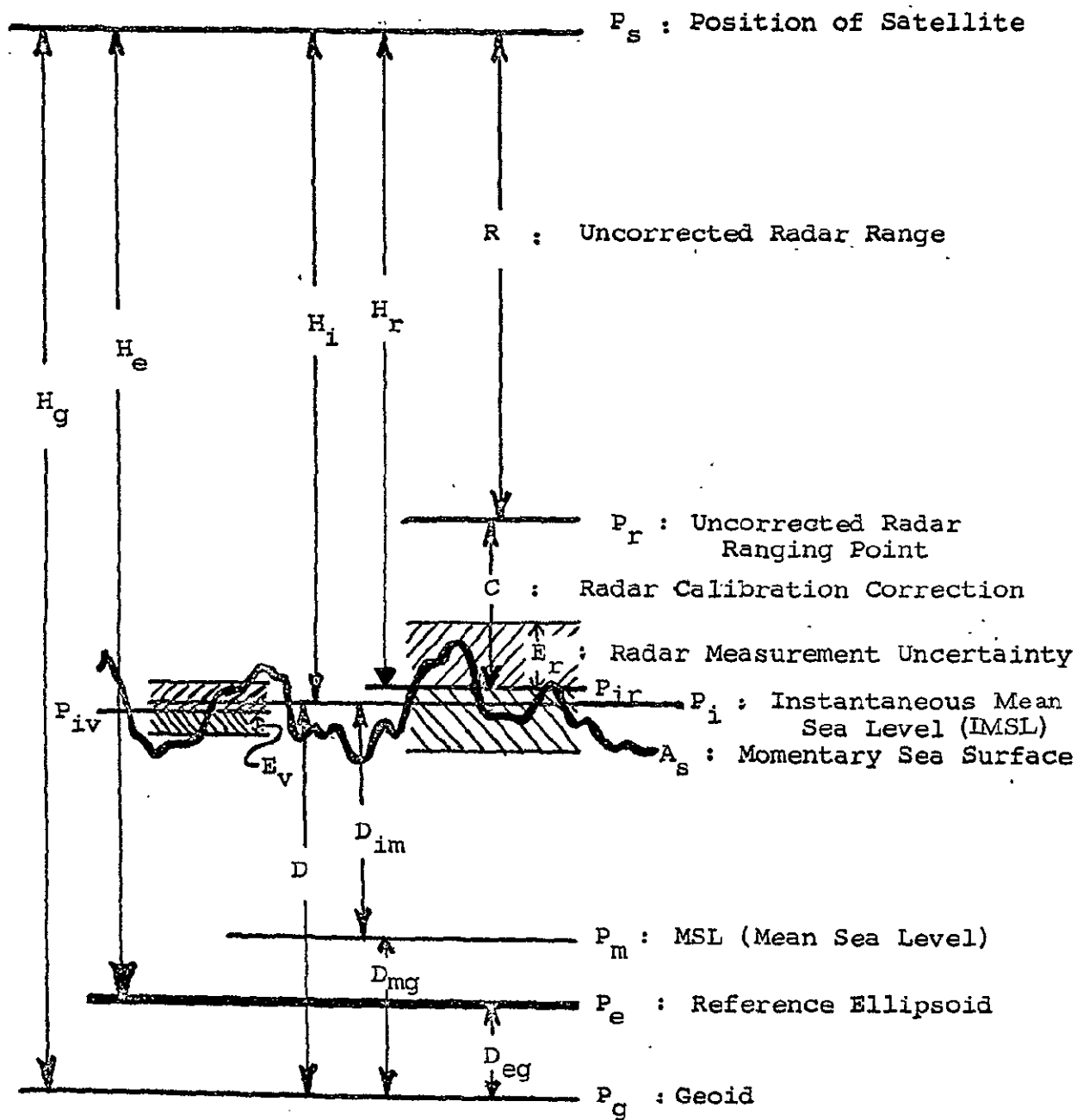


Figure N-1. VEDS Geometry

APPENDIX O  
OCEAN SURFACE CONDITIONS (OCEAN TRUTH)

B. Kinsman

O-1 Descriptions of the Ocean Surface and Their Relation to Radar Altimetry

O-1.1 Descriptions of the Ocean Surface

Were the ocean at rest on the rotating earth and free of all forces except gravity, the surface of the ocean would be singularly easy to describe. In a word, it would coincide with a level geopotential surface. But the ocean is neither at rest nor is it free of driving forces. The great oceanic circulations powered by the differences in solar energy reaching the earth tilt the surface over great distances and over long time intervals. At lesser scales the sun and moon induce periodic displacements, and earth movements cause intermittent tsunamis. At still smaller scales the wind generates waves, while at the smallest scales even a fish breaking water makes ripples. The simple geopotential surface (whose precise determination is anything but simple) is never encountered in nature.

If the level geopotential surface is taken as a reference, and  $\eta$  is the departure from it, then a complete description of the sea surface would require a specification of  $\eta$  for all positions on the two-dimensional curved surface of the earth and for all time. We ask for  $\eta = \eta(\vec{x}, t)$  where  $\vec{x}$  is a suitably restricted two dimensional position vector and  $-\infty < t < +\infty$ . Clearly the request is preposterous. The sea is far too large, and the forces too many and too little known. Instead of a complete description of the ocean surface, we have many partial descriptions, each fashioned to meet some need sufficiently well. The seaman has fashioned a crude description which permits him to communicate to other seamen the aspects of the ocean important to him. George Darwin, studying tides, describes an ocean surface which varies smoothly with a complex periodicity

Current tilts, tsunamis, wind waves, and ripples have all disappeared, but tidal predictions based on his partial description are of the greatest utility to shipping. The scientist studying wind waves may have trouble "removing the tide" from his actual record, but in the end he describes his wind waves as though the ocean were tideless. Corresponding to each problem on which attention is focused, there is a conceptually ideal partial description and a number of more or less satisfactory practical partial descriptions which have actually been created. The problem of radar altimetry is no different from other problems. It sets the requirements of a useful partial description. If we must first create the appropriate partial description, gather the data, verify the description, and, in short, hatch the whole thing ab ovum before we can attempt radar altimetry, we are clearly in a bad way.

Our first task is to review briefly the requirements of the radar altimetry problem and then, just as briefly, inspect the partial descriptions of the ocean surface created for other problems. We can hope that with luck some one among them will also be useful to us, and at the very least, there will be clues and usable fragments.

#### O-1.2 The Requirements of Radar Altimetry

At root the measurement of distance with a radar altimeter consists of illuminating a distant target with a burst of energy of a specific sort and sensing the energy reflected from the target. If both instrument characteristics, e.g., beam width, burst duration, frequency, etc., and the nature of the illuminated target, e.g., surface shape, orientation, dielectric properties, etc., are known, the reflected signal is easily interpretable and can be used to compute a distance to the precision of the instrument. The instrument characteristics are well known. However, application of radar altimetry to the real world ocean presents it with a poorly known target which makes the reflected signals difficult to interpret and decreases our confidence in the distance we compute.

One of the important parameters of radar altimetry which depends on both the instrument and the target is the scattering cross section per unit area denoted by  $\sigma^\circ$ . The area to be illuminated can be designed into the instrument and is of the order of 7 kilometers or so. This at once tells us that gross structure -- features with the scales of the current tilts, tsunamis, and tides -- need not appear in our descriptions. They will tilt the entire target only slightly; departures of the order of a few seconds of arc at the most are a reasonable expectation. It is also immediately clear that we will want to know the fine structure of the sea surface -- the wind waves and possibly the ripples. Further, if we are to mount our instrument in an orbiting satellite which passes over the entire ocean in a few hours, we will find a description that incorporates the variation with time of the fine structure over the world ocean of the greatest utility.

Among the characteristics of the sea surface target that will affect  $\sigma^\circ$  we may mention:

1. The wave heights, both their size and their distribution over the illuminated area,
2. The slopes of the sea surface within the target area,
3. The gross tilts of the area, and
4. The dielectric properties of the sea water.

It is characteristics such as these which, because they cannot be controlled as the instrument characteristics can be, pose the real problem of determining proper values for  $\sigma^\circ$ . Of those enumerated, it is 1 and 2, the structural height and slope properties of the sea surface, which are most important at radar frequencies. For a normally incident beam, a surface reasonably describable as "rough" returns a smaller signal than does a "smooth" surface. However, at

grazing incidence the "rough" surface returns much the stronger signal. Property 3, the gross tilts, will have its greatest effect indirectly through 1 and 2 by changing the nominal incidence of the beam. The effect of 4 is minor. To radio waves the dielectric properties of sea water are sensibly constant over the entire range of salinities and temperatures encountered in the open ocean.

It thus becomes clear that two kinds of description of the sea surface are pertinent to radar altimetry. One kind will address itself to the "fine structure," the other to global variations of the fine structure. Unless a description of the sea surface promises information of these kinds, we can ignore it.

## O-2 A Review of Likely Descriptions of the Ocean Surface

### O-2.1 The Fundamental Theoretical Sinusoid

In the early part of the 19th Century, George B. Airy produced an approximate solution of the equations of motion and continuity for an inviscid, incompressible fluid with a free surface under the influence of gravity. He found that a permanent sinusoidal deformation of infinitesimal amplitude was compatible with Newton's second law if it moved, i. e., exhibited wave behavior, at a phase speed  $c = L/T$ , where  $L$ , the wave length, and  $T$ , the wave period, are functionally related. The depth of the fluid,  $h$ , also plays a role. For a wave in deep water, one whose length is no more than twice the water depth ( $h/L < 1/2$ ), the relation between  $T$  and  $L$  is  $T = (2\pi L/g)^{1/2}$  where  $g$  is the acceleration of gravity. For radar altimetry, the size of the illuminated patch makes waves with lengths greater than 4000 feet uninteresting. Any wave with  $L < 4000$  ft will be in deep water whenever the depth  $h > 2000$  ft. Since most of the world



has depths in excess of 2000 ft, it is clear that within the context of our interest we will usually be dealing with deep water (or alternatively "short") waves.

Airy's sinusoidal wave gained importance when Fourier created an analysis that permitted the decomposition of the most complicated sea surfaces into sums of pure sinusoids of appropriate amplitudes, periods, lengths, phases, and directions of propagation. The interpretation of these Fourier component sinusoids as Airy waves is attractive but requires caution. It is exact only if the equations governing the sea surface are linear, which they usually aren't. However, we are fortunate that in many cases we are not led seriously astray by the identification. Most descriptions of the sea rely on Fourier decomposition into Airy waves when theoretical support is required, and they usually violate the conditions of the highly simplified theoretical model in at least one of two ways. They either assume that a result derived for waves with infinitesimal heights which you can't see will do just as well for a wave a foot high which you can see, or they assume that it will do no harm to deduce results from an extrapolation of a linear combination of the Fourier components as though they were Airy waves.

#### O-2.2 A Collection of Material From Simple Descriptions

For centuries seamen have been watching waves and recording what they saw in their logs. More recently scientists began to observe waves with instruments which have become increasingly more sensitive and sophisticated. Not one of them has ever seen an Airy wave. The component sinusoid has one height, one length, one period -- one of anything you choose to talk about. The waves of the sea have many heights, many lengths, many periods -- many of anything. If you want a simple description of the sea, you must single out some particular feature, say a height you consider characteristic, or you must boil down the chaos with statistics. For example, you might report some average wave height. The simpler the description, the more of the essential welter of the sea surface you lose. If you will keep this firmly in mind, you will be better able to see

what the following material tells you and, even more important, what has been left out. It is a collection which mixes observations, deductions from Airy waves, and very simple energy transfer considerations.

We have seen that both the height and the slope structures of the sea surface are important. Table O-1 shows a common classification code for the condition of the sea surface with respect to height,  $H$ , the difference in elevation between any crest and the succeeding trough.

Table O-1. Sea State Classification  
(Douglas Sea Scale)

<u>Term</u>	<u>Code</u>	<u>H (ft)</u>
Calm	0	0
Smooth	1	1
Slight	2	3
Moderate	3	5
Rough	4	8
Very Rough	5	12
High	6	20

The values of  $H$  given in the third column are supposed to be the maximum wave heights corresponding to each class. The table is carried only to 20 ft waves since waves higher than this are rare.

A crude measurement of the slope of the sea surface is the wave steepness,  $H/L$ . Clearly, a wave 5 feet high and 35 feet long ( $H/L = 1/7$ ) is a much different thing than one 5 ft high and 350 ft long ( $H/L = 1/70$ ). Table O-2 gives a code in terms of steepness. "Instability" indicates that many of the wave creasts are breaking.

Table O-2. Wave Classification by Steepness

<u>Wave Types</u>	<u>Criterion</u>
Low	$H/L \leq 0.01$
Moderate	$0.010 < H/L \leq 0.040$
Great	$0.040 < H/L \leq 0.143$
Instability	$0.143 < H/L$

Wave heights, as even Ulysses knew, are related to the wind speed. A simple empirical relation suggests that we use  $H = 0.026U^2$  with  $H$  in feet and  $U$ , the wind speed in knots at anemometer height (10 m) above the water. The sea gains energy from the wind, and as it does, the waves grow. The process cannot go on indefinitely. For any given wind speed, there is a wave state which loses energy as fast as it gets it. Such a saturated sea is called fully developed or fully arisen. A certain minimum time and sea room are necessary if the sea is to become fully arisen. The length of time a wind of a given speed has blown is the duration  $D$  and the extent of the water surface over which it blows is the fetch,  $F$ . Table O-3 gives for each sea state the requisite wind speed, the representative wave height, and the length, phase speed, and period of three characteristic waves. Table O-4 gives the minimum fetch and the minimum duration necessary for a given wind to produce a fully developed sea. Table O-5 gives empirically based frequencies of occurrence for wave height in the various oceans while Table O-6 gives observed maximum and minimum wave lengths. The large range of wave lengths in all oceans is striking.

### O-2.3 The Power Spectral Representation of the Ocean Surface

Visual observations and simple descriptions of the sea surface are not without their value, but the currently fashionable representation uses the power spectral density. Very compactly, the power spectral density function corresponding to a sea surface is the Fourier transform of its autocorrelation function. It

Table O-3. Deep-Wave Relationships For Fully Developed Sea

Sea State Code	Wave Type:		Low			Moderate			Great		
	U(knots)	H(m)*	L(ft)	C(knots)	T(sec)	L(ft)	C(knots)	T(sec)	L(ft)	C(knots)	T(sec)
0	0	0	0	0	0	0	0	0	0	0	0
1	6.2	0.3	100	13.4	4.2	25	6.7	2.1	7	3.6	1.1
2	10.7	1.0	300	23.2	7.3	75	11.6	3.7	21	6.2	1.9
3	13.9	1.5	500	30.0	9.5	125	15.0	4.7	35	7.9	2.5
4	17.5	2.5	800	37.9	12.0	200	19.0	6.0	56	10.0	3.2
5	21.5	4.0	1,200	46.6	14.6	300	23.2	7.3	84	12.3	3.9
6	27.8	6.0	2,000	60.0	18.9	500	30.0	9.5	140	15.9	5.0
		**C/U=		2.16			1.08			0.58	

Thus, for sea states 1-6 the variation in period, T, is approximately from 1 to 19 seconds and in wave length, L, from 7 to 2,000 feet for a fully developed sea.

\*Wave Height, H, is crest-to-trough (peak-to-peak).

\*\* The wave age, C/U, is a dimensionless measure of the length of time necessary for the wave to grow.

Table O-4.  
Minimum Fetch & Duration vs. Wind Speed  
for a Fully Developed Sea

Wind Speed U (knots)	Minimum Fetch F min (n mi)	Duration D min. (hr.)
10	10	2.4
20	75	10
30	280	23
40	710	42
50	1,420	69

Table O-5. Relative Frequency of Waves of Different Heights in Different Regions

Ocean Region	Wave Height: (feet)	0-3	3-4	4-7	7-12	12-20	≥20
		%	%	%	%	%	%
North Atlantic		20	20	20	15	10	15
Mid-equatorial Atlantic		20	30	25	15	5	5
South Atlantic		10	20	20	20	15	10
North Pacific		25	20	20	15	10	10
East equatorial Pacific		25	35	25	10	5	5
West wind belt of South Pacific		5	20	20	20	15	15
North Indian Ocean (Northeast monsoon season)		55	25	10	5	0	0
North Indian Ocean (Southwest monsoon season)		15	15	25	20	15	10
Southern Indian Ocean		35	25	20	15	5	5
West wind belt of southern Indian Ocean		10	20	20	20	15	15

(Bigelow and Edmondson, 1962)

Table O-6. Length of Storm Waves Observed in Different Oceans

Ocean Area	Maximum	Wave Length (Feet)		Average	Number of Cases
		Minimum			
North Atlantic	599	115		303	15
South Atlantic	701	82		226	32
Pacific	765	80		242	14
Southern Indian	1121	108		360	23
China Sea	261	160		197	3

(Bigelow and Edmondson, 1962)

is a function of vector wave number and frequency and contains vector position and time as parameters. In more immediately accessible terms, the power spectral density function is a bookkeeping device that takes the energy stored in a wave system and sorts it into the energy of the various Fourier component waves by period, wave length, and direction of travel. It carries vastly more information than the simpler descriptions, and, if the energy of the system is what your problem requires, it can be very useful. From it such statistics as the average heights of component waves within specified frequency and wave number bands can be calculated. However, these are still statistics. The precise details of the time and space histories are lost. Another way of saying this is that the phase relations among the Fourier components vanish. All disturbances in which the components have the same energies appear the same to the power spectral density no matter how they are put together. It is clear that seas differing widely in detail will be regarded as the same so long as their energy structures are the same.

The full wave number-frequency energy density spectrum is inaccessible because it requires too much input information of kinds we cannot now get. It is therefore the practice to use various reduced versions. The simplest is the frequency power spectral density function which can be computed from a time history of the water elevation at a single point. It is a function of frequency and has time and the probe position as parameters. It reports the energy correctly and sorts it by component periods, but it is totally unable to tell you from what directions the energy in waves of a given period is reaching the probe. A somewhat more elaborate version is the line spectrum which can be computed from a record of water elevation along a line made at some instant of time. It will sort the energy by wave number (wave length) as it appears to the line. If you are willing to assume that the Fourier components are Airy waves, then the relation between period and wave length will allow you to deduce directional information with a bilateral ambiguity. If you can get a record of the water

elevations over an area at an instant of time, then the vector wave number spectrum, sometimes called the two-dimensional spectrum, becomes possible. An engineer I know once called this "the fingerprint of the sea." Since the record from which it comes is instantaneous, there is a  $180^\circ$  ambiguity about which way the components are traveling. In this case, since waves generally run with the wind, you can resolve the ambiguity.

Many attempts, some of which have met with reasonable success, have been made to relate the spectrum to be expected when the wind field is known. This is of interest to our problem since wind fields can be deduced from weather maps. Complete success would permit us to describe the sea state by the energy spectrum for the entire globe, given a complete weather net.

Another line of endeavor which is still in its infancy bears on the propagation of waves. Waves run and a storm off New Zealand can furnish waves for Bermuda days later. Forecasts of wave propagation based on a linear superposition of Airy waves is simple in principal, although tedious to execute. Most methods in use today have this as their base. However, wave propagation is a non-linear problem, and, while the non-linear effects are small, the distances and running times are so long that non-linear effects can build up to the point where a linear analysis can lead us astray. So far, a beginning has been made at understanding the physics of non-linearity, but little has been achieved that permits practical application.

#### O-2.4 Very Fine Structure

For radar altimetry surface slope is one of the most important parameters. On the sea surface, the most extreme slopes are associated with the ripples or capillary waves. Except in flat calms and very light airs, the ripples are always there. The first waves that appear at the onset of a wind strong enough to make waves are capillaries with lengths of the order of a centimeter, and in mountainous



storm seas the ripples are still found riding the large waves. Studies of capillaries frequently handle their slopes by considering them as facets set in the larger gross structure. To give you a feeling for this description, we can hardly do better than quote from Marks, W. (1965) "The application of airborne radar to the measurement of the state of the sea:"<sup>(1)</sup>

"The radar observes reflections from facets on the surface of a wave; the strength of the reflected signal depends on the size and orientation of the facets with respect to the angle of incidence and frequency of the radiated signal."

"The wind speed is the primary factor that influences the roughness and slope distributions of the tiny wavelets in the sea and (that) these distributions are significantly unique in different states of sea. By carrying out a dimensional analysis, it was shown that air momentum (M) and air viscosity ( $\eta$ ) acting on a water surface that resists deformity through gravity (g), water density ( $\rho_w$ ) and surface tension (T), produces a roughness condition (R), characterized by a slope distribution(s)

$$s = f \left[ R, \frac{g \rho_w \rho_a}{T \eta} (F h v) \right]$$

In this expression, the air momentum is expressed in terms of air density ( $\rho_a$ ), fetch (distance over which wind blows) (F), the effective height of the wind (h) and the wind speed (v). The term

$$\frac{g \rho_w \rho_a}{T \eta}$$

is considered to be constant. The fetch determines the state of wave development for any given wind speed and the effective height prescribes uniformity in correlation of wind speed with sea state. Therefore, it is the wind speed that primarily governs the slope characteristics of the waves."

(1) "Oceanography from Space," edited by G. C. Ewing, WHOI, Ref. No. 65-10, 1965.

### O-3 Sources for Occasional or Continuing Information About the State of the Sea and Pertinent Associated Qualities

#### O-3.1 The Fleet Numerical Weather Center (FNWC)

Numerical wave and swell analyses have been made twice daily at FNWC, Monterey, Calif., since 1961. Wave and swell (waves which have propagated away from their generating area) fields are merged by an rms technique to provide wave heights, directions, and frequencies. From the accumulating analyses, monthly means and standard deviations for the wave heights are computed as well as mean and modal propagation directions. For computational details consult Hamilton and Corkum (1969).

FNWC uses a number of procedures. In one, stereophotos from four aircrafts are used when the waves are medium to large. In another, oceanic scale predictions of winds are used to deduce wave spectra. The FNWC maintains a regular program of verification in its effort to improve the accuracy of its forecasts by making observations in areas available to it. Sources of records for verification include a variety of airborne, shipborne, and tower mounted instrument systems.

#### O-3.2 The Applications Technology Satellites (ATS)

Valuable information on the sea surface structure at scales of interest down to capillary waves and in areas where no direct observations are available may be derived from the Applications Technology Satellites (ATS). These satellites are space-stationary at an altitude of about 36,000 km, and each views continuously a fixed region of earth. When the region is oceanic, the glitter patterns of reflected sunlight are indicative of the sea state condition. A calm ocean would show only a single intense reflection from the point appropriate to the laws of geometric optics. A wave covered sea surface reflects the sun's light from any surface that happens to be tipped at the right angle, and the sun glint then appears as a much larger, more diffuse source. A dark spot in the sun

glint pattern arises from a relatively calm patch within the illuminated area. When such a calm patch passes through the position which the sun's calm-water specular point would occupy, it reveals itself by returning a much more intense light and then blackening again as it moves away. One source of such patches is the upwelling of cold, deeper waters. This has been observed in several places, e.g., west of the Gulf of Guayaquil and north of the mouth of the Amazon. In such areas the more steeply sloped ripples are reduced, producing the "dark-patch" effect.

Unfortunately, ATS observations are restricted to an equatorial band between  $11^{\circ}$  N and  $11^{\circ}$  S latitude.

For further information, see Bowley et al (1969), Greaves (1969), and Duntley and Edgerton (1966).

### O-3.3 The Global Atmospheric Research Program (GARP)

The Global Atmospheric Research Program (GARP) is included here for completeness, since it is not yet operational. As projected, it includes an international weather watch, and among its intended observations, we may list the following as potentially useful:

- a. Cloud motion pictures taken from four geosynchronous satellites with both infrared and visible light sensitive systems.
- b. Similar cloud photographs from two polar-orbiting satellites.
- c. Assorted data taken from a global network of balloons, buoys, and automated stations.
- d. Continuous wind profiles from several thousand free balloons set to hold at the 920 mb level (roughly at 600 m).
- e. Radiosonde measurements on a global scale.

#### O-3.4 Data Repositories

A number of centers are involved to a greater or lesser extent with the collection, processing, analysis, storage, and retrieval of oceanographic data. Some also provide for the calibration and standardization of oceanographic instruments. The oceanographic institutions connected with the various universities should be mentioned in passing. Their data is collected for their specific interests, and they are usually cooperative about sharing it. The difficulty is that it is usually not easily retrievable, and word of mouth is often the only way of finding out what's where. The organizations listed here are important to the VED study because it is known that they hold useful data, and further, because they have a mission to process and preserve scientific data for the use of others.

##### a. National Oceanographic Data Center (NODC)

NODC is a subcenter for the World Data Center (WDC). The designations for the subcenters are WDC-A, United States; WDC-B USSR; WDC-C, England, western Europe, Australia, and Japan. At each, data is held in separately administered categories according to subject. The categories are meteorology, geomagnetism, aurora and airglow, solar activity, cosmic rays, longitude and latitude, glaciology, oceanography, rockets and satellites, seismology, gravimetry, nuclear radiation, and upper mantle project. The address of the national headquarters of WDC-A is

WDC-A Coordination Office  
National Academy of Sciences  
2101 Constitutional Ave., N.W.  
Washington, D. C. 20418  
Phone: (202) 961-1478

The address of three other offices whose holdings are of interest to the study are:

WDC-A Oceanography  
Building 1602  
Second and N Street, S.E.  
Washington, D. C. 20390  
Phone: (202) 698-3753

WDC-A: Meteorology  
National Weather Records Center  
Ashville, N. C. 28801  
Phone: (704) 253-0481

and

WDC-A: Upper Atmosphere Geophysics E. S. S. A.  
Boulder, Colorado 80302  
Phone: (303) 447-100 X-3654

- b. Smithsonian Oceanographic Sorting Center
- c. National Oceanographic Instrumentation Center
- d. National Bureau of Standards
- e. National Space Science Data Center

The holdings of NSSDC include data from earth satellites, sounding rockets, high-altitude aircraft, and balloons, together with supporting ground-based measurements.

Table O-7 shows the principal sources from which one may expect data on the sea surface per se.

Table O-7. Sources of Ocean Surface Data

National Oceanographic Data Center  
National Weather Records Center  
U.S. Navy - Fleet Numerical Weather Center  
U.S. Coast & Geodetic Survey  
British Admiralty

#### O-4 Description of the Ocean Surface for Operational Use and for Verification of the Radar Altimeter

##### O-4.1 Operational Description

Once the radar altimeter is put in orbit, a continuing knowledge of the sea states of the global ocean will be necessary for the interpretation of the data. For a routine job of this magnitude, computerized wave forecasting techniques which depend for their input on the world weather net are the only possibility. Computerized forecasting techniques, while far from perfect, have reached the point where their employment would be both feasible and reasonable. The first complete computerized method is due to Baer (1962). Since then, many investigators have experimented with computerized forecasts in the hope of improving them and reducing the amount of computer time required. The chief difficulty for our required application arises from the old problem of representing a spherical surface on a "flat" piece of paper. All of the methods produce satisfactory forecasts for more or less limited areas but grave difficulties are encountered when it becomes necessary to splice the regional forecasts together to form a forecast on a global scale. Adamo, Baer, and Hosmer (1968) have given their attention to this problem and have devised an icosahedral-gnomonic map projection together with a grid network which permits the extension of a wave forecast to global scales. Pierson et al (1966), describes a somewhat similar method. At present, we have no system for a global forecast that would gain the assent of all wave forecasters as satisfactory. However, the icosahedral gnomonic projection does provide a geometric procedure that meets the necessities of the computer. It can be done, and for the present, it is the best available. It should be used until a better one comes along. In short, there is no need to be delayed for want of a global picture of the state of the ocean surface.

An important further point is that unless the distances measured by the radar altimeter are wanted in something approaching real time, the required description of the sea state is a hindcast, not a forecast. This is a considerable advantage. The "forecast" on the basis of the wind field over the earth can be used as the zero order approximation. It can be improved by modifying it to agree with any knowledge of the actual state of the sea that we can gather. Such supplementary information can range from visual observations radioed in from ships at sea to the most sophisticated data telemetered from satellites. The extent to which it is desirable to correct the zero order description depends on the use to which the distance measurements will be put and obviously requires a cost-effectiveness decision.

#### O-4.2 Verification Description

The description of the sea surface required for the initial verification of the radar altimeter must obviously be much more detailed than that required for operational work once we have satisfied ourselves that it gives meaningful data. If one were too bemused by the usual "textbook" presentation of science, one would demand that every parameter conceivably associated with the problem be measured. Science doesn't proceed like that. One would drown in a mass of irrelevant data, and the detection of an unexpected significant effect would be a matter of chance. The proper approach is to include those parameters for whose importance that is strong support from previous experience or theoretical argument and add to them as many more parameters which persuasive speculative argument can justify and your budget can afford. The items included in this section are offered as a reasonable basis for the verification of the radar altimeter.

##### O-4.2.1 Visual Wave Observations

It will be well to dispose first of this crude but necessary method of securing wave information. Trained observers and experienced seamen are

often surprisingly accurate in their estimates of the condition of the sea surface, whether these estimates are the result of simply looking at the sea or come from the instruments normally found on any well equipped ship. Such estimates are open to questions of precision, repeatability, and personal bias, but they serve as the rock bottom for data from more sophisticated instruments. It is all very well to make the elaborate measurements necessary for a spectrum, carry out the extensive calculations, and finally deduce by a long chain of theoretical argument, which inevitably involves assumptions and approximations, that the average height of the waves was 20 feet. If the trained observer replies, "I was there and the biggest wave I saw the whole time you were working was 10 feet," you can only conclude that your sophisticated system is in error somewhere along the line. The visual observer cannot give you the detail you need, but he can see to it that your description of the sea surface is not infected with gross error.

Among the parameters that may be expected to be estimated by an observer on the spot, either by direct observation or with the aid of simple instruments, are:

1. dominant wave direction (heading)
2. wave heights
3. wave lengths
4. wave periods
5. facet lengths
6. wave slopes
7. surface wind speed
8. surface wind direction
9. air temperature
10. water temperature
11. barometric pressure
12. surface current speed
13. surface current direction



### O-4.2.2 Power Spectral Densities

Since the data from verification studies must be interpreted, and since modern ocean wave theory for waves with lengths in our range of interest are couched almost exclusively in terms of the power spectral density function, it is this function which must be the prime requisite for the description of the target. Realizable estimates of the power spectral density function are of three kinds:

1. The two-dimensional spatial spectrum at an instant of time
2. The one-dimensional spatial spectrum at an instant of time
3. The frequency spectrum at a fixed point.

The first contains the most information and requires the most input data, while the third contains the least and requires the least.

#### O-4.2.2.1 The Two-Dimensional Spatial Spectrum

This spectrum, more usually called the wave number spectrum, begins with a record of the water elevations over an area of the sea surface at some instant of time. The analysis then gets a measure of the wave energy contained in that particular area and sorts it into the energy to be attributed to each of the Fourier component waves according to their vector wave number, i. e., according to their lengths and directions. Direction of travel is uncertain to 180° but can be decided by an appeal to visual observation of the wind direction.

For our purposes, this is the most desirable, most detailed, and most useful spectrum we can have. If another instantaneous record of the same area is taken at a later time, another wave number spectrum may be calculated. If the sea has taken on a different character, its spectrum will be different from the first. If it has remained much the same, the two spectra will be indistinguishable within the limits of statistical uncertainty. For

verification in the field, this is important, since the target size relative to the sizes of the wind systems which generate waves is such that periods ranging from hours to days can be expected when the sea surface in the working area will retain its characteristics. The costs of data acquisition and computation for spectra are not trivial. Characterizing the sea surface by spectra only intermittently during a working period rather than with each radar burst is what makes the spectrum a feasible tool.

Data for estimates of the wave number spectrum have been secured by three instruments systems: laser holography\* (the Stilwell method), stereophotography (operation SWOP), and floating accelerometer-tilt meters (the NIO Buoy).

The laser transform method developed by Denzil Stilwell at NRL begins by photographing the sea surface. The negative is then illuminated through a lens system with a laser, and the output, which is effectively the desired Fourier transform, is recorded on a second negative. A densitometer reading of the second negative produces the final contoured relative energy spectrum in wave number space. The altitude and azimuth of the camera are required. The longest wave length detected depends on the camera altitude and the field of view, while the lower limit is set by the grain size of the negative. A range in the wave number of 100:1 is attainable. If one wants absolute energy values, some auxiliary information is needed for scaling. Stilwell's method is the best existing method for the inexpensive rapid acquisition of large numbers of wave number spectral density estimates. Like any method, however, it is not without its limitations. Its use is restricted to the daylight hours with the best results in the early morning or late afternoon. Optimum results require either a cloudless sky or a uniform overcast, and uncertainties about the effects of extensive whitecapping have not yet been resolved.

---

\* Stilwell, D., Directional Energy Spectra of the Sea From Photographs, J. Geophys. Res., 74, 1974-1986, (1969).

The stereophotographic method requires the coordinated use of two camera and an expensive, tedious analysis of the pairs of plates. Katz (1964)\* reports his experiences with the stereophotographic method. Airborne stereo-cameras were proven inadequate for radar clutter studies since the height sensitivity of airborne systems is on the order of one (1) foot. (For radar studies, a height sensitivity of one-tenth the radar wave length is desired; at X-band (3 cm), a sensitivity of 0.3 cm is required.) A shipborne system was subsequently developed which under optimum lighting conditions wave-height measurements to a sensitivity of 0.8 mm were made. The system consisted of a pair of specially modified aircraft stereo cameras was mounted on a rigging 20 ft above the water and about the same distance forward of the bow of a ship. The cameras were spaced on 11.5-ft centers, facing downward in such a way as to provide a 60% overlap of the two pictures. The cameras were T-5 Fairchild cartographic cameras refocused to the 20-ft distance. Their shutters were reworked to provide a 1/1000<sup>th</sup> sec exposure. Two 6-inch selected Metrogon lenses were installed. The wave-height information is used in two ways. Profiles of height-versus-distance, are obtained along lines that parallel the direction of flight of the airplane making the radar backscattering measurements. For each pass of the airplane, the standard deviation of the surface can be related with the radar signal strength returned at any preselected viewing angle of the radar; the larger the roughness, the greater the returned signal.

The second use to which wave-height data can be put is in the form of spectra; that is space spectrum, as distinguished from frequency spectrum. In other words, the correlative function of the surface, which is the Fourier transform of the space spectrum is desired. There exist many theoretical treatments relating the wave-number spectrum (or correlative function) with the angular dependence of the backscattered radar signal. If the radar backscatter function is measured simultaneously with the sea in this more meaningful statistical manner, the most accurate theory can then be selected.

\* I. Katz, Ocean Wave Measurements, APL Technical Digest, Sept. -Oct. 1964.

This technique, too, has its limitations. It has been found that with cloudy skies, the stereo-photos are of excellent quality. However, when the skies are clear, good quality stereo photographs can be obtained only during the early morning and late-afternoon hours when the sun was at a relatively low angle in the sky.

The stereophotographic method, however, has distinct strengths when the problem is to describe precisely the facets associated with capillary waves. As we have seen, the facet structure has an important effect on backscattering at radar frequencies.

Figure O-1 shows some portions of wave profiles (originally 6 meters long) obtained from different stereo-photographs of waves made in the same sea condition. Figure O-2 is an enlargement of a small section of a wave profile. This profile lies in the dominant direction of the waves. Some basic definitions can be derived from Figure O-2. Flatness tolerance is defined as  $1/10$  the radar wavelength. At any point on the wave profile, the slope is found by a line drawn tangent to the profile at that point (A). The angle  $\theta$  of the tangent line with respect to the horizontal will be referred to as the slope of the tangent. The flatness tolerance is then drawn parallel to the tangent line and equidistant from it. The two lines representing the flatness tolerance will intersect the wave profile and thereby define the facet length associated with the slope  $\theta$ . At the point B, the facet length is obtained by intersection of only one parallel of the flatness tolerance with the profile. The ratio of flatness tolerance to facet length is called roughness factor.

If the profile is sampled randomly, a sequence of facet lengths appropriate to each slope is obtained. The facet lengths are collected in equally-spaced intervals and averaged. The result is a relation between average facet length and slope as shown in Figure O-3. Negative slopes correspond to the downwind direction of wave travel.

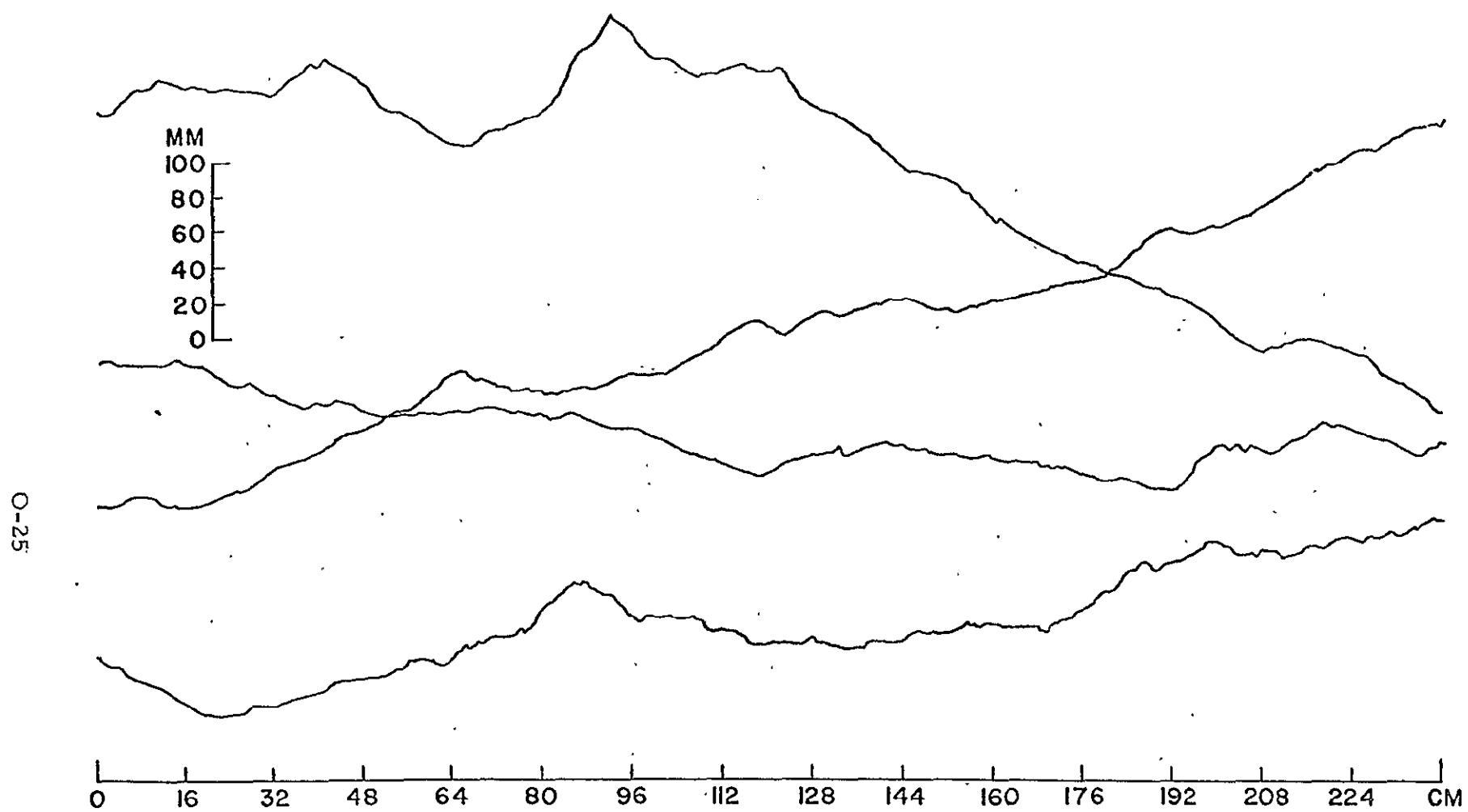


Figure O-1. Portions of Wave Profiles Obtained From Stereophotographs

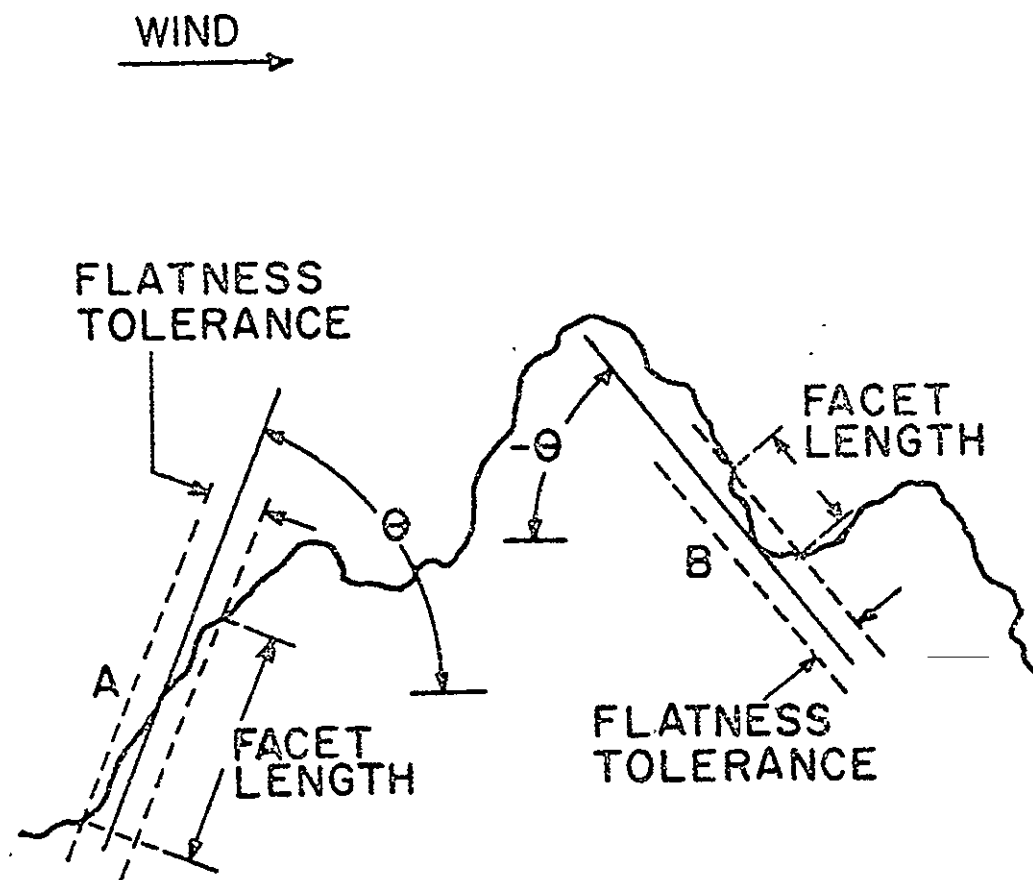


Figure O-2. Facet Length as Determined by Flatness Tolerance

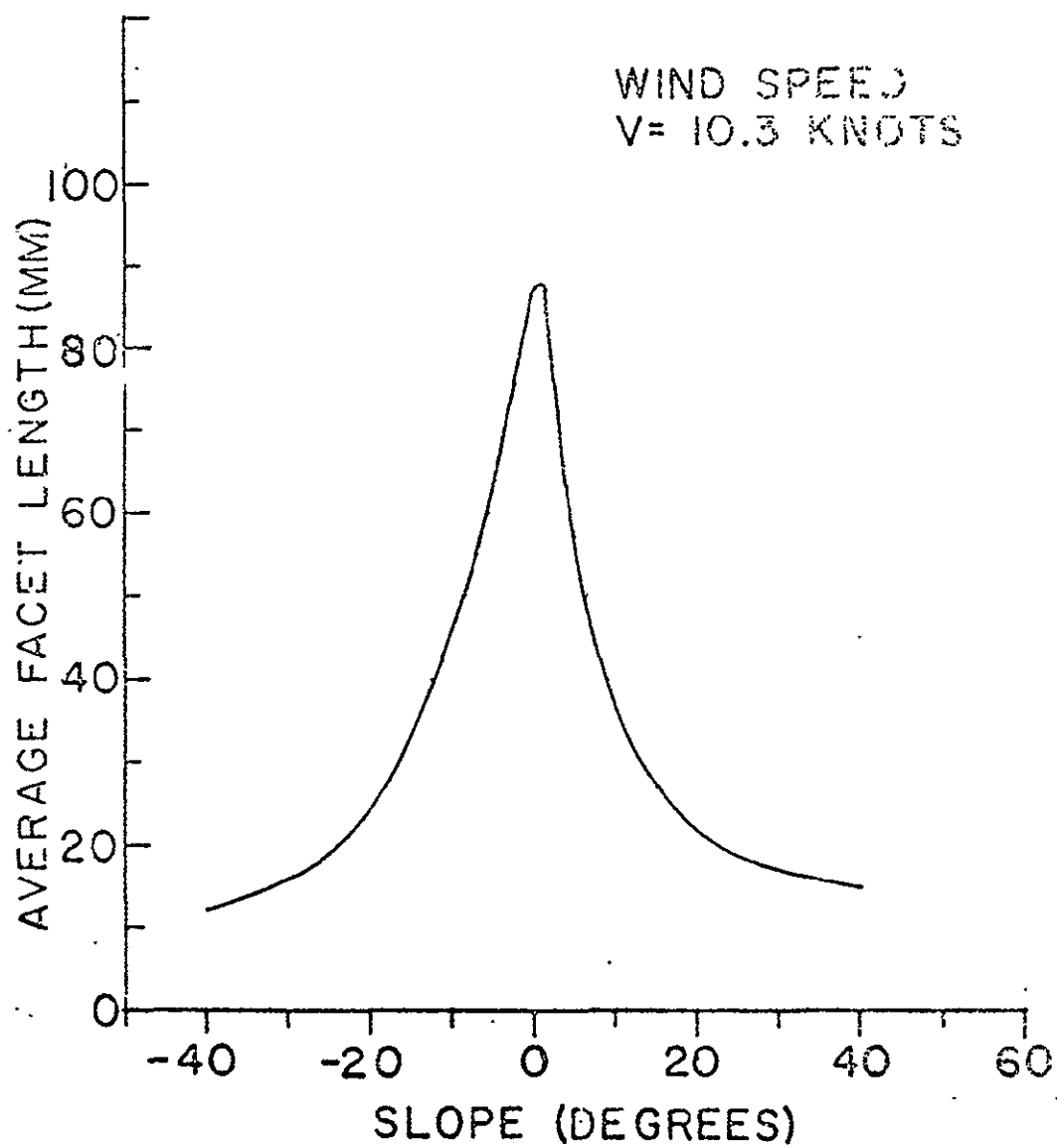


Figure O-3. Average Facet Length Versus Slope for Waves  
1-1.5 Feet High (radar wavelength = 3 cm)

The contribution to the radar return or backscatter depends not only on the slopes of the facets and their size, but upon their frequency of occurrence as well. Consequently, the next step is to obtain a relationship between probability of occurrence of average facet length and associated slope. Such a relationship is shown in Figure O-4.

In order to estimate the quantity of radiation reflected from the irregular wave surface, it is necessary to consider the effective radar scattering area of the facets. This is done by first considering the return of radar waves impinging on disks of known area. If the wave facets are assumed to be circular then the facet area is known and the theoretical results of Schmitt may be used to infer the effective radar scattering area for the real condition. Furthermore, the information in Figure O-4 permits a table to be calculated that describes the probability density of effective radar scattering area with respect to slope.

Each facet receives and reradiates energy over a limited angle which is greatest at normal incidence ( $90^\circ$ ). This effective beamwidth is a function of facet size and radar wavelength. The effective beamwidth thus obtained relates also to the effective radar scattering area.

The radar depression angle ( $\phi$ ) is the angle the radar beam (center) makes with respect to the horizontal. For a constant radar depression angle, the facets that have sufficient beamwidth to contribute to the total radar return from the water surface are known and so is the probability density of facet occurrence. Thus, the total effective scattering area for different depression angles may be obtained for all the facets oriented in the upwind and downwind direction. If the ratio of effective scattering area in the upwind and downwind directions is plotted (in decibels) against the depression angle, then this statistic is equivalent to the radar measurements and a direct comparison can be made.



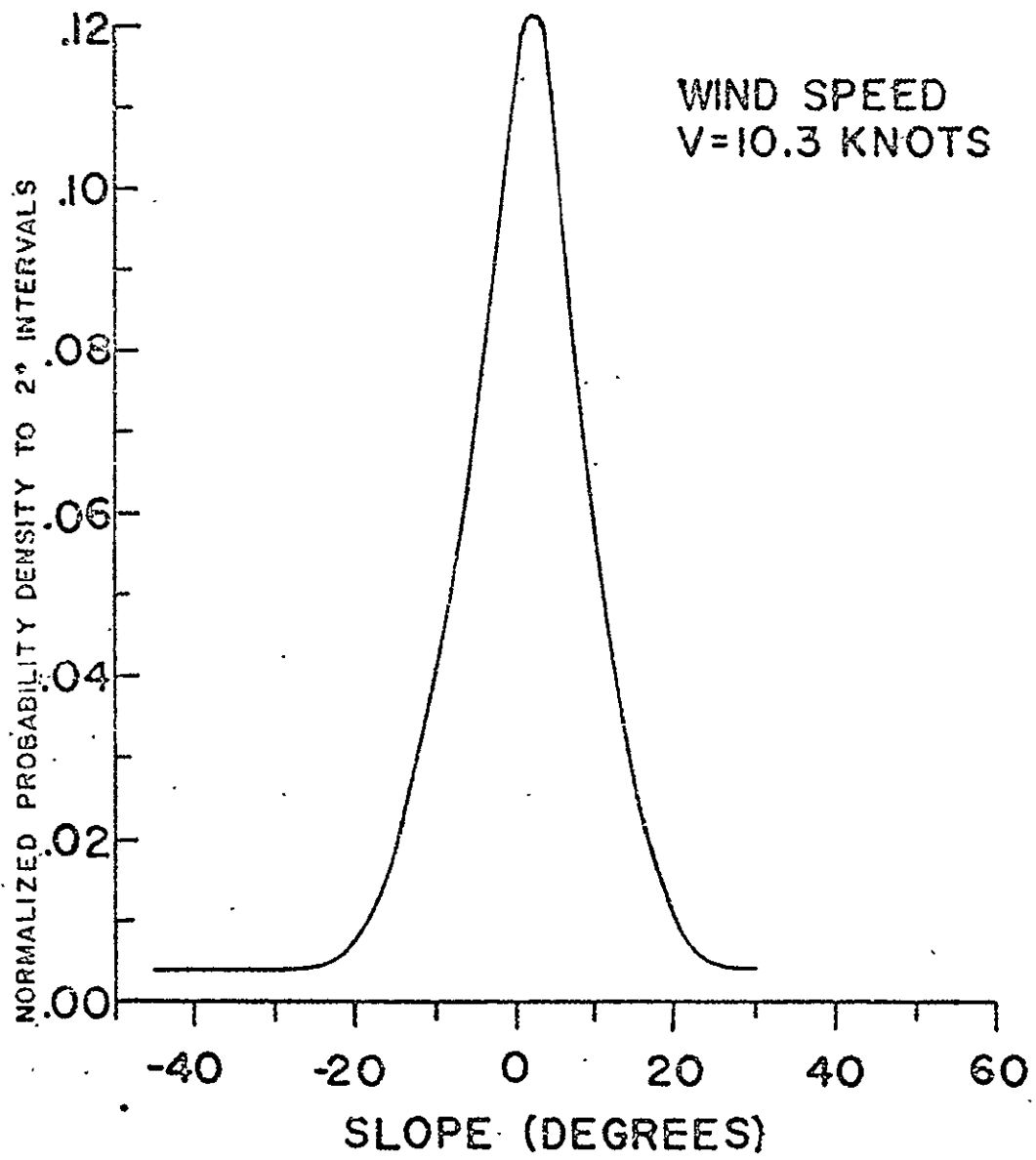


Figure O-4. Slope Probability for Waves 1-1.5 Feet High

The use of floating accelerometers associated with tiltmeters as worked out in the NIO Buoy is an expedient rather than a method of choice. The quantities to be had from the data are surface displacement and the surface slopes along two orthogonal directions. From this information, the first two terms of an infinite series expansion of the wave-number spectrum can be computed. If you feel that the series converges rapidly enough to sustain such an early truncation, you may be satisfied with the estimate of the wave number spectrum the method provides. Buoys large enough to carry the sensor, power supply, and recorder load are rather large and will not respond to the smaller waves.

#### O-4.2.2.2 The One-Dimensional Spatial Spectrum

This spectrum, more briefly the line spectrum, begins with a record of water elevation at some instant of time along a line made by the intersection of a plane normal to the sea surface. There is no need to elaborate here on the calculations by which it is converted to a power spectrum. It should be mentioned that the wave lengths (wave numbers) it sees are as they appear to the line -- smallest whenever the wave component runs parallel to the line and infinite when the component runs perpendicular to the line. If the components are assumed to be small amplitude Airy waves, then they can be mapped to their true lengths. The line spectrum can be thought of as a section through the wave-number spectrum. The wave-number spectrum can be built up by taking line spectra along many different headings. The more nearly the line records coincide in time, the more confidence one has in the correctness of the resulting mosaic.

The laser profilometer looks to be a promising instrument for line records. Typical laser profilometers are built for airborne use at altitudes up to 7000 ft during the day over the ocean. The instrument measures the distance from the aircraft to the laser illuminated spot on the ocean surfaces.

The small size of the illuminated spot and the fast response time allow for accuracies of less than 6 inches at 500 ft, decreasing to about one foot at 2000 ft. The output signal is an analog voltage recorded on a strip chart or on magnetic tape. A barometric pressure altimeter is usually included with the system which allows variations in the height of the aircraft either above or below the desired altitude to be removed from the final output. Because of the small spot size, the output is a ocean line spectra. However, a spatial spectrum may be derived by flying the profilometer at many different heading in a short period of time over an ocean area. This instrument is manufactured by Spectra-Physics Inc., Mountain View, California, and is a 30-MW AM-CW helium neon laser of red light at  $6328\text{\AA}$ .

#### O-4.2.2.3 The Frequency Spectrum

This spectrum is the easiest to estimate, requires the least sophistication in its recording devices, and yields the least information. The starting point is a record of the sea surface displacement at a fixed location over a length of time selected by the use you intend for your results. The following summary of instruments which have been used is taken from L. Katz (1964)\*.

Various methods for measuring waves have been used. Among these, the more popular are:

1. Pressure gages
2. Step gages (resistance or relay-activated)
3. Wire gages (resistance or capacitance)
4. Altimeter
5. Accelerometer buoy.

---

\* Ibid

Pressure Gage -- The pressure gage is a device mounted underwater that is sensitive to the amount of water between it and the surface. As the waves move past the point directly above the gage, the pressure changes; hence, a recording of pressure versus time is equivalent to wave-height versus time. This device is usually connected to a recording meter on shore.

Step Gate -- The step-resistance gage consists of a thin, vertical support which is partially immersed in the water, and on the support is a set of exposed electrodes. Each electrode is in series with a fixed resistor. As the water moves up on the gage staff, more electrodes are shorted out and the total gage resistance becomes less. Wave height is then simply a measurement of resistance versus time. A fast-response recorder, 60-cps or better, is useful in that it makes the instrument self-calibrating. With the fast-response recorder, one can see the discrete steps in the record as the water rises on the gage. As the water falls, on the other hand, it pours slowly off each electrode and the step function is not discernible. Since each step corresponds to a fixed increment of water height, one can check on the calibration as frequently as desired.

A modification of this gage is one in which the electrodes are replaced by small floats. The water rises and causes a float to move; in turn, the float activates a relay in series with a resistor. We then have a device that does not change its calibration with time. Its use is in those applications where long-term calibration stability is required.

Wire Gage -- The wire gage is similar in concept to the step gage except that the conducting wire is the exposed measuring device. As the water moves up and down, the total wire resistance changes. One can also use the capacitance of an insulated wire as the measuring

element. In fact, if two wires are mounted vertically a short distance apart, the difference in reading between the two is a measure of water slope. Although the inherent sensitivity of the continuous wire gage is greater than that of the step gage, it, too, is limited by the surface tension of the water.

Altimeter Gage -- Devices using the altimeter principle have been developed to measure wave height from an airplane. If one flew over the water at a relatively low altitude and measured the transit time of a radio pulse transmitted to the surface and returned, he would have a measure of his height. The fluctuations in height versus time are dependent on the irregularities in the water height as long as the airplane motion is constant in altitude above a mean water level. Some measure of success has been achieved with this type of gage. It has the advantage that it can cover a large area in a relatively short time. However, this type of gage does not seem to be gaining in popularity.

Accelerometer Buoy -- A buoy floating in the water moves up and down with the waves; thus the accelerometer buoy is a device that measures wave accelerations. The accelerations are integrated twice to get displacement versus time. However, this type of gage is useful only for measuring the larger waves since the buoy, because of its size and mass, cannot respond to the capillary or small gravity waves.

All the gages just discussed (with the possible exception of the wire gage) have in common the difficulty that small waves are hard to measure.

#### O-4.3 Possible Helpful Supplements

- a. Warnecke (1968) has analyzed recent television pictures and radiation measurements from near-Earth and geo-synchronous orbits to provide large-scale features of the global cloud distribution.

- b. The Gulf Environmental Measurement Program (GEP) and the ESSA Gulf Study are directed specifically to problems in the Gulf of Mexico, but outputs from their projected studies in air-sea interaction will be of interest to the verification experiment.
- c. Mitchel and Rotz (1969) have applied coherent optics to the determination of two-dimensional power spectra of water waves.
- d. Arnold (1967) used ESSA I satellite photographs to show that there is a correlation between low-level clouds and the sea-surface temperature.
- e. Barnett and Sutherland (1969) have discussed a surface-wave parameter which although not very well understood, may have a critical effect on the success of the verification experiment. It is known as "overshoot" and can have an extreme effect on the specular characteristics of an ocean surface. Its effect is complicated by the fact that overshoot is not always present, not even within otherwise similar sea states.
- f. Schwartz and Marchello (1968) found that, particularly in the case of sudden onset of a relatively strong wind, the initially generated resonant waves may run almost orthogonally to the mean wind field. Needless to say, this complicates and renders somewhat useless, any scheme which assumes that directions of wind and waves are always roughly the same.
- g. Another forecasting technique may be based on the good correlation between water currents at the ocean bottom and tidal heights at the ocean surface. This close correlation arises from the fact that ocean-bottom currents are produced primarily by tidal heights. Instrumentation for this experiment has been installed at the ocean bottom by Nowroozi et al (1968).

- h. Monahan (1968) has recently devised instrumentation for determining the concentration and size distribution of sea spray in the 1-meter interval just above the sea surface in the deep, open ocean. By simultaneously measuring the wind, he was able to show that there is an abrupt increase in sea spray as the wind increases from about 8.5 to 9.5 m/sec. This is consistent with other indications that there is a critical or transition velocity in numerous other sea-surface and near-surface phenomena. (See for example, Mandelbaum, 1956).
- i. The Institute for Meteorology and Geophysics of the Free University of Berlin publishes daily weather maps from sea level up to 10 mb level (i. e., about 30 km), covering the whole of the northern hemisphere. The daily map includes surface temperature and wind data. Details are in Scherhag (1969).
- j. There is some indication that the behavior of the ocean-air interface is dependent on the heat budget at that interface. Schooley (1969) has recently reviewed this area with particular attention to:
1. short- and long-wave radiation heating of the sea surface
  2. short-wave radiation reflected from the sea surface
  3. long-wave radiation from the sea surface.

This area was also covered by Neumann & Pierson (1966), in less detail but including also the ocean-air interface heat budget involving:

1. heat transported by advection
2. heat transported by convection and conduction
3. heat lost from the surface by evaporation or gained by condensation.

- k. Adem (1969) has recently perfected a rudimentary model for predicting month-to-month changes in ocean surface temperatures. Based on observational data from various sources and using a time-averaged thermodynamic model, the system is already producing good results and promises to form the basic framework for more sophisticated models involved other sea-state parameters. Related studies include those by Namias (1959), Clark (1967), and Jacobs (1967).
- l. Chang (1969) found that there is a large low-frequency oscillation above the mean drift of deep-water, long-crested waves. Observational data confirm, therefore, that Stokes' classical mass-transport velocity equation is an unsatisfactory one for use in connection with ocean surface models.
- m. Ewing (1969) has studied the problems associated with identifying the basic parameters of so-called confused seas. His analysis is an updated version of a similar study done by Longuet-Higgins (1967) on a random, moving surface.
- n. Aagaard (1969) has determined that the field of wind stress at the sea surface depends approximately on the square of the surface wind speed.
- o. Williams (1969) has outlined an indirect method for obtaining over-the-ocean wind velocity and direction information using the outputs from a satellite radiometer.
- p. Schwartz and Marchello (1968) found that, although the amplitude of a wind wave should grow linearly with time during the initial stage of wave development, the amplitude actually increases as the square root of time. This complicates and renders somewhat



inaccurate any algorithm or other analytical scheme which ignores the myriad nonlinearities in the actual behavior of the real-world ocean surface.

- q. Wu (1969) has found evidence that the ocean-surface roughness is governed by the amplitude of the short gravity waves. He also summarized some of the parameters related to wind stress acting at the ocean-air interface as important factors affecting the wind-wave interaction:

1. the generation of water surface "setup"
2. drift current
3. surface waves
4. heat-mass transfer across the interface and its effect on the nature of the interface roughness.

Wu concluded, among other things, that the split between ocean-air interface roughness, below and above wavelengths of interest to this study ( $1 < L < 10$  cm)> is at about: \_\_\_\_\_

1. wind velocity: 14 m/sec
2. sea state: 5
3. Beaufort number: 7
4. Aerodynamic flow: rough
5. wind stress dependence: function of square root of wind velocity for  $L < 1.5$  cm; independent of wind velocity for  $L > 1.5$  cm.

#### O-4.4 Examples of Type of Measurements Taken on Other Experiments

The following three problems were investigated and reported in "Earth Resources Program. Ground Truth Session\*,"

---

\* Prepared by Test and Operations Office Science and Applications Directorate, NASA-Houston, Final Report - Nov. 1967.

1. Sea State Measurements
2. Surface Temperature Measurements
3. Air-Sea Interactions.

APPENDIX O  
BIBLIOGRAPHY AND REFERENCES ON  
OCEAN SURFACE CONDITIONS

Aagaard, K., Relationship between geostrophic and surface winds at Weather Ship M, J. Geophys. Res., 74, 3440-3442, 1969.

Adamo, L.C., L. Baer, and J.P. Hosmer, Icosahedral-gnomonic projection and grid of the world ocean for wave studies, J. Geophys. Res, 73, 5125-5132, 1968.

Adem, J., Numerical prediction of mean monthly ocean temperatures, J. Geophys. Res. 74, 1104-1108, 1969.

Anon, Marine environmental forecasting, in Under Sea Technology Handbook, A61-A64, Compass, 1968.

Arnold, J.E., Reflection of the sea surfaces temperature field in low level cloud development: an observational air-sea interaction study from space, preliminary report, ONR contract Nonr 2119 (04), Texas A & M Research Foundation, 1967.

Baer, L., An experiment in numerical forecasting of deep-ocean waves, New York University, 1962.

Bailey, L.F., The Use of Historical Tsunami Wave Height Data in Forecasting Runup, ESSA Symp. on Earthquake Prediction, GPO, 1966.

Baker, B.B., et al, Glossary of Oceanographic Terms, SP-35, USNOO, 204 p, 1966.

Barnett, T.P., On the Generation, Dissipation, and Prediction of Ocean Wind Waves, J. Geophys. Res. 73(2), 513-529, 1968.

Barnett, T.P. and H.L. Sutherland, A note on an overshoot effect in wind-generated waves, J. Geophys. Res. 73, 6879-6891, 1969.

Barton, D.K., and H.R. Ward, Handbook of Radar Measurement, Prentice-Hall, 1969.

- Beckman, P., and A. Spizzichino, The Scattering of Electromagnetic Waves from Rough Surfaces, Macmillan, 445 p, 1963.
- Bowley, C.J., J.R. Greaves, and S.L. Spiegel, Sun glint patterns: unusual dark patches, Sci, 165, 1360-1362, 1969.
- Burt, K.H., Autoprobe: a free-floating, mid-water observational platform for oceanographic studies, WHOI, 95 p, 1969.
- Challinor, J., Dictionary of Geology, Oxford, 289 p, 1964.
- Chang, M.S., Mass Transport in deep-water, long-crested random gravity waves, J. Geophys. Res. 74, 1515-1536, 1969.
- Clark, N.E., Report on an investigation of large scale heat transfer processes and fluctuations of sea-surface temperature in the north Pacific, Ph.D. thesis, MIT, 148 p, 1967.
- Duntley, S., and C. Edgerton, The use of meteorological satellite photographs for the measurement of sea state, Scripps, 1966.
- Ewing, J.A., and N. Hogben, Some wave and wind data from trawlers, Marine Observer London, 36, 71, 1966.
- Ewing, J.A., and N. Hogben, A note on the lengths and periods of irregular unidirectional waves, National Physical Laboratory, England, TM 218, 1968.
- Ewing, J.A., A note on wavelength and period in confused seas, J. Geophys. Res. 74, 1406-1408, 1969.
- Fairbridge, R.W., Encyclopedia of Oceanography, Reinhold, 1020 p, 1966.
- Greaves, J., and C. Bowley, Satellite augmented oceanographic studies, Phase II, WHOI, in press, 1969.
- Hamilton, G.D., and R.C. Corkrum, Monthly combined wave height means and standard deviation and combined wave mean and modal directions, FNW Cen, AD-691-247, 55 p. 1969.
- Hogben, N., and F.E. Lumb, Ocean Wave Statistics, H.M. Stationary Office, London, 1967.

Howell, J. V., Glossary of Geology and Related Sciences, Amer Geol Inst., 397 p, 1962.

Jacob, W. J., Numerical Semiprediction of Monthly Mean Sea Surface Temperature, J. Geophys. Res. 72, 1681-1689; 1967.

Katz, I., Radar Backscatter from the Sea, in Oceanography from Space, WHOI, 367, 1965.

Kaula, W. M. Tests and Combination of Satellite Determinations of the Gravity Field with Gravimetry, J. Geophys. Res. 71, 5303-5314, 1966.

Kaula, W. M., Comparison and Combination of Satellite Data with Other Results for Geodetic Parameters, in The Use of Artificial Satellites for Geodesy, Nor Holland, 1967.

Kaula, W. M., Geodetic Satellites: Evaluation of Results Relative to Those Obtained by Other Means, Trans Amer Geophys Un, 48, 343-345, 1967.

Kauth, R., Backgrounds, in Handbook of Military Infrared Technology, GPO, 1965.

Kinsman, B., Win Waves - Their Generation and Propagation on the Ocean Surface, Prentice-Hall, Inc., Englewood Cliffs, N. Y., 1965.

Koch, K. R., Orbit Perturbations of Artificial Earth Satellites as Functions of Gravity Anomalies and Differential Corrections of Orbit and Station Coordinates, Ohio State, 43 p, 1968.

Köhnlein, W., Interface with Oceanography, in Scientific Horizons from Satellite Tracking, SAO Spl Rpt 236, 203-211, 1966.

Lee, W. H. K., and W. M. Kaula, A spherical harmonic analysis of the Earth's topography, J. Geophys. Res. 72, 753-758, 1967.

Longuet-Higgins, M. S., The statistical analysis of a random, moving surface, Phil Trans Ray Soc, London A 249 (966), 321, 1957.

Lundquist, C. A., and G. Veis, eds, Geodetic Parameters for a 1966 Smithsonian Institution Standard Earth, 3 vols, 683 p, 1966.

Mandelbaum, H., Evidence for a critical wind velocity for air-sea boundary processes, Trans Am Geophys Un, 37, 685, 1965.

- Miller, R. L., and J. S. Kahn, Statistical Analysis in the Geological Sciences, Wiley, 483 p, 1962.
- Mitchel, R. H. and F. B. Rotz, Applications of coherent optics to geological imagery, Mich Univ., Ad-691-267, 58 p, 1969.
- Momoi, T., Long Waves Around a Convex or Concave Bottom, Tokyo Uni Earthquake Res Inst Bull 44, 1966.
- Monahan, E. C., Sea spray as a function of low elevation wind speed, J. Geophys Res, 73, 1127-1137, 1968. .
- Moore, R. K., Satellite Radar and Oceanography, an Introduction; Oceanography from Space, W. H. O. I., Ref. No. 65-10, 1965.
- Moskowitz, L. I., Evaluation of Spectral Wave Hindcasts Using the Automated Wave Prediction Program of the Naval Oceanographic Office, NOO, 1967.
- Munk, W. H., Low-Frequency Tail of Wave Spectra, 6th Naval Hydrodynamics Symposium, 1966.
- Myers, J. J., C. H. Holm, and R. F. McAllister, Handbook of Ocean and Underwater Engineering, McGraw Hill, 1100 p. 1969.
- Namias, J., Recent seasonal interactions between north Pacific waters and the overlying atmospheric circulation, J. Geophys. Res, 64, 631-646, 1959.
- Nathan, A., Geodetic and Oceanographic Applications of Satellite Radar Altimetry, Trans Amer Geophys Un, 48, 126, 1967.
- Neumann, G., and W. J. Pierson, Principles of Physical Oceanography, 545 p, Prentice-Hall 1966.
- Nowroozi, A. A., M. Ewing, J. E. Nafe, and M. Fliegel, Deep Ocean current and its correlation with the ocean tide off the coast of northern California, J. Geophys. Res. 73, 1921, 1968.
- Orlin, H., Gravity sensing instruments, Trans Am Geophys Un, 48, 351-355, 1967.
- Phillips, O. M., On internal wave interactions, Sixth Hydrodynamics Symposium, 1966.
- Phillips, O. M., Dynamics of the Upper Ocean, Cambridge, 1966.

Pierson, W. J., An interpretation of the observable properties of sea waves in terms of the energy spectrum of a Gaussian record, Trans Amer Geophys Union, 35, 747, 1954.

Pierson, W. J., and L. Moskowitz, A proposed spectral form for fully developed wind seas based on the similarity theory of Kitaigorodskii, J. Geophys. Res. 69, 5181, 1964.

Pierson, W. J., L. J. Tick, and L. Baer, Computer-based procedures for preparing global wave forecasts and wind field analyses capable of using wave data obtained by a spacecraft, Sixth Naval Hydrodynamic Symposium, 1966.

Pierson, W. J., Gravity Waves, Trans Amer Geophys Union, 48, 584-588, 1967.

Rapp, R. H., The equatorial radius of the Earth and the zero-order undulations of the geoid, J. Geophys. Res. 72, 589-593, 1967.

Ross, D. B., Recent Developments in Remote Sensing of Deep Ocean Waves, USNOO, 1967.

Rouse, J. W., et al, Use of Orbital Radars for Geoscience Investigations, Proc Third Space Cong, 77-94, 1966.

Runcorn, S. K., Satellite gravity observations and convection in the mantle, in World Rift System, Can Geol Surv Ppr 66-14, 364-372, 1966.

Runcorn, S. K., Satellite gravity measurements and a laminar viscous flow model of the Earth's mantle, J. Geophys. Res. 64, 4389-4394, 1964.

Scheffer, V., The relation between the European geoid undulations and the distribution of the terrestrial heat flow values, Acad Sci Hung Acta Geod, 1, 43-48, 1966.

Scheibe, D. M., and H. W. Howard, Classical Methods for Reduction of Gravity Observations, USAF, ACID Ref Publ 12, 65 p, 1964.

Schmid, H. H., Geodetic Satellites: Reduction of geometric data, Trans Amer Geophys Un, 48, 333-337, 1967.

- Schooley, A. H., Radiation measurements at sea, J. Geophys. Res. 74, 958-961, 1969.
- Scherhag, R., Daily weather maps, J. Geophys. Res. 74, 1704, 1969.
- Schwartz, R. J., and J. M. Marchello, Onset of wind-driven waves, JGR, 73, 5133-5143, 1968.
- Shepard, T. P., Submarine Geology, Harper and Row, 2nd ed, 557 p, 1963.
- Slichter, L. B., Earth tides, Trans Amer Geophys Un, 48, 355-357, 1967.
- Smathers, S. E., et al, Preliminary Measurements with a laser geodimeter, ESSA Tech 1, 1966.
- Stewart, H. B., Sea level and tsunamis, in Oceanography from Space, WHOI, 1965.
- Stillwell, D., Directional energy spectra of the sea from photographs, Jour Geophys Res, 74, 1974-1986, 1969.
- Strange, W. E., A comparison of satellite gravity with surface gravity and other physical parameters, in SAO Spl Rpt 237, 1967.
- USNOO, Techniques of Forecasting Wind Waves and Swell, H. O. Pub. 604, 1966.
- Van Bemmelen, R. W., On the interpretation of the apparent form of the geoid and of the terrestrial heat flow, Tectonophysics, 4, 101-106, 1967.
- Van Bemmelen, R. W., The evolution of mega-undations: a mechanical model for large-scale geodynamic phenomena, in World Rift Systems, Can Geol Sur Ppr 66-14, 373-399, 1966.
- Von Arx, W. S., An Introduction to Physical Oceanography, Addison-Wesley, 422 p, 1962.
- Vastano, A. C., and R. O. Reid, Tsunami response for islands, Jour Mar Res, 25, 1967.



Von Arx, W.S., Absolute dynamic topography, Soc Limnol and Oceanog, 10, R265-R273, 1965.

Wang, C.Y., On the Distribution of Surface Heat Flows and the Second Order Variations in the External Gravitational Field, SAO Spl Rpt 134, 13 p, 1963.

Warnecke, G., Interconnections between the extra-tropical and the tropical circulation as revealed by satellite observations, Trans Amer Geophys Un, 49, 183, 1968.

Waters, O.D., Ocean Science Program of U.S. Navy, USNOO, 1967.

WDC, Catalogue of Data Oceanography, World Data Center, A, 1967.

Wexler, H., and J.E. Coskey, Rocket and Satellite Meteorology, North-Holland, 1963.

Williams, G.F. Microwave radiometry of the ocean and the possibility of marine wind velocity determination from satellite observations, JGR, 18, 4591-4594, 1969.

Wolff, P.M., et al, Synoptic Analyses and Prediction of Conditions and Processes in the Surface Layers of the Sea, Fleet Numerical Weather Facility, Monterey, 1967.

Worzel, J.L., and J.C. Harrison, Gravity at sea, in The Sea, vol 3, Wiley, 134-174, 1963.

Wu, J., Wind stress and surface roughness at air-sea interface, J. Geophys Res. 74, 444-455, 1969.

Wunderlich, H.G., On the meaning of the geoid and heat flow anomalies of the Earth, Tectonophysics, 4, 107-115, 1967.

Zetler, B.D., Tides and other long period waves, Trans Amer Geophys Un, 48, 591-595, 1967.

APPENDIX P  
SURFACE VERIFICATION OF ALTITUDE UTILIZING  
ALTIMETER SIGNAL\*

Satellite altitude verification utilizing the altimeter signal could be performed either from the satellite or from the surface. Performing the measurement from the altimeter (using, for example, transponders on the surface) complicates the altimeter excessively. It would be simpler for satellite instrumentation if the altitude were determined at the surface. There are several ways of doing this; the two most easily put into practice are one in which ground clocks and satellite clocks are synchronized, and one in which only the ground clocks are synchronized. Both shall be considered but only to the extent of outlining the method and identifying the major difficulties.

1. All Clocks Synchronized (Calibrated)

Consider a satellite containing an electronic oscillator with short-term (1-second) stability of 1 part in  $10^{11}$  and with long-term (1 month) stability of 1 part in  $10^{10}$ . Also consider a set of three (Earth) surface radio receivers and oscillators with the same characteristics. Oscillators with stabilities as good as this or better are already available on the commercial market, and an oscillator of 1 in  $10^{11}$  stability is in fact specified for GEOS-C. A typical rubidium frequency standard (Ref.C-7) which is very conservatively rated quotes stabilities of  $6 \cdot 10^{-12}$  per second and  $6 \cdot 10^{-11}$  per year, with setting accuracy of  $2 \cdot 10^{-12}$ . The satellite clock emits pulses 1 second apart in time; these are received at the surface radio receivers, and sent to oscillator-controlled counters, and time of arrival noted. Assuming a requirement that the distance from satellite to surface station be in error by no more than 1 meter, the time of transit of the signal from satellite to surface station should be in error by less than 3 nsec. Assuming a stability (over 1 second) of  $\pm 6 \cdot 10^{-12}$ , a 3 nsec.

---

\* See also Appendix C

error will have accumulated after 4 days. A synchronization of satellite and surface clocks every 2 days is therefore sufficient. Synchronization of the surface clocks with a common master clock to 100 nsec. is already being done (1969 - frequency) by secondary standards laboratories; synchronization to 1 nsec. is entirely feasible. Getting synchronization between the surface clocks themselves to better than 1 nsec. is of course a simple matter if the clocks can (and in the present scheme that is the case) be brought together periodically for checking.

In the ideal case, the location of the altimeter is then determined by the set of three equations

$$\Delta t_i = \frac{1}{c} \sqrt{\sum_j (\chi_{sj} - \chi_{ij})^2} \quad i, j = 1, 3$$

where  $\{\chi_{sj}\}$  and  $\{\chi_{ij}\}$  are the coordinates of the satellite and of receiver  $i$ , respectively, and  $\Delta t_i$  is the time difference at receiver  $i$  between time of transmission of pulse and time of reception. In the actual case, these equations will have to be modified to allow for, among other things,

1. non-instantaneous pulse rise time;
2. refractive index of atmosphere;
3. transmitter, receiver, and counter delay times  $\xi$  and calibration constants;
4. frequency calibration constants;
5. doppler shift in frequency, as it affects pulse shape.

This method is simple, accurate, and inexpensive. It makes use, with little modification, of the altimeter as a clock-pulse source, so that the satellite portion of the system is already in existence. The major drawback is in the need for keeping synchronization between satellite clock and surface counters for two years. Once the satellite clock has left the ground, it is no longer available for adjustment or for synchronization in proximity to surface

clocks. After a few days, therefore, the satellite clock will no longer be synchronized with ground clocks but must be calibrated against them. The problem of calibration is not difficult but will require introduction of a time-standard station into the general verification.

Using time-standard stations with artificial satellites for world-wide calibration of time is not a new idea; it has often been suggested ever since artificial satellites were first proposed. Using the stations for the double purpose of time and altimeter calibration is therefore a minor extension of the time calibration scheme and has undoubtedly been suggested already by others in slightly different forms.

Suppose there is a time-standard station close to a radar station within the zone covered by a satellite. If the radar station range error,  $\sigma_r$ , is  $\pm 1$  meter, the uncertainty  $\sigma_t$  in the time of transmission of timing impulse from the satellite clock is

$$\sigma_t = \left( \frac{\sigma_r}{c} \right)^2 + \left( \frac{\sigma_c t_r}{c} \right)^2$$

where  $\sigma_c$  is the standard deviation in the velocity of light,  $c$ , and  $\left( \frac{\sigma_c}{c} \right)$  is reported in recent literature as  $3 \times 10^{-7}$ . The range time,  $t_r$ , is given by  $\frac{r}{c}$ , where  $r$  is the range. Then

$$\begin{aligned} \sigma_t &= \frac{1}{c} \sqrt{\sigma_r^2 + \left( \frac{\sigma_c r}{c} \right)^2} \\ &= \frac{1}{3 \times 10^8} \sqrt{1 + (3 \times 10^{-7} \times 10^6)^2} \\ &= 3 \times 10^{-9} \text{ sec} \end{aligned}$$

so the second term in  $\sigma_t$  does not contribute significantly.

Assuming a frequency variations of better than  $1.10^{-11}$  per day, and assuming that the time-standard station is able to check the time at least once per day, the time error between check times is less than  $3.10^{-8}$  second or, in distance, about 9 m. The r.m.s. error half-way between check times is of course more significant; this is about 5 m, and represents the error incurred by an observation that was made 12 hours after a time-check. Most stations should be able to make their observations within three revolutions of the satellite after a time check; for these the r.m.s. error is less than 3 meters. The principal stations in the Caribbean could be caught on the first or second revolution by a time standard station tied to the US Naval Observatory.

## 2. Only Surface Clocks Synchronized (Calibrated)

The second method does not require that the surface station time be synchronized with or calibrated against the satellite time or even that the satellite pulses be regular. This considerably eases the calibration problem since calibration of the satellite clock is otherwise the most difficult part of the experiment. But the experiment pays for the greater ease of calibration by losing, in effect, one coordinate of the altimeter. Consider three cases:

1. There are three stations at the surface and no knowledge of altimeter pulse transmission times is assumed;
2. there are three stations, and the altimeter pulses are assumed to be sent out at intervals of precisely  $\Delta t_s$  seconds, although the times of emission are irrelevant;
3. there are four non-coplanar stations.

These time differences constitute the observations; they are converted to distance differences by multiplying the average signal transit speeds over the respective paths. The three distance differences are not independent, since any one can be found by differencing the other two. Hence only two independent functions relating  $d_1$ ,  $d_2$ , and  $d_3$  can be found. Each of these functions locates the source on the surface of a hyperboloid of revolution with

the corresponding pair of surface receivers as foci, so that the two functions together locate the source on a space curve that is the intersection of two hyperboloids. In order for a complete set of three coordinates to be found, an independent measurement must be available. The simplest way of getting an independent measure is to use a range-measurement from a radar or laser ranging station; or a direction from a Baker-Nunn ballistic camera station.

#### B. Three Surface Clocks Synchronized; Altimeter Pulses at Equal Intervals

In Case 1 above no special requirement was laid on the altimeter pulses other than the obvious ones that they be sharp and of adequate strength. As a consequence, each set of three (two independent) time differences had to be accompanied by an independent measure of distance or direction. If a condition is set that the altimeter pulses be emitted at precisely-spaced ( $\pm 3$  nsec.) intervals, all but one independent range or direction measurement can be dispensed with. This is because the equation

$$d_1 = d_0 + \sum \Delta t_j \cdot c_1$$

defines a set of spheres about point  $P_1$  (for example). The reference sphere of radius  $d_0$  is established from an independent range or direction measurement; the intervals  $\Delta t_j \cdot c_1$  are determined by the increase or decrease  $\Delta t_j$  between the observed intervals between pulse reception and the known intervals between emission.

#### C. Four Synchronized Surface Clocks

The last case is mentioned because it has a theoretical interest and a possible future application, although no practical way of applying it at present is known. As shown for Case 1 above, three surface stations provide two altimeter coordinates. The third coordinate can be found, if there is a fourth time difference.

$$\Delta \tau_4 = (d_1 - d_4)/c_4,$$

provided point  $P_4$  is not coplanar with points  $P_1, P_2, P_3$ . A rigorous analysis of the altimeter location errors resulting from time interval measurement errors for different arrangements of the surface points is not necessary. It is obvious that any arrangement leading to acceptably small errors in altimeter location would require  $P$  to be at distances above the  $P_1 P_2 P_3$  plane not achievable with a surface location for  $P_4$ . Only if  $P_4$  were itself a satellite point would reasonable errors result, and such an arrangement is not relevant to the GEOS-C verification experiment.

Of the three different cases described above, that requiring only synchronization among surface clocks (Case 2) appears to be the one most readily realized. In the western portion of the Caribbean the relation of radar stations to the clock stations would be poor, but the optical tracking station relationships would be excellent. Nevertheless, the advantage of requiring only one simultaneous range or direction measurement per pass over the clock stations rather than a range or direction measurement with every time difference measurement is so great that the system of Case 2 above is recommended rather than that of Case 1.

APPENDIX Q  
TROPOSPHERIC AND IONOSPHERIC EFFECTS

Q-1 Summary

An analysis was performed of the influences of the troposphere and ionosphere in the determination of range from a satellite at close to vertical incidence. The standard deviation in the determination of one-way atmospheric error is estimated at 30 cm at 3 GHz and 4.5 cm at 10 GHz.

Q-2 Introduction

In a number of projects, the accurate determination of range from a satellite to a known reference related to the earth is of fundamental importance. Such projects include satellite geodesy and Very Long Base-Line Interferometers (VLBI). With desired ultimate accuracies for these applications on the order of a few centimeters<sup>1</sup>, the necessity for assessing and correcting range errors resulting from atmospheric uncertainties becomes extremely important. It is the purpose here to summarize the magnitude of these errors.

Interest for this study is centered on the microwave portion of the RF spectrum. The two regions of the earth's atmosphere which produce significant refractive errors, (hence range errors), are the troposphere and the ionosphere, particularly the  $F_2$  region, which exhibits the maximum ionosphere electron density.

Q-3 Tropospheric Errors

The influence of the troposphere is such as to produce an estimated positive one-way bias error in range at zenith of approximately 2.4 meters. The standard error of the estimate is  $3.7 \text{ cm}^2$ . The bias error is positive,



indicating that the troposphere slows down RF energy traversing it thus making the estimate of range an overestimate. The troposphere is nondispersive, at least up to 20 GHz, and probably into the millimeter wave region. The limiting factors in the determination of refractivity  $N_s$  are the measurement of the physical parameters of the atmosphere at sea level, (total air pressure, temperature, and relative humidity), with relative humidity exerting the greater influence<sup>2</sup>. These errors are summarized in Table Q-1.

Table Q-1  
One-Way Troposphere-Induced Range Errors (m)

<u>Frequency GHz</u>	<u>Tropospheric Bias Error (m)</u>	<u>Tropospheric Standard Deviation (m)</u>
3	+2.4	0.037
7	+2.4	0.037
10	+2.4	0.037

#### Q-4 Ionospheric Errors

The ionosphere is a dispersive medium and errors in range in the microwave region are inversely proportional to the square of the carrier-frequency. At zenith, the one-way bias error (which is negative) ranges from 0.1 meters at X-band (10 GHz) to 1.3 meters at S-band (3 GHz) assuming daylight operation. At night, the range is from 0.1 to 0.8 meters respectively.

If the electron density profile at a given location and time were precisely known, the standard error of the estimate in range would be negligible. Taking into account all that is predictable about the pertinent ionospheric parameters at microwave frequencies, such as the maximum electron density of the  $F_2$  layer, these parameters can be predicted at best to provide a fluctuation error which is  $\pm 50\%$  of the bias error<sup>1</sup>.

Ionospheric data from the world-wide network of land-based vertical ionosondes is capable of specifying pertinent ionospheric parameters to provide a fluctuation error which is within  $\pm 25\%$  of the bias error<sup>1</sup>.

Thus, standard one-way errors in estimates can be expected to be from 2.5 cm at X-band to 30. cm at S-band, as shown in Table Q-2. for daytime (worst case).

Table Q-2  
One-Way Ionosphere-Induced Range Errors (m)

<u>Frequency (GHz)</u>	<u>Ionospheric Bias Error (m)</u>	<u>Ionospheric Standard Deviation (m)</u>
3	+1.3	0.30
7	0.2	.05
10	+0.1	0.025

#### Q-5 Total Atmospheric Errors

Based upon available state-of-the-art techniques and data, Table Q-3 shows the expected bias and standard errors induced by the atmosphere in determining range from a satellite at zenith to established reference level, (such as the geoid) using carrier frequencies between 3 and 10 GHz. More accurate information is dependent primarily upon better information about the ionosphere at specific location and time.

If the standard errors in range estimates for troposphere and ionosphere are assumed to be independent, the total standard errors in range estimate are on the order of 4.5 cm at X-band and 30 cm at S-band. If the standard errors are assumed to be Gaussian, then using all data that normally exists, over 99% of the one-way errors are expected to be less than 14 cm at X-band ( $3\sigma$ ).

Table Q-3  
One-Way Atmospherically-Induced Range Errors (m)

<u>Frequency (GHz)</u>	<u>Atmospheric Bias Error (m)</u>	<u>Atmospheric Standard Deviation (m)</u>
3	+3.7	0.30
7	2.6	.062
10	+2.5	0.045

If special instrumentation is employed, such as a radar to make back-scatter measurements near the location, the standard error would probably be reduced to 12 cm.

#### Q-6 Ionospheric Effects on Range Estimation

When radar measurements are made on targets above 100 km, the effects of the ionospheric layers must be considered. Refractivity, the main effect of the ionosphere, is a function of frequency:

$$N_i = (n-1) \times 10^6 \approx \frac{1}{2} \frac{f_c^2}{f} \quad (Q-1)$$

Where

- $N_i$  = refractivity of ionosphere
- $n$  = refractive index
- $f_c$  = critical frequency
- $f$  = frequency (8 to 10 GHz for VEDS)

The critical frequency,  $f_c$ , is solved in the following manner:

$$\omega_c^2 = (2\pi)^2 f_c^2 = \frac{N_e e^2}{\epsilon_o m} \quad (Q-2)$$

Where

- $\omega_c$  = angular frequency
- $N_e$  = electron density per  $m^3$
- $e/m$  =  $1.759 \times 10^{11}$  coulomb/kg
- $e$  =  $1.602 \times 10^{-19}$  coulomb (electron charge)
- $\epsilon_o$  =  $\frac{1}{36\pi} \times 10^{-9}$  farad/m

$$\therefore f_c^2 = \frac{N_e e^2}{4\pi^2 \epsilon_o m} \quad (Q-3)$$

$$\therefore f_c^2 = (80.727) N_e \quad (Q-4)$$

$$\therefore N_i = \frac{1}{2} \frac{(80.727) N_e}{f^2} \quad (Q-5)$$

The range bias error,  $\Delta R$ , is found in the following manner:

$$\Delta R = \frac{1}{2f^2} \int f_c^2 dS \quad (Q-6)$$

$$\approx \frac{40.4}{f^2} \int N_e(z) dz \text{ (at } 90^\circ \text{ elevation angle)} \quad (Q-7)$$

Where

$S$  = the slant range distance between target and observer

$z$  = the vertical distance between target and observer  
(elevation angle =  $90^\circ$ )

Figure Q-1<sup>3</sup> shows typical day and night profiles of electron density vs altitude based on backscattering data (Bowles 1961).

Expressing electron density as per  $\text{cm}^3$  rather than as per  $\text{m}^3$ , equation (7) becomes:

$$\Delta R = \frac{40.4 \times 10^6}{f^2} \int N_e'(z) dz \quad (Q-8)$$

If a parabolic profile for electron density (see Figure Q-1) is assumed for both the day and nighttime data, we get:

a. During daylight conditions

$$N_e' = - \frac{16 z^2 - (9.6 \times 10^6)z + 12.4 \times 10^{11}}{10^5} \quad (Q-9)$$

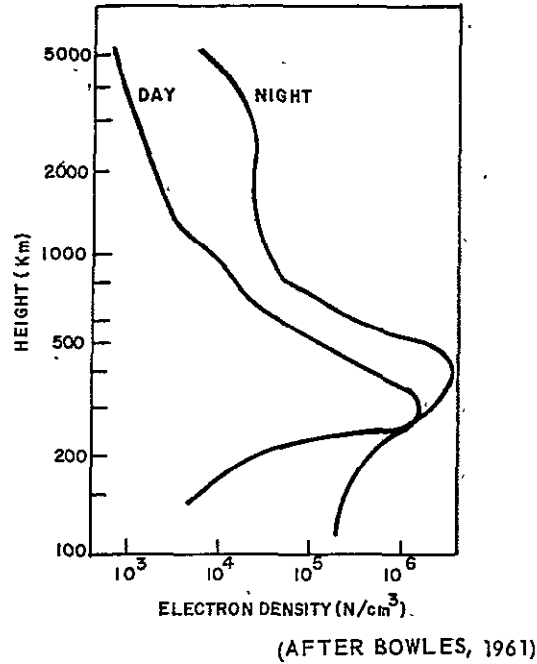


Figure Q-1. Typical Day and Night Profiles:  
Electron Density vs. Altitude.

b. During night conditions

$$N_e = - \frac{3 z^2 - 2.4 \cdot 10^6 z + 4.0 \times 10^{11}}{10^5} \quad (Q-10)$$

After examining Figure Q-1, it can be seen that the ionosphere will have its greatest effect during the day from about 200 km to 400 km. During the night, these limits are from 250 km to 500 km. These values were used as integration limits in equation (Q-8).

#### Q-7 Tropospheric Effects on Range Estimation

Range error in the troposphere is due to refraction and geometric range errors. Since the geometric range error is only significant for elevation angles of less than 3°, this Appendix analyzes only the error due to refraction<sup>2</sup>. The following analysis is only valid for frequencies less than 30 GHz because of the dispersive effects of the 22.5 GHz water vapor absorption line and the 60 GHz oxygen absorption line<sup>2</sup>.

In the temperature range of -50°C to 40°C, the refractivity of the troposphere can be expressed with an error of less than 0.3 percent as<sup>4</sup>:

$$N_t = (n-1) \times 10^6 = \frac{K_1}{T} \left( P + \frac{K_2 e}{T} \right) \quad (Q-11)$$

where

- $N_t$  = refractivity (meters)
- $n$  = refractive index
- $T$  = temperature (° Kelvin)
- $P$  = total atmospheric pressure (millibars)
- $e$  = partial water vapor pressure (millibars)

Using the "Smith and Weintraub" constants for  $K_1$  and  $K_2$ , the following expression is obtained:

$$N = \frac{77.6}{T} \left( P + \frac{4810e}{T} \right) \quad (Q-12)$$

The above equation is sometimes written as:

$$N = \frac{77.6}{T} \left( P + \frac{4810e}{T} \right) (RH) \quad (Q-13)$$

where

$e_s$  = the saturation vapor pressure in millibars at temperature T

RH = relative humidity in percent.

Equation (Q-13) is the refractivity at any given point. To find the range error due to the total troposphere, the refractivity must be summed over the entire troposphere:

$$\Delta R = 10^{-6} \int_0^{h_t} N \csc \theta \, dh \quad (Q-14)$$

where

$\Delta R$  = range error

$h_t$  = height of troposphere

$\theta$  = elevation angle

For VEDS,  $\theta = 90^\circ \therefore \csc \theta = 1$ . Therefore, equation (Q-14) can be expressed as:

$$\Delta R = 10^{-6} \int_0^{h_t} N \, dh \quad (Q-15)$$

This equation can be approximated by the following equation (see Figure Q-1<sup>2</sup>).

$$\Delta R = 1.4588 + 0.0029611 N_s \text{ (meters) (one-way error)} \quad (Q-16)$$

where

$N_s$  = surface refractivity.

At sea level,  $N_s$  is typically between 300 and 350 <sup>3</sup>. Results of a large number of observations of surface refractivity have been published, (Bean, Horn, and Ozanich, 1960), which show variations in  $N_s$  as a function of time and of season, with diurnal changes of 20 to 40 N-units peak to peak, added to seasonal changes of about 10 N-units rms <sup>3</sup>. Thus, at a given site, the refractivity may change by 100 N-units or more during the course of a year. Therefore, the range of  $N_s$  at sea level should vary at the most from 250 N (i. e., 300-50) to 400 N (i. e., 350+50), with a two-way range correction factor of about 4.3 meters to 5.3 meters (using equation (Q-16).

#### Q-8 Errors in Measurement of N

The degree of accuracy of the measurement of N is a function of the accuracies of the sensors for sea level conditions, and is found by differentiating equation (Q-12):

$$dN = \frac{\partial N}{\partial T} dT + \frac{\partial N}{\partial e} de + \frac{\partial N}{\partial P} dP \quad (Q-17)$$

or:

$$\Delta N = a \Delta T + b \Delta e + c \Delta P \quad (Q-18)$$

Typical values of the constants a, b, and c based on the International Civil Aviation Organization (ICAO) are shown in Table Q-4.

Table Q-4

Values of Constants a, b, and c Based on ICAO

<u>Alt. (km)</u>	<u>Temp. (°C)</u>	<u>e (mb)</u>	<u>RH (%)</u>	<u>P (mb)</u>	<u>a</u>	<u>b</u>	<u>c</u>
0	15.0	10.2	60	1013	-1.27	4.50	0.27



The ICAO has found that the effect of pressure variation is relatively constant with altitude; the effect of water vapor pressure increases with altitude.

The indirect method of obtaining the above parameters is through standard weather observations. While fairly accurate measurements of atmospheric pressure and temperature are readily obtained, relative humidity measurements are only accurate to a few percent giving an optimistic measurement accuracy of the refractive index to approximately  $\pm 1.0$  N units and a very pessimistic accuracy of  $\pm 15.0$  N units<sup>4</sup>. (An error of  $\pm 30$  N units would result in a one-way  $\Delta R$  error of  $\pm 0.1$  meters.) Another source of data is the current world-wide system of radiosondes which measure temperature, pressure and humidity. The standard deviation in the determination of refractivity from radiosonde data "under ideal conditions" at sea level is approximately 3 N units.

Direct measurements of refractivity through the use of refractometers are relatively expensive, somewhat complex, and require technical personnel to maintain, calibrate, and operate them<sup>4</sup>. For these reasons, the increased accuracy obtained from refractometers do not warrant their use for VEDS. It appears that both current and synoptic data from the world-wide weather services will be accurate enough to obtain the two-way error to  $\pm 0.2$  meter.

## APPENDIX Q

### REFERENCES

- "The Long-Baseline Radio Interferometer and Methods for Refractive Corrections," M. R. Pearlman & M. D. Grossi, Paper presented at the International Symposium on Electromagnetic Distance Measurement and Atmospheric Refraction, Boulder, Colorado, 23-27 June 1969.
2. Bean, B., and Dutton, E., Radio Meteorology, National Bureau of Standards Monograph 92, 1966, p. 337, 2, 339.
  3. Barton, D., and Ward, H., Handbook of Radar Measurement, Prentice Hall, 1969, p. 388, 366, 370.
  4. McGavin, R., Measuring the Radio Refractive Index, p. 1, 26, 5ff.

# APPENDIX R CONTRIBUTIONS TO MEAN SEA LEVEL IN THE OPEN OCEAN

This section presents a brief enumeration of the factors which contribute to mean sea level in ocean areas in general (i. e., open ocean, not too close to shore). The orders of magnitude of the effects vary greatly depending on specific location.

## R-1 Errors in the Determination of Mean Sea Level Due to Wind Waves

A radar at incident angles near vertical operating at centimeter wavelengths views an ocean surface which is almost always rough. The following discussion will attempt to quantify that statement.

The wind-driven sea surface is best represented as a random process. This is true with the possible exception of a duration-limited sea<sup>1</sup>. At most frequencies lower than the microwave region, (f 1 GHz), the probability distributions representing elevation can be assumed Gaussian. Such a representation is:

$$P(H)dH = (2\pi\sigma^2)^{-1/2} \exp\left(-\frac{H^2}{2\sigma^2}\right) \quad (R-1)$$

where

$P(H)$  = Probability that a given wave height, will occur between  $H$  and  $(H+dH)$ ,  
and  $\sigma^2$  = Second moment of surface height distribution.

Equation (T-1) is adjusted to assume that  $\bar{H}$ , (Instantaneous Mean Sea Level), is zero (i. e., that the sea surface varies about instantaneous mean level).

Thus, considering the effect of the wind-driven sea surface on the radar returns, the period,  $T$ , of a surface is analogous to the correlation distance; and wave

height,  $H$ , corresponds to  $2\sigma(2)$ . The roughness criterion under these conditions becomes:

$$\frac{4\pi H \cos \theta}{\lambda} \leq 1.57 = \pi/2, \quad (R-2)$$

for a surface to be smooth. Except for the extremely rare case of a perfectly calm sea, this criterion is never satisfied for a wind-driven sea. For example, when  $\lambda = 3$  cm.,  $H = 0.3$  cm, (Sea State 1),  $\theta$  (Incident Angle) =  $0^\circ$ ,

$$\frac{4\pi H \cos \theta}{\lambda} = 126.$$

The representation of the sea surface by a symmetrical distribution, such as the Gaussian distribution of Equation (T-1) is not adequate in the case of centimeter radar wavelengths, since it fails to account properly for capillary waves, whose wavelengths are of the same order of magnitude as the X-band radar wavelengths.

If this probability distribution is symmetrical, up to the first order, the radar measurement of height above the surface will be a height above instantaneous mean sea level (IMSL). This ignores effects such as differences in reflection characteristics between the crest and troughs of the waves. It may be that these effects are relatively unimportant; i.e., of second order. Failure of the radar to measure IMSL can then be calculated by the asymmetries in the actual measured probability distribution representing waves. There have been very few detailed measurements made of this phenomenon. One set of results is shown in Figure R-1, which shows the result of a detailed statistical analysis of measured waves<sup>1</sup>. The writer has not been able to find any probability distribution describing wave slope as a function of height with respect to IMSL.

The error  $\sigma_w$ , due to asymmetry in the water surface distribution is given by:

$$\sigma_w = \frac{\gamma_1 \sigma}{2} \quad \text{where} \quad (R-3)$$

$\gamma_1$  = Skewness factor, and

$\sigma$  = Standard deviation of wave height.

Total number of data points	11,786
Mean anemometer height (m)	1.21
Mean wind speed (m/sec)	4.63
Mean air temperature (C)	27.64
Mean water temperature (C)	26.68
Mean estimated fetch(m)	2100

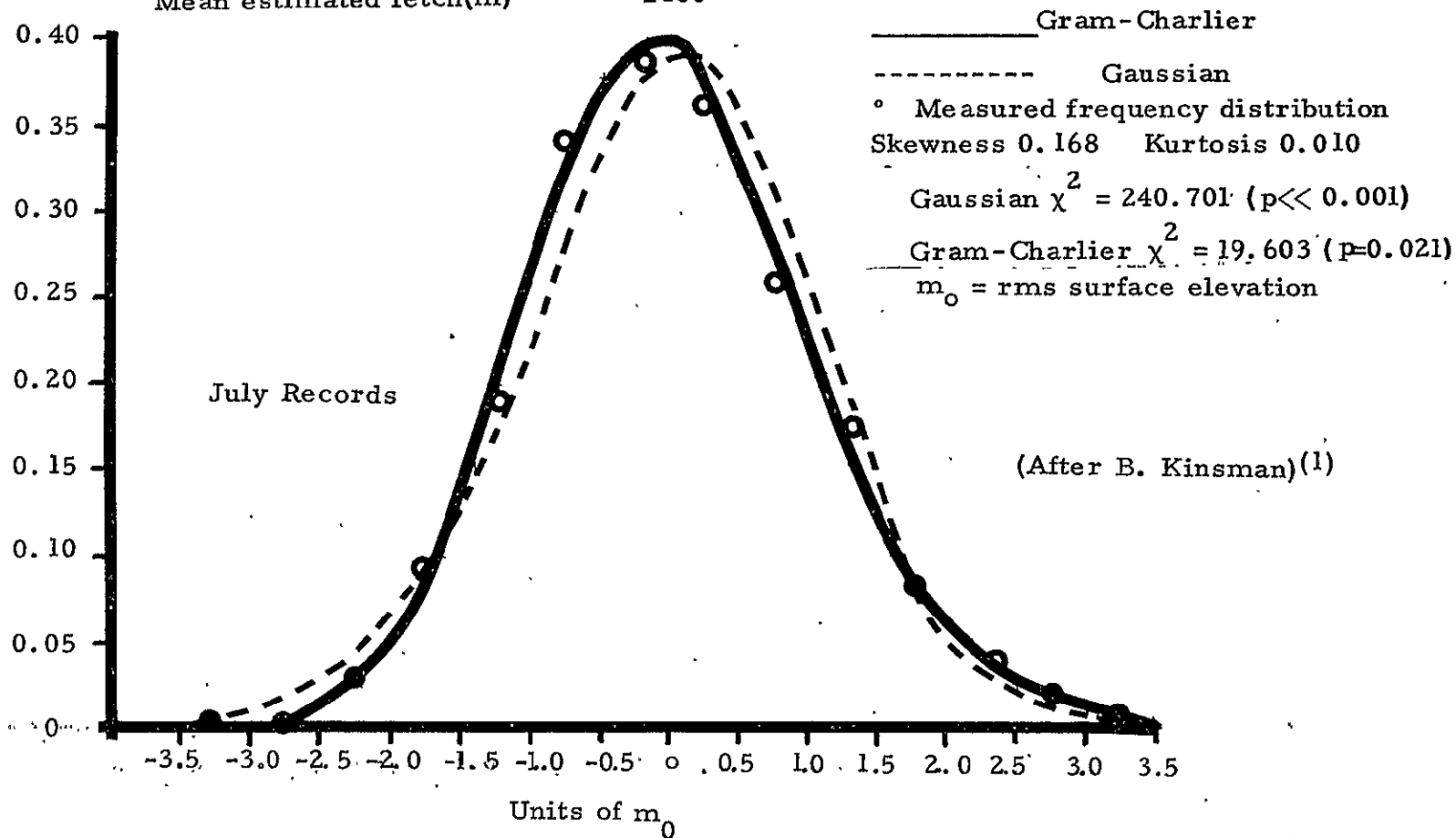


Figure R-1A. Distributions of Water Surface Displacement (July)

Total number of data points	12,634
Mean anemometer height (m)	1.25
Mean wind speed(m/sec)	7.05
Mean air temperature at 2.25m (C)	10.45
Mean air temperature at 0.50m (C)	10.22
Mean water temperature (C)	12.65
Mean estimated fetch (m)	2800

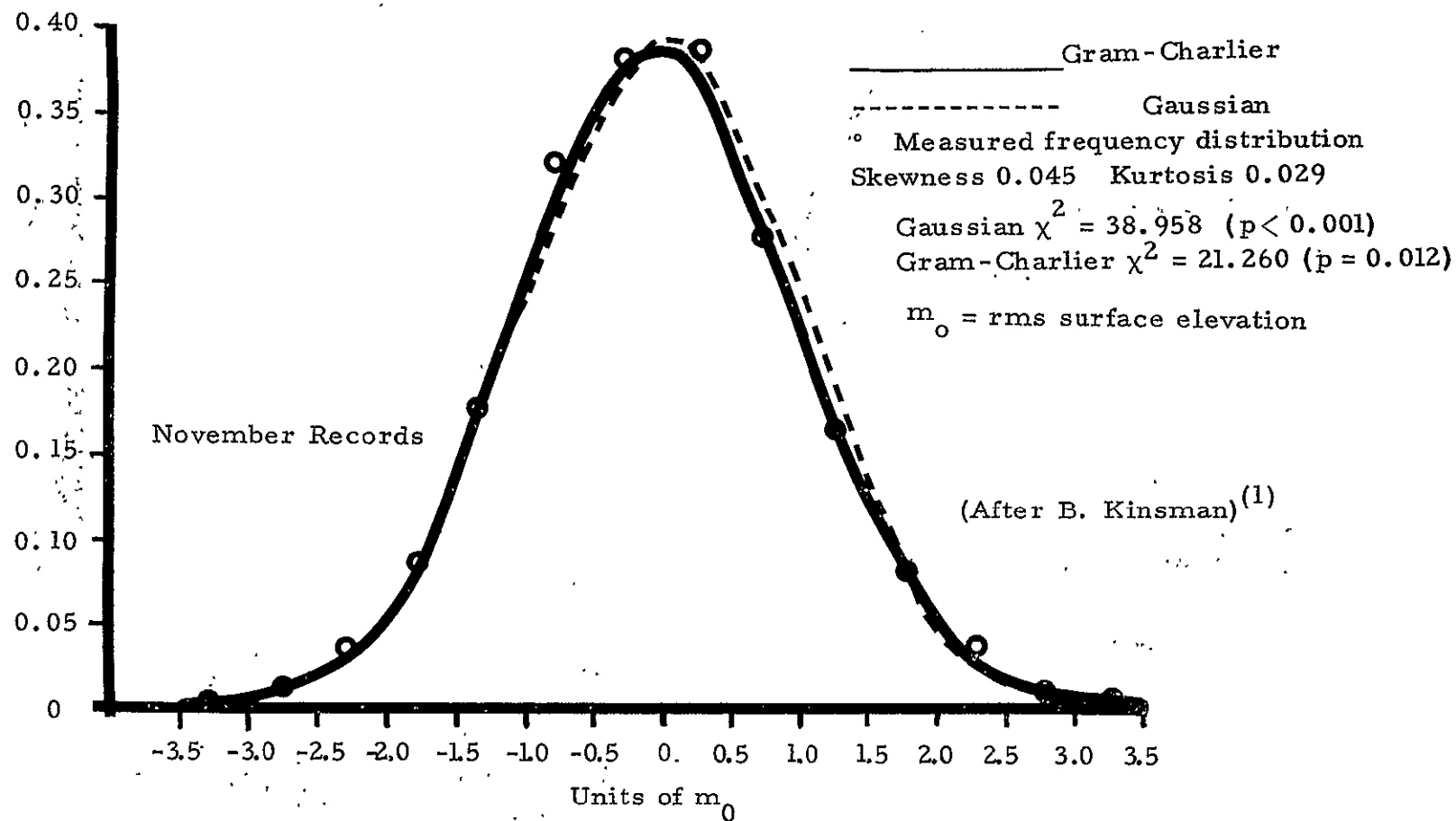


Figure R-1B. Distributions of Water Surface Displacement (November)

It is seen from Equation (R-3) that the displacement error is proportional to the sea state. If it is assumed that  $\gamma_1$  does not vary with sea state, then the error in radar measurement due to waves,  $\sigma_w$  for the case of Figure R-1, (July), and a wave  $\sigma$  of 6 meters (Code 6):

$$\sigma_w = \frac{(0.168)(6)}{4} = 0.252 \text{ meters.}$$
 In the absence of wave slope data this value will be taken to be an estimate of the fluctuation error in IMSL due to waves, since it describes the asymmetrical wave shape.

## R-2. The Influence of Factors Other Than Waves

In reference 3 a total of 11 factors were listed as influencing mean sea level. These factors were:

- Long Period Changes
- Coriolis Effect
- Waves
- Tides
- Tsunamis
- Storm Tides
- Meteorologic Effects
- Solar Activity
- Specific Volume (Temperature/Salinity)
- Earth Tides
- Gravitational Anomalies

The influence of each of these factors will be discussed in turn.

### R-2.1 Long Period Changes

Long period changes in mean sea level have been observed to range about 200 meters total. In the present geological era, this change has been observed over the last 50 years to correspond to an increase of 1.2 mm/year.

### R-2.2 Coriolis Effect

Due to currents on a rotating earth, the Coriolis effect is to shift northward-bound currents in the northern hemisphere to the east. For example, the mean sea level is 590 mm higher in the Bahamas than it is in Miami due to the Gulf Stream. It will be assumed that measurements over seas containing appreciable currents will be excluded from consideration.

### R-2.3 Waves

These effects have been discussed in detail in Section 1. Waves of rms height up to 6 meters have been considered.

### R-2.4 Tides

The total tidal range in the open ocean, particularly in equatorial regions, is given in terms of the equilibrium tides. In the open ocean the magnitude of the range is 3.04 feet. \* If it is assumed that the tide at any point in the ocean can be estimated to within 25% of the range, the expected error due to tides in estimating mean sea level,  $\sigma_T = 0.25$  meters.

### R-2.5 Tsunamis

Although tsunamis have been known to reach shores with tremendous heights, they are only about a few feet high at sea.<sup>1</sup> This fact, coupled with their relatively infrequent occurrence should make their importance to an experiment negligible.

### R-2.6 Storm Tides

These phenomena are similar to tsunamis in their magnitude, although they occur more frequently. Being transient in nature, they can probably be neglected.

### R-2.7 Meteorologic Effects

Pressure changes have a direct influence on the ocean's surface. The sea acts as an inverted barometer, the surface rising approximately 1 cm for each millibar the air pressure falls.<sup>4</sup> In regions bounded by 20° N and 20° S latitude, the normal pressure variations are small, amounting to a maximum standard deviation of 4 millibars.<sup>5</sup> This corresponds, therefore, to a change of sea level of 4 cm.



The equilibrium tides due to moon and sun are given in Table R-1 below:

Table R-1.\* Equilibrium Tides Due to Moon and Sun

<u>Source</u>	<u>Rise (ft)</u>	<u>Fall (ft)</u>	<u>Total</u>
Moon	1.46	0.73	2.19
Sun	<u>0.57</u>	<u>0.28</u>	<u>0.85</u>
	2.03	1.01	3.04

\* Robert Cummings, United States Coast and Geodetic Survey, private communication.

#### R-2.8 Solar Activity

Sea level variations are known to occur during variations of solar activity. The amount of the annual variation is in the order of 5 cm.<sup>4</sup>

#### R-2.9 Specific Volume Changes due to Temperature and Salinity

Steric changes are the major contributions to the isostatic changes in mean sea level at low latitude. The total range of variation annually is on the order of 20 cm.<sup>6</sup>

#### R-2.10 Earth Tides

The solid portion of the earth's surface, the lithosphere, is also subject to tidal variation. Variations in height are thought to range from 7.3 to 40.4 cm. Very little measurements have been made to define the variation more carefully. The principal measuring instruments used in obtaining data are the horizontal pendulum, gravimeter, and the linear strain-seismometer.<sup>7</sup>

#### R-2.11 Gravitational Anomalies

Variations in the shape and mass of the lithosphere with respect to position also affect the position of IMSL. Determination of the geoid from a satellite are known to within  $\pm 20$  m of the true value. Other methods, such

as measurements on or near the ocean surface appear to predict the position of the geoid with respect to IMSL within  $\pm 2$  to  $\pm 3$  meters. With more knowledge of a particular geographic location, the uncertainty could be reduced to perhaps  $\pm 1$  m.<sup>8</sup>

### R-3 Summary

The various factors which influence IMSL variation can be grouped into three categories:

- Very Long Period Factors
- Moderately Long Period Factors
- Short Period Factors

#### R-3.1 Very Long Period Factors

These factors consist of those which have cyclic variations ranging from eons to years. They are very long in comparison to the GEOS measurement period, which is in the order of seconds. The factors which fit into this category include:

- Long period changes
- Changes due to solar activity variation
- Changes due to ocean currents (Coriolis effect)
- Gravitational anomalies

The first two factors should have little effect on VEDS. The third, the Coriolis effect, should be taken into account when a particular geographic location is considered for the experiment. The last, the variation in the Geoid is not a factor in a radar altimeter measurement which relates to IMSL.

#### R-3.2 Moderately Long Period Factors

Factors which have periods ranging from months to hours fit into this general category. Among these are:

Tsunamis  
Storm Tides  
Specific Volume  
Meteorologic  
Ocean Tides  
Earth Tides

Tsunamis and storm tides occur infrequently. It should generally be possible to predict their occurrence after the fact by using auxiliary weather data. Since the occurrence of these phenomena is so infrequent, measurements made when they occur can be eliminated 'a posteriori'.

Since the change in Specific Volume at low latitudes is small, it contributes little to the overall error in predicting IMSL at a specific point on the ocean at a given time. Pressure changes, (meteorological changes), occur on a continuous basis and can probably be predicted to some extent due to auxiliary data.

Tidal variations are well known in general, but less well known in particular for the deep ocean. Knowledge of the geographic location and time of measurement would be more effective in reducing the predicted variation in ocean tides than for earth tides, which are less well documented.

### R-3.3 Short Period Factors

Of all the factors discussed, Waves are the only phenomena whose periods are on the order of the satellite measurement period (i. e., seconds). Over a large enough area (e. g., an area on the ocean much larger than the satellite altimeter footprint.), there appears to be no evidence of measurable departure from IMSL with time. Thus, at present the IMSL variation due to Wind Waves is thought to be negligible.

However, since waves tend to depart from symmetry as their height increases, the distribution of slope with respect to IMSL will become asymmetrical, tending to introduce an error in radar measurement, as discussed in Section 4. Table R-2 is a summary of the various factors influencing IMSL.

Table R-2 summarizes contributions to the IMSL error. The root sum square of the estimated irreducible error is of the order of one-third of a meter.

Table R-2. Errors in Instantaneous Mean Sea Level (IMSL)  
Relative to Mean Sea Level (MSL) For Deep Oceans

	Factor	Maximum (Peak-to-Peak) Variation (m)	Estimated Irreducible rms Error (m)
Long Period	Long Period ( $10^2$ - $10^7$ yrs)	200	---
	Solar Activity (11 years)	0.2	0.1
	Ocean Currents (Coriolis)	---	---
	Gravitation (Geoid)	---	---
Moderate	Ocean Tides	1.0	0.30
	Earth Tides	0.4	0.20
	Meteorological (Pressure)	1.0	0.10
	Specific Volume (Temp/Salinity)	0.2	0.10
	Storm Tides	3.0	---
	Tsunamis	3.0	---
Short	Wind Waves	6 *	0.25*

\* Probability 0.9

## APPENDIX R

### REFERENCES

1. "Wind Waves - Their Generation and Propagation on the Ocean Surface, " B. Kinsman, Prentice-Hall, Inc., Englewood Cliffs, N.J., 1965, p. 330-331, 342-345, p. 15.
2. "The Scattering of Electromagnetic Waves from Rough Surface, " P. Beckman & A. Spizzichino, Pergamon Press, MacMillan Co., New York, 1963, pp. 90-91, 246-248, 477, 480.
3. "VEDS: Progress Report for August - Task 3.0 - Environmental Parameter Analysis, " W.A. Fordon, File No. SE 06-443, 12 September 1969.
4. "The Encyclopedia of Oceanography, " R. W. Fairbridge, Ed., Reinhold Publishing Corp., New York, (1966).
5. "Handbook of Geophysics, " United States Air Force, Air Research and Development Command, Air Research Division, Geophysics Research Directorate, The MacMillan Company, New York, 1961, p. 3-2, 3-3.
6. "The Principal Factors Influencing the Seasonal Oscillation of Sea Level, " E. Lisitzin & J. G. Pattullo, JGR, Vol. 66, No. 3, March 1969, pp. 845-852.
7. "Encyclopedia of Science & Technology, " McGraw-Hill, 1966, Vol. 4, pp. 346-351.
8. Private Communication, S. W. Henriksen.

## APPENDIX S

### THE FIGURE OF THE SEA: AN ESTIMATE OF ERROR

by W. S. von Arx

The satellite-borne radar altimeter measures the distance from the satellite to a small area of sea surface along a path very nearly parallel with the local spheroidal normal. This path is assured by the fact that, except for wind-waves and swell, the sea surface is everywhere convex upward -- even in regions of very strong free-air gravity anomaly -- with the result that the path of specular reflection will also be that of minimum distance or first return.

In this discussion it will be assumed that the sea surface is free of wind-waves and swell, i. e., is glassy smooth, and that the problem is to define the figure of the sea surface as a function of time in hours. It will also be assumed that the area of concern is one in which both the field of gravity and the various hydrographic and meteorological forces are well known -- the Caribbean for example.

#### Procedure

Step 1. Calculate, from the observed values of gravity<sup>1</sup> in the area, the free-air gravity anomaly field  $\Delta g = \gamma - \gamma_0$  where  $\gamma_0$  is some standard gravity value such as that given by the International Gravity Formula<sup>2</sup> of 1930 for  $f = 1/297$ .

Step 2. Calculate from the field of free-air gravity anomalies the corresponding deflections of vertical using the Vening Meinesz formulas<sup>2</sup> and from these the undulations of an equipotential surface.

Step 3. From available tide gauge records of at least 10 year's duration<sup>3</sup> in and around the Caribbean determine the long-term average water level; mean sea level, "MSL".

Step 4. From available oceanographic information<sup>4, 5, 6</sup> correct the MSL at each station for the specific volume anomaly of the regional water column, and from climatological mean values of atmospheric pressure<sup>7</sup> correct MSL to standard atmospheric pressure.

Step 5. Adjust the height of the equipotential surface found in step 2 to fit corrected MSL by least squares. This surface may be considered to represent the equipotential surface of the "standard ocean" and indeed to be virtually identical with the oceanographic geoid.

Step 6. Upon the assumption that the oceanographic geoid has the same figure as an equipotential surface at the "level of no motion," add the sea surface elevations contributed by

- a. the vertically integrated specific volume anomaly above the "level of no motion" in all interior ocean areas,
- b. the observed mean atmospheric pressure anomalies,
- c. the amphidromic contribution of the astronomical tide (use linear approximation along co-phase lines across the basin from shore points), and
- d. a correction of approximately 10 cm/1000 km slope due to Trade Wind set-up.<sup>8</sup>

### Errors

The accumulated error in the procedure outlined above can be estimated as follows:

Step 1. Given gravity observations good to 1 mgal the free-air anomalies are also correct to that figure and are consistent insofar as standard gravity is reckoned in each case from the same formula.

Step 2. From the near-field formulas, deflections of the vertical can be calculated from 1 mgal gravity data for 200 km circles of influence to 1" accuracy. When these deflections are expressed as undulations of an equipotential surface the height error may be in the order of 1 meter for a run of 200 km between successive stations. Increased station density should reduce this error as  $1/\sqrt{n}$ , but even so this conversion is by far the source of largest error.

Step 3. Mean sea level is normally given to 0.1 ft. (3 cm) accuracy for 10-year runs of data but may be found to even greater refinement especially where runs of many decades are available.

Step 4. The specific volume anomaly for sea water is usually expressed to 1-cm accuracy or better but is given with reference to an assumed "level of no motion." Arguments based on the 1500 decibar reference surface can differ from those for the 4000 decibar reference surface by as much as 10's of cm in extreme cases.

Corrections of surface height to standard barometric pressure are made by the hydrostatic equivalent that 1 cm of water is supported by 1 mb of atmospheric pressure. The error in this correction is probably in the order of 1 cm.

Step 5. The accuracy of fitting the equipotential surface to MSL is dependent on the quality of the geodetic net which ties the tide gauge stations together. Presumably this accuracy is far greater than that of the calculated equipotential undulations. It may be estimated that the height of the least squares fit may be in error by at least 1 meter and possibly more.

Step 6. The height of the physical sea surface may be expressed relative to the equipotential surface mentioned in Step 5 to an accuracy of 10 cm or better, the largest error coming from the choice of a depth for the assumed reference surface in expressing the specific volume anomaly.



The tidal regimes in the Caribbean are well enough known to make linear estimates of the interior tidal amplitudes with an error of less than 10 cm. The so-called "meteorological tides" or shallow water waves generated by non-astronomical forces can be large but are ephemeral.

The set-up due to mean winds such as the Trades are probably of the order stated, i.e., 10 cm per 100 km.

In sum then it seems probable that the accuracy with which the figure of the ocean surface can be predicted is in the 2 to 3 meter range because of the large uncertainty in the geoidal topography.

APPENDIX S  
REFERENCES

1. Bowin, C.O. (unpublished) Gravity observations in Caribbean Basin Woods Hole Oceanographic Institution.
2. Heiskanen, W.A. and F.A. Vening Meinesz, 1959, The Earth and its Gravity Field, McGraw-Hill, New York, 470 pp.
3. U.S. Coast and Geodetic Survey, 1942, Tidal Harmonic Constants TH-1 Atlantic Ocean, 137 pp.
4. Wust, G., 1964, Stratification and Circulation in the Antillean-Caribbean Basins, Columbia Univ. Press, New York, 201 pp.
5. Wust, G., 1963, "On the stratification and the circulation in the cold water sphere of the Antillean-Caribbean Basins, " *Deep-Sea Res.*, 10:165-187.
6. Parr, A.E., 1937, "A contribution to the hydrography of the Caribbean and Cayman Seas, " *Bull. Bingham Oceanogr. Coll.*, V:1-110.
7. Mintz, Y. and G. Dean, 1952, Observed Mean Field of Motion of the Atmosphere, Geophys. Res. Pap 17, Geophysics Research Directorate, Air Force Cambridge Research Center.
8. Montgomery, R.B., 1940, *Bull. Am. Meteor. Soc.* 21:87-94.

## GENERAL REFERENCES

1. Opportunities for Participation in Space Flight Investigation, Memo Change No. 20, March 20, 1969, signed J. Naugle, NASA OSSA, entitled "GEOS-C Radar Altimeter Experiment".
2. Fischer, I., M. Slutsky, R. Shirley, and P. Wyatt - Geoid Charts of North and Central America, Army Map Service, Washington, D. C., 1967.
3. Berry, F., E. Bolay and N. Beers (eds). - Handbook of Meteorology, McGraw-Hill Book Co., New York, pp. 989-992.
4. Anonymous - World Chart of Observations in 5° x 5° - Squares, National Oceanographic Data Center, Washington, D. C.
5. Worzel, J. - Pendulum Gravity Measurements at Sea 1946-1959, J. Wiley & Sons, New York, 1965.
6. Anderle, R. J. - Computational Methods Employed in Deriving Geodetic Results from Doppler Observations of Artificial Earth Satellites, U.S. Naval Weapons Lab., Dahlgren, Va., 1965.
7. Bursa, M. - Geopotential, Geoidal Surface, and Earth's Figure Parameters as Determined from Satellite and Terrestrial Data, Research Inst. of Geodesy, Prague, 1969.
8. Sherr, P. T., et al., - World-Wide Cloud-Cover Distribution for use in Computer Simulation, NASA CR-61226, CFSTI, Springfield, Va., 1968.
9. Kalil, F. - Optical and Microwave Communications, NASA TN D-3984, CFSTI, Washington, D. C., p. 18, 1968.
10. Hogben, N. and Lumb, F., Ocean Wave Statistics, H. M. Stationery Office, London, Area 16, 1967.
11. Hospers, J. and J. C. van Wynen - Gravity Field of the Venezuelan Andes and Adjacent Basins (Verh. Kon. Med. Akad. Wet. 23.1), N. V. Noord-Hollandsche Uit. Amsterdam, 1959.
12. VonArx, W. S., "Level Surface Profiles Across the Puerto Rico Trench," Science 154: 1651-1654, 1966.
13. Morgan, W. J., "Gravity Anomalies and Convection Currents, 2. The Puerto Rico Trench and the Mid-Atlantic Rise," J. Geophys. Res., 70(24): 6189-6204, 1965.
14. VonArx, W. S., "A New Navigation System," Navigation Vol. 9, #3 pp. 224-230, 1962.
15. Hospers, J., "Gravity Field of Northern S. America and the West Indies," Geol. en Mijnbouw 20: 358-365, 1958.

16. Von Arx, W.S., "Relationship Between Marine Geodesy and Oceanographic Measurements" Proceedings of the First Marine Geodesy Symposium Columbus, Ohio, Sept. 28-30, 1966, pp. 37-42.
17. Butera, A., J. Goelowski, and J. Dematteo - Direct Measurement of Deflection of the Vertical Using a Ship's Inertial Navigation System (SINS). Paper presented at Marine Geodesy Symposium, New Orleans, 1969.
18. Rice, D., private communication, 1970.
19. Sturges, W., "Water Characteristics of the Caribbean Sea," J. Marine Res. 23 (2): 147-162, 1965.
20. Gordon, A., D. Grim and M. Lampetter, "Layer of Abnormally Cold Bottom Water Over S. Aves Ridge," Science 151 (3733): 1525-1526, 1966.
21. LaFond, E. and LaFond, K., Vertical and Horizontal Thermal Structures in The Sea, U.S. Navy Electronics Lab, San Diego, Calif., 1966.
22. Bush, N., Atlantic Missile Range, Engineering Tech. Staff, Private Communication, 1970.
23. Anonymous, Gezeitentafeln 1966, B. II. Deutsches Hydrographische Institute, Hamburg, 1965.
24. Anonymous, East Coast Tide Tables 1969, U.S. Coast & Geodetic Survey, Washington, D.C., 1969.
25. Anonymous, Admiralty Tide Tables 1970 - Volume III, Hydrographer of the Navy, London, 1969.
26. Simmons, L., "How Accurate is First-Order Triangulation?", J.C. & C.S. 3:, 1950.
27. Various Authors, Proc. IEEE 54 (2), 1966.
28. Anonymous (Geonautics) - Goddard Directory of Tracking Station Locations (2nd ed.), Data Operations Branch, Goddard Space Flight Center, Greenbelt, Md. Part II. Section 3.
29. Schumacker, A., "Sterophotogrammetrische Wellenaufnahmen," Wissen. Ergeb. Deutsche Atlantischen Exped....."Meteor" 1925-1929, Vol. 7, No. 2., 1939.
30. M. Kolker & E. Weiss, Space Geodesy Altimetry Study, NASA CR-1298, Raytheon Company, Sudbury, Mass., 1969.
31. Izsak, I.G., Tesseral Harmonics of the Geopotential and Corrections to Station Coordinates, J. Geoplug, Res. 69: 2621-2630, 1964.
32. Defant, A., Physical Oceanography, Vol. 1, Pergamon Press, N.Y., 1961.

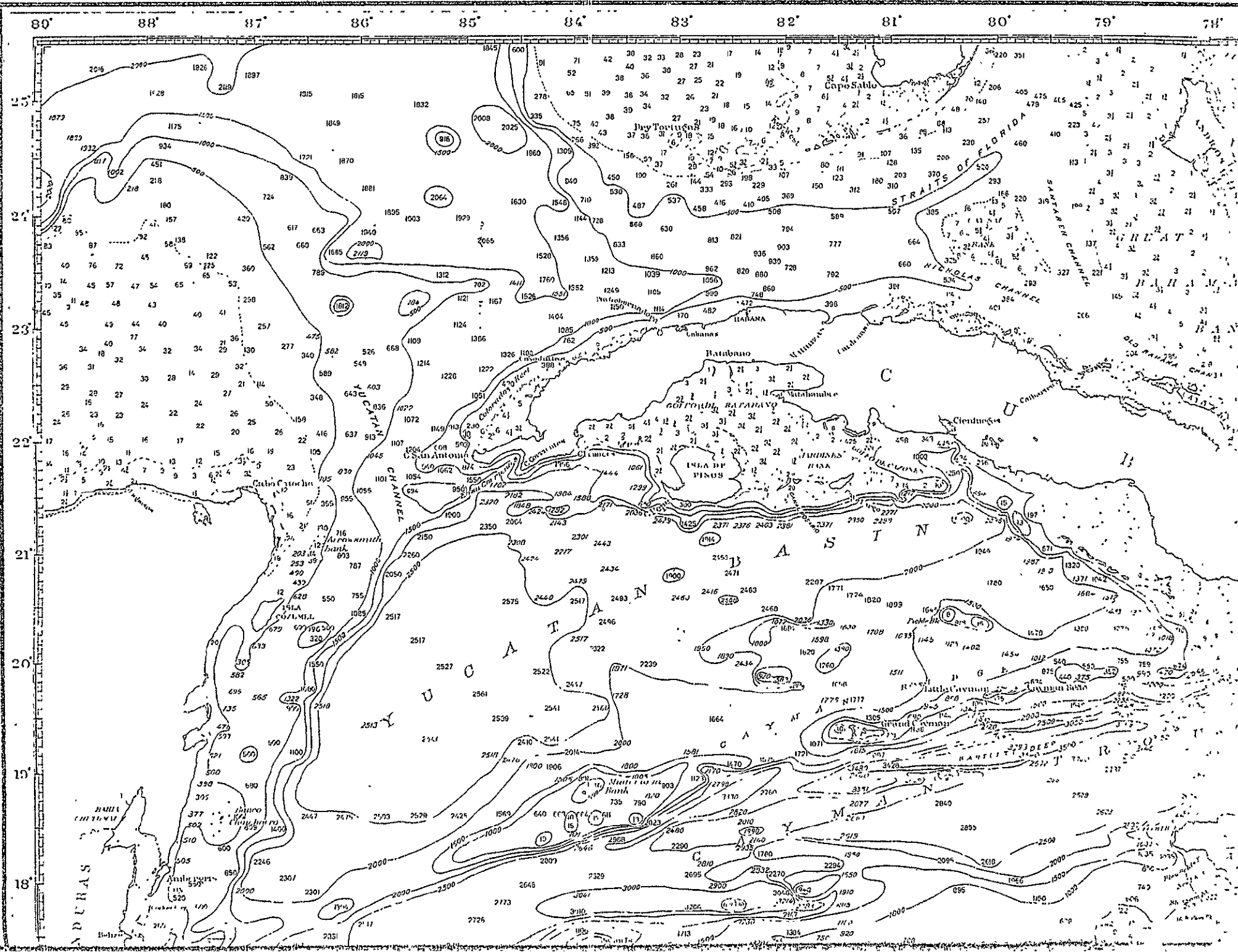
33. Sverdrup, H., M. Johnson and R. Fleming, The Oceans, Prentice-Hall, Inc., New York, 1942.
34. Sturges, W., "Slope of Sea Level Along the Pacific Coast of the United States," J. Geophys. Res. 72(14): 3627-3637, 1967.
35. Bigelow, H. and D. Edmundson, Wind Waves at Sea, Breakers and Surf, Publ. No. 602, U.S. Navy Hydrographic Office, Washington, D.C., 1962.
36. Robert Day - Private Communication.
37. M. Greenspan and C.E. Tscheigg, "Sing Around Velocimeter for Liquids," Rev. Sci Inst., Vol. 28, 897-901, (1957).
38. Paul Brumberg, Code 813, NASA, Goddard Space Flight Center, Private Communication.
39. Paul Putnam, Convair General Dynamics, Quincy, Mass., Private Communication.
40. John Alvey, NASA, Goddard, Private Communication.
41. Kinsman, Blair. Wind Waves, Prentice-Hall, 1965
42. Keller, Apollo Inertial Ship Evaluation, August 1968, pgs. 832-68-323, NASA, Goddard Space Flight Center.
43. Apollo 101 AS-505 MSFN Metric Tracking Performance Preliminary Report X832-69-224, May 1969, NASA, Goddard Space Flight Center.
44. MSFN Metric Tracking Performance Report AS-506 X-832-69-362, August 1969, NASA, Goddard Space Flight Center.
45. Pratt, D.E., Bond, D.A., Unified S Band System Ranging Performance and Transponder Integration for GEOS Satellites, Report #R-4035-51-21, Communication & Systems, Inc., Falls Church, Va.
46. Moss, S.J., C Band Accuracy Estimates for Wallops Island Colocation Experiment; GEOS B C Band System Project Technical Conference and Working Group, June 1969, NASA, Goddard Space Flight Center.
47. Brooks, R.L., Beacon Skin Tracks of GEOS II Satellite by Wallops AN/FPQ-6 Radar; IBID.
48. Leito, C.D., Brooks, R.L., C Band Range Measurements: An Assessment of Accuracy. International Association of Geodesy, International Symposium of Electromagnetic Distance Measurement and Atmospheric Refraction, Boulder, Colorado, June 1969.
49. McGoogan, J., Private Communication.
50. Stanley, H.R., Private Communication.

51. "AROD Application," Motorola, Government Electronics Division, Aerospace Center (NAS 8-11835).
52. Radar Altimeter Experiment for GEOS-C, Communications and Systems Report No. R-4035-53-2, December, 1968.
53. Preprocessing Electronic Satellite Observations, by Joseph E. Gross, Ohio State University, prepared under NASA grant NGR 36-008-093, published as NASA CR-1183 dated November, 1968.
54. Brouwer, D. and G. Clemence, Celestial Mechanics, Academic Press—New York, 1961.
55. Guenther, W. and Thomas, P., "Some Graphs Useful for Statistical Inference," Am. Statistical Ass. J. 60 (309), 334-343, 1965.
56. Veis, G. (ed.) Use of Artificial Satellites for Geodesy Vol. II. National Technical University, Athens. 1967
57. Schmid, H. "Accuracy Aspects of a World Wide Passive Satellite Triangulation System" Photogram. Eng. 31(1): 104-117 (1965).
58. Lambeck, K., Comments on the Accuracy of Baker-Nunn Observations, Smithsonian Institute Astrophysical Obs., Cambridge, Mass. 1968
59. Moss, S. and Wells, W., A Laser Satellite Ranging System II. An Analysis of the GSFC Laser Ranging Data. Wolf Research and Development Corp. 16 June 1967.
60. Bretterbauer, K., New Results Concerning the Atmospheric Effect on Laser-Ranges to Artificial Satellites. International Symposium on E.D.M. and Atmospheric Refraction. Boulder, Colorado 1969.
61. Carney, D.; Hlavin, J.; Berbert, J., C-Band, SECOR, TRANET and GRRR Tracking Data Comparisons with Laser/Optical Short-Arc Orbits, 50th Annual Meeting, (Washington, D.C.) American Geophysical Union, Washington, D.C. 1969.
62. Veis, G., "Results from the Orbital Method", Geodetic Parameters for a 1966 Smithsonian Institution Standard Earth Vol. 2 (C. Lundquist, ed.). 1966 pp. 59-66.
63. B. Chovetz private communication, 1969.
64. Jury, H. Marine Geodesy and Navigation at the Air Force Eastern Test Range Second Symposium on Marine Geodesy (New Orleans) Marine Technological Society. 1969
65. NASA/Wallops Station, GEOS-II C-Band Project 1969.

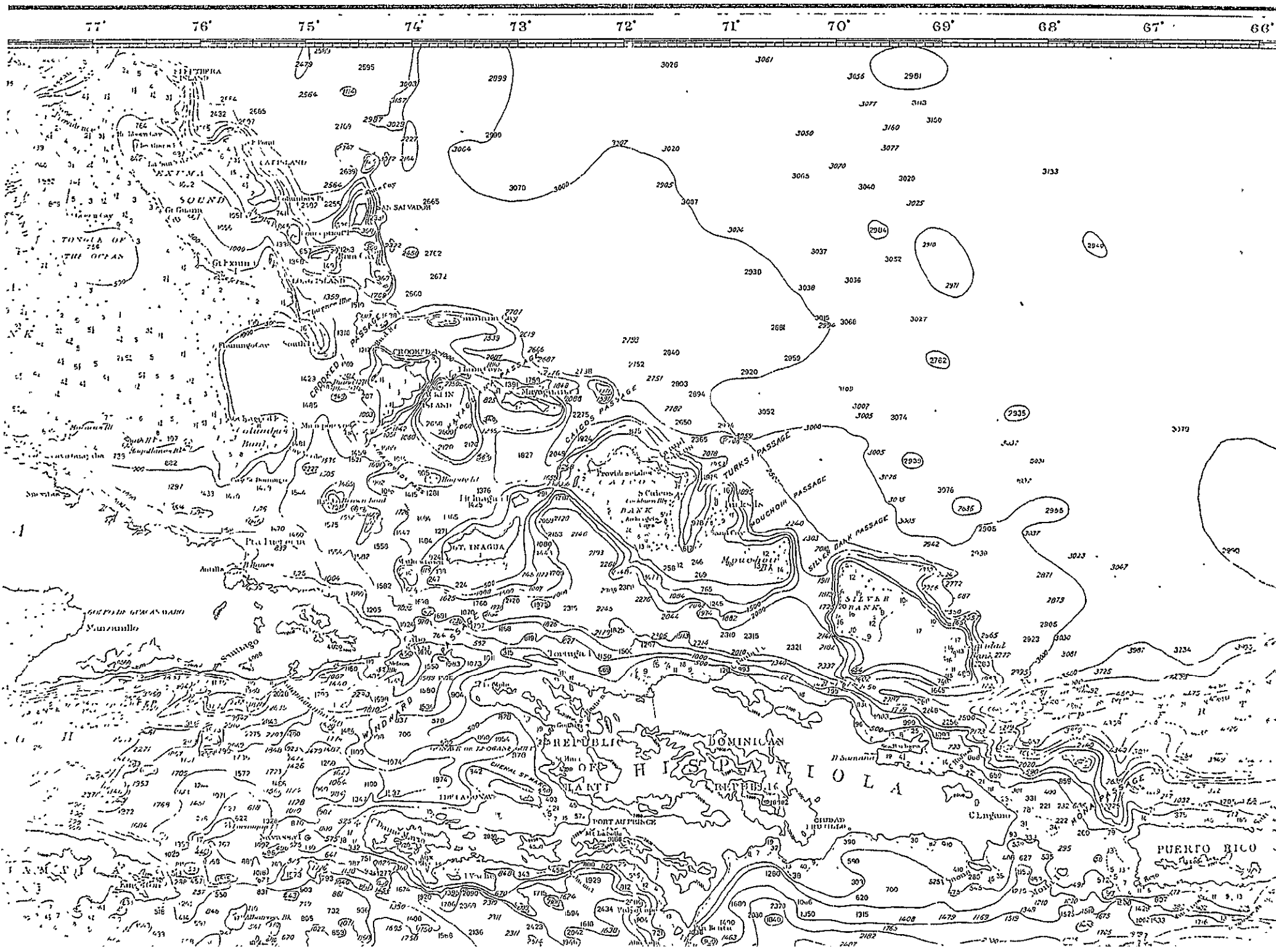
66. Meinez, F.A. Venning, "Interpretations of Gravity Anomalies on the West Coast of South America and in the Caribbean", Neth. Geod. Comm. Publ. on Geodesy 2(1): 5-22 (1964).
67. Talwani, M.; Poppe, H.; Rabinowitz, P. Recent Progress in Marine Gravimetry and a Gravimetric Geoid for the Western North Atlantic, 51st Annual Meeting, American Geophysical Union, Washington, D. C. (1970).
68. Irving Salsburg, NASA Goddard Space Flight Center, private communication.
69. J. Tomlin, Pickard & Burns Electronics, Waltham, private communication.
70. Anonymous, "AN/FPS-16(V) Shipborne Precision Radar," (Brochure), RCA Defense Electronics Products, Missile and Surface Radar Division, Moorestown, N.J.

A

B







K

F

66° 65° 64° 63° 62° 61° 60° 59° 58° 57° 56°

To Accompany Report of Navy-Geophysical  
Union Gravity Expedition, 1936-1937,  
by H. H. Hess



# BATHYMETRIC CHART OF THE CARIBBEAN SEA

Compiled at the U. S. Hydrographic Office, mainly  
from sounding data obtained by U. S. Navy Vessels

SOUNDINGS IN FATHOMS

HEIGHTS IN FEET

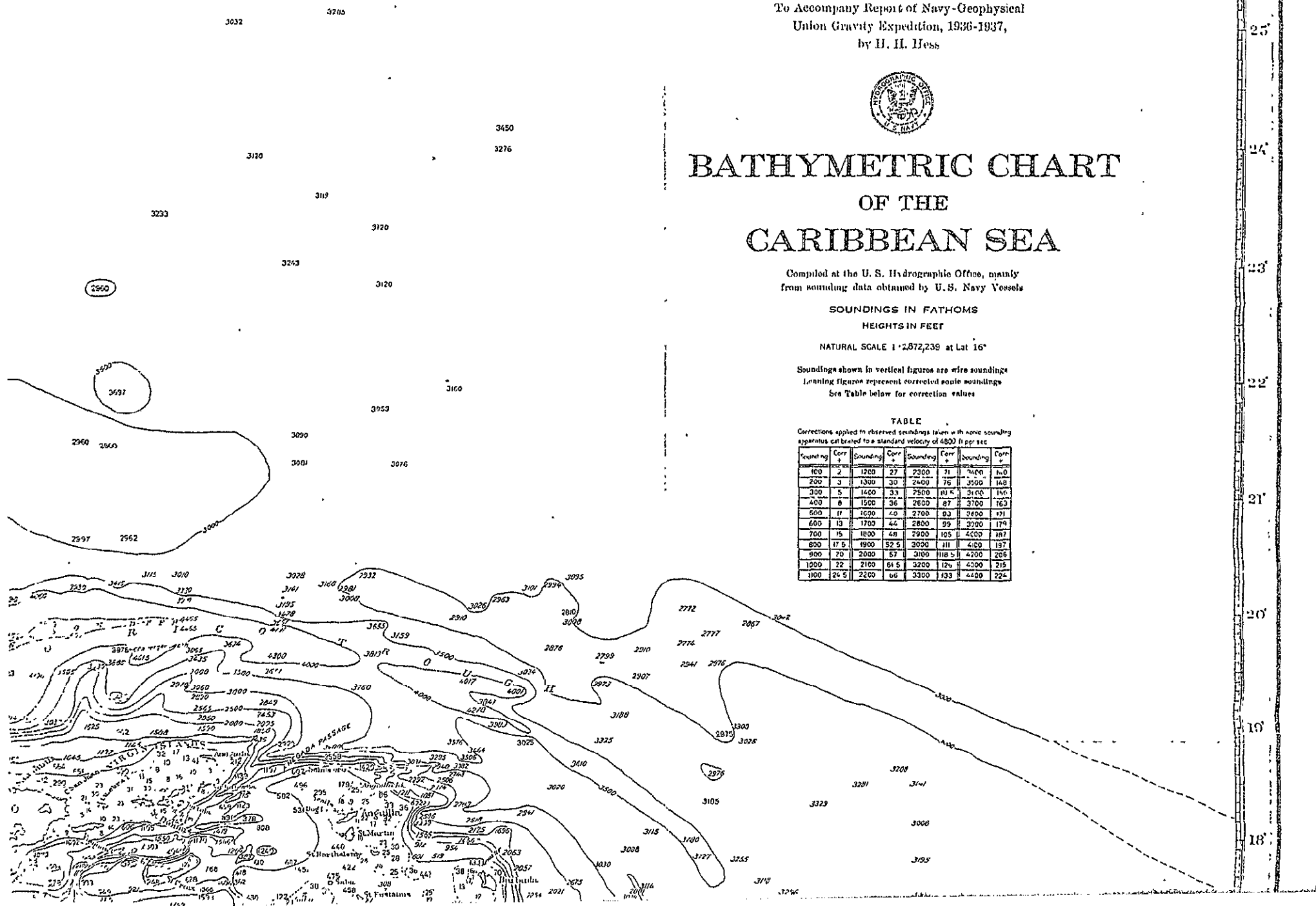
NATURAL SCALE 1:2872,239 at Lat 16°

Soundings shown in vertical figures are wire soundings  
Leading figures represent corrected soundings  
See Table below for correction values

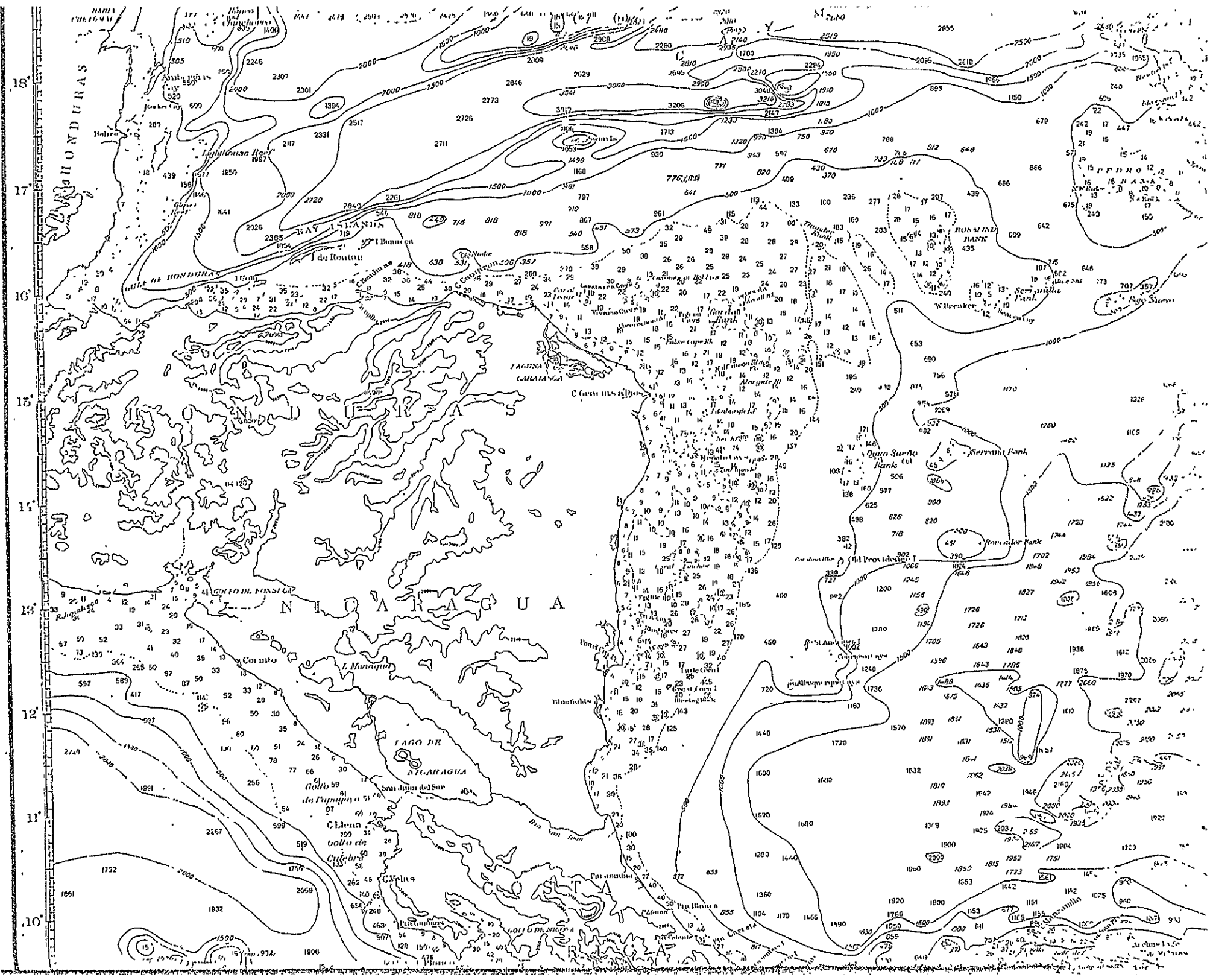
TABLE

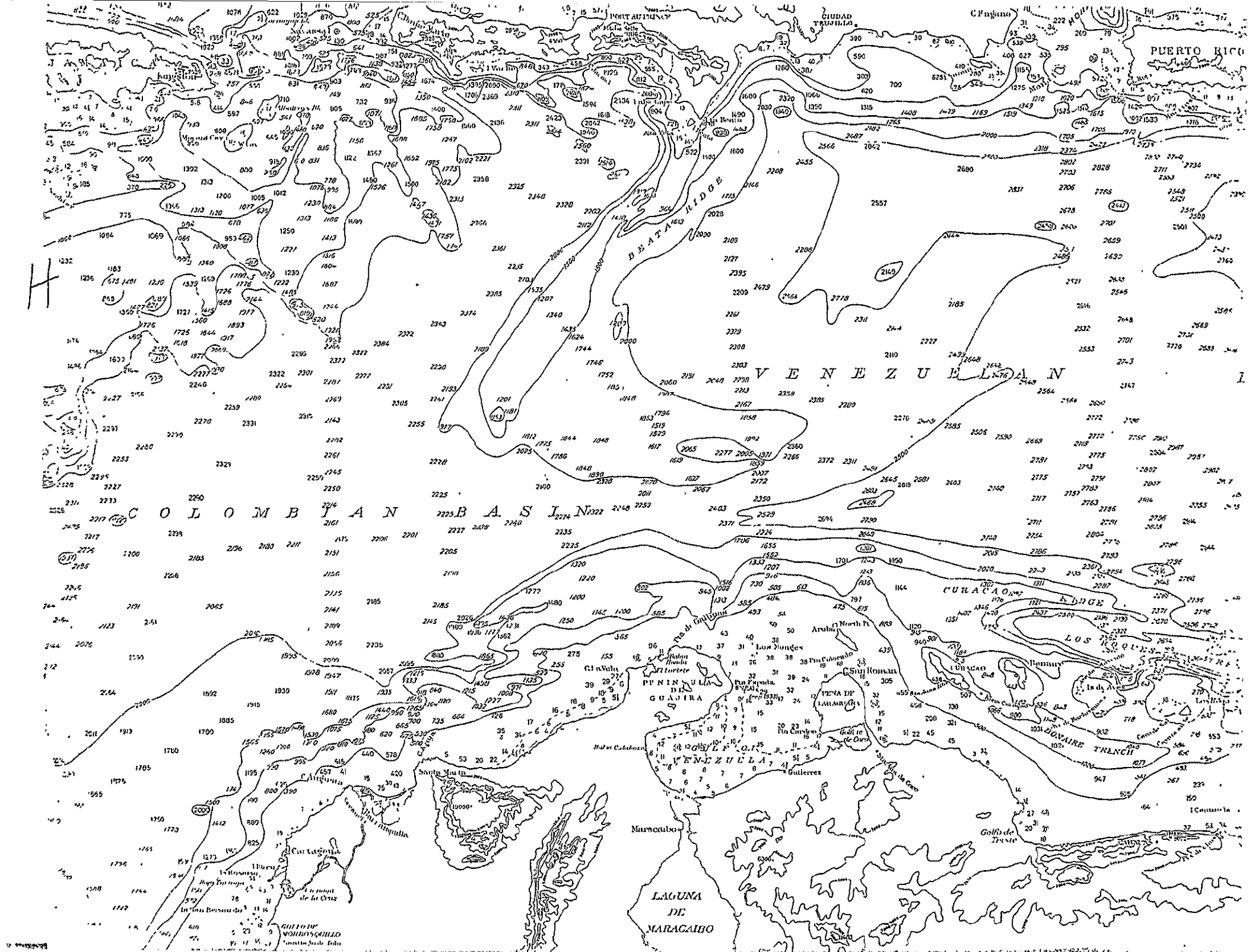
Corrections applied to observed soundings taken with sonic sounding  
apparatus calibrated to a standard velocity of 4800 ft per sec

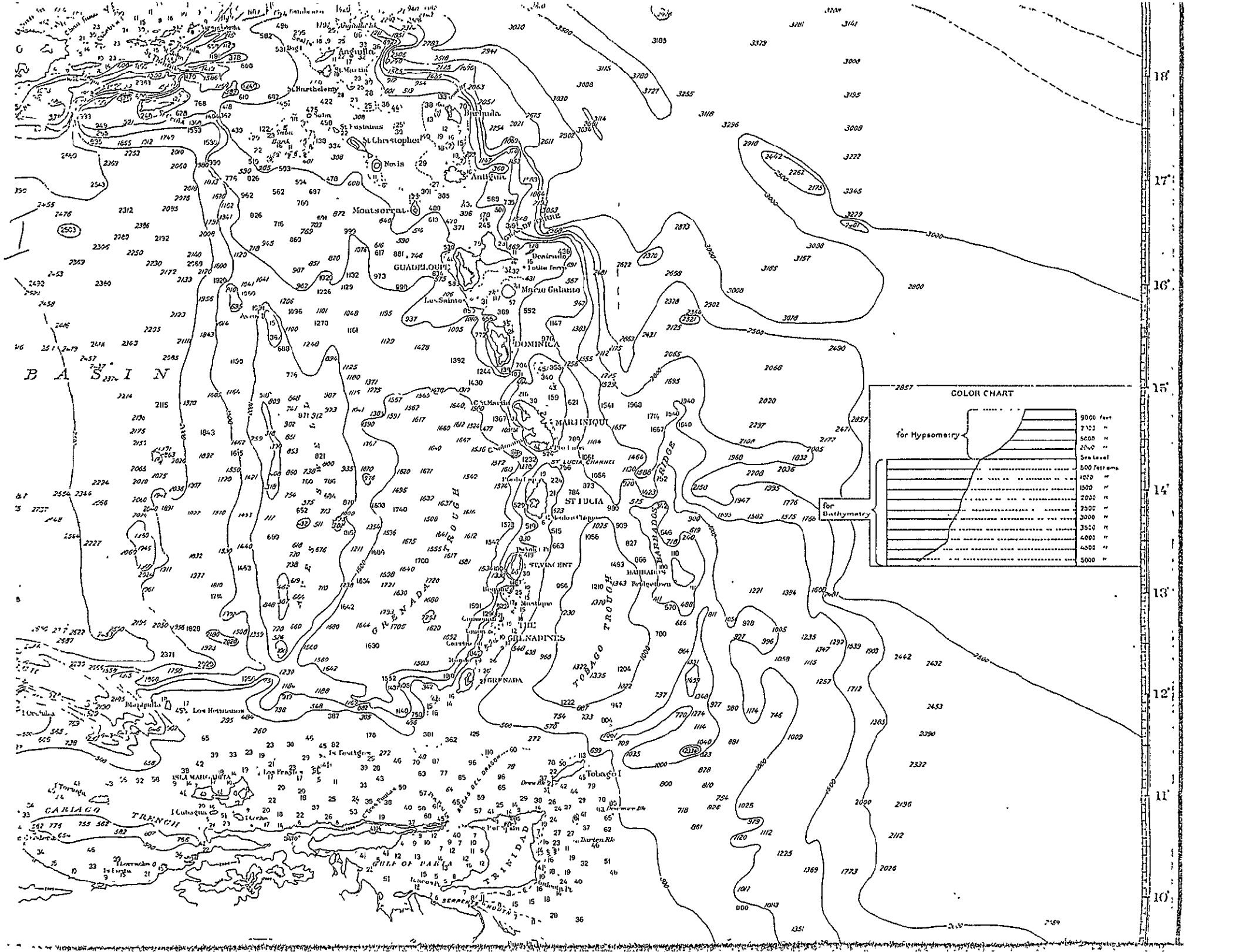
Sounding	Corr	Sounding	Corr	Sounding	Corr	Sounding	Corr
100	2	1200	27	2300	71	3400	110
200	3	1300	30	2400	76	3500	116
300	5	1400	33	2500	81	3600	121
400	6	1500	36	2600	87	3700	126
500	11	1600	40	2700	93	3800	131
600	13	1700	44	2800	99	3900	137
700	15	1800	48	2900	105	4000	142
800	17	1900	52	3000	111	4100	147
900	20	2000	57	3100	118	4200	152
1000	22	2100	61	3200	124	4300	157
1100	24	2200	66	3300	133	4400	162

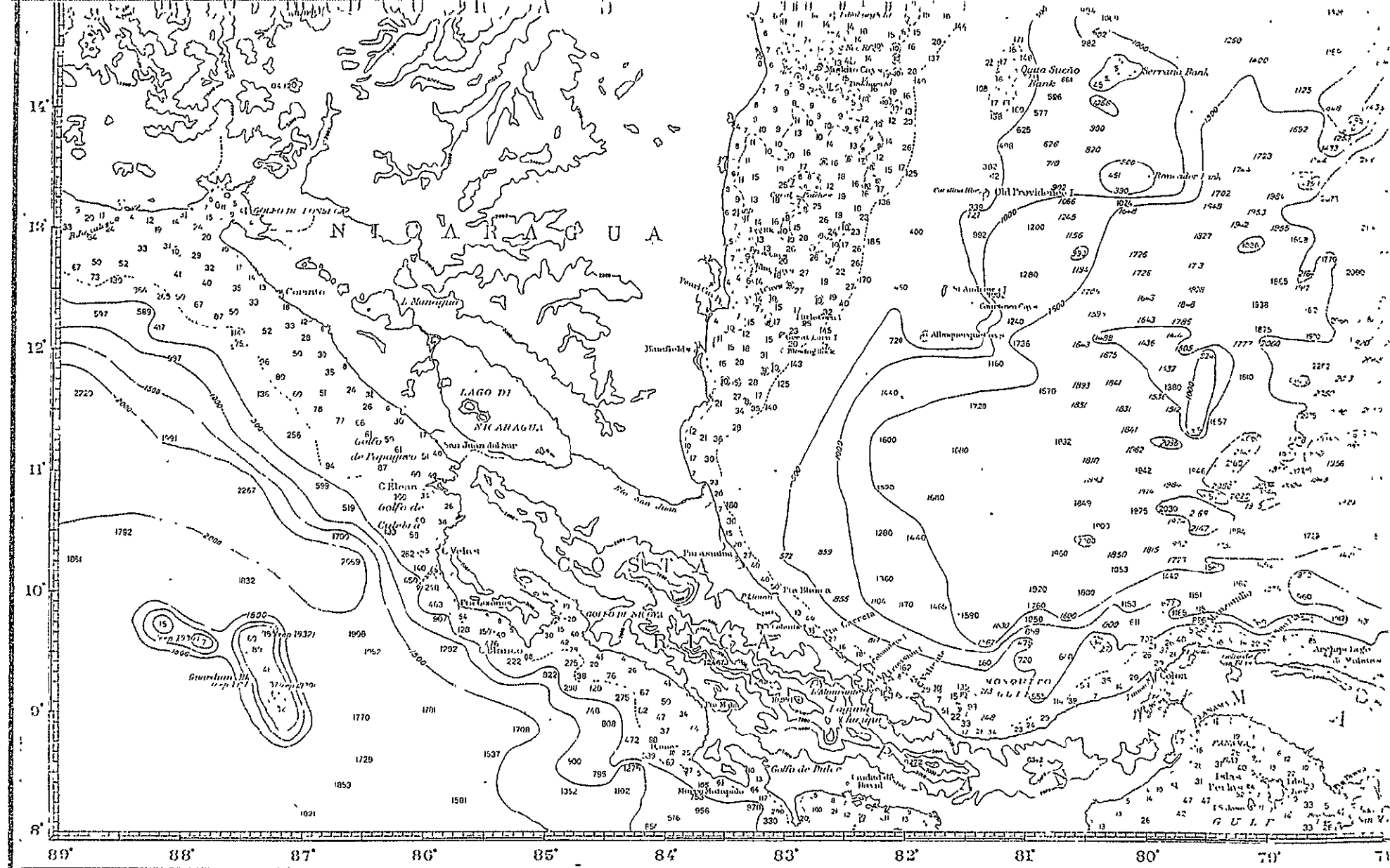


5



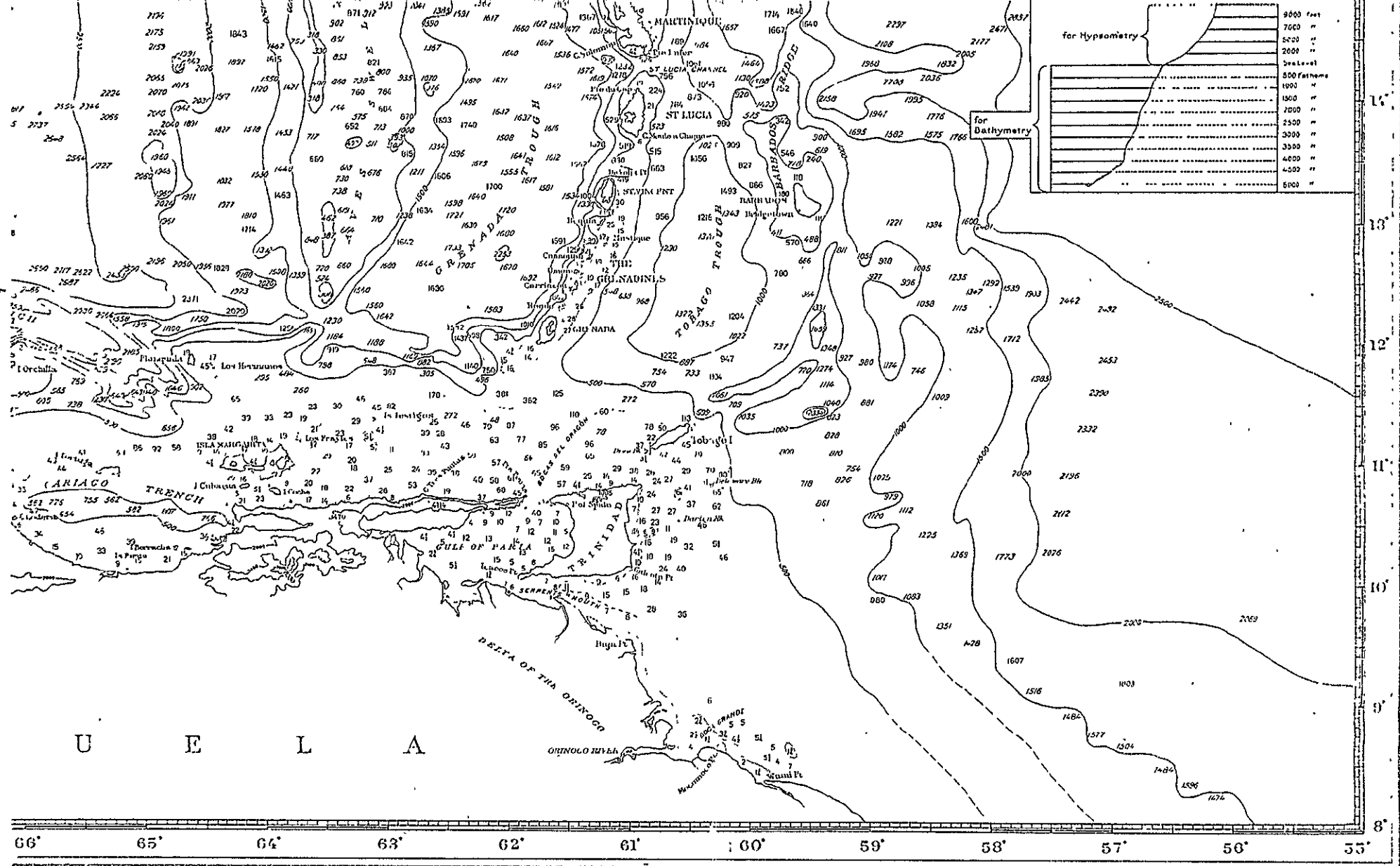




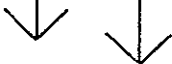


Small corrections  
from Notices to Mariners  
from other sources









RAYTHEON COMPANY  
EQUIPMENT DIVISION